Nanostructured emulsions and nanolaminates: an approach toward food protection and delivery of active ingredients

Alejandra Acevedo Fani

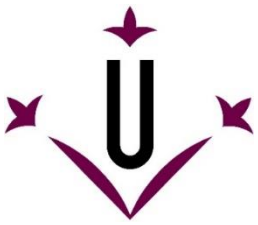

Universitat de Lleida

Tesi Doctoral

Nanostructured emulsions and nanolaminates: an approach toward food protection and delivery of active ingredients

Alejandra Acevedo Fani

Memòria presentada per optar al grau de
Doctor por la Universitat de Lleida
(Programa de Doctorat en Ciència i Tecnologia Agrària i Alimentària)

Director/a :
Dr. Olga Martín Belloso
Dr. Robert Soliva Fortuny

Lleida, Octubre 2016

The current research has been performed in the Laboratory of Novel Technologies for Food Processing and the Pilot Plant of the Department of Food Technology, under the supervision of Prof. Olga Martín Belloso and Prof. Robert Soliva Fortuny.

This Doctoral Thesis was supported by the Spanish Ministry of Science and Innovation through the following projects:

- **ALG2009-11475**: 'Development of nanostructured edible coatings as carriers of active compounds'
- **ALG2012-35635**: "Improving quality and functionality of food products by incorporating lipid nanoparticles into edible coatings"

The Ph.D candidate granted a fellowship of the University of Lleida to pursue the Ph.D degree.

Experiments concerning to the optimization in formation, physicochemical stability and gastrointestinal fate of multilayer emulsions, as delivery systems of resveratrol, were carried out in the Laboratory of Industry and Process (LIP) of the Centre of Biological Engineering at the University of Minho (Braga-Portugal), under the supervision of Prof. Antonio Vicente.

Permanence, perseverance and persistence in spite of all obstacles, discouragements, and impossibilities: It is this that in all things distinguishes the strong soul from the weak.

-*Thomas Carlyle*

All our dreams can come true if we have the courage to pursue them

-*Walt Disney*

A mis abuelos maternos: Amada (que en paz descanse) y Omero (¡larga vida!), y como no, a mi adorada madre Barbara.

Este logro es también de ellos.

AGRADECIMIENTOS / ACKNOWLEDGMENTS

Comenzaré por agradecer a mi directora, la Prof. Olga Martín Belloso, por haberme introducido en el mundo de la investigación y brindarme su apoyo incondicional a lo largo de mi tesis. Gracias por confiar en mí, por toda la paciencia que has tenido, y sobre todo, por haberme dado la libertad para avanzar hacia cualquier objetivo que me platease. Me has brindado numerosas oportunidades para hacerme florecer como investigadora y terminar amando lo que he hecho todos estos años. A nivel personal, quiero agradecerte también por haberme hecho sentir como en casa, aún cuando estaba a muchos kilómetros de ella. De corazón, muchas gracias 'mamá' Olga.

También quisiera agradecer a mi co-director Robert Soliva Fortuny por el apoyo académico brindado durante esta larga travesía. Agradezco todas esas largas charlas en tu despacho que, gracias a tus consejos, siempre acababan teniendo un efecto calmante. Estos momentos también han sido cruciales para seguir caminando hacia la gran meta. Te agradezco la inmensa paciencia, incondicional disponibilidad y gran implicación que has tenido en todo momento.

A mis ex compañeras y grandes amigas, Dra. Laura Salvia y Dra. M. Alejandra Rojas, quienes me contagiaron con su pasión por la ciencia en los primeros años de mi tesis. Laura, contigo dí mis primeros nano-pasitos y me llevaste de la mano a comprender el mundo a escala nanométrica. Alejandra, la reina de los recubrimientos comestibles. Gracias por transmitirme tus conocimientos científicos en el tema y por ser mi hermana de la vida. Ambas han estado allí para darme ánimos y aconsejarme en todos los aspectos. No tengo palabras para expresar mi agradecimiento.

A todos mis compañeros del laboratorio de nuevas tecnologías, tanto a los que están ahora como a los que ya marcharon. Tengo muchos recuerdos bonitos, que sin duda alguna, han hecho mucho más agradable mis años como doctoranda. En especial quisiera agradecer a Ariadna, Mariona, Mauro y Blanca por cuidarme siempre y darme ánimos para seguir adelante.

No puedo dejar de mencionar a mis queridos técnicos de laboratorio, Magda, Manel y Gemma. Muchisisisimas gracias por ser 'mi botón de emergencia'.

Más de una vez tuve que ‘romper el cristal’, y afortunadamente siempre han estado allí para rescatarme. Por eso les estoy muy agradecida.

Moreover, I would like to thank Prof. Ph.D. Antonio Vicente for the excellent guidance during my stay in his Laboratory at the University of Minho. Sincerely, my experience was completely positive and beneficial. Also, I would like to thank all my lab mates (meninos do LIP) for being so kind with me, making my stay an spectacular story to remember. Hélder, many thanks for all the patience and interest in helping me in the lab. My ‘meninas’: Isabel, María-kiki, Ana Cristina, Heloisa, Adriana and Liliana, thank you very much for all the awsome stories.

A mis amigos Ana Ramos, Armando Moreno, Ana Sanhueza, Lady Aguilera, Antonio y Rafael Castillo, Juan Vallenilla, Asdrubal Miranda. Más cerca o más lejos, han estado allí para regalarme “oxígeno” y buenos recuerdos. Por supuesto, gracias a mis compañeras de piso, hermanas y amigas, Eimys Ortiz, Soraia Oliveira, Anna Trenc y Hadaly Serrano. Todos estos años han sido mi familia putativa, brindándome un soporte emocional increíble… Me siento afortunada de haberlas conocido y tenido a mi lado en esta etapa de mi vida.

Y por último pero no menos importante, muchas gracias a mi familia. Mamí, gracias por todos los valores que me has inculcado y por todo el esfuerzo que has hecho por mí. Tengo la certeza que sin tu apoyo y confianza, no hubiese sido capaz de llegar hasta aquí. Al resto de mi familia (Abuelos, tíos y primos) tengo mucho que agradecerles…han aplaudido cada uno de mis logros y me han impulsado a seguir adelante en los momentos más difíciles. Alguna vez leí que la familia es donde comienza la vida y el amor nunca termina…Por eso les amo y me siento bendecida por tenerles.

RESUM

Actualment, els consumidors demanen aliments més segurs, saludables i amb una qualitat nutricional elevada. És per això que, incorporar substàncies actives als aliments representa una estratègia prometedora. Aquestes substàncies poden ser químicament inestables, poc solubles en aigua, presentar una biodisponibilitat baixa i a més a més, provocar canvis organolèptics en el producte final. Per tant, existeix un interès destacat en els sistemes alimentaris nanoestructurats com una eina per poder contrarestar aquests inconvenients. La importància d'aquests sistemes es basa en la possibilitat de controlar les seves característiques a nivell molecular, aconseguint així una funcionalitat específica. L'objectiu d'aquesta tesi doctoral va ser avaluar els factors més importants que afecten la formació i les propietats fisicoquímiques de nanoemulsions, emulsions multicapa i nanolaminats, així com la seva capacitat per encapsular, protegir i alliberar les substàncies actives.

En primer lloc es van obtenir nanoemulsions contenint olis essencials de farigola, citronela i sàlvia en la fase dispersa i alginat sòdi en la fase contínua, mitjançant microfluidització per ser aplicades com a pel·lícules comestibles. Les característiques de les gotes en les nanoemulsions, principalement diàmetre de partícula i potencial zeta, van determinar les propietats físiques de les pel·lícules. Aquelles formades amb nanoemulsions d'oli de sàlvia van ser més translúcidas, flexibles i resistents a la transferència de vapor d'aigua. No obstant això, l'activitat antimicrobiana de les pel·lícules enfront de *Escherichia coli* va estar governada pel tipus d'oli essencial empleat. En particular, les pel·lícules comestibles amb oli de farigola van exhibir l'activitat antimicrobiana més forta.

En segon lloc, es van elaborar emulsions d'una capa (gotes recobertes amb lactoferrina) i multicapa (gotes recobertes amb lactoferrina/alginat i lactoferrina/alginat/poli-L-lisina), contenint resveratrol com a substància nutracéutica hidrofòbica. Es va estudiar l'efecte de la concentració de biopolímer en la formació i estabilitat d'aquests sistemes. A concentracions molt baixes o molt altes de biopolímer, les emulsions multicapa van ser bastant inestables. Es van aconseguir formar emulsions secundàries estables (amb gotes cobertes per lactoferrina/alginat) usant concentracions de alginat de 0.22% a 0.28 % p/p, mentre les emulsions terciàries (amb gotes cobertes

per lactoferrina/alginat/poli-L-lisina) es van obtenir a 0.036% de poli-L-lisina. Les emulsions multicapa van ser més estables que les emulsions d'una capa durant l'emmagatzematge. La capacitat antioxidant de totes les emulsions contenint resveratrol va romandre estable durant l'emmagatzematge, comparat amb el resveratrol sense encapsular. D'altra banda, la composició de la capa interfacial va afectar l'estabilitat de les partícules durant una digestió *in vitro*. Les emulsions terciàries van ser més estable que les primàries i secundàries sota condicions gastrointestinals simulades. Després de la digestió, la bioaccesibilidad més alta del resveratrol es va observar en les emulsions terciàries.

Finalment, es van formar nanolaminats d'alginat/quitosà mitjançant la tècnica de capa-a-capa per incloure a més àcid fólic com a substància nutracéutica hidrofílica. Els canvis en la càrrega elèctrica de les solucions de alginato i quitosano van permetre modular les propietats macroscòpiques dels nanolaminats. L'àcid fólic fou encapsulat efectivament dins dels nanolaminats pel mètode de post-difusió. El contingut de vitamina en els nanolaminats va augmentar en usar solucions de càrrega més concentrades, o augmentant el temps d'immersió en la solució de càrrega. L'encapsulació de l'àcid fólic dins dels nanolaminats va aportar una millor protecció enfront de la degradació per llum UV. També, els perfils d'alliberament de l'àcid fólico des dels nanolaminats van poder ser controlats canviant el pH del mitjà. En condicions alcalines (pH 7), la vitamina va ser ràpidament alliberada, mentre que en condicions àcides (pH 3) l'alliberament va ser molt baixa.

Els resultats obtinguts en el present treball aporten informació útil per al disseny d'emulsions nanoestructurades i nanolaminats, i demostren que l'encapsulació d'additius naturals en aquests sistemes pot millorar la seva estabilitat i funcionalitat. Per tant, aquests sistemes d'alliberament poden ser considerats com una via per aconseguir l'ús més efectiu i racional de compostos actius alimentaris, obrint noves perspectives a l'elaboració de productes alimentaris amb beneficis excepcionals per als consumidors.

RESUMEN

Actualmente, los consumidores demandan alimentos seguros, sanos y de alta calidad. Para alcanzar este objetivo, la incorporación de ingredientes activos a los alimentos representa una estrategia prometedora. Estos compuestos pueden ser químicamente inestables, poco solubles en agua, presentar baja biodisponibilidad, y dar lugar a cambios organolépticos en el producto. Por lo tanto, existe un gran interés en los sistemas nanoestructurados como una herramienta para superar estos inconvenientes. La importancia de los sistemas alimentarios nanoestructurados radica en la posibilidad de controlar sus características a nivel molecular, alcanzando una funcionalidad específica. El objetivo de la presente tesis doctoral fue evaluar los factores más importantes que afectan la formación y las propiedades de las nanoemulsiones, emulsiones multicapa y nanolaminados, así como también, su habilidad para encapsular, proteger y liberar ingredientes alimentarios activos.

En primer lugar, se obtuvieron nanoemulsiones conteniendo aceites esenciales de tomillo, citronela y salvia en la fase dispersa y alginato de sodio en la fase continua, por microfluidización para ser aplicadas como películas comestibles. Las características de las gotas en las nanoemulsiones, principalmente tamaño y potencial zeta, determinaron las propiedades físicas de las películas. Aquellas formadas con nanoemulsiones de aceite de salvia fueron más translúcidas, flexibles y resistentes a la transferencia de vapor de agua. Sin embargo, la actividad antimicrobiana de las películas frente a *Escherichia coli* estuvo gobernada por el tipo de aceite esencial empleado. En particular, las películas comestibles con aceite de tomillo exhibieron la actividad antimicrobiana más fuerte.

En segundo lugar, se elaboraron emulsiones de una capa (gotas recubiertas con lactoferrina) y multicapa (gotas recubiertas con lactoferrina/alginato y lactoferrina/alginato/poli-L-lisina), conteniendo resveratrol como sustancia nutracéutica hidrofóbica. Se estudió el efecto de la concentración de biopolímero en la formación y estabilidad de estos sistemas. A concentraciones muy bajas o muy altas de biopolímero, las emulsiones multicapa fueron bastante inestables. Se lograron formar emulsiones secundarias estables (con gotas cubiertas por lactoferrina/alginato) usando concentraciones de alginato de 0.22% a 0.28 % p/p, mientras las emulsiones

terciarias (con gotas cubiertas por lactoferrina/alginato/poli-L-lisina) se obtuvieron a 0.036% de poli-L-lisina. Las emulsiones multicapa fueron más estables que las emulsiones de una capa durante el almacenamiento. La capacidad antioxidante de todas las emulsiones conteniendo resveratrol permaneció estable durante el almacenamiento, comparado con el resveratrol sin encapsular. Por otra parte, la composición de la capa interfacial afectó la estabilidad de las partículas durante una digestión *in vitro*. Las emulsiones terciarias fueron más estable que las primarias y secondarias bajo condiciones gastrointestinales simuladas. Después de la digestión, la bioaccesibilidad más alta del resveratrol se observó en las emulsiones terciarias.

Finalmente, se formaron nanolaminados de alginato/quitosano mediante la técnica de capa-a-capa para incluir además ácido fólico como sustancia nutracéutica hidrofílica. Los cambios en la carga eléctrica de las soluciones de alginato y quitosano permitieron modular las propiedades macroscópicas de los nanolaminados. El ácido fólico fue encapsulado efectivamente dentro de los nanolaminados por el método de post-difusión. El contenido de vitamina en los nanolaminados aumentó al usar soluciones de carga más concentradas, o aumentando el tiempo de inmersión en la solución de carga. La encapsulación del ácido fólico dentro de los nanolaminados aportó una mejor protección frente a la degradación por luz UV. Adicionalmente, los perfiles de liberación del ácido fólico desde los nanolaminados pudieron ser controlados cambiando el pH del medio. En condiciones alcalinas (pH 7), la vitamina fue rápidamente liberada, mientras que en condiciones ácidas (pH 3) la liberación fue muy baja.

Los resultados obtenidos en el presente trabajo aportan información útil para el diseño de emulsiones nanoestructuradas y nanolaminados, y demuestran que la encapsulación de aditivos naturales en estos sistemas puede mejorar su estabilidad y funcionalidad. Por lo tanto, estos sistemas de liberación pueden ser considerados como una vía para alcanzar el uso más efectivo y racional de compuestos activos alimentarios, abriendo nuevas perspectivas a la elaboración de productos alimentarios con beneficios excepcionales para los consumidores.

ABSTRACT

Nowadays, consumers are demanding safer, healthier and high-quality food products. To reach this goal, incorporating active ingredients to foods represent a promising strategy. Nevertheless, these compounds may be chemically unstable, poor-water soluble, scarce bioavailable or change the organoleptic properties of the product. A great interest in nanostructured delivery systems is emerging as a tool to overcome these issues. The importance of food nanostructured systems lies on the possibility to control their properties at molecular level, achieving a specific functionality. The objective of this doctoral thesis was to evaluate the most relevant factors affecting the formation and properties of nanoemulsions, multilayer emulsions and nanolaminates, as well as their capability to encapsulate, protect and deliver active compounds.

Firstly, nanoemulsions containing thyme, lemongrass and sage essential oils in the disperse phase, and sodium alginate in the continuous phase, were obtained by microfluization to be applied as edible films. The droplets characteristics of nanoemulsions, mainly size and ζ-potential, determined the physical properties of the resulting films. Those formed from sage oil nanoemulsions were the most translucent, flexible and resistance to water vapor transference. However, antimicrobial activity of films against *Escherichia coli* was governed by the type of essential oil used. In particular, thyme EO edible films exhibited the strongest antimicrobial effect.

Secondly, single-layer emulsions (lactoferrin-coated droplets) and multilayer emulsions (lactoferrin/alginate- and lactoferrinn/alginate/poly-L-lysine-coated droplets) were fabricated containing resveratrol as hydrophobic nutraceutical compound. The effect of biopolymer concentration on the formation and stability of these systems was investigated. At too low or too high concentrations of biopolymer, multilayer emulsions were highly unstable. Stable secondary emulsions (with lactoferrin/alginate-coated droplets) could be formed using alginate concentrations from 0.22% to 0.28% w/w, whereas stable tertiary emulsions (with lactoferrin/alginate/poly-L-lysine-coated droplets) were obtained at 0.036% w/w of poly-L-lysine. Multilayer emulsions were more stable than single-layer emulsions during storage. The antioxidant activity of all resveratrol-loaded emulsions remained stable during storage, compared to non-encapsulated resveratrol. On the other hand, the interfacial

layer composition affected the droplets stability during an *in vitro* digestion. Tertiary emulsions were more stable than primary and secondary emulsions under simulated gastrointestinal conditions. After digestion, the highest resveratrol bioaccessibility values was also found in tertiary emulsions.

Finally, alginate/chitosan nanolaminates were formed by the layer-by-layer technique to further include folic acid as hydrophilic nutraceutical. Changes in the initial electrical charge of alginate and chitosan solutions allowed modulating the macroscopic properties of nanolaminates. Folic acid was effectively encapsulated within nanolaminates by the post-diffussion method. Vitamin content in nanolaminates increased using more concentrated loading solutions, or increasing the inmersion time in the loading solution. The encapsulation of folic acid into nanolaminates provided better protection against UV-light degradation. Additionally, the release profiles of folic acid from nanolaminates could be controlled by changing the pH of the media. In alkaline conditions (pH 7), the vitamin was rapidly released from nanolaminates, while in acidic condition (pH 3) the release was very low.

The results obtained in this work provide useful information for the design of nanostructured emulsions and nanolaminates, and demonstrate that the encapsulation of natural additives into these systems can improve their stability and functionality. Therefore, these delivery systems can be considered as a way to achieve a more effective and rational use of active food ingredients, opening new perspective to the design food products with outstanding benefits for consumers.

TABLE OF CONTENTS

INTRODUCTION

LITERATURE REVIEW: ***NANOSTRUCTURED EMULSIONS AND NANOLAMINATES AS DELIVERY SYSTEMS OF ACTIVE INGREDIENTS: IMPROVING FOOD SAFETY AND FUNCTIONALITY***

Acevedo-Fani, A., Soliva-Fortuny, R., & Martín-Belloso, O.

Trends in Food Science & Technology (accepted: http://dx.doi.org/10.1016/j.tifs.2016.10.027)

Background

Nowadays, consumers are increasingly demanding high-quality, safe and healthy food products. Nanostructured emulsions and nanolaminates may have the potential to protect and transport lipophilic and hydrophilic active compounds commonly incorporated to food products, such as natural antimicrobials and nutraceuticals, while protecting or even enhancing their functional properties.

Scope and approach

This review deals with the most important aspects concerning to the use of nanostructured emulsions and nanolaminates as delivery systems of active ingredients, including the advantages and challenges of incorporating plant-derived antimicrobials and nutraceuticals in foods, relevant factors affecting the formation of these nanostructures, fabrication methods, their advantages as delivery systems, and the current trends in food applications. In addition, concerns regarding the potential toxicity of nanomaterials are also discussed.

Key findings and conclusions

The successful production of nanostructured emulsions and nanolaminates depends on several physicochemical factors that should be controlled in order to reach stable systems. Research evidences that nanostructured emulsions and nanolaminates are able to improve the delivery and biological activity of encapsulated active compounds. Antimicrobial and bioactive nanostructured emulsions and nanolaminates exhibit some promising advantages in food preservation and may represent a new strategy to produce functional foods. However, the knowledge in this area is still limited. The potential toxicological effects of nanostructured delivery systems are a current concern. Therefore, future investigations should be directed toward more comprehensive studies to shed light on the formation, physicochemical stability, functional performance, interactions with food matrices and toxicity of nanostructured delivery systems before their commercialization.

1. Introduction

The increasing consumer's demand of fresh-like food products and the rejection of synthetic additives are driving the scientific community to pursue natural alternatives that can enhance food preservation while having a minimum effect on the organoleptic and nutritional attributes of the product. Moreover, consumption patterns are changing toward a healthy diet owing to an evident relationship between food and health. As a result, there is a global trend toward the intake of food products with health-promoting properties beyond their nutritional value. There are a number of antimicrobials and nutraceuticals from natural sources with great performance that allow reducing or even replacing the use of their synthetic counterparts in foods (Irkin & Esmer, 2015; Oliveira, Ramos, Ramos, Piccoli, & Cristianini, 2015). However, an effective incorporation of active compounds to foods may be restricted by their physicochemical properties, stability under certain conditions or low bioavailability. As a result, there is a need of encapsulating them into delivery systems, understood as those in which an active compound is entrapped into a carrier (Fathi, Mozafari, & Mohebbi, 2012) , that allow overcoming these issues.

Nanotechnology is offering innumerable approaches in the food field (Cushen, Kerry, Morris, Cruz-Romero, & Cummins, 2012; Durán & Marcato, 2013). Nanostructured delivery systems constitute one of the most explored approaches. Their nanostructured architecture enables to improve protection of encapsulated compounds, increase solubility and dispensability of lipophilic ingredients in water-based environments, modulate the compound release, or even increase bioavailability of nutraceuticals, exhibiting better performance than micro-size systems (Augustin & Hemar, 2009; Ezhilarasi, Karthik, Chhanwal, & Anandharamakrishnan, 2013). In particular, emulsion-based delivery systems of either one single layer, such as nanoemulsions, or multiple layers have been proposed as those capable of effectively encapsulating lipophilic active compounds (Augustin & Hemar, 2009). On the other hand, nanolaminates are systems that can be applied directly onto food surfaces as an edible coating or to functionalize the surface of conventional packaging. The most important advantage is their ability of serving as reservoirs of active compounds, either hydrophilic or lipophilic, protecting them and modulating its release in response to certain triggers (Kuan, Yee-Fung, Yuen, & Liong, 2012;

Rojas-Graü, Soliva-Fortuny, & Martín-Belloso, 2009). The use of nanostructured emulsions and nanolaminates for delivery of active ingredients to foods represents a promising alternative to improve the quality, safety and functionality of food products. In this review we discuss the properties and limitations of incorporating plant-based antimicrobials and nutraceuticals in foods, and overview the recent developments concerning the formation, physicochemical characteristics, fabrication techniques, advantages as delivery systems, and food applications of a selected number of nanostructured emulsions and nanolaminates (Fig 1). Finally, the toxicological aspects associated to the incorporation of nanomaterials in foods are presented.

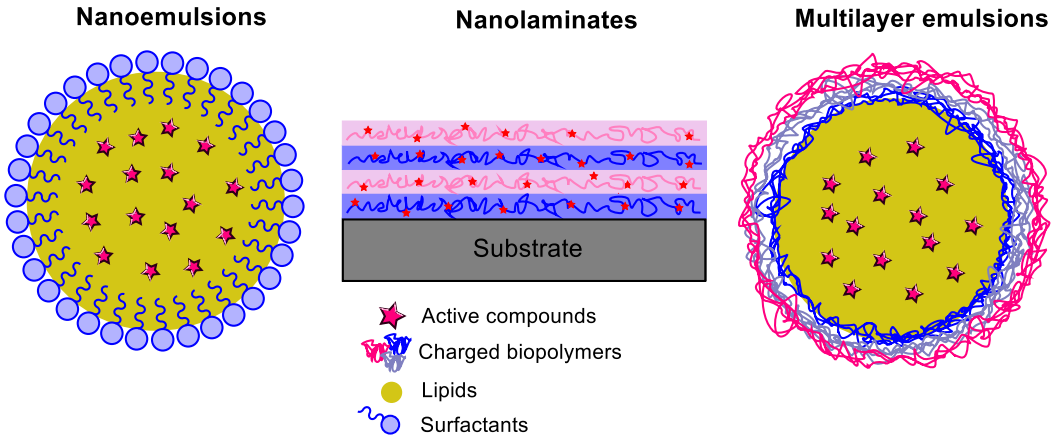

Fig. 1. Food nanostructured systems for encapsulating active ingredients with potential applications in beverages or edible coatings.

2. Active ingredients: advantages and limitations of their incorporation in foods

Plant-based antimicrobials

Antimicrobial compounds that come from plant sources exhibit outstanding efficacy against most pathogenic microorganisms responsible of foodborne illnesses and food spoilage (Tiwari et al., 2009). There is a strong consumer's perception that natural preservatives have less side effects to health that their non-natural counterparts, although in some cases the concentration required to achieve an antimicrobial effect is greater than that needed with synthetic preservatives (Carocho, Barreiro, Morales, & Ferreira, 2014). Antimicrobials derived from plants are substances originated from their secondary

metabolism, which plays a protective role against predators or stressing conditions (Solórzano-Santos & Miranda-Novales, 2012). Table 1 summarizes some types of plant-based antimicrobials commonly used in foods. Essential oils (EOs), the most significant group of plant-based antimicrobials, are complex mixtures of volatile compounds present in many herbs and spices (Burt, 2004). The main groups of compounds responsible for their antimicrobial and antioxidant properties include phenolic acids, quinones, saponins, flavonoids, tannins, coumarins, terpenoids and alkaloids (Bassolé & Juliani, 2012; Lai & Roy, 2004).

Table 1. Plant-derived antimicrobials and nutraceuticals that can be encapsulated within nanostructured emulsions and nanolaminates.

Compound	Types	Bioactivities
Plant-based antimicrobials		
EOs	Thyme, oregano, sage, lemongrass, cinnamon, rosemary, marjoram, clove	Antimicrobial, antioxidant
Active compounds of EOs	Carvacrol, cinnamaldehyde, thymol,eugenol, citral	Antimicrobial, antioxidant
Nutraceuticals		
Micronutrients	Lipophilic and hydrophilic vitamins (vit. A, vit. D, folic acid). Minerals (zinc, magnesium)	Co-enzymes for metabolic process, antioxidants, modulation of gene transcription
Phytochemicals	*Carotenoids* (carotene, lycopene), *terpenoids and isoterpenoids* (resveratrol), *phenolics* (isoflavones, anthocyanins)	Antoxidants, anti-inflammatory, anti-hyperlipidemic, chemopreventive activity
Fatty acids	omega-3 fatty acids, omega-6 fatty acids	Brain development, cardio-protection, anti-inflammatory action
Bioactive peptides and proteins	Val-Tyr-Pro, lactoglobulin and lactoferrin	Cardio-protection, anti-inflammatory action

Adapted from (Gleeson et al., 2016) and (Bassolé & Juliani, 2012)

Despite the increasing interest in applying EOs for food preservation, there are several factors affecting their antimicrobial activity, such as the poor-water solubility, partitioning behavior, mass transfer, volatility or reactivity can influence its efficacy in food systems (Donsì & Ferrari, 2016; Prakash, Kedia, Mishra, & Dubey, 2015). In addition, the use of EOs significantly changes the organoleptic profile of foods or may be toxic at high concentrations (Dima & Dima, 2015). Antimicrobial efficacy of EOs may be also influenced by the pH, fat content or water activity present in the food matrix. Plant-derived antimicrobials may bind to lipids, proteins or carbohydrates in foodstuffs, requiring higher concentrations than those used in *in vitro* studies to achieve the same effect (Weiss, Loeffler, & Terjung, 2015).

Nutraceuticals

There are several nutraceuticals that can be incorporated into food formulations with the purpose of providing well-being while reducing the incidence of diseases in humans. Table 1 presents some of the nutraceutical compounds that could be potentially included in foods. The intake of recommended doses of these compounds has been associated with prevention of coronary heart disease, diabetes, obesity, hypertension, and cancer (Cencic & Chingwaru, 2010; Espín, García-Conesa, & Tomás-Barberán, 2007). Being isolated from natural sources, nutraceuticals are expected to exhibit relatively less toxicity and less secondary side effects than drugs used to treat similar symptoms (Ting, Jiang, Ho, & Huang, 2014).

However, effective enrichment and fortification of food products using nutraceuticals suppose a major challenge. The chemical stability of most bioactive compounds is highly influenced by pH, temperature, oxygen, light or specific chemicals that promote the loss of the biological properties. Moreover, the oral bioavailability of nutraceuticals depends on their solubility in the gastrointestinal tract, stability during digestion and intestinal permeability (Gleeson, Ryan, & Brayden, 2016). Therefore, nutraceuticals may have poor oral bioavailability as a result of several physicochemical and physiological processes occurring after intake in the gastrointestinal tract.

3. Nanostructured delivery systems

Nanoemulsions

Nanoemulsions are oil-in-water systems containing oil droplets with mean diameters between 20 nm and 200 nm (Solans, Izquierdo, Nolla, Azemar, & Garcia-Celma, 2005). In an emulsion, two immiscible liquids (e.g. oil and water) are combined so that one liquid (disperse phase) is incorporated as droplets within a second liquid (continuous phase). These two phases are often combined by a process known as homogenization, in which the use of energy is required for increasing the surface area of the disperse phase and create droplets. As the total free energy of formation is always positive and the interfacial tension between both phases is large, emulsions are thermodynamically unstable (Tadros, Izquierdo, Esquena, & Solans, 2004). Nanoemulsions are also thermodynamically unstable but the rate of destabilization is lower than in conventional emulsions because the Brownian motion effect is sufficient to overcome the gravitational forces (Mason, Wilking, Meleson, Chang, & Graves, 2006; Tadros et al., 2004). For this reason, nanoemulsions are more stable to sedimentation, creaming, flocculation and coalescence than conventional emulsions. There are some important differences in terms of physicochemical properties, such as the fact that nanoemulsions are less opaque than conventional emulsions, since droplet diameters are smaller than the wavelength of light, and hence, droplets scatter light weakly (McClements, 2011). This feature makes nanoemulsions suitable systems to be incorporated into food products such as beverage, sauces, dressing or soups, having a little impact on their sensorial properties.

Factors affecting the formation and fabrication methods

The formulation of oil-in-water nanoemulsions is a key factor that determines their overall properties including droplet size, interfacial properties, physical stability or their functionality (Salvia-Trujillo, Rojas-Graü, Soliva-Fortuny, & Martín-Belloso, 2014). The physicochemical characteristics of the oil phase have an important impact on the formation and stability of nanoemulsions. For instance, when viscosity of the oil phase is high, droplets disruption is more difficult by mechanical means (Jafari, Assadpoor, He, & Bhandari, 2008). The viscosity ratio between oil phase and aqueous phase also affects the final droplet size achieved. The closer the viscosity ratio between the oil and

aqueous phase is to the unit, the more efficient the homogenization and the smaller the droplet size in nanoemulsions (Qian & McClements, 2011). The oil solubility also plays an important role in nanoemulsions stability. Oils with considerable water-solubility give rise to Ostwald ripening destabilization phenomenon, which consists in the formation of bigger droplets fueled by small ones driven by their fast diffusion along the continuous phase of nanoemulsions (Wooster, Golding, & Sanguansri, 2008). Many essential oils have significant water-solubility and Ostwald ripening has been described as the most frequent reason of destabilization of nanoemulsions containing them (Guerra-Rosas, Morales-Castro, Ochoa-Martínez, Salvia-Trujillo, & Martín-Belloso, 2016). The surfactant type and concentration have been found to exhibit a great impact in the formation of nanoemulsions. Each surfactant acts differently at the oil/water interface of emulsions depending on their molecular structure, which determines their hydrophilic-lipophilic balance (HLB) and their ability to adsorb to the oil/water interface and reduce the interfacial tension. The droplet size of nanoemulsions normally decreases as the surfactant concentration increases (Silva, Cerqueira, & Vicente, 2015). Small molecule surfactants (Tweens, sucrose esters, spans, SDS) are able to generate nano-sized emulsions (Silva, Cerqueira, & Vicente, 2012). However, there is a marked trend in using natural-derived surface-active molecules in nanoemulsions to develop “label-friendly” food products. In this case, proteins, polysaccharides or phospholipids, have been reported as feasible alternatives (Bai, Huan, Gu, & McClements, 2016; Gupta & Ghosh, 2015). Another important component in nanoemulsions formulation is the presence of texturizing agents in the aqueous phase. The incorporation of biopolymers, such as polysaccharides or proteins, at sufficient concentrations modifies the viscosity and improve emulsion stability, by delaying collision between droplets (McClements & Rao, 2011), as well as to provide specific textural properties, such as the film-forming ability.

There are two main approaches commonly used to produce fine emulsions. The high-energy methods (Mason et al., 2006) and low-energy methods (Conxita Solans & Solé, 2012). High energy methods are based in the input of large amounts of energy to reach emulsification. To prepare nanoemulsions, preliminary coarse emulsions are normally obtained by high shear mixing, which are further subjected to a second homogenization. High pressure homogenization or sonication are the most commonly known

techniques to produce nanoemulsions, which involve the use of mechanical forces, able to create intensive disruptive forces such as, turbulence, shear or cavitation, that break down the droplets. The smallest droplet size that can be obtained by high energy methods depends on the type of homogenizer, operating conditions, emulsion composition, and the physicochemical characteristics of the emulsion components (Mason et al., 2006). The low-energy methods consists on the spontaneous emulsification by controlling the physicochemical properties of the system. Self-emulsification and phase inversion have been described as reliable techniques to fabricate nanoemulsions. Both use the internal chemical energy generated in the system, either by the dilution process with the continuous phase, or by the phase transitions taking place during emulsification, to produce nano-sized droplets (Conxita Solans & Solé, 2012).

Advantages as delivery systems

These systems are able to encapsulate lipophilic active compounds within the oil phase of nanoemulsions. A reduction in the droplet size down to the nanoscale increases the surface area per volume unit of the disperse phase, having important impact on the physicochemical characteristics and functionality of nanoemulsions (Gupta, Eral, Hatton, & Doyle, 2016). The fact that nanoemulsions are translucent systems represents a major advantage, since they may have little impact on the visual properties of the food product, while contributing to enhance other food characteristics. In fact, this feature has been already observed in nanoemulsions containing some types of EOs which, beyond their antimicrobial effect, are often more translucent than conventional emulsions (Salvia-Trujillo, Rojas-Graü, Soliva-Fortuny, Martín-Belloso, & Rojas-Graü, 2012).

Nanoemulsions also improve the biological activity of lipophilic compounds, such as EOs, due to their capacity of increasing solubility and dispensability in water-based foods, allowing to reach places where microorganisms proliferate (Donsì & Ferrari, 2016). Several studies have demonstrated that nanoemulsions containing EOs have greater antimicrobial activity than the bulk oil (Table 2), since nano-sized droplets can interact more efficiently with the microbial cell membranes causing the microorganism death (Donsì & Ferrari, 2016). The nanometric particle size also allows minimizing the impact

of EOs on food organoleptic properties and the risk of toxicity, by lowering the concentration needed for microbial inactivation. Recently, it has been reported that the minimal concentration of EO required to inhibit several pathogenic bacteria decreases using nanoemulsions (Moghimi, Aliahmadi, McClements, & Rafati, 2016). Bioactive nanoemulsions have greater bioavailability than conventional emulsions. Table 3 presents recent research works dealing with nanoemulsions as delivery systems of nutraceuticals. Lipophilic nutraceuticals encapsulated within nano-sized droplets are more soluble in the gastrointestinal fluids, so that higher concentrations of the bioactive compound can reach to the target site (Fathi et al., 2012). The lipid digestion occurs more rapid for nanoemulsions owing to the greater surface area exposed to the gastrointestinal fluids, which results in the release of encapsulated bioactive compounds in a greater extent.

Food applications

Nanoemulsions containing natural antimicrobials, such as EOs, have been used in fluid foods to increase their safety. For instance, Ghosh et al. (2014) incorporated nanoemulsions of eugenol in orange juice (0.3 % eugenol in the juice) and evaluated their inhibitory effect on native bacteria at 25ºC and 4ºC for 72 h. The microbial growth in orange juice significantly decreased after 6 h at both storage temperatures, but the inhibitory effect was greater at 4ºC after 72 h. In another work, Jo et al. (2015) incorporated nano-sized (<200 nm) cinnamaldehyde emulsions to watermelon juice at different concentrations of cinnamaldehyde-Tween, using a ratio of 1:3 (0.8 %, 2.4 % and 4 % w/w). The pathogenic bacteria growth lessened using the lowest antimicrobial concentration, compared with a control treatment.

The addition of polysaccharides with film-forming properties in the aqueous phase of nanoemulsions allow their application as edible films. Otoni et al. (2014) obtained antifungal films prepared from nanoemulsions of methylcellulose and clove or oregano oils to extend the shelf life of packaged bread slides. They observed a clear reduction of the fungal growth on bread slides stored for 15 days. In another study, edible films from nanoemulsions of cinnamaldehyde, pectin and papaya puree and were effective in inactivating pathogenic bacteria (Otoni, Moura, et al., 2014). Our group investigated the inhibitory effect against *E.coli* of alginate-based edible films formulated with nanoemulsions of three different essential oils. The antimicrobial effect was

found to depend on the EO type, whereas the physicochemical properties of nanoemulsions significantly affected the physical and mechanical film properties. (Acevedo-Fani, Salvia-Trujillo, Rojas-Graü, & Martín-Belloso, 2015).

Nanoemulsions have been as well applied as edible coatings. Salvia-Trujillo et al., (2015b) applied conventional emulsions and nanoemulsions of lemongrass oil and sodium alginate as edible coatings on fresh-cut apples. Nanoemulsion-based coatings were more effective inactivating spoilage and pathogenic microorganisms than conventional emulsion-based coatings. The shelf life of other fruits and vegetables including plums, berries, arugula, lettuce and green beans has been as well extended using nanoemulsion-based edible coatings of plant-based antimicrobials (Bhargava, Conti, da Rocha, & Zhang, 2015; Kim et al., 2013; Kim, Oh, Lee, Song, & Min, 2014; Sessa, Ferrari, & Donsì, 2015; Severino et al., 2015).

Multilayer emulsions

Multilayer emulsions can be defined as oil-in-water systems containing droplets with at least two interfacial membranes composed by surfactants and biopolymers, which are created by the layer-by-layer assembly. Normally, an initial stable emulsion of nano-sized droplets is used to produce multilayer emulsions, and then several interfacial membranes are created by the alternative deposition of oppositely charged biopolymers; therefore, the multilayering process is driven mostly by electrostatic interactions, although other non-electrostatic forces may also play a role (Zeeb, Thongkaew, & Weiss, 2014). The presence of a multilayered membrane on droplets increases the physical stability of emulsions under certain environmental conditions, such as pH, ionic strength, heating, chilling or freeze-drying cycles, compared with single-layer emulsions (Aoki, Decker, & McClements, 2005; Fioramonti, Arzeni, Pilosof, Rubiolo, & Santiago, 2015). There are two principal mechanisms that promote the stability of multilayer emulsions: i) the steric stabilization caused when biopolymers adsorb at the oil/water interface, which create a shield that protect particles from aggregation, and ii) the electrostatic stabilization driven by the strong Coulombic forces that provoke repulsion between droplets (Kuroiwa, Kobayashi, Chuah, Nakajima, & Ichikawa, 2015). Recently, multilayer emulsions have been proposed as

potential delivery systems of active ingredients, owing to their outstanding physicochemical characteristics.

Factors affecting the formation and fabrication methods

The composition of multilayer emulsions and the preparation conditions significantly influences the formation of the interfacial membranes and the system stability. The biopolymer concentration in the aqueous phase has a significant impact in the multilayer emulsion formation. At very low concentrations, a biopolymer chain tends to adsorb to the interface of several droplets because there is insufficient material to coat all the interfacial area, causing then droplet aggregation by bridging flocculation. When the biopolymer concentration in the aqueous phase is high enough to saturate the entire droplets surface, then multilayer emulsions become physically stable. However, if the biopolymer concentration is too high there is an excess of non-adsorbed material remaining in the aqueous phase, which may cause droplets aggregation by depletion flocculation (Mun, Decker, & McClements, 2005). Another factor to consider is the droplets concentration and biopolymer-particle ratio. Mathematical analyses demonstrated that, as the particle concentration decreases the rate of flocculation also decreases because the biopolymer chains are adsorbed to the droplet surface more rapidly than the droplet collision (McClements, 2005). The preparation conditions such as pH, ionic strength or solvent quality have an important impact on the characteristics of the multilayered membranes, such as charge, thickness or porosity (Guzey & McClements, 2006). One of the most important factors affecting the formation and membranes characteristics is the pH of the system. Normally, most food-grade biopolymers behave as weak polyelectrolytes, which means that their charge density is strongly affected by the pH of the system. Either if they are adsorbed to droplets interface acting as surfactants or forming electrostatic complexes with another pre-adsorbed layer, the magnitude and sign of the electrical charge of such (macro) molecules would be changed by the protonation or deprotonation of the functional groups that provides that charge (Fioramonti, Martinez, Pilosof, Rubiolo, & Santiago, 2015). Therefore, stronger or weaker interactions between oppositely charged species on the droplet surface would determine: i) the ability of forming electrostatic complexes or not, and ii): the characteristics of such multilayered membranes, such as the thickness, degree of porosity or electrical charge.

To produce multilayer emulsions, an oil-in-water "primary" emulsion is prepared, normally, by high-energy methods using an ionic surfactants or surface-active biopolymers with an electrical charge (Zeeb et al., 2014). In a further step, an oppositely charged biopolymer is incorporated into primary emulsions allowing their adsorption to the droplet interface, thus forming a new "secondary" emulsion. The process can be repeated several times to obtain emulsions with oil droplets coated by a desirable number of layers (Guzey & McClements, 2006). A schematic representation of the process of formation is presented in Fig.2.

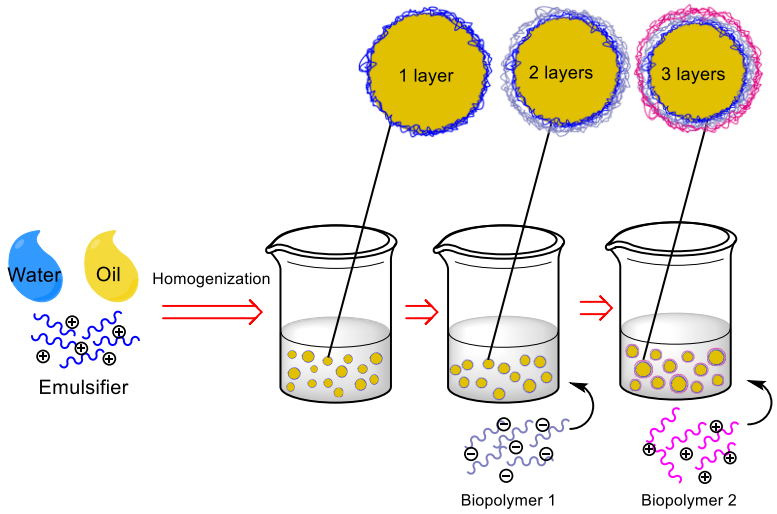

Fig. 2. Schematic representation of the fabrication process of multilayer emulsions.

The most widely used method to fabricate multilayer emulsions is by adding exactly the amount of polyelectrolyte needed to saturate the droplets surface (Fioramonti, Martinez, et al., 2015; Pinheiro, Coimbra, & Vicente, 2016; Yang, Tian, Ho, & Huang, 2012). This method allows saving time in the process because the adsorption of polyelectrolytes occurs quickly, and there is no loss of polyelectrolytes because only the required amount is used. However, the correct balance of the components in the system is crucial to avoid bridging flocculation or depletion flocculation. Finding the polyelectrolyte concentration where a saturated layer is formed, either by empirical methods (monitoring the ζ-potential until stabilization) or by theoretical calculations, is a key factor to fabricate stable multilayer emulsions.

Table 2. Recent studies regarding the use of nanoemulsions and nanolaminates for plant-derived antimicrobials delivery.

	Active compound	Technique	Materials	Particle size / film thickness	Outcomes	References
Nanoemulsions	Sage oil	Sonication	Emulsifiers: Tween 80 and Span 80	≈200 nm	Greater antimicrobial activity than bulk oil against pathogenic bacteria	(Moghimi et al., 2016)
	Anise oil	HPH	Disperse phase: MCT oil Emulsifier: Soy lecithin	<276 nm	Better long-term stability and antimicrobial activity than bulk oil	(Topuz et al., 2016)
	Thyme oil	HPH	Disperse phase: corn oil Emulsifiers: lauric arginate and Tween 80	<250 nm	Enhanced antimicrobial activity against spoilage yeast combining lauric arginate and thyme oil	(Chang, McLandsborough, & McClements, 2015)
	Lemongrass, clove, tea tree, thyme, geranium, marjoram, palmarosa, rosewood, sage and mint	MF	Emulsifier: Tween 80 Texturizing agent: sodium alginate	<20 nm	Nanoemulsions exhibited faster inactivation of E.coli than cconventional emulsions	(Salvia-Trujillo, Rojas-Graü, Soliva-Fortuny, & Martín-Belloso, 2015a)
	Carvacrol	Spontaneous emulsification	Disperse phase: MCT oil	≈55 nm	The antimicrobial activity against spoilage yeast increased with oil concentration.	(Chang, McLandsborough, & McClements, 2013)

	Peppermint	HPH	Emulsifiers: Tween 20, 40, 60, 80 and 85 Disperse phase: MCT oil Emulsifier: modified starch	<200 nm	Nanoemulsion stability was better at low oil concentrations Greater antimicrobial activity against pathogenic bacteria than bulk oil. High long-term stability	(Liang et al., 2012)
Nanolaminates	Carvacrol	Layer-by-layer	Bulding blocks: alginate, zein-carvacrol nanocapsules, chitosan and chitosan-carvacrol emulsions Substrate: PET sheet	Not reported	Water and oxygen transmission rate decreased compared with net alginate or chitosan films. Nanolaminates exhibit antifungal activity against Alternaria ssp.	(Fabra et al., 2016)

HPH: high pressure homogenization; MF: microfluidization

Table 3. Recent studies regarding the use of nanostructured emulsions for lipophilic nutraceutical delivery.

	Active compound	Technique	Materials	Particle size	Outcomes	References
Nanoemulsions	Green tea catechins	HPH	Disperse phase: Sunflower oil Emulsifier: soy protein	240-270 nm	High physical and chemical stability in cold storage Cathechins nanoemulsions exhibited greater bioaccessibility and permeability through caco-2 cell monolayers than non-encapsulated cathechins	(Bhushani, Karthik, & Anandharamakrishnan, 2016)
	Vitamin E	MF	Disperse phase: Sunflower oil Emulsifier: saponins	≈ 300 nm	High physical stability during storage at different temperatures Nanoemulsions exhibited higher vitamin E bioavailability than conventional emulsions, assessed by *in vivo* studies	(Parthasarathi, Muthukumar, & Anandharamakrishnan, 2016)
	Vitamin D_3	HPH	Disperse phase: LCT* oils (corn and fish oils), MCT* oil, indigestible oils (mineral and orange oils)	≈ 190 nm	Vitamin D bioaccessibility increased in LCT nanoemulsions, compared to MCT nanoemulsions.	(Ozturk, Argin, Ozilgen, & McClements, 2015)

			Emulsifier: Quillaja saponin		Undigested oil nanoemulsions presented greater vitamin bioaccessibility than MCT nanoemulsions	
	Resveratrol	HPH	Disperse phase: peanut oil Emulsifiers: combinations of lecithins, sugar esters, Tween 20 and glycerol monooleate	130 – 240 nm	Transport though caco-2 cells monolayers was enhanced in resveratrol nanoemulsions with the smallest droplet size. The resveratrol metabolization by caco-2 cells and the *in vitro* release was lower in nanoemulsions	(Sessa et al., 2014)
	β-carotene	MF	Disperse phase: corn oil Emulsifier: Tween 20	23 – 0.2 um	The initial droplet size affected β-carotene bioaccessibility. It increased by decreasing droplet size of emulsions.	(Salvia-Trujillo, Qian, Martín-Belloso, & McClements, 2013)
Multilayer emulsions	Curcumin	HPH and LbL	Disperse phase: corn oil Emulsifier: lactoferrin Coatings composition: lactoferrin and lactoferrin/alginate	> 150 nm	Interfacial membranes allowed controlling lipid digestion and curcumin release in different stages of the small intestine	(Pinheiro et al., 2016)

β-carotene	HPH and LbL	Disperse phase: MCT* oil Emulsifier: lactoferrin and lactoferrin-polyphenol conjugates Coatings composition: lactoferrin, lactoferrin-polyphenols, lactoferrin/lactoferrin-polyphenols	≈ 300 – 1300 nm	The presence of polyphenol in the interfacial layers helped to improve the physical and chemical stability of β-carotene encapsulated. The type of polyphenol affected the stability profiles of emulsions.	(Liu et al., 2016)
Carotenoids	MF and LbL	Disperse phase: MCT oil Emulsifier: soy protein isolate (SPI) Coatings composition: SPI, SPI/alginate, SPI/chitosan	≈ 280 nm	Lipid digestion decreased when the outer layer on droplets was chitosan. Carotenoids bioaccessibility increased in SPI/alginate emulsions.	(Zhang et al., 2015)
Lutein	HPH and LbL	Disperse phase: MCT* oil Emulsifiers: WPI*, DTAB and fish gelatin (FG) Coatings: WPI/sugar beet pectin, DTAB/sugar beet pectin and FG/sugar beet pectin Crosslinked coatings with lacasse	< 200 nm	Multilayer emulsions significantly diminished lutein release in comparison with single-layer emulsions. The release profiles of crosslinked emulsions were similar to multilayer emulsions	(Beicht et al., 2013)

*MCT: medium chain triglyceride oils; LCT: long chain triglyceride oils; WPI: whey protein isolate; LbL: layer-by-layer deposition; HPH: high pressure homogenization; MF: microfluidization

Advantages as delivery systems

These systems allow encapsulating both lipophilic and hydrophilic active compounds, locating them either in the lipid phase or in the interfacial coating. The high physical stability of multilayer emulsions under different environmental stresses is a major advantage when they are intended to be incorporated to food matrices. It is desirable that a delivery system maintains the functional properties of the encapsulated active compounds in presence of other food components. It has been described that multilayer emulsions have the capacity of increase the chemical stability of encapsulated active compounds, since interfacial membranes protect lipophilic substances from degradation reactions (oxidation or light-induced) (Hou et al., 2010). The deposition of charged antioxidant molecules (e.g. polyphenols) at the oil/water interface of droplets can reduce oxidative degradation of β-carotene encapsulated in the lipid core (Liu, Wang, Sun, McClements, & Gao, 2016).

Furthermore, the thickness, porosity, composition or surface charge of the interfacial layers can be tuned in order to provide stimuli-responsive properties to emulsions, which is a great advantage for controlling the release of encapsulated active compounds. For instance, it is possible to slow down the lipophilic bioactive release by adding several interfacial membranes on droplets, and also to accelerate the release by changing the pH of the system. The pH might alter the conformation of the interfacial membranes, and in turn, can modulate the release rate of the active compound (Beicht, Zeeb, Gibis, Fischer, & Weiss, 2013). Lipid digestibility or bioaccessibility of nutraceuticals in the gastrointestinal tract (GIT) can be controlled using multilayer emulsions. The presence of protein-polysaccharide membranes on droplets may cause a delay or acceleration of the lipid digestion, which depend on the characteristics on the interfacial membranes and their physicochemical behavior in the different gastrointestinal fluids (Tokle, Lesmes, Decker, & McClements, 2012; Zeeb, Lopez-Pena, Weiss, & McClements, 2015). Within GIT, droplets stability may be influenced by the pH, ionic strength, enzymes, bile, among others components conforming the gastrointestinal fluids. Therefore, a tailored design of the interfacial membranes characteristics in multilayer emulsions can be a promising strategy to rationally develop efficient delivery systems for food ingredients. Most of the ongoing studies are exploring their behavior under gastrointestinal conditions, as they might be a promising alternative for

enhancing the delivery of nutraceuticals. However, to the best of our knowledge, multilayer emulsions have not been yet explored as delivery systems of plant-based antimicrobials.

Food applications

The practical application of multilayer emulsions in food products is still scarce. However, there is an approach that suggests the use of multilayer emulsions containing bioactive lipids as a strategy to enhance the fat quality of food products. Jo et al., (2015) prepared fish oil (high omega-3 fatty acids content) multilayer emulsions by the electrostatic deposition of Tween (primary), Tween-chitosan (secondary), and Tween-alginate-pectin (tertiary). Pork patties were enriched with fish oil encapsulated in primary, secondary and tertiary emulsions. The chemical stability of the fat contained in the product was assessed by the degree of lipid oxidation during storage, and it was found that the fish oil content in the pork patties had better chemical stability as the number of layers increased in multilayer emulsions.

Nanolaminates

Nanolaminates are thin films formed by two or more layers of food-grade materials alternatively deposited on a substrate through the layer-by-layer assembly technique. Typical layer thickness ranges from several Å to up to 100 nm, which depends on the adsorption conditions and material properties (Clark & Hammond, 1998). However, the final film thickness is governed by the number of layers deposited. The layer-by-layer assembly can be carried out *via* several chemical interactions, including electrostatic bonding, hydrogen bonding, hydrophobic interactions, charge-transfer interactions, covalent bonding, among others (Borges & Mano, 2014). So far, electrostatic interactions is the only mechanism explored to prepare nanolaminates in the food field (Flores-López, Cerqueira, de Rodríguez, & Vicente, 2016). The process starts with the adsorption of a charged specie (e.g. polysaccharides, proteins or nanoparticles) to a substrate that also has an electrical charge. The first adsorption step leads to a charge reversal on the surface that allows the adsorption of another oppositely charged specie. After each layer assembly, a washing step is required to remove the excess of unbound material, thus self-regulating the layer thickness. The sequential adsorption of oppositely charge building blocks is usually repeated to obtain nanolaminate

structures. Numerous research works published in other science fields concerning the layer-by-layer technique point out that the mechanisms behind recharging and the driving forces that give rise to the nanolaminates buildup are still not fully understood (Borges & Mano, 2014). The intervention of other types of non-coulombic interactions acting synergistically with electrostatic attractions has been proposed (Schoeler, Sharpe, Hatton, & Caruso, 2004). Lately, some studies suggest that nanolaminates prepared from polysaccharides may exhibit exceptional physicochemical characteristics, such as gas barrier properties, water vapor resistance or different wetting properties and surface charge, compared to conventional materials (Li, Biagioni, Finazzi, Tavazzi, & Piergiovanni, 2013; Pinheiro et al., 2012). Additionally, a high swelling capacity has been observed in polysaccharide-based nanolaminates (Crouzier, Boudou, & Picart, 2010), which may have important implications in the diffusion of the other molecules (e.g. small active molecules) inside the structure.

Factors affecting the formation and fabrication methods

There are several experimental parameters that affect the formation and physicochemical properties of nanolaminates, such as the pH, ionic strength, concentration and temperature of the solutions containing the building blocks (e.g. polysaccharides or proteins), the molecular weight or charge density of the building blocks, number of layers deposited, the terminal layer, adsorption and washing time, and film drying procedure (Klitzing & Klitzing, 2006). The pH and ionic strength of the adsorbing solutions are among the most important factors affecting the nanolaminates assembly. The pH has a profound effect on the conformation and charge density of polysaccharides in solution and hence, on their kinetics of adsorption on the substrate. This directly changes the nanolaminate growth and, aspects such as film thickness, surface charge, wettability or roughness will be affected. For instance, the conformation of ionic biopolymers may vary from well-extended to globular depending on the solution pH, therefore, the amount of mass adsorbed per layer will be different in each condition (Acevedo-Fani, Salvia-Trujillo, Soliva-Fortuny, & Martín-Belloso, 2015). The ionic strength also affects the formation of nanolaminates. The concentration of salt in the solution influences the conformation of biopolymers due to the screening of the charges along the chains, resulting in

coiled structures. Thereby, the nanolaminate thickness can be increased if the ionic concentration is increased (Klitzing & Klitzing, 2006).

There are three main ways to prepare nanolaminates by the LbL technique: i) dipping, ii) spraying and iii) spin coating (Benkirane-Jessel et al., 2011). The dipping method is most commonly used to form nanolaminates and can be carried out manually by simply submerging the charged substrate on an adsorbing solution, or mechanically, using a device that controls the number of immersion steps and the duration of adsorption and washing steps. In this case, adsorption steps can last between 1 min and 1 h (Bertrand, Jonas, Laschewsky, & Legras, 2000). The layer-by-layer deposition by spraying and spin-coaters has also been confirmed but it has not been used in the food field. Such methods present the advantages of using a small amount of material to coat a surface and the velocity of the adsorption process, which can occur more rapidly in comparison to the dipping approach (Aoki et al., 2014).

Advantages as delivery systems

One of the most promising advantages of nanolaminates is their ability of entrap a payload of active compounds within the film structure and then release it in response to external stimulus such as pH, ionic strength, light, temperature, etc (Keeney et al., 2015). So far, nanolaminates have mostly been explored as food-grade coatings on packaging materials and some commodities. Moreover, the incorporation of active substances within nanolaminates is also possible, either by changing the nature of the building blocks adsorbed in each layer or by the loading of small active molecules. Therefore, these nanolaminates can work as carriers of active ingredients with antimicrobial or health-promoting properties. Nanolaminates can be designed to control the release of encapsulated substances under specific triggers, enhancing their targeted delivery. As far as we are concerned, this topic has been scarcely investigated. Therefore, there is a lack of information that opens the possibility to a future research trend, so that the potential advantages of nanolaminates for active ingredients delivery can be explored in a greater extent, being a promising alternative to improve safety, quality and functionality of foodstuffs. The versatility of the layer-by-layer assembly could allow the design of countless types of food-grade nanolaminates with tuned physicochemical and functional properties, either by modulating the layer

composition or assembly parameters, which would have a positive impact in food preservation or fortification.

Food applications

The application of nanolaminates in foods is in the early stage. Nanolaminates have been formed on food surfaces or conventional packaging materials. A schematic representation of the procedure to create nanolaminate structures onto solid foods is shown in Fig. 3.

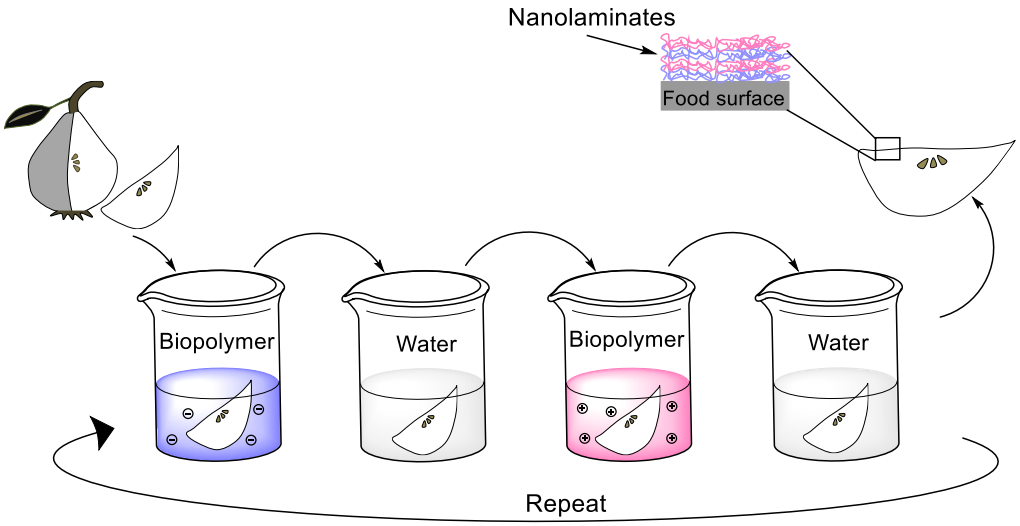

Fig. 3. Schematic representation of the layer-by-layer assembly on food surfaces.

The formation and characterization of nanolaminates on planar materials is a crucial preliminary step to their application as edible coatings. This is considered as an 'in vitro' study that allows confirming the actual formation and properties of nanolaminates. The typical microstructure of a nanolaminate formed onto a polyethylene terephthalate sheet is presented in Fig. 4.

For instance, Pinheiro et al., (2012) reported the structural and transport properties of κ-carragenan and chitosan nanolaminates created on a polyethylene terephthalate film (PET). The layer-by-layer deposition of both oppositely charged polysaccharides forming nanolaminates was confirmed, and their influence on wetting and gas barrier properties of the substrate were also assessed. Our group studied the influence of the electrical charge of alginate and chitosan solutions on the buildup and physicochemical properties of the resulting nanolaminates created on PET and quartz slides (Acevedo-Fani, Salvia-Trujillo, Soliva-Fortuny, et al., 2015). As nanolaminates may

serve as reservoirs of active molecules, some authors have demonstrated their ability to hold antimicrobial molecules and nanoparticles within the film structure.

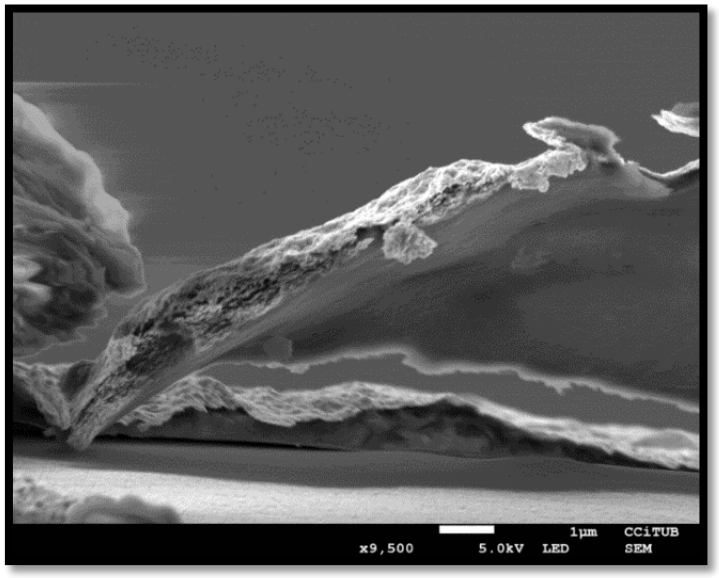

Fig. 4. SEM micrograph of alginate/chitosan nanolaminates formed on polyethylene terephthalate sheet.
(Acevedo-Fani, Salvia-Trujillo, Soliva-Fortuny, et al., 2015)

In fact, nanofibrous mats with antimicrobial activity were successfully obtained by applying a nanolaminate coating of alginate (negative) and a lysozyme-chitosan-rectorite complex (positive) on the surface. Coated mats exhibited higher antimicrobial activity when the nanolaminate was made of the lysozyme-chitosan-rectorite complex and their use on pork preservation extended the shelf life for about 3 days (Huang et al., 2012). In another case, it was possible to fabricate nanolaminate films of PET using nanocapsules or emulsions containing carvacrol as building blocks. This improved the antifungal properties of the packaging material (Fabra et al., 2016).

The use of nanolaminates as edible coatings has also been demonstrated. For instance, chitosan, alginate, κ-carragenan or lysozyme were used to produce nanolaminates that were able to preserve the quality and safety of fresh-cut and whole pears and mangoes (de S. Medeiros, Pinheiro, Carneiro-da-Cunha, & Vicente, 2012; Medeiros, Pinheiro, Teixeira, Vicente, & Carneiro-da-Cunha, 2012; Souza et al., 2015). The same approach has been used for extending the shelf life of cheese (de S. Medeiros et al., 2014).

4. Toxicological aspects

Nowadays, the number of nanotech patents and nano-products being released to the food market is increasing, but there is also a great concern about the potential toxicological effects related to their intake through foodstuffs. It is noteworthy that the potential advantages of nanostructured delivery systems arising from the manipulation of materials in the nanometric scale (e.g. greater reactivity, higher bioavailability, enhanced cellular transport) may also have an important impact on their toxicity in the human body. For example, some nutraceuticals are toxic at high concentrations and their intake is recommended at certain doses. Nutraceuticals encapsulated within nanostructured delivery systems may cause toxicity due to their greater bioavailability, thereby, increasing the bioactive concentration in the target site. Essential (EOs) oils may also have some toxic effects associated to their potential ability to interact with the human cellular membranes in the same way that EOs acts on microbial membranes. Therefore, if EOs are encapsulated in nanostructured systems their increased reactivity may represent a latent issue in terms of safety. Moreover, some nanoparticulates may not be digested in the GIT, being able to pass across the epithelium cells and increasing the exposure to biological tissues, which could lead to unpredictable interactions or bioaccumulation in some organs. However, if nanomaterials are transformed into bigger structures in the food matrix before ingestion or they are completely degraded and solubilized in the GIT, then the toxicity risk may be insignificant. Therefore, the evaluation of toxicological profiles and potential risks associated with the use of nanomaterials in foods is required. The toxicity of nanomaterials strongly depends on their physicochemical properties including chemical composition, size, shape, solubility, surface charge, surface reactivity, among others, as well as their behavior within the GIT and final fate in the human body after adsorption. In this regard, risk assessment must be done considering such characteristics and following an approach based in the case-by-case study.

5. Concluding remarks

There is an evident interest in the design and production of food-grade nanostructures able to encapsulate, protect and enhance functionality of some types of active ingredients. Plant-derived antimicrobials and nutraceuticals are

potential natural additives that can be incorporated within foodstuffs, representing a promising strategy to satisfy the current consumer's claims. The proper formation of nanostructured delivery systems have to be carefully controlled in order to reach stable systems. There are a number of factors that intervene differently in each type of delivery system. In the case of nanostructured emulsions, the surfactant type, surfactant concentration, viscosity of the aqueous media, the biopolymer concentration, pH, ionic strength are among the most important factors affecting the formation and stability of droplets. The assembly of nanolaminates is highly influenced by the conditions of biopolymer solutions (e.g. pH, ionic strength), but also by different experimental parameters (e.g. adsorption and washing times, number of layers, terminal layer, drying procedure). Several research works has indicated that nanostructured emulsions and nanolaminates are able to encapsulate both plant-derived antimicrobials and nutraceuticals, providing enhanced physicochemical stability and functional properties. Their ability to modulate the biological fate of bioactive ingredients within GIT, and to control their release under certain conditions seems to be a promising advantage for the design of functional foods. Applications in food models are still incipient. Up to date, some research works conducted suggest that both nanostructured emulsions and nanolaminates have the potential to improve food preservation and food fortification, but there are still unknown aspects that required further research. Another latent concern is the potential toxicity effect of food nanostructures in the human body. The novel properties arising from manipulation of materials and active ingredients at the nanoscale may have important consequences in the toxicity after consumption, which should be considered in a case-by-case basis. Therefore, future investigations have to be directed to a more comprehensive approach of all the factors implied in the use of nanostructured delivery systems in foodstuffs, starting from their physicochemical stability and functional performance, stability in food matrices during storage, behavior during digestion, potential toxicological effects, until the economic analysis of the costs implicit in the industrial scale-up.

6. Acknowledgments

This research work was supported by the Ministry of Science and Innovation (Spain) [ALG2009-11475, ALG2012-35635, ALG2015-65975-R]. Also, author Acevedo-Fani thanks to the University of Lleida for the pre-doctoral grant.

7. References

Acevedo-Fani, A., Salvia-Trujillo, L., Rojas-Graü, M. A., & Martín-Belloso, O. (2015). Edible films from essential-oil-loaded nanoemulsions: Physicochemical characterization and antimicrobial properties. *Food Hydrocolloids*, *47*, 168–177.

Acevedo-Fani, A., Salvia-Trujillo, L., Soliva-Fortuny, R., & Martín-Belloso, O. (2015). Modulating Biopolymer Electrical Charge to Optimize the Assembly of Edible Multilayer Nanofilms by the Layer-by-Layer Technique. *Biomacromolecules*, *16*(9), 2895–2903.

Aoki, P. H. B., Alessio, P., Volpati, D., Paulovich, F. V, Riul, A., Oliveira, O. N., & Constantino, C. J. L. (2014). On the distinct molecular architectures of dipping- and spray-LbL films containing lipid vesicles. *Materials Science and Engineering: C*, *41*, 363–371.

Aoki, T., Decker, E. A., & McClements, D. J. (2005). Influence of environmental stresses on stability of O/W emulsions containing droplets stabilized by multilayered membranes produced by a layer-by-layer electrostatic deposition technique. *Food Hydrocolloids*, *19*(2), 209–220.

Augustin, M. A., & Hemar, Y. (2009). Nano- and micro-structured assemblies for encapsulation of food ingredients. *Chem. Soc. Rev.*, *38*(4), 902–912.

Bai, L., Huan, S., Gu, J., & McClements, D. J. (2016). Fabrication of oil-in-water nanoemulsions by dual-channel microfluidization using natural emulsifiers: Saponins, phospholipids, proteins, and polysaccharides. *Food Hydrocolloids*, *61*, 703–711.

Bassolé, I. H. N., & Juliani, H. R. (2012). Essential Oils in Combination and Their Antimicrobial Properties. *Molecules*, *17*(12), 3989–4006.

Beicht, J., Zeeb, B., Gibis, M., Fischer, L., & Weiss, J. (2013). Influence of layer thickness and composition of cross-linked multilayered oil-in-water emulsions on the release behavior of lutein. *Food & Function*, *4*(10), 1457.

Benkirane-Jessel, N., Lavalle, P., Ball, V., Ogier, J., Senger, B., Picart, C., Schaaf, P., Voegel, J-C., & Decher, G. (2011). Polyelectrolyte Multilayer Films - A General Approach to (Bio)functional Coatings. In K. Matyjaszewski, Y. Gnanou, & L. Leibler (Eds.), *Macromolecular Engineering* (Vol. 2, pp. 1249–1305). Weinheim, Germany: Wiley-VCH Verlag GmbH & Co. KGaA.

Bertrand, P., Jonas, A., Laschewsky, A., & Legras, R. (2000). Ultrathin polymer coatings by complexation of polyelectrolytes at interfaces: suitable materials,

structure and properties. *Macromolecular Rapid Communications*, *21*(7), 319–348.

Bhargava, K., Conti, D. S., da Rocha, S. R. P., & Zhang, Y. (2015). Application of an oregano oil nanoemulsion to the control of foodborne bacteria on fresh lettuce. *Food Microbiology*, *47*, 69–73.

Bhushani, J. A., Karthik, P., & Anandharamakrishnan, C. (2016). Nanoemulsion based delivery system for improved bioaccessibility and Caco-2 cell monolayer permeability of green tea catechins. *Food Hydrocolloids*, *56*, 372–382.

Borges, J., & Mano, J. F. (2014). Molecular Interactions Driving the Layer-by-Layer Assembly of Multilayers. *Chemical Reviews*, *114*(18), 8883–8942.

Burt, S. (2004). Essential oils: their antibacterial properties and potential applications in foods—a review. *International Journal of Food Microbiology*, *94*(3), 223–253.

Carocho, M., Barreiro, M. F., Morales, P., & Ferreira, I. C. F. R. (2014). Adding Molecules to Food, Pros and Cons: A Review on Synthetic and Natural Food Additives. *Comprehensive Reviews in Food Science and Food Safety*, *13*(4), 377–399.

Cencic, A., & Chingwaru, W. (2010). The Role of Functional Foods, Nutraceuticals, and Food Supplements in Intestinal Health. *Nutrients*, *2*(6), 611–625.

Chang, Y., McLandsborough, L., & McClements, D. J. (2013). Physicochemical Properties and Antimicrobial Efficacy of Carvacrol Nanoemulsions Formed by Spontaneous Emulsification. *Journal of Agricultural and Food Chemistry*, *61*(37), 8906–8913.

Chang, Y., McLandsborough, L., & McClements, D. J. (2015). Fabrication, stability and efficacy of dual-component antimicrobial nanoemulsions: Essential oil (thyme oil) and cationic surfactant (lauric arginate). *Food Chemistry*, *172*, 298–304.

Clark, S. L., & Hammond, P. T. (1998). Engineering the Microfabrication of Layer-by-Layer Thin Films. *Advanced Materials*, *10*(18), 1515–1519.

Crouzier, T., Boudou, T., & Picart, C. (2010). Polysaccharide-based polyelectrolyte multilayers. *Current Opinion in Colloid & Interface Science*, *15*(6), 417–426.

Cushen, M., Kerry, J., Morris, M., Cruz-Romero, M., & Cummins, E. (2012). Nanotechnologies in the food industry – Recent developments, risks and regulation. *Trends in Food Science & Technology*, *24*(1), 30–46.

de S. Medeiros, B. G., Pinheiro, A. C., Carneiro-da-Cunha, M. G., & Vicente, A. A. (2012). Development and characterization of a nanomultilayer coating of pectin and chitosan – Evaluation of its gas barrier properties and application on "Tommy Atkins" mangoes. *Journal of Food Engineering*, *110*(3), 457–464.

de S. Medeiros, B. G., Souza, M. P., Pinheiro, A. C., Bourbon, A. I., Cerqueira, M. A., Vicente, A. A., & Carneiro-da-Cunha, M. G. (2014). Physical Characterisation of an Alginate/Lysozyme Nano-Laminate Coating and Its Evaluation on "Coalho" Cheese Shelf Life. *Food and Bioprocess Technology*, *7*(4), 1088–1098.

Dima, C., & Dima, S. (2015). Essential oils in foods: extraction, stabilization, and toxicity. *Current Opinion in Food Science*, *5*, 29–35.

Donsì, F., & Ferrari, G. (2016). Essential oil nanoemulsions as antimicrobial agents in food. *Journal of Biotechnology*, *233*, 106–120.

Durán, N., & Marcato, P. D. (2013). Nanobiotechnology perspectives. Role of nanotechnology in the food industry: a review. *International Journal of Food Science & Technology*, *48*(6), 1127–1134.

Espín, J. C., García-Conesa, M. T., & Tomás-Barberán, F. A. (2007). Nutraceuticals: Facts and fiction. *Phytochemistry*, *68*(22-24), 2986–3008.

Ezhilarasi, P. N., Karthik, P., Chhanwal, N., & Anandharamakrishnan, C. (2013). Nanoencapsulation Techniques for Food Bioactive Components: A Review. *Food and Bioprocess Technology*, *6*(3), 628–647.

Fabra, M. J., Flores-López, M. L., Cerqueira, M. A., de Rodriguez, D. J., Lagaron, J. M., & Vicente, A. A. (2016). Layer-by-Layer Technique to Developing Functional Nanolaminate Films with Antifungal Activity. *Food and Bioprocess Technology*, *9*(3), 471–480.

Fathi, M., Mozafari, M. R., & Mohebbi, M. (2012). Nanoencapsulation of food ingredients using lipid based delivery systems. *Trends in Food Science & Technology*, *23*(1), 13–27.

Fioramonti, S. A., Arzeni, C., Pilosof, A. M. R., Rubiolo, A. C., & Santiago, L. G. (2015). Influence of freezing temperature and maltodextrin concentration on

stability of linseed oil-in-water multilayer emulsions. *Journal of Food Engineering*, *156*, 31–38.

Fioramonti, S. A., Martinez, M. J., Pilosof, A. M. R., Rubiolo, A. C., & Santiago, L. G. (2015). Multilayer emulsions as a strategy for linseed oil microencapsulation: Effect of pH and alginate concentration. *Food Hydrocolloids*, *43*, 8–17.

Flores-López, M. L., Cerqueira, M. A., de Rodríguez, D. J., & Vicente, A. A. (2016). Perspectives on Utilization of Edible Coatings and Nano-laminate Coatings for Extension of Postharvest Storage of Fruits and Vegetables. *Food Engineering Reviews*, *8*(3), 292–305.

Ghosh, V., Mukherjee, A., & Chandrasekaran, N. (2014). Eugenol-loaded antimicrobial nanoemulsion preserves fruit juice against, microbial spoilage. *Colloids and Surfaces B: Biointerfaces*, *114*, 392–397.

Gleeson, J. P., Ryan, S. M., & Brayden, D. J. (2016). Oral delivery strategies for nutraceuticals: Delivery vehicles and absorption enhancers. *Trends in Food Science & Technology*, *53*, 90–101.

Guerra-Rosas, M. I., Morales-Castro, J., Ochoa-Martínez, L. A., Salvia-Trujillo, L., & Martín-Belloso, O. (2016). Long-term stability of food-grade nanoemulsions from high methoxyl pectin containing essential oils. *Food Hydrocolloids*, *52*, 438–446.

Gupta, A., Eral, H. B., Hatton, T. A., & Doyle, P. S. (2016). Nanoemulsions: formation, properties and applications. *Soft Matter*, *12*(11), 2826–2841.

Guzey, D., & McClements, D. J. (2006). Formation, stability and properties of multilayer emulsions for application in the food industry. *Advances in Colloid and Interface Science*, *128-130*, 227–248.

Hou, Z., Gao, Y., Yuan, F., Liu, Y., Li, C., & Xu, D. (2010). Investigation into the Physicochemical Stability and Rheological Properties of β-Carotene Emulsion Stabilized by Soybean Soluble Polysaccharides and Chitosan. *Journal of Agricultural and Food Chemistry*, *58*(15), 8604–8611.

Huang, W., Xu, H., Xue, Y., Huang, R., Deng, H., & Pan, S. (2012). Layer-by-layer immobilization of lysozyme–chitosan–organic rectorite composites on electrospun nanofibrous mats for pork preservation. *Food Research International*, *48*(2), 784–791.

Irkin, R., & Esmer, O. K. (2015). Novel food packaging systems with natural antimicrobial agents. *Journal of Food Science and Technology*, *52*(10), 6095–111.

Jafari, S. M., Assadpoor, E., He, Y., & Bhandari, B. (2008). Re-coalescence of emulsion droplets during high-energy emulsification. *Food Hydrocolloids*, *22*(7), 1191–1202.

Jo, Y.-J., Chun, J.-Y., Kwon, Y.-J., Min, S.-G., Hong, G.-P., & Choi, M.-J. (2015). Physical and antimicrobial properties of trans-cinnamaldehyde nanoemulsions in water melon juice. *LWT - Food Science and Technology*, *60*(1), 444–451.

Jo, Y.-J., Kwon, Y.-J., Min, S.-G., & Choi, M.-J. (2015). Changes in Quality Characteristics of Pork Patties Containing Multilayered Fish Oil Emulsion during Refrigerated Storage. *Korean Journal for Food Science of Animal Resources*, *35*(1), 71–9.

Keeney, M., Jiang, X. Y., Yamane, M., Lee, M., Goodman, S., & Yang, F. (2015). Nanocoating for biomolecule delivery using layer-by-layer self-assembly. *J. Mater. Chem. B*, *3*(45), 8757–8770.

Kim, I.-H., Lee, H., Kim, J. E., Song, K. Bin, Lee, Y. S., Chung, D. S., & Min, S. C. (2013). Plum Coatings of Lemongrass Oil-incorporating Carnauba Wax-based Nanoemulsion. *Journal of Food Science*, *78*(10), E1551–E1559.

Kim, I.-H., Oh, Y. A., Lee, H., Song, K. Bin, & Min, S. C. (2014). Grape berry coatings of lemongrass oil-incorporating nanoemulsion. *LWT - Food Science and Technology*, *58*(1), 1–10.

Klitzing, R. V, & V Klitzing, R. (2006). Internal structure of polyelectrolyte multilayer assemblies. *Physical Chemistry Chemical Physics : PCCP*, *8*(43), 5012–33.

Kuan, C.-Y., Yee-Fung, W., Yuen, K.-H., & Liong, M.-T. (2012). Nanotech: propensity in foods and bioactives. *Critical Reviews in Food Science and Nutrition*, *52*(1), 55–71.

Kuroiwa, T., Kobayashi, I., Chuah, A. M., Nakajima, M., & Ichikawa, S. (2015). Formulation and stabilization of nano-/microdispersion systems using naturally occurring edible polyelectrolytes by electrostatic deposition and complexation. *Advances in Colloid and Interface Science*, *226*(Pt A), 86–100.

Lai, P., & Roy, J. (2004). Antimicrobial and Chemopreventive Properties of Herbs and Spices. *Current Medicinal Chemistry*, *11*(11), 1451–1460.

Li, F., Biagioni, P., Finazzi, M., Tavazzi, S., & Piergiovanni, L. (2013). Tunable green oxygen barrier through layer-by-layer self-assembly of chitosan and cellulose nanocrystals. *Carbohydrate Polymers*, *92*(2), 2128–34.

Liang, R., Xu, S., Shoemaker, C. F., Li, Y., Zhong, F., & Huang, Q. (2012). Physical and antimicrobial properties of peppermint oil nanoemulsions. *Journal of Agricultural and Food Chemistry*, *60*(30), 7548–55.

Liu, F., Wang, D., Sun, C., McClements, D. J., & Gao, Y. (2016). Utilization of interfacial engineering to improve physicochemical stability of β-carotene emulsions: Multilayer coatings formed using protein and protein–polyphenol conjugates. *Food Chemistry*, *205*, 129–139.

Mason, T. G., Wilking, J. N., Meleson, K., Chang, C. B., & Graves, S. M. (2006). Nanoemulsions: formation, structure, and physical properties. *Journal of Physics: Condensed Matter*, *18*(41), R635–R666.

McClements, D. J. (2005). Theoretical analysis of factors affecting the formation and stability of multilayered colloidal dispersions. *Langmuir : The ACS Journal of Surfaces and Colloids*, *21*(21), 9777–85.

McClements, D. J. (2011). Edible nanoemulsions: Fabrication, properties, and functional performance. *Soft Matter*, *7*(6), 2297–2316.

McClements, D. J., & Rao, J. (2011). Food-grade nanoemulsions: formulation, fabrication, properties, performance, biological fate, and potential toxicity. *Critical Reviews in Food Science and Nutrition*, *51*(4), 285–330.

Medeiros, B. G. de S., Pinheiro, A. C., Teixeira, J. A., Vicente, A. A., & Carneiro-da-Cunha, M. G. (2012). Polysaccharide/Protein Nanomultilayer Coatings: Construction, Characterization and Evaluation of Their Effect on “Rocha” Pear (Pyrus communis L.) Shelf-Life. *Food and Bioprocess Technology*, *5*(6), 2435–2445.

Moghimi, R., Aliahmadi, A., McClements, D. J., & Rafati, H. (2016). Investigations of the effectiveness of nanoemulsions from sage oil as antibacterial agents on some food borne pathogens. *LWT - Food Science and Technology*, *71*, 69–76.

Mun, S., Decker, E. A., & McClements, D. J. (2005). Influence of Droplet Characteristics on the Formation of Oil-in-Water Emulsions Stabilized by Surfactant−Chitosan Layers. *Langmuir*, *21*(14), 6228–6234.

Oliveira, T. L. C. de, Ramos, A. L. S., Ramos, E. M., Piccoli, R. H., & Cristianini, M. (2015). Natural antimicrobials as additional hurdles to preservation of foods

by high pressure processing. *Trends in Food Science & Technology*, *45*(1), 60–85.

Otoni, C. G., Moura, M. R. de, Aouada, F. A., Camilloto, G. P., Cruz, R. S., Lorevice, M. V., Soares, N. de F. F., & Mattoso, L. H. C. (2014). Antimicrobial and physical-mechanical properties of pectin/papaya puree/cinnamaldehyde nanoemulsion edible composite films. *Food Hydrocolloids*, *41*, 188–194.

Otoni, C. G., Pontes, S. F. O., Medeiros, E. A. A., & Soares, N. de F. F. (2014). Edible films from methylcellulose and nanoemulsions of clove bud (Syzygium aromaticum) and oregano (Origanum vulgare) essential oils as shelf life extenders for sliced bread. *Journal of Agricultural and Food Chemistry*, *62*(22), 5214–9.

Ozturk, B., Argin, S., Ozilgen, M., & McClements, D. J. (2015). Formation and stabilization of nanoemulsion-based vitamin E delivery systems using natural biopolymers: Whey protein isolate and gum arabic. *Food Chemistry*, *188*, 256–263.

Parthasarathi, S., Muthukumar, S. P., & Anandharamakrishnan, C. (2016). The influence of droplet size on the stability, in vivo digestion, and oral bioavailability of vitamin E emulsions. *Food Funct.*, *7*(5), 2294–2302.

Pinheiro, A. C., Bourbon, A. I., Medeiros, B. G. de S., da Silva, L. H. M., da Silva, M. C. H., Carneiro-da-Cunha, M. G., Coimbra, M. A., & Vicente, A. A. (2012). Interactions between κ-carrageenan and chitosan in nanolayered coatings—Structural and transport properties. *Carbohydrate Polymers*, *87*(2), 1081–1090.

Pinheiro, A. C., Coimbra, M. A., & Vicente, A. A. (2016). In vitro behaviour of curcumin nanoemulsions stabilized by biopolymer emulsifiers – Effect of interfacial composition. *Food Hydrocolloids*, *52*, 460–467.

Prakash, B., Kedia, A., Mishra, P. K., & Dubey, N. K. (2015). Plant essential oils as food preservatives to control moulds, mycotoxin contamination and oxidative deterioration of agri-food commodities – Potentials and challenges. *Food Control*, *47*, 381–391.

Qian, C., & McClements, D. J. (2011). Formation of nanoemulsions stabilized by model food-grade emulsifiers using high-pressure homogenization: Factors affecting particle size. *Food Hydrocolloids*, *25*(5), 1000–1008.

Rojas-Graü, M. A., Soliva-Fortuny, R. C., & Martín-Belloso, O. (2009). Edible coatings to incorporate active ingredients to fresh-cut fruits: a review. *Trends in Food Science & Technology*, *20*(10), 438–447.

Salvia-Trujillo, L., Qian, C., Martín-Belloso, O., & McClements, D. J. (2013). Influence of particle size on lipid digestion and β-carotene bioaccessibility in emulsions and nanoemulsions. *Food Chemistry*, *141*(2), 1472–80.

Salvia-Trujillo, L., Rojas-Graü, A., Soliva-Fortuny, R. C., & Martín-Belloso, O. (2015a). Physicochemical characterization and antimicrobial activity of food-grade emulsions and nanoemulsions incorporating essential oils. *Food Hydrocolloids*, *43*, 547–556.

Salvia-Trujillo, L., Rojas-Graü, M. A., Soliva-Fortuny, R. C., & Martín-Belloso, O. (2014). Formulation of Antimicrobial Edible Nanoemulsions with Pseudo-Ternary Phase Experimental Design. *Food and Bioprocess Technology*, *7*(10), 3022–3032.

Salvia-Trujillo, L., Rojas-Graü, M. A., Soliva-Fortuny, R. C., & Martín-Belloso, O. (2015b). Use of antimicrobial nanoemulsions as edible coatings: Impact on safety and quality attributes of fresh-cut Fuji apples. *Postharvest Biology and Technology*, *105*, 8–16.

Salvia-Trujillo, L., Rojas-Graü, M. A., Soliva-Fortuny, R. C., Martín-Belloso, O., & Rojas-Graü, A. (2012). Physicochemical Characterization of Lemongrass Essential Oil–Alginate Nanoemulsions: Effect of Ultrasound Processing Parameters. *Food and Bioprocess Technology*, *6*(9), 2439–2446.

Schoeler, B., Sharpe, S., Hatton, T. A., & Caruso, F. (2004). Polyelectrolyte Multilayer Films of Different Charge Density Copolymers with Synergistic Nonelectrostatic Interactions Prepared by the Layer-by-Layer Technique. *Langmuir*, *20*(7), 2730–2738.

Sen Gupta, S., & Ghosh, M. (2015). Formulation development and process parameter optimization of lipid nanoemulsions using an alginate-protein stabilizer. *Journal of Food Science and Technology*, *52*(5), 2544–57.

Sessa, M., Balestrieri, M. L., Ferrari, G., Servillo, L., Castaldo, D., D'Onofrio, N., … Tsao, R. (2014). Bioavailability of encapsulated resveratrol into nanoemulsion-based delivery systems. *Food Chemistry*, *147*, 42–50.

Sessa, M., Ferrari, G., & Donsì, F. (2015). Novel edible coating containing essential oil nanoemulsions to prolong the shelf life of vegetable products. *Chemical Engineering Transactions*, *43*, 55–60.

Severino, R., Ferrari, G., Vu, K. D., Donsì, F., Salmieri, S., & Lacroix, M. (2015). Antimicrobial effects of modified chitosan based coating containing nanoemulsion of essential oils, modified atmosphere packaging and gamma irradiation against Escherichia coli O157:H7 and Salmonella Typhimurium on green beans. *Food Control*, *50*, 215–222.

Silva, H. D., Cerqueira, M. A., & Vicente, A. A. (2012). Nanoemulsions for Food Applications: Development and Characterization. *Food and Bioprocess Technology*, *5*(3), 854–867.

Silva, H. D., Cerqueira, M. A., & Vicente, A. A. (2015). Influence of surfactant and processing conditions in the stability of oil-in-water nanoemulsions. *Journal of Food Engineering*, *167*, 89–98.

Solans, C., Izquierdo, P., Nolla, J., Azemar, N., & Garcia-Celma, M. J. (2005). Nano-emulsions. *Current Opinion in Colloid & Interface Science*, *10*(3), 102–110.

Solans, C., & Solé, I. (2012). Nano-emulsions: Formation by low-energy methods. *Current Opinion in Colloid & Interface Science*, *17*(5), 246–254.

Solórzano-Santos, F., & Miranda-Novales, M. G. (2012). Essential oils from aromatic herbs as antimicrobial agents. *Food Biotechnology - Plant Biotechnology*, *23*(2), 136–141.

Souza, M. P., Vaz, A. F. M., Cerqueira, M. A., Texeira, J. A., Vicente, A. A., & Carneiro-da-Cunha, M. G. (2015). Effect of an Edible Nanomultilayer Coating by Electrostatic Self-Assembly on the Shelf Life of Fresh-Cut Mangoes. *Food and Bioprocess Technology*, *8*(3), 647–654.

Tadros, T., Izquierdo, P., Esquena, J., & Solans, C. (2004). Formation and stability of nano-emulsions. *Advances in Colloid and Interface Science*, *108*, 303–318.

Ting, Y., Jiang, Y., Ho, C. T., & Huang, Q. (2014). Common delivery systems for enhancing in vivo bioavailability and biological efficacy of nutraceuticals. *Journal of Functional Foods*, *7*(1), 112–128.

Tiwari, B. K., Valdramidis, V. P., O' Donnell, C. P., Muthukumarappan, K., Bourke, P., & Cullen, P. J. (2009). Application of Natural Antimicrobials for Food Preservation. *Journal of Agricultural and Food Chemistry*, *57*(14), 5987–6000.

Tokle, T., Lesmes, U., Decker, E. A., & McClements, D. J. (2012). Impact of dietary fiber coatings on behavior of protein-stabilized lipid droplets under simulated gastrointestinal conditions. *Food & Function*, *3*(1), 58–66.

Topuz, O. K., Özvural, E. B., Zhao, Q., Huang, Q., Chikindas, M., & Gölükçü, M. (2016). Physical and antimicrobial properties of anise oil loaded nanoemulsions on the survival of foodborne pathogens. *Food Chemistry*, *203*, 117–23.

Weiss, J., Loeffler, M., & Terjung, N. (2015). The antimicrobial paradox: why preservatives lose activity in foods. *Current Opinion in Food Science*, *4*, 69–75.Wooster, T. J., Golding, M., & Sanguansri, P. (2008). Impact of oil type on nanoemulsion formation and ostwald ripening stability. *Langmuir*, *24*(22), 12758–12765.

Yang, X., Tian, H., Ho, C.-T., & Huang, Q. (2012). Stability of Citral in Emulsions Coated with Cationic Biopolymer Layers. *Journal of Agricultural and Food Chemistry*, *60*(1), 402–409.

Zeeb, B., Lopez-Pena, C. L., Weiss, J., & McClements, D. J. (2015). Controlling lipid digestion using enzyme-induced crosslinking of biopolymer interfacial layers in multilayer emulsions. *Food Hydrocolloids*, *46*, 125–133.

Zeeb, B., Thongkaew, C., & Weiss, J. (2014). Theoretical and practical considerations in electrostatic depositioning of charged polymers. *Journal of Applied Polymer Science*, *131*(7), n/a–n/a.

Zhang, C., Xu, W., Jin, W., Shah, B. R., Li, Y., & Li, B. (2015). Influence of anionic alginate and cationic chitosan on physicochemical stability and carotenoids bioaccessibility of soy protein isolate-stabilized emulsions. *Food Research International*, *77*, 419–425.

HYPOTHESIS AND OBJECTIVES

The hypothesis underlying this Doctoral Thesis was that the encapsulation of active ingredients into food-grade nanostructured delivery systems would allow increasing the physicochemical stability and functional performance of the encapsulated substances. In this regard, it was theorized that nanostructured delivery systems could be a promising approach to facilitate the use of natural-origin food additives in foods, boosting therefore their quality, safety and/or functional properties.

The main objective of this Doctoral Thesis was to study the most important factors affecting the formation and physicochemical properties of three types of food nanostructures (nanoemulsions, multilayer emulsions and nanolaminates), and to assess their ability to encapsulate, protect and deliver plant-based antimicrobials or nutraceuticals. Their potential application in edible films was also explored.

To achieve this main objective, the following specific objectives were proposed:

i. To obtain food-grade nanoemulsions containing antimicrobial lipids (essential oils) for their application in edible films, and to study the impact of the physicochemical properties of nanoemulsions on the final features of the resulting edible films.

ii. To evaluate the feasibility of using food-grade multilayer emulsions as delivery systems of hydrophobic active ingredients (resveratrol); firstly, by investigating the effect of biopolymer concentration on their formation and stability; and eventually, by studying their behavior under simulated gastrointestinal conditions.

I. To assess the influence of the conditions of preparation on the formation of polysaccharide-based nanolaminates using the layer-by-layer technique, and to study their ability to encapsulate, protect and release hydrophilic nutraceuticals (folic acid) in a controlled way.

MATERIALS AND METHODS

MATERIALS

Table 1 summarizes the different food-grade materials and active ingredients used in the fabrication of nanostructured emulsions and nanolaminates investigated in this work.

Table 1. Materials required to produce the nanostructured delivery systems.

Type	**Active ingredient**	**Materials**
Nanoemulsions	Essential oils: Sage, thyme and lemongrass	*Disperse phase:* essential oils *Emulsifier*: Tween 80 *Texturizing agent*: sodium alginate Plasticizer: glycerol
Multilayer emulsions	Resveratrol	*Disperse phase*: corn oil *Emulsifier*: lactoferrin *Coatings composition:* lactoferrin, lactoferrin/alginate, lactoferrin/alginate/poly-L-lysine
Nanolaminates	Folic acid	*Substrates:* Quartz slides and polyethylene terephthalate (PET) sheets *Building blocks*: Sodium alginate and chitosan

METHODS

1. SECTION I. Essential oil nanoemulsions and edible films

Nanoemulsions formation

The continuous phase was prepared by dissolving 3% w/v of sodium alginate in hot deionized water (70ºC) and stirring for at least 4 h. The disperse phase consisted of 1% v/v of the different essential oils used (Table 1). The emulsifier at 3% v/v and the plasticizer at 2% v/v were also incorporated to the formulation. All the components were homogenized using a high-speed blender (Ultra-turrax, Jake & Kunkel, Staufen, Germany). The resulting coarse emulsions were treated in a microfluidizer (M110P, Microfluidics, Massachusetts, USA), with 150 MPa and 3 passes, in order to obtain emulsions of smaller oil droplet sizes.

Fig. 1 present a schematic representation of microfluidization process and the device used in these experiments.

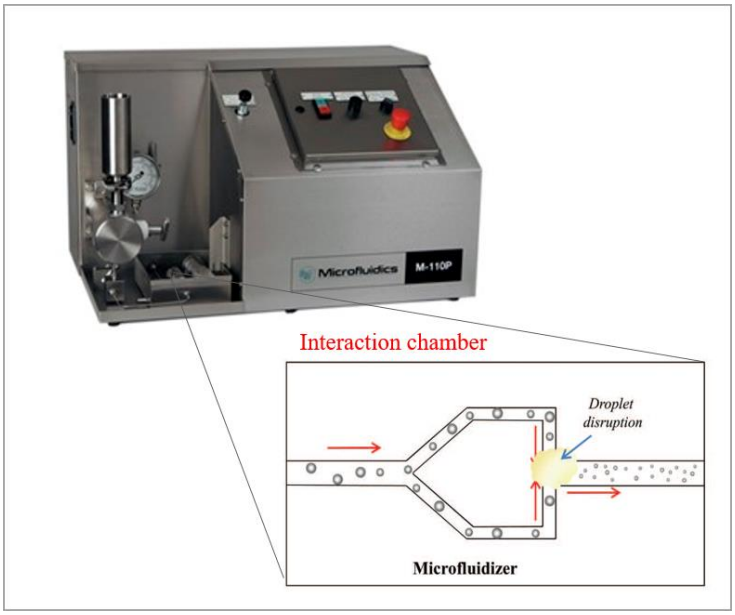

Fig. 1. Microfluidizer M-110P. Schematic representation of microfluidization. Adapted from (McClements & Rao, 2011)

Characterization of nanoemulsions

Nanoemulsions were characterized in terms of droplet size, droplet charge, viscosity and color of the systems. The particle size was measured by dynamic light scattering using a laser diffractometer (Zetasizer NanoZS, Malvern

Instruments, U.K.), from diluted nanoemulsions with water in ratio of 1:20. The ζ-potential of nanoemulsions was assessed by phase-analysis light scattering in the same device used for particle size analysis, and measurements were carried out using diluted nanoemulsions.

Viscosity of nanoemulsions was measured in a vibro-viscometer SV-10 (A&D Company, Tokyo, Japan), from aliquots of 10 mL, vibrating at 30 MHz and constant amplitude. The temperature of samples was recorded simultaneously by the same equipment.

The color of nanoemulsions was determined in a colorimeter Minolta CR-400 colorimeter (Konica Minolta Sensing, Inc., Osaka, Japan), using an illuminant D_{65} and the 10º observer angle. Whiteness index was calculated from the CIE L^*, a^* and b^* parameters, according to Eq. (1) (Vargas, Cháfer, Albors, Chiralt, & González-Martínez, 2008):

$$WI = 100 - \sqrt{(100 - L^*)^2 + \left(a^{*^2} + b^{*^2}\right)} \quad (1)$$

Formation of edible films from nanoemulsions

Essential oil nanoemulsions were spread uniformly using a casting bar on the surface of crystal plates of 30 x 40 cm, coated with PET sheets (Mylar®). Alginate films without essential oils (3% sodium alginate, 3% emulsifier and 2% plasticizer) were also prepared. Films were dried for 24 h at room temperature and peeled off from PET for further determinations.

Characterization of edible films and antimicrobial activity

Microscopic images of the surface were recorded in a scanning electron microscope (DSM 940 A, Zeiss, Germany), with an acceleration voltage of 10 kV and a working distance of 10 mm.

Film color and film opacity were measured using a colorimeter Minolta CR-400 colorimeter (Konica Minolta Sensing, Inc., Osaka, Japan), with an illuminant D_{65} and the 10º observer angle. The color difference (ΔE^*) between films and a white background was calculated by E.q (2); while opacity was obtained through E.q. (3) (Pires et al., 2013):

$$\Delta E^* = ((L^* - L_o)^2 + (a^* - a_o)^2 + (b^* - b_o)^2)^{0.5} \quad (2)$$

where L^*, a^*, b^* are the color coordinates of the films, and L_o, a_o, b_o values are those corresponding to the white background (L_o = 90.97, a_o = 0.08, b_o = -0.28).

$$Opacity = {}^{Y_b}/_{Y_w} \times 100 \quad (3)$$

where Y_b is the Y coordinate measured on the black background, and Y_w is the Y coordinate measured on the white background.

Film thickness was determined using a micrometer IP 65 (Mitutoyo Manufacturing, Tokio, Japan), taking measurements at five different points of the film.

The water vapor permeability (WVP) of films was assessed gravimetrically at 25 ºC, using a modified version of the ASTM standard method E96-00 (ASTM, 2000). Briefly, circular film pieces were placed onto methylmethacrylate test cups, previously filled with water, and sealed using a cap with a rubber O-ring. The cups containing films were entered in glass containers with hermetic covers equilibrated at 33 % of relative humidity and room temperature. The cups were weighted hourly, and data of weight loss versus time were fitted with a linear regression. The WVP was calculated as described in Eqs. (4) and (5) (Chinnan & Park, 1996; Kaya & Kaya, 2000).

$$WVTR = m_1/A \quad (4)$$

$$WVP = L \times WVTR/(\rho_i - \rho_a) \quad (5)$$

where A (m^2) is the exposed film area, ρ_i (Pa) and ρ_a (Pa) are the vapor pressures of saturated air and air with 33% RH, respectively, at 25 ºC. L is the average film thickness (m).

Film mechanical properties were evaluated by tensile and puncture tests in a TA-TX2 texture analyzer (Stable Micro Systems, Goldaming, Surrey, U.K.). The tensile tests were determined by ASTM standard method D882-97 (ASTM, 1991), and the tensile strength (TS) and elongation at break (EAB) were calculated by E.q. (6) and (7):

$$TS = F_{max}/A \quad (6)$$

$$EAB = \left({}^{L}/_{L_o}\right) \times 100 \quad (7)$$

The puncture analyses were carried out using the ASTM D6241-04 standard method (ASTM, 2004), and the puncture force (PF) was obtained from the force-displacement curves recorded by Texture Exponent 32 software (Stable Micro Systems, Goldaming, Surrey, U.K.).

Finally, *the antimicrobial activity* of films against *Escherichia coli* was determined by a modification of the method proposed by Kristo et al., (2008) and Sánchez-González et al., (2011). Briefly, films were place on the surface of inoculated agar plates (Triptone soy agar with 3% NaCl). The uncoated agar plates were used as controls. Straightaway, coated and uncoated agar plates were left at room temperature for 12 h. During the first 4 h, the antimicrobial activity of films was evaluated hourly. Afterwards, assays were carried out every 2 h. For this purpose, 10 g of agar were aseptically removed from Petri dishes and put into sterile stomacher bags with 90 mL of saline peptone, homogenized for 2 min, and then, serial dilutions were prepared and McConkey-Sorbitol Agar plates were inoculated (Biokar Diagnostics, France). Plates were incubated at 37 ºC for 24 h.

2. SECTION II. Multilayer emulsions as delivery systems of hydrophobic compounds

Multilayer emulsions preparation

Primary emulsions

The continuous phase was prepared by dissolving different concentrations of lactoferrin (1%, 1.5% and 2% w/w) in water, under continuous stirring overnight. The disperse phase consisted of the corn oil loaded with resveratrol. First, powdered resveratrol was dissolved in ethanol, working as a co-solvent, and then, this mixture was added to the corn oil, so that the final concentrations of both corn oil and resveratrol in the emulsion were 5% w/w and 0.01% w/w, respectively. Continuous and disperse phases were homogenized in a high-speed blender (Ultra-turrax T25, IKA Werke, Staufen, Germany), and then the resulting coarse emulsions were treated in a high pressure homogenizer (Nano DeBEE, BEE International, USA), at 22,000 psi and 5 cycles. The final composition of primary emulsions was 0.01% w/w resveratrol, 0.2% w/w ethanol, 5% w/w corn oil, and 0.95% w/w, 1.42% w/w or 1.90% w/w lactoferrin. Primary emulsions were adjusted to pH 5. Emulsions containing the smallest droplet size and sufficiently strong droplet charge were used in secondary emulsions.

Secondary emulsions

An aliquot of 5 mL of primary emulsions was added to a previous mixture of 5 mL of sodium alginate solution (at different concentrations) and 15 mL of water, under continuous stirring for 15 min. The system was adjusted to 5 to promote alginate adsorption at the oil/water interface. The resulting secondary emulsions were sonicated for 10 min to disrupt possible flocs created during the alginate adsorption to the interface of lactoferrin coated droplets. The final composition was 0.002% w/w resveratrol, 1% w/w corn oil, 0.38% w/w lactoferrin, and alginate from 0.02% to 0.28% w/w. The most stable formulation was used to prepare tertiary emulsions.

Tertiary emulsions

Similarly, a 5 mL aliquot of secondary emulsions were combined with a previous mixture of 5 mL of poly-L-lysine solution (at different concentrations)

and 45 mL of water under continuous stirring for 15 min. The system was adjusted to pH 5 to promote poly-L-lysine adsorption at the oil/water interface. Tertiary emulsions were then sonicated for 10 min. The final composition was 0.0002% w/w resveratrol, 0.090% corn oil, 0.038% w/w lactoferrin, 0.022% w/w alginate, and from 0.009% to 0.045% w/w poly-L-lysine. A schematic representation of the procedure carried out in the formation of multilayer emulsions is presented in Fig. 2.

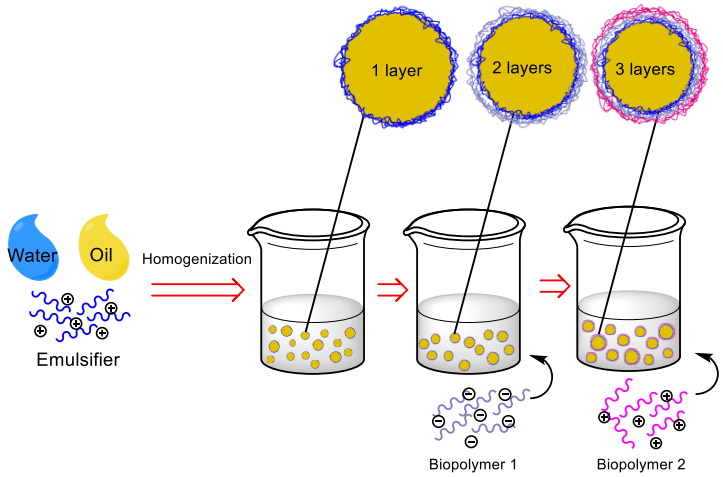

Fig. 2. Schematic representation of the formation of multilayer emulsions.

Effect of biopolymer concentration on emulsions formation

The influence of incorporating different concentrations of alginate and poly-L-lysine to the emulsion stability was assessed through the changes in droplet size and droplet charge. The droplet size allow determining the physical stability of particles in suspensions, while the droplet charge (ζ-potential) indicates the degree of saturation of droplets interface by the oppositely charged biopolymers.

Droplet size and ζ-potential measurements were performed in diluted emulsions (1:100, primary emulsions and 1:10, secondary and tertiary emulsions), through dynamic light scattering and phase-analysis light scattering, using a laser diffractometer (Zetasizer NanoZS, Malvern Instruments, U.K).

The best formulations of each type of emulsion was analyzed by Transmission Electron Microscopy, to obtain crucial insights of the formation of the interfacial membranes of droplets. The morphology of single-layer emulsions and multilayer emulsions was evaluated by transmission electron microscopy

(TEM) (EM 902A, ZEISS, Germany) operating at 80 kV. TEM samples were prepared by depositing the single-layer emulsions and multilayer emulsions suspensions on a carbon-coated copper grid, and negatively stained with 1 % (w/v) uranyl acetate for observation. Samples were air-dried before analyses.

Physical and chemical stability during storage

Changes in the droplet size and droplet charge of single-layer, multilayer emulsions were stored with lighting at room temperature and monitored during 4 weeks. Analyses of droplet size and droplet charge were performed weekly, as described in the previous section.

The chemical stability of resveratrol encapsulated in multilayer emulsions was assessed by their antioxidant activity using the DPPH method, following the procedure described in a previous work (Pinheiro et al., 2015). Briefly, 1 mL of each emulsion was blended with 4 mL of ethanol absolute to promote the emulsion leakage and release of encapsulated resveratrol. Then, an aliquot of 0.3 mL was mixed with 0.2 mL of ethanol absolute and 2.5 mL of DPPH• solution (60 µM in ethanol). Solutions were kept under dark conditions during 30 min at room temperature. Absorbance was measured at 515 nm using a Multi-Detection Microplate Reader SynergyTM HT (Biotek, Winooski, USA). The scavenging effect of emulsions was calculated through Eq. (8) as follows:

$$SE\ (\%) = \left(\frac{A_0 - A}{A_0}\right) \times 100 \qquad (8)$$

where A_0 is the absorbance of the DPPH• solution and A is the absorbance of the sample with DPPH•.

In vitro digestion

Optimal formulation of multilayer emulsions were subjected to an *in vitro* digestion process, which was carried out through a harmonized static standard protocol (Minekus et al., 2014). The conditions of the mouth, stomach and small intestine were simulated. The simulated salivary fluid (SSF), simulated gastric fluid (SGF) and simulated intestinal fluid (SIF) solutions were prepared according to Table 2. Calcium chloride was added in every stage of the digestion, rather than in the electrolyte solutions to avoid precipitation. The simulated digestion fluids were warmed up at 37 ºC in a water bath before starting the process.

Table 2. Composition of the simulated salivary (SSF), gastric (SGF) and intenstinal (SIF) fluids.

Salts added	SSF (pH 7)	SGF (pH 3)	SIF (pH 7)
	Salt concentration (mmol/L)	**Salt concentration (mmol/L)**	**Salt concentration (mmol/L)**
KCl	15.1	6.9	6.8
KH_2PO_4	3.7	0.9	0.8
$NaHCO_3$	13.6	25	85
NaCl	-	47.2	38.4
$MgCl_2(H_2O)_6$	0.15	0.12	0.33
$(NH_4)_2CO_3$	0.06	0.5	-
$CaCl_2(H_2O)_2$	1.5	0.15	0.6
HCl	1.1	15.6	8.4

Oral phase: aliquots of 4 mL of SSF, 5 mL of the multilayer emulsions (primary, secondary or tertiary), 25 µL of $CaCl_2$ 0.3 M and 0.475 mL of ultrapure water were added to conical centrifuge tubes of 50 mL to obtain a final ratio of emulsions and SSF of 50:50 (v/v). Tubes were incubated for 2 min at 37ºC, under agitation in a water bath. Afterwards, aliquots of 1 mL of sample were taken from the tubes.

Gastric phase: a porcin pepsin solution (3600 U/mL) was prepared in ultrapure water and left on ice. The "bolus" sample from the oral phase (9 mL) was mixed with 7.2 mL of SGF, 1 mL of pepsin (to obtain a final activity of 2000 U/mL) and 4.5 µL of $CaCl_2$, 0.3 M. The pH was adjusted to 3 by adding 1 M HCl and the volume required was recorded. The amount of ultrapure water needed to complete a volume of 18 mL was added, in order to reach a final ratio of bolus to SGF of 50:50 (v/v). The sample was incubated for 2 h at 37 ºC, under agitation in a water bath. After incubation, an aliquot of 1 mL was removed from the sample and the pH was increased to 7 using 1 M NaOH and stored ion ice to stop the enzymatic reactions.

Intestinal phase: a pancreatin solution (680 U/mL) was prepared in SIF and left on ice. Bile salts (80 mg/mL) were dissolved in SIF under stirring until complete dissolution. The "chyme" sample from the gastric phase (17 mL) was mixed with 8.6 mL of SIF, 5 mL of pancreatin (to reach a final activity of 100 U/mL), 2.07 mL of bile (to reach 10 mM in the final mixture), and 34 µL of 0.3 M $CaCl_2$. The pH was adjusted to 7 adding 1 M NaOH and the volume required was recorded. The amount of ultrapure water necessary to complete a volume of 34 mL was added in order to obtain a final ratio of chyme to SIF of 50:50 (v/v). The sample was incubated for 2 h at 37 ºC under agitation in a water bath. Afterwards, an aliquot of 340 µL of 1 mM Pefabloc was added to the sample and stored ion ice to inhibit enzymatic activities.

Physical stability of digested emulsions

The physical stability of single-layer, two-layer and three-layer emulsions were assessed by monitoring their changes in droplet size, droplet charge and morphology.

The initial droplet size and ζ-potential of oil droplets, as well as in each stage of the digestion (mouth, stomach and intestine) were measured by dynamic light scattering and phase-analysis light scattering, using a laser diffractometer (Zetasizer, NanoZS, Malvern Instruments, U.K.). Emulsions were diluted in a ratio 1:10 with water adjusted to the corresponding pH of each digested sample.

The morphology of oil droplets in the different digestion stages were assessed by an epifluorescence microscope (BX51 266 OLYMPUS, Tokyo, Japan) and with a ×100 oil immersion objective lens. Samples were dyed with Nile Red with a ratio of 1:10 (dye:sample). Slides were prepared by taking 10 µL of the dyed emulsion solution and placing in a glass microscope slide and covering with a glass cover slip.

Resveratrol bioaccessibility assessment

Resveratrol bioaccessibility of multilayer emulsions were analyzed in the digesta, using a previously published protocol (Pinheiro, Coimbra, & Vicente, 2016). Briefly, digested emulsions of the intestinal phase were centrifuged at 60000 rpm, for 60 min at 25 ºC. The supernatant was collected, assuming that it corresponded to the micelle fraction, in which resveratrol molecules were

entrapped within mixed micelles. A standard extraction procedure was then carried out twice, by mixing 5 mL of the micelle phase and 5 mL of chloroform, vortexed and centrifuged at 1750 rpm for 10 min at 25 ºC. The chloroform containing the extracted resveratrol was quantified spectrophotometrically in a Multi-Detection Microplate Reader SynergyTM HT (Biotek, Winooski, USA) at 307 nm (absorbance peak). The concentration of resveratrol was quantified through a calibration curve in chloroform (0.5 – 7 µg/mL, R2 = 0.9986). The bioaccessibility of resveratrol was calculated by Eq. (9):

$$\%Bioaccessibility = \frac{C_m}{C_0} \times 100 \quad (9)$$

where C_m is the concentration of resveratrol in the micelle fraction after digestion, and C_0 is the initial concentration of resveratrol in the emulsions.

3. SECTION III. Nanolaminates as delivery systems of hydrophilic compounds

Substrate pre-treatment

Treatment applied to quartz slides was carried out through a method previously published (Lukomska, Malicka, Gryczynski, & Lakowicz, 2004). Briefly, quartz were cleaned in Hellmanex solution for 2 h. Then, slides were immersed in APTS (1% v/v) for 30 min, rinsed with water and left in a desiccator containing silica gel. This procedure generated a superficial positive charge in the substrate.

PET (polyethylene terephthalate) were treated using a modified method previously described for aminolysis (Bech, Meylheuc, Lepoittevin, & Roger, 2007). PET rectangles (6 cm x 2 cm) were washed in propanol/water solution for 3 h. Clean substrates were submerged in 1 M 1,6-hexanediamine/methanol solution for 4 h at 50 ºC to promote aminolysis, then washed in methanol and dried. Finally, they were immersed in 0.1 M HCl for 3 h, and left under vacuum until their use in nanolaminates formation.

The grafting of amino groups was confirmed using a protocol previously published that measures the concentration of amino groups on the surface (Irena, Jolanta, & Karolina, 2009). Briefly, substrates were immersed in a BPB/DMF solution (0.1 mg/mL) for 30 min, and then washed with copious ethanol. Both substrates were submerged in a piperidine/DMF solution (20%), and the absorbance of piperidine solutions was measured at λ = 605 nm. The surface concentration of amine groups was calculated from Lambert-Beer's law following Eq. (10):

$$A=\varepsilon\, l\, c \qquad (10)$$

where A is the absorbance of the sample, ε is the molar extinction coefficient ($BPB_{\varepsilon 605}$ = 91,800 $L.mol^{-1}.cm^{-1}$), l is the path length (1 cm), and c is the sample concentration.

Preparation of polysaccharide solutions

Alginate and chitosan solutions were prepared in water and lactic acid 1% v/v, respectively, varying the concentration (0.1-1% w/v), pH (3-11) and ionic

0.1strength (0.1-0.5 M). The solution pH was adjusted using either 1 M NaOH or 1 M lactic acid. The ionic strength was changed by incorporating different NaCl content in the solutions. Washing solutions for the layer-by-layer assembly procedure were prepared with water at the same pH and ionic strength of polysaccharide solutions.

Influence of experimental parameters on the colloidal characteristics of polysaccharides

Changes in the colloidal characteristics of polysaccharide solutions, at different concentrations, pH and ionic strength were analyzed in terms of ζ-potential, viscosity and color of solutions.

The ζ-potential of both alginate and chitosan solutions was used as an indicator of the changes in the charge density of chains under certain conditions, and it was measured by phase-analysis light scattering in a laser diffractometer (Zetasizer NanoZS, Malvern Instruments, U.K.), directly on polysaccharide solutions without previous dilution.

Viscosity of the hydrocolloids was determined in a vibro-viscometer SV-10 (A&D Company, Tokyo, Japan), from aliquots of 10 mL, vibrating at 30 MHz and constant amplitude. The temperature of samples was recorded simultaneously by the same equipment.

Whiteness index of the colloidal systems was measured in a colorimeter Minolta CR-400 (Konica Minolta Sensing, Inc., Osaka, Japan), using an illuminant D_{65} and a 10º observer angle. Whiteness index was calculated from the CIE L^*, a^* and b^* parameters, according to Eq. (1).

Layer-by-layer assembly of nanolaminates

The aminolyzed substrates (positively charged), were immersed in alginate solutions (negatively charged) for 10-20 min. Then, substrates were washed twice during 1-5 min. A subsequent immersion of the substrates in chitosan solutions (positively charged) was performed for 10-20 min, followed by two rinsed steps for 1-5 min. This cycle was repeat until obtaining a desired number of layers (10 or 20 layers). The pH and ionic strength of polysaccharide solutions was adjusted in order to create different types of assemblies. In some cases, solutions were under stirring during the assembly

process. After deposition was finished, substrates coated by the nanolaminates were dried using a nitrogen gas flow, and stored into desiccators with silica.

A schematic representation of the layer-by-layer assembly is shown in Fig.2.

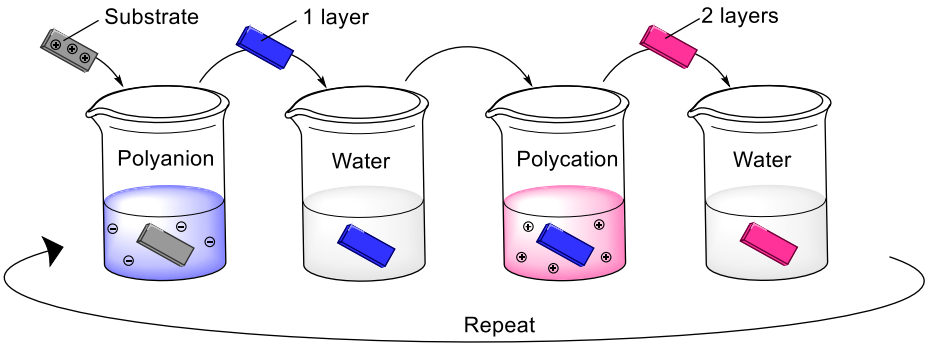

Fig. 3. Schematic representation of the layer-by-layer assembly technique performed by dipping approach.

Physicochemical characterization of nanolaminates

The nanolaminates buildup in quartz slides was monitored using a UV-visible-NIR spectrophotometer (V670, Jasco Corporation, Tokio, Japan). Absorbance spectra were recorded from 190 to 400 nm.

Infrared spectroscopy was used to determine the formation of nanolaminates on PET sheets. Spectra were collected on a FT/IR-6600 spectrophotometer (Jasco Corporation, Tokyo, Japan) fitted with an ATR cell.

The surface ζ-potential of nanolaminates created on PET sheets was evaluated after each layer deposition, which also allowed confirming the alternative adsorption of oppositely charged polysaccharides. Analyses were performed in a laser diffractometer (Zetasizer NanoZS, Malvern Instruments, U.K.), using a cell unit (ZEN1020) specially designed to measure the ζ-potential of flat surfaces. Briefly, PET coated with nanolaminates were attached to a sample holder and placed between two electrodes located in the cell. Then, samples were immersed in an appropriated aqueous solution containing, either positive or negative tracer particles, depending of layer to be analyzed. The ζ-potential of the tracer particles was measured by phase-analysis light scattering (PALS) at 5 distances from the sample surface. By plotting the zeta potential as a function of displacement from the surface, the

software equipment extrapolated this relationship to zero displacement, hence obtaining the surface ζ-potential of the layer.

Wettability of nanolaminates on PET was assessed after each layer deposition. Measurements were carried out in a DSA25 Krüss goniometer (Krüss GmbH, Hamburg, Germany) equipped with image analysis software (Drop Shape Analysis System, Krüss GmbH, Germany), through the sessile drop method. The contact angle was calculated using the Young-Laplace fit.

The thermal properties of nanolaminates on PET were determined using a differential scanning calorimeter (DSC822e, Mettler Toledo S.A.E., Barcelona, Spain). Samples were heated from 0 ºC to 400 ºC at a rate of 10 ºC/min under an atmosphere of inert nitrogen. The glass transition temperature (T_g), the melting temperature (T_m) and the enthalpy of melting (ΔH_m) were reported from the thermograms.

Finally, micrographs of nanolaminates on PET were obtained by Scanning Electron Microscopy, using a microscope JEOL J-6510 (JEOL Ltd., Tokio, Japan, working with an acceleration voltage of 5 kV.

Incorporation of folic acid

Folic acid was encapsulated into 20-layer nanolaminates throughout post-diffusion (Jiang, Bingbing Li, 2009). Nanolaminates assembled on quartz and PET substrates were dipped into folic acid solutions at pH 9, at different immersion times (1-420 min). Additionally, folic acid loading was carried out using different concentrations of folic acid in solution (1-12.5 mg/mL). Then, substrates with the nanolaminates containing encapsulated folic acid were washed with copious water to remove non-encapsulated molecules, and then dried at room temperature.

The loading process of folic acid into nanolaminates was confirmed by measuring the absorbance of the samples from 190 to 400 nm, in a UV-visible-NIR spectrophotometer (V-670, Jasco Corporation, Tokyo, Japan). Quantification of folic acid encapsulated was carried out by sonicating samples in phosphate buffer, pH 9 for 30 min, which was repeated until absorption peaks of folic acid disappeared from the spectrum. Then, the absorbance of sonicated solutions was measured at 364 nm and the folic acid

concentration was calculated through a calibration curve (0.5-10 µg/mL - R2 0.995126).

Micro-Raman determinations of powdered folic acid and nanolaminates containing the encapsulated compound were also performed, using a Jobin-Yvon LabRam H800 system (HORIBA Scientific, Kyoto, Japan), equipped with an Olympus BXFM optical microscope (objective 50x) and a CCD detector cooled at -70 ºC. The excitation source was a diode laser at 785 nm.

Photo-stability of encapsulated folic acid and release from nanolaminates

The stability of encapsulated and non-encapsulated folic acid under UV light was assessed by a previously published procedure, with some modifications (Aceituno-Medina, Mendoza, Lagaron, & López-Rubio, 2015). The PET sheets (0.7 x 2 cm) coated with folic acid nanolaminates (≈ 91 µg/ml folic acid) and a buffered solution at pH 9, containing the micronutrient (91 µg/ml) were placed below an UV light lamp (Osram Ultra-vitalux, 300 W) for 120 min, at a distance of 20.5 cm from the lamp, to accelerate molecules' degradation. At certain times, aliquots of irradiated folic acid solution and samples of folic acid nanolaminates were taken off, and PET sheets were submerged in 2 ml of phosphate buffer at pH 9, and sonicated for 30 min. Then, absorbance spectra of both non-encapsulated folic acid solution and that coming from the sonicated nanolaminates, were recorded from 190 to 400 nm in a UV-visible-NIR spectrophotometer (V-670, Jasco Corporation, Tokyo, Japan).

Finally, the release behavior of folic acid from nanolaminates was evaluated through a published method for active molecules release from layer-by-layer structures (Shukla, Fang, Puranam, & Hammond, 2012), with some modifications. The PET sheets coated with nanolaminates (0.7 x 2 cm) and loaded in 12.5 mg/mL FA solutions for 30 min, were used for the release experiments. Each PET sheet was immersed in 2 ml of phosphate-citrate buffer at pH 3 or pH 7, for 7 h at 37ºC. These pH values were selected in order to simulate the conditions of the gastrointestinal tract. At predetermined times, buffer solutions were removed and stored in ice under darkness for further analysis, and 2 ml of fresh buffer were added to continue the film release. The buffer solutions containing folic acid released at pH 7 were directly analyzed by UV-visible spectroscopy at 347 nm. The buffer solutions with the

micronutrient released at pH 3 were adjusted to pH 7 using 1.2 ml of 1 M sodium phosphate, and absorbance was then measured at 347 nm. The concentration of the compound released at each time was quantified using a calibration curve at pH 7 (0.5-10 µg/mL - R^2 0.991046). Release curves were generated by plotting the percentage of folic acid released versus the immersion time.

4. References

Alboofetileh, M., Rezaei, M., Hosseini, H., & Abdollahi, M. (2014). Antimicrobial activity of alginate/clay nanocomposite films enriched with essential oils against three common foodborne pathogens. Food Control, 36(1), 1–7.

ASTM. (1991). Standard test methods for tensile properties of thin plastic sheeting, method D 882-91. Philadelphia, PA: American Society for Testing Materials.

ASTM. (2000). Standard test methods for water vapor transmission of materials, method E 96-00. Philadelphia, PA: American Society for Testing Materials.

ASTM. (2004). Test method for the static puncture strength of geotextiles and geotextile-related products using a 50-mm probe, method D 6241-04. Philadelphia, PA: American Society for Testing Materials.

Atarés, L., Bonilla, J., & Chiralt, A. (2010). Characterization of sodium caseinate-based edible films incorporated with cinnamon or ginger essential oils. Journal of Food Engineering, 100(4), 678–687.

Ayhan, Z., Cimmino, S., Esturk, O., Duraccio, D., Pezzuto, M., & Silvestre, C. (2015). Development of Films of Novel Polypropylene based Nanomaterials for Food Packaging Application. Packaging Technology and Science, 28(7), 589–602.

Bech, L., Meylheuc, T., Lepoittevin, B., & Roger, P. (2007). Chemical surface modification of poly(ethylene terephthalate) fibers by aminolysis and grafting of carbohydrates. Journal of Polymer Science, Part A: Polymer Chemistry, 45(11), 2172–2183.

Bhargava, K., Conti, D. S., da Rocha, S. R. P., & Zhang, Y. (2015). Application of an oregano oil nanoemulsion to the control of foodborne bacteria on fresh lettuce. Food Microbiology, 47, 69–73.

Bieker, P., & Schönhoff, M. (2010). Linear and Exponential Growth Regimes of Multilayers of Weak Polyelectrolytes in Dependence on pH. Macromolecules, 43(11), 5052–5059.

Bilbao-Sáinz, C., Avena-Bustillos, R. de J., Wood, D. F., Williams, T. G., & McHugh, T. H. (2010). Nanoemulsions prepared by a low-energy emulsification method applied to edible films. Journal of Agricultural and Food Chemistry, 58(22), 11932–8.

Boddohi, S., Killingsworth, C. E., & Kipper, M. J. (2008). Polyelectrolyte multilayer assembly as a function of pH and ionic strength using the polysaccharides chitosan and heparin. Biomacromolecules, 9(7), 2021–2028.

Bonilla, J., Atarés, L., Vargas, M., & Chiralt, A. (2012). Effect of essential oils and homogenization conditions on properties of chitosan-based films. Food Hydrocolloids, 26(1), 9–16.

Buranasuksombat, U., Kwon, Y. J., Turner, M., & Bhandari, B. (2011). Influence of emulsion droplet size on antimicrobial properties. Food Science and Biotechnology, 20(3), 793–800.

Burt, S. (2004). Essential oils: their antibacterial properties and potential applications in foods—a review. International Journal of Food Microbiology, 94(3), 223–253.

Carneiro-da-Cunha, M. G., Cerqueira, M. A., Souza, B. W. S., Carvalho, S., Quintas, M. A. C. C., Teixeira, J. A., & Vicente, A. A. (2010). Physical and thermal properties of a chitosan/alginate nanolayered PET film. Carbohydrate Polymers, 82(1), 153–159.

Chang, Y., McLandsborough, L. A., & McClements, D. J. (2012). Physical properties and antimicrobial efficacy of thyme oil nanoemulsions: influence of ripening inhibitors. Journal of Agricultural and Food Chemistry, 60(48), 12056–63.

Chantrapornchai, W., Clydesdale, F., & McClements, D. J. (1998). Influence of Droplet Size and Concentration on the Color of Oil-in-Water Emulsions. Journal of Agricultural and Food Chemistry, 46, 2914–2920.

Chinnan, M. S., & Park, H. J. (1996). Effect of plasticizer level and temperature on water vapor transmission of cellulose-based edible films. Journal of Food Process Engineering, 18(4), 417–429.

Cramer Flores, F., Fagundes Ribeiro, R., Ferreira Ourique, A., Bueno Rolim, C. M., De Bona Da Silva, C., Raffin Pohlmann, A., Ruver Beck, R. C., & Stanisçuaski Guterres, S. (2011). Nanostructured systems containing an essential oil: protection against volatilization. Química Nova, 34(6), 968–972.

Davidov-Pardo, G., & McClements, D. J. (2015). Nutraceutical delivery systems: resveratrol encapsulation in grape seed oil nanoemulsions formed by spontaneous emulsification. Food Chemistry, 167, 205–12.

de Oliveira Santos, R. P., Castro, D. O., Ruvolo-Filho, A. C., & Frollini, E. (2014). Processing and thermal properties of composites based on recycled PET, sisal fibers, and renewable plasticizers. Journal of Applied Polymer Science, 131(12), 40386.

de Villiers, M. M., Otto, D. P., Strydom, S. J., & Lvov, Y. M. (2011). Introduction to nanocoatings produced by layer-by-layer (LbL) self-assembly. Advanced Drug Delivery Reviews, 63(9), 701–715.

Deng, J., Liu, X., Ma, L., Cheng, C., Shi, W., Nie, C., & Zhao, C. (2014). Heparin-mimicking multilayer coating on polymeric membrane via LbL assembly of cyclodextrin-based supramolecules. ACS Applied Materials & Interfaces, 6(23), 21603–14.

Dickinson, E. (2003). Hydrocolloids at interfaces and the influence on the properties of dispersed systems. Food Hydrocolloids, 17(1), 25–39.

Dickinson, E. (2009). Hydrocolloids as emulsifiers and emulsion stabilizers. Food Hydrocolloids, 23(6), 1473–1482.

Donsì, F., Cuomo, A., Marchese, E., & Ferrari, G. (2014). Infusion of essential oils for food stabilization: Unraveling the role of nanoemulsion-based delivery systems on mass transfer and antimicrobial activity. Innovative Food Science & Emerging Technologies, 22, 212–220.

Dufresne, A., & Vignon, M. R. (1998). Improvement of starch film performances using cellulose microfibrils. Macromolecules, 31(8), 2693–2696.

Edris, A. E., & Malone, C. F. R. (2012). Preferential solubilization behaviours and stability of some phenolic-bearing essential oils formulated in different microemulsion systems. International Journal of Cosmetic Science, 34(5), 441–450.

Emiroğlu, Z. K., Yemiş, G. P., Coşkun, B. K., & Candoğan, K. (2010). Antimicrobial activity of soy edible films incorporated with thyme and oregano essential oils on fresh ground beef patties. Meat Science, 86(2), 283–8.

Etienne, O., Schneider, A., Taddei, C., Richert, L., Schaaf, P., Voegel, J.-C., Egles, C., & Picart, C. (2005). Degradability of polysaccharides multilayer films in the oral environment: an in vitro and in vivo study. Biomacromolecules, 6(2), 726–33.

Fabra, M. J., Pérez-Masiá, R., Talens, P., & Chiralt, A. (2011). Influence of the homogenization conditions and lipid self-association on properties of sodium caseinate based films containing oleic and stearic acids. Food Hydrocolloids, 25(5), 1112–1121.

Farris, S., Introzzi, L., Biagioni, P., Holz, T., Schiraldi, A., & Piergiovanni, L. (2011). Wetting of Biopolymer Coatings: Contact Angle Kinetics and Image Analysis Investigation. Langmuir, 27(12), 7563–7574.

Fu, J., Ji, J., Yuan, W., & Shen, J. (2005). Construction of anti-adhesive and antibacterial multilayer films via layer-by-layer assembly of heparin and chitosan. Biomaterials, 26(33), 6684–6692.

Grant, C. A., Alfouzan, A., Gough, T., Twigg, P. C., & Coates, P. D. (2013). Nano-scale temperature dependent visco-elastic properties of polyethylene terephthalate (PET) using atomic force microscope (AFM). Micron (Oxford, England : 1993), 44, 174–8.

Gu, C.-H., Wang, J.-J., Yu, Y., Sun, H., Shuai, N., & Wei, B. (2013). Biodegradable multilayer barrier films based on alginate/polyethyleneimine and biaxially oriented poly(lactic acid). Carbohydrate Polymers, 92(2), 1579–85.

Gutierrez, J., Rodriguez, G., Barry-Ryan, C., & Bourke, P. (2008). Efficacy of plant essential oils against foodborne pathogens and spoilage bacteria associated with ready-to-eat vegetables: Antimicrobial and sensory screening. Journal of Food Protection, 71(9), 1846–1854.

Hammer, K. A., Carson, C. F., & Riley, T. V. (1999). Antimicrobial activity of essential oils and other plant extracts. Journal of Applied Microbiology, 86(6), 985–990.

Han, J., & Gennadios, A. (2005). Edible films and coatings: a review. In Innovations in Food Packaging (pp. 239–262).

Harding, S. E. (1997). The intrinsic viscosity of biological macromolecules. Progress in measurement, interpretation and application to structure in dilute solution. Progress in Biophysics and Molecular Biology, 68(2), 207–262.

Haynie, D. T., Zhang, L., Rudra, J. S., Zhao, W., Zhong, Y., & Palath, N. (2005). Polypeptide Multilayer Films. Biomacromolecules, 6(6), 2895–2913.

Helander, I. M., Alakomi, H.-L., Latva-Kala, K., Mattila-Sandholm, T., Pol, I., Smid, E. J., Gorris, L. G. M., & Von Wright, A. (1998). Characterization of the Action of Selected Essential Oil Components on Gram-Negative Bacteria. Journal of Agricultural and Food Chemistry, 46(9), 3590–3595.

Hernandez, R. J. (1994). Effect of water vapor on the transport properties of oxygen through polyamide packaging materials. Journal of Food Engineering, 22(1-4), 495–507.

Heurtault, B. (2003). Physico-chemical stability of colloidal lipid particles. Biomaterials, 24(23), 4283–4300.

Heydenreich, A. (2003). Preparation and purification of cationic solid lipid nanospheres—effects on particle size, physical stability and cell toxicity. International Journal of Pharmaceutics, 254(1), 83–87.

Indest, T., Laine, J., Ribitsch, V., Johansson, L.-S., Stana-Kleinschek, K., & Strnad, S. (2008). Adsorption of chitosan on PET films monitored by quartz crystal microbalance. Biomacromolecules, 9(8), 2207–14.

Irena, G., Jolanta, B., & Karolina, Z. (2009). Chemical modification of poly(ethylene terephthalate) and immobilization of the selected enzymes on the modified film. Applied Surface Science, 255(19), 8293–8298.

Jafari, S. M., Assadpoor, E., He, Y., & Bhandari, B. (2008). Re-coalescence of emulsion droplets during high-energy emulsification. Food Hydrocolloids, 22(7), 1191–1202.

Jiang, Bingbing Li, B. (2009). Tunable drug loading and release from polypeptide multilayer nano fi lms. International Journal of Nanomedicine, 4, 37–54.

Jiménez, A., Fabra, M. J., Talens, P., & Chiralt, A. (2012). Influence of hydroxypropylmethylcellulose addition and homogenization conditions on properties and ageing of corn starch based films. Carbohydrate Polymers, 89(2), 676–686.

Jouki, M., Mortazavi, S. A., Yazdi, F. T., & Koocheki, A. (2014). Characterization of antioxidant-antibacterial quince seed mucilage films containing thyme essential oil. Carbohydrate Polymers, 99, 537–46.

Junka, K., Sundman, O., Salmi, J., Osterberg, M., & Laine, J. (2014). Multilayers of cellulose derivatives and chitosan on nanofibrillated cellulose. Carbohydrate Polymers, 108, 34–40.

Juven, B. J., Kanner, J., Schved, F., & Weisslowicz, H. (1994). Factors that interact with the antibacterial action of thyme essential oil and its active constituents. Journal of Applied Bacteriology, 76(6), 626–631.

Kaya, S., & Kaya, A. (2000). Microwave drying effects on properties of whey protein isolate edible films. Journal of Food Engineering, 43(2), 91–96.

Kim, S. O., Ha, T. V. A., Choi, Y. J., & Ko, S. (2014). Optimization of homogenization-evaporation process for lycopene nanoemulsion production and its beverage applications. Journal of Food Science, 79(8), N1604–10.

Klitzing, R. V, & V Klitzing, R. (2006). Internal structure of polyelectrolyte multilayer assemblies. Physical Chemistry Chemical Physics : PCCP, 8(43), 5012–33.

Kralova, I., & Sjöblom, J. (2009). Surfactants used in food industry: a review. Journal of Dispersion Science and Technology, 30(9), 1363–1383.

Kristo, E., Koutsoumanis, K. P., & Biliaderis, C. G. (2008). Thermal, mechanical and water vapor barrier properties of sodium caseinate films containing antimicrobials and their inhibitory action on Listeria monocytogenes. Food Hydrocolloids, 22(3), 373–386.

Krochta, J. M., Baldwin, E., & Nisperos-Carriedo, M. (1994). Edible Coatings and Films to Improve Food Quality. (J. Krochta, E. Baldwin, & M. Nisperos-Carriedo, Eds.). Lancaster, PA: Technomic.

Ladam, G., Schaad, P., Voegel, J. C., Schaaf, P., Decher, G., & Cuisinier, F. (2000). In Situ Determination of the Structural Properties of Initially Deposited Polyelectrolyte Multilayers. Langmuir, 16(3), 1249–1255.

Lagoueyte, N., & Paquin, P. (1998). Effects of microfluidization on the functional properties of xanthan gum. Food Hydrocolloids, 12(3), 365–371.

Lambert, R. J. W., Skandamis, P. N., Coote, P. J., & Nychas, G.-J. E. (2001). A study of the minimum inhibitory concentration and mode of action of oregano

essential oil, thymol and carvacrol. Journal of Applied Microbiology, 91(3), 453–462.

Liang, R., Xu, S., Shoemaker, C. F., Li, Y., Zhong, F., & Huang, Q. (2012). Physical and antimicrobial properties of peppermint oil nanoemulsions. Journal of Agricultural and Food Chemistry, 60(30), 7548–55.

Lukomska, J., Malicka, J., Gryczynski, I., & Lakowicz, J. R. (2004). Fluorescence enhancements on silver colloid coated surfaces. Journal of Fluorescence, 14(4), 417–23.

Lundin, M., Blomberg, E., & Tilton, R. D. (2010). Polymer dynamics in layer-by-layer assemblies of chitosan and heparin. Langmuir, 26(5), 3242–3251.

Lundin, M., Solaqa, F., Thormann, E., MacAkova, L., & Blomberg, E. (2011). Layer-by-layer assemblies of chitosan and heparin: Effect of solution ionic strength and pH. Langmuir, 27(12), 7537–7548.

Ma, X., Chang, P. R., & Yu, J. (2008). Properties of biodegradable thermoplastic pea starch/carboxymethyl cellulose and pea starch/microcrystalline cellulose composites. Carbohydrate Polymers, 72(3), 369–375.

Maizura, M., Fazilah, A., Norziah, M. H., & Karim, A. A. (2007). Antibacterial activity and mechanical properties of partially hydrolyzed sago starch-alginate edible film containing lemongrass oil. Journal of Food Science, 72(6), C324–30.

Martins, G. V, Mano, J. F., & Alves, N. M. (2011). Dual Responsive Nanostructured Surfaces for Biomedical Applications. Langmuir, 27(13), 8415–8423.

McClements, D. J. (2005). Food emulsions : principles, practices, and techniques. (C. Press, Ed.). Boca Raton, Fla. : CRC Press.

McClements, D. J. (2011). Edible nanoemulsions: Fabrication, properties, and functional performance. Soft Matter, 7(6), 2297–2316.

McClements, D. J., & Rao, J. (2011). Food-grade nanoemulsions: formulation, fabrication, properties, performance, biological fate, and potential toxicity. Critical Reviews in Food Science and Nutrition, 51(4), 285–330.

Milani, J., & Maleki, G. (2012). Hydrocolloids in food industry. In B. Valdez (Ed.), Food Idustrial Processes–Methods and Equipment (pp. 17–38). Intech.

Morariu, S., Brunchi, C. E., & Bercea, M. (2012). The Behavior of Chitosan in Solvents with Different Ionic Strengths. Industrial & Engineering Chemistry Research, 51(39), 12959–12966.

Norajit, K., Kim, K. M., & Ryu, G. H. (2010). Comparative studies on the characterization and antioxidant properties of biodegradable alginate films containing ginseng extract. Journal of Food Engineering, 98(3), 377–384.

Nuchuchua, O., Sakulku, U., Uawongyart, N., Puttipipatkhachorn, S., Soottitantawat, A., & Ruktanonchai, U. (2009). In vitro characterization and mosquito (Aedes aegypti) repellent activity of essential-oils-loaded nanoemulsions. AAPS PharmSciTech, 10(4), 1234–42.

Oriani, V. B., Molina, G., Chiumarelli, M., Pastore, G. M., & Hubinger, M. D. (2014). Properties of cassava starch-based edible coating containing essential oils. Journal of Food Science, 79(2), E189–94.

Otoni, C. G., Moura, M. R. de, Aouada, F. A., Camilloto, G. P., Cruz, R. S., Lorevice, M. V., Soares, N. de F.F., & Mattoso, L. H. C. (2014). Antimicrobial and physical-mechanical properties of pectin/papaya puree/cinnamaldehyde nanoemulsion edible composite films. Food Hydrocolloids, 41, 188–194.

Otoni, C. G., Pontes, S. F. O., Medeiros, E. A. A., & Soares, N. de F. F. (2014). Edible films from methylcellulose and nanoemulsions of clove bud (Syzygium aromaticum) and oregano (Origanum vulgare) essential oils as shelf life extenders for sliced bread. Journal of Agricultural and Food Chemistry, 62(22), 5214–9.

Pérez-Gago, M. B., & Krochta, J. M. (2001). Lipid particle size effect on water vapor permeability and mechanical properties of whey protein/beeswax emulsion films. Journal of Agricultural and Food Chemistry, 49(2), 996–1002.

Picart, C. (2008). Polyelectrolyte multilayer film: From physico-chemical properties to the control of cellular processes. Current Medicinal Chemistry, 15(7), 685–697.

Picart, C., Lavalle, P., Hubert, P., Cuisinier, F. J. G., Decher, G., Schaaf, P., & Voegel, J.-C. (2001). Buildup Mechanism for Poly(l -lysine)/Hyaluronic Acid Films onto a Solid Surface. Langmuir, 17(23), 7414–7424.

Picart, C., Mutterer, J., Richert, L., Luo, Y., Prestwich, G. D., Schaaf, P., … Lavalle, P. (2002). Molecular basis for the explanation of the exponential growth of polyelectrolyte multilayers. Proceedings of the National Academy of Sciences of the United States of America, 99(20), 12531–5.

Pinheiro, A. C., Bourbon, A. I., Medeiros, B. G. de S., da Silva, L. H. M., da Silva, M. C. H., Carneiro-da-Cunha, M. G., Coimbra, M. A., & Vicente, A. A. (2012).

Interactions between κ-carrageenan and chitosan in nanolayered coatings—Structural and transport properties. Carbohydrate Polymers, 87(2), 1081–1090.

Pires, C., Ramos, C., Teixeira, B., Batista, I., Nunes, L., & Marques, A. (2013). Hake proteins edible films incorporated with essential oils: Physical, mechanical, antioxidant and antibacterial properties. Food Hydrocolloids, 30(1), 224–231.

Qian, C., & McClements, D. J. (2011). Formation of nanoemulsions stabilized by model food-grade emulsifiers using high-pressure homogenization: Factors affecting particle size. Food Hydrocolloids, 25(5), 1000–1008.

Radeva, T., Kamburova, K., & Petkanchin, I. (2006). Formation of polyelectrolyte multilayers from polysaccharides at low ionic strength. Journal of Colloid and Interface Science, 298(1), 59–65.

Rao, J., & McClements, D. J. (2012a). Food-grade microemulsions and nanoemulsions: Role of oil phase composition on formation and stability. Food Hydrocolloids, 29(2), 326–334.

Rao, J., & McClements, D. J. (2012b). Impact of lemon oil composition on formation and stability of model food and beverage emulsions. Food Chemistry, 134(2), 749–57.

Raybaudi-Massilia, R. M., Mosqueda-Melgar, J., & Martin-Belloso, O. (2008). Edible alginate-based coating as carrier of antimicrobials to improve shelf-life and safety of fresh-cut melon. International Journal of Food Microbiology, 121(3), 313–327.

Rhim, J.-W., Lee, J.-H., & Hong, S.-I. (2006). Water resistance and mechanical properties of biopolymer (alginate and soy protein) coated paperboards. LWT - Food Science and Technology, 39(7), 806–813.

Richert, L., Lavalle, P., Payan, E., Shu, X. Z., Prestwich, G. D., Stoltz, J.-F., Schaaf, P., Voegel, J. -C., & Picart, C. (2004). Layer by Layer Buildup of Polysaccharide Films: Physical Chemistry and Cellular Adhesion Aspects. Langmuir, 20(2), 448–458.

Rojas-Graü, M. A., Avena-Bustillos, R. de J., Friedman, M., Henika, P. R., Martin-Belloso, O., & McHugh, T. H. (2006). Mechanical, barrier, and antimicrobial properties of apple puree edible films containing plant essential oils. Journal of Agricultural and Food Chemistry, 54(24), 9262–7.

Rojas-Graü, M. A., Avena-Bustillos, R. de J., Olsen, C., Friedman, M., Henika, P. R., Martin-Belloso, O., Pan, Z., & McHugh, T. H. (2007). Effects of plant essential

oils and oil compounds on mechanical, barrier and antimicrobial properties of alginate-apple puree edible films. Journal of Food Engineering, 81(3), 634–641.

Sæther, H. V., Holme, H. K., Maurstad, G., Smidsrød, O., & Stokke, B. T. (2008). Polyelectrolyte complex formation using alginate and chitosan. Carbohydrate Polymers, 74(4), 813–821.

Salehi, A., Desai, P. S., Li, J., Steele, C. A., & Larson, R. G. (2015). Relationship between Polyelectrolyte Bulk Complexation and Kinetics of Their Layer-by-Layer Assembly. Macromolecules, 48(2), 400–409.

Salvia-Trujillo, L., Rojas-Graü, M. A., Soliva-Fortuny, R. C., & Martín-Belloso, O. (2013). Effect of processing parameters on physicochemical characteristics of microfluidized lemongrass essential oil-alginate nanoemulsions. Food Hydrocolloids, 30(1), 401–407.

Sánchez-González, L., Cháfer, M., Hernández, M., Chiralt, A., & González-Martínez, C. (2011). Antimicrobial activity of polysaccharide films containing essential oils. Food Control, 22(8), 1302–1310.

Sánchez-González, L., Chiralt, A., González-Martínez, C., & Cháfer, M. (2011). Effect of essential oils on properties of film forming emulsions and films based on hydroxypropylmethylcellulose and chitosan. Journal of Food Engineering, 105(2), 246–253.

Schoeler, B., Sharpe, S., Hatton, T. A., & Caruso, F. (2004). Polyelectrolyte Multilayer Films of Different Charge Density Copolymers with Synergistic Nonelectrostatic Interactions Prepared by the Layer-by-Layer Technique. Langmuir, 20(7), 2730–2738.

Sessa, M., Tsao, R., Liu, R., Ferrari, G., & Donsì, F. (2011). Evaluation of the Stability and Antioxidant Activity of Nanoencapsulated Resveratrol during in Vitro Digestion. Journal of Agricultural and Food Chemistry, 59(23), 12352–12360.

Severino, R., Ferrari, G., Vu, K. D., Donsì, F., Salmieri, S., & Lacroix, M. (2015). Antimicrobial effects of modified chitosan based coating containing nanoemulsion of essential oils, modified atmosphere packaging and gamma irradiation against Escherichia coli O157:H7 and Salmonella Typhimurium on green beans. Food Control, 50, 215–222.

Shimoni, G., Shani Levi, C., Levi Tal, S., & Lesmes, U. (2013). Emulsions stabilization by lactoferrin nano-particles under in vitro digestion conditions. Food Hydrocolloids, 33(2), 264–272.

Shiratori, S. S., & Rubner, M. F. (2000). pH-Dependent Thickness Behavior of Sequentially Adsorbed Layers of Weak Polyelectrolytes. Macromolecules, 33(11), 4213–4219.

Shirazi, M. H., Ranjbar, R., Eshraghi, S., Amin, G., Nouri, M. S., & Bazzaz, N. (2008). Inhibitory Effects of Sage Extract on the Growth of Enteric Bacteria. Pakistan Journal of Biological Sciences, 11(3), 487–489.

Shojaee-Aliabadi, S., Hosseini, H., Mohammadifar, M. A., Mohammadi, A., Ghasemlou, M., Hosseini, S. M., & Khaksar, R. (2014). Characterization of κ-carrageenan films incorporated plant essential oils with improved antimicrobial activity. Carbohydrate Polymers, 101, 582–91.

Solans, C., Izquierdo, P., Nolla, J., Azemar, N., & Garcia-Celma, M. J. (2005). Nano-emulsions. Current Opinion in Colloid & Interface Science, 10(3), 102–110.

Stang, M., Karbstein, H., & Schubert, H. (1994). Adsorption kinetics of emulsifiers at oil—water interfaces and their effect on mechanical emulsification. Chemical Engineering and Processing: Process Intensification, 33(5), 307–311.

Tokle, T., & McClements, D. J. (2011). Physicochemical properties of lactoferrin stabilized oil-in-water emulsions: Effects of pH, salt and heating. Food Hydrocolloids, 25(5), 976–982.

Ultee, A., Bennik, M. H. J., & Moezelaar, R. (2002). The phenolic hydroxyl group of carvacrol is essential for action against the food-borne pathogen Bacillus cereus. Applied and Environmental Microbiology, 68(4), 1561–1568.

Vargas, M., Cháfer, M., Albors, A., Chiralt, A., & González-Martínez, C. (2008). Physicochemical and sensory characteristics of yoghurt produced from mixtures of cows' and goats' milk. International Dairy Journal, 18(12), 1146–1152.

Vargas, M., Perdones, Á., Chiralt, A., Cháfer, M., & González-Martínez, C. (2011). Effect of homogenization conditions on physicochemical properties of chitosan-based film-forming dispersions and films. Food Hydrocolloids, 25(5), 1158–1164.

Vidyasagar, A., Sung, C., Losensky, K., & Lutkenhaus, J. L. (2012). pH-Dependent Thermal Transitions in Hydrated Layer-by-Layer Assemblies Containing Weak Polyelectrolytes. Macromolecules, 45(22), 9169–9176.

Xu, J., Yang, L., Hu, X., Xu, S., Wang, J., & Feng, S. (2015). The effect of polysaccharide types on adsorption properties of LbL assembled multilayer films. Soft Matter, 11(9), 1794–9.

Yoo, D., Shiratori, S. S., & Rubner, M. F. (1998). Controlling Bilayer Composition and Surface Wettability of Sequentially Adsorbed Multilayers of Weak Polyelectrolytes. Macromolecules, 31(13), 4309–4318.

Yuan, W., Dong, H., Li, C. M., Cui, X., Yu, L., Lu, Z., & Zhou, Q. (2007). pH-Controlled Construction of Chitosan/Alginate Multilayer Film: Characterization and Application for Antibody Immobilization. Langmuir, 23(26), 13046–13052.

Zhang, J., Senger, B., Vautier, D., Picart, C., Schaaf, P., Voegel, J.-C., & Lavalle, P. (2005). Natural polyelectrolyte films based on layer-by layer deposition of collagen and hyaluronic acid. Biomaterials, 26(16), 3353–61.

Ziani, K., Fang, Y., & McClements, D. J. (2012). Fabrication and stability of colloidal delivery systems for flavor oils: Effect of composition and storage conditions. Food Research International, 46(1), 209–216.

Zúñiga, R. N., Skurtys, O., Osorio, F., Aguilera, J. M., & Pedreschi, F. (2012). Physical properties of emulsion-based hydroxypropyl methylcellulose films: effect of their microstructure. Carbohydrate Polymers, 90(2), 1147–58.

PUBLICATIONS

SECTION I. NANOEMULSIONS AND EDIBLE FILMS

CHAPTER I: *EDIBLE FILMS FROM ESSENTIAL-OIL-LOADED NANOEMULSIONS: PHYSICOCHEMICAL CHARACTERIZATION AND ANTIMICROBIAL ACTIVITY*

Acevedo-Fani, A., Salvia-Trujillo, L., Rojas-Graü, M. A., & Martín-Belloso, O

Food Hydrocolloids (2015); 47: 168-177

ABSTRACT

Edible films including active ingredients can be used as an alternative to preserve food products. Essential oils (EOs) exhibit antimicrobial activity against pathogenic microorganisms but their low water solubility limits the application in foods. To improve water dispersion and protect EOs from degradation, nano-sized emulsions emerge as a viable alternative. Nanoemulsions containing EOs and polysaccharides could be used to form edible films with functional properties. This study was focused on the evaluation of physical, mechanical and antimicrobial properties of alginate-based edible films formed from nanoemulsions of EOs. Nanoemulsions containing thyme (TH-EO), lemongrass (LG-EO) or sage (SG-EO) oil as dispersed phase and sodium alginate solution as continuous phase were prepared. The average droplet size of nanoemulsions was reduced after the microfluidization treatment exhibiting multimodal size distributions. The ζ-potentials of nanoemulsions were between -41 mV and -70 mV depending on the type of EO used. The lowest whiteness index was found in SG-EO nanoemulsions, whereas those containing TH-EO showed the highest value. Films formed from SG-EO nanoemulsions exhibited higher transparency, water vapor resistance and flexibility than films formed from TH-EO or LG-EO. Edible films containing TH-EO were those with the strongest antimicrobial effect against inoculated *Escherichia coli,* achieving up to 4.71 Log reductions after 12 h. Results obtained in the present work evidence the suitability of using nanoemulsions with active ingredients for the formation of edible films, with different physical and functional properties.

Keywords: Nanoemulsions, microfluidization, essential oils, edible films, antimicrobial activity, sodium alginate

1. Introduction

Edible films have been proposed as an alternative of food packaging to improve the quality and safety of food products. This technology protects foods from dehydration and acts as gases barrier with the surrounding media. In addition, edible films may serve as carriers of active compounds such as antimicrobials, antioxidants and texture enhancers, among others. Sodium alginate is a polysaccharide isolated from marine brown algae, widely used in the food industry as thickening agent, which also has film-forming properties (Krochta, Baldwin, & Nisperos-Carriedo, 1994). Essential oils (EOs) are aromatic oily liquids extracted from plant materials and commonly utilized as flavoring in foodstuffs (Burt, 2004). Their antimicrobial properties against several pathogenic microorganisms involved in foodborne illness have been demonstrated in previous investigations (Alboofetileh, Rezaei, Hosseini, & Abdollahi, 2014; Oriani, Molina, Chiumarelli, Pastore, & Hubinger, 2014). For this reason, the scientific community and food industry are considering the use of EOs as potential preservatives of natural origin. Nevertheless, their incorporation in food systems is mainly limited by flavor considerations, since effective antimicrobial doses may exceed organoleptic acceptance levels (Lambert, Skandamis, Coote, & Nychas, 2001). In addition, EOs have low-water solubility, meaning their dispersion within aqueous-based products is rather difficult.

Nanoemulsions are being increasingly used to encapsulate, protect and deliver lipophilic ingredients to liquid foods or minimally processed fruits and vegetables (Bhargava, Conti, da Rocha, & Zhang, 2015; Donsì, Cuomo, Marchese, & Ferrari, 2014; Kim, Ha, Choi, & Ko, 2014). Literature refer nanoemulsions as emulsions with very small droplet size, below 100 nm (McClements, 2011; Solans, Izquierdo, Nolla, Azemar, & Garcia-Celma, 2005). The small particle size in nanoemulsions has two important consequences: i) the possibility of enhancing physicochemical properties and stability; and ii) the ability of improving biological activity of lipophilic compounds by increasing the surface area per unit of mass (McClements & Rao, 2011). This fact also allows using lower doses of active ingredients. Recent studies have shown an enhancement of the physical properties of EOs-loaded nanoemulsions regarding to their equivalent conventional emulsions (Salvia-Trujillo, Rojas-Graü, Soliva-Fortuny, & Martín-Belloso,

2013). In addition, it has been also observed a higher antibacterial activity in nanoemulsions containing EOs (Buranasuksombat, Kwon, Turner, & Bhandari, 2011; Liang et al., 2012; Severino et al., 2015).

In this sense, nanoemulsions based on polysaccharides such as alginate and EOs as antimicrobial agents may be used for edible films formation, which could be considered a new generation of edible packaging. The particular properties observed in nanoemulsions regarding to the conventional emulsions could be extrapolated to the physicochemical and functional properties of the edible films formed from them. Previous studies have evaluated the formation of films based on nanoemulsions prepared by low-energy methods and high-energy techniques such as ultrasounds or high-speed homogenization (Bilbao-Sáinz, Avena-Bustillos, Wood, Williams, & McHugh, 2010; Otoni, Pontes, Medeiros, & Soares, 2014; Otoni, Moura, et al., 2014). However, up to our knowledge, systematic studies have not been reported about the properties of polysaccharide-based films made from EOs-loaded nanoemulsions prepared by microfluidization. Therefore, the purpose of this study was to evaluate the antimicrobial, physical and mechanical properties of edible films obtained from alginate-based nanoemulsions loaded with EOs (Thyme, TH-EO; lemongrass, LG-EO or sage, SG-EO), as well as characterizing the physicochemical properties of the EO nanoemulsions relating them with the edible film properties.

2. Materials and methods

Food grade sodium alginate was supplied by FMC Biopolymers Ltd (Scotland, U.K.). Nonionic surfactant (Tween 80) was purchased from Scharlau (Spain), and plasticizer (glycerol) was provided by Fisher Scientific (U.K.). Thyme (TH-EO; *Thymus vulgaris*), lemongrass (LG-EO; *Cymbopogon citratus*) and sage (SG-EO; *Salvia officinalis*) essential oils were purchased from Essential arôms (Spain).

2.1. Preparation of Film-Forming Nanoemulsions (FFN)

Sodium alginate dispersions were prepared by dissolving 3% w/v in double distilled water at 70°C. A coarse emulsion was obtained by mixing alginate dispersions at room temperature, glycerol (2% v/v), Tween 80 (3% v/v) and TH-EO, LG-EO or SG-EO (1% v/v) in a high-speed blender at 17,500 rpm for

2 min (Ultra-turrax, Jake & Kunkel, Staufen, Germany). To prepare nanoemulsions, coarse emulsions were pumped into the microfluidizer (M110P, Microfluidics, Massachusetts, USA) at 150 MPa for three cycles. Temperature of nanoemulsions during processing was maintained below 15 ºC with an external coiling coil immersed in an ice-water bath and placed at the exit of the interaction chamber. All samples were prepared using ultra-pure water obtained from a Milli-Q filtration system. Alginate films (ALG) were also made without the addition of EO (alginate 3% w/v, Tween 80 3% v/v and glycerol 2 % v/v) to be considered as control.

2.2. Characterization of Film-Forming Nanoemulsions (FFN)

2.2.1. Particle size and ζ-potential

Particle size, polydispersity index and ζ-potential were analyzed with a Zetasizer Nano ZS laser diffractometer (Malvern Instruments Ltd, Worcestershire, U.K.). Particle size was measured by dynamic light scattering (DLS) at 633 nm, 25 ºC and using a backscatter detector of 173º. FFN were first diluted with ultra-pure water to 1:20 to avoid multiple scattering effects. The average droplet size (z-average) and polydispersity index were reported. Polydispersity index (PDI) value is a measure of heterogeneity in the droplet size distribution. PDI values close to 0 indicate homogenous size distributions, whereas PDI values close to 1 indicate heterogenous size distributions. The surface charge at the interface of oil droplets within FFN (ζ-potential) was measured by phase-analysis light scattering (PALS).

2.2.2. Whiteness index and viscosity

The color of the FFN was determined with a Minolta CR-400 colorimeter (Konica Minolta Sensing, Inc., Osaka, Japan), using an illuminant D_{65} and the 10º observer angle. The device was calibrated in a white standard plate (Y = 94, x = 0.3158, y = 0.3222). A crystal flat-faced cuvette was filled with FFN and then placed at the top of the measuring device of the colorimeter. CIE L^*, a^* and b^* values were utilized to calculate whiteness index (WI) throughout Eq. (1) (Vargas et al., 2008):

$$WI = 100 - \sqrt{(100 - L^*)^2 + \left(a^{*^2} + b^{*^2}\right)} \quad (1)$$

The viscosity of FFN was measured in aliquots of 10 mL using a vibro-viscometer SV-10 (A&D Company, Tokyo, Japan), vibrating at 30 Hz and constant amplitude.

2.3. Film formation

Nanoemulsions and alginate film-forming solutions were treated with a vacuum pump to remove air bubbles and avoid the presence of micro-holes in film structure. Then, oil-containing and control films were formed by casting in crystal plates of 30 x 40 cm, previously covered with Mylar paper. Films were dried at room temperature for 24 h and peeled off from Mylar paper for further determinations.

2.4. Characterization of edible films

2.4.1. Scanning Electron Microscopy

Aluminum stubs with films were dried in a heater at 60 ºC for 48 h. Films were fixed with carbon and metalized with evaporated gold in a Blazers SCD 050 sputter coater (Balzers Union AG, Liechtenstein) to grant electrical conductive properties. Microstructure of films surface were examined using a Scanning Electron Microscope with an acceleration voltage of 10 kV and a working distance of 10 mm (DSM 940 A, Zeiss, Germany).

2.4.2. Color and opacity

Film color and opacity were measured with a colorimeter (CR-400, Konica Minolta Sensing, Inc., Osaka, Japan), using an illuminant D_{65} and the 10º observer angle. The instrument was calibrated with a standard white plate (Y = 94.00, x = 0.3158, y = 0.3222). Measurements were performed by placing film squares of 30 mm x 30 mm onto a white background. Chromaticity coordinates CIE L^*, a^*, b^* were recorded to obtain the color difference (ΔE^*), which was calculated using Eq. (2) (Pires et al., 2013):

$$\Delta E^* = ((L^* - L_o)^2 + (a^* - a_o)^2 + (b^* - b_o)^2)^{0.5} \quad (2)$$

where L^*, a^*, b^* are the color coordinates of the films, and L_o, a_o, b_o values are those corresponding to the white background (L_o = 90.97, a_o = 0.08, b_o = -0.28).

Film opacity was obtained by measuring the CIE *Y* coordinates of edible films (30 mm x 30 mm) onto a white and black background. Opacity was calculated by Eq. (3) (Pires et al., 2013):

$$Opacity = {}^{Y_b}/_{Y_w} \times 100 \quad (3)$$

where Y_b is the *Y* coordinate measured on the black background, and Y_w is the *Y* coordinate measured on the white background.

2.4.3. Film thickness

Film thickness was determined with IP 65 micrometer (Mitutoyo Manufacturing, Tokio, Japan). Thickness was taken in five random points of the film.

2.4.4. Water vapor permeability

Water vapor permeability (WVP) of films was evaluated gravimetrically at 25 ºC using a modified version of ASTM standard method E96-00 (ASTM, 2000). Methylmethacrylate test cups (internal diameter of 3 cm, outer diameter 4.5 cm and depth of 2.0 cm) were used to determine WVP. Cups were filled with distilled water (6 ml) and circular samples of films were placed over the cups and sealed using a cap with a rubber O-ring. The diameter of film exposure was 3 cm. Cups with films were placed in glass containers with hermetic covers containing a saturated solution of magnesium chloride ($MgCl_2.6H_2O$), with 33 % of relative humidity at 25 ºC. Cups weights were recorded at 60 min intervals over 6 h.

Weight loss data versus time were analyzed by lineal regression to obtain the slope (m_1) of the curve in g/s. Water vapor transmission rates (WVTR) through the film and WVP were calculated as described in Eqs. (4) and (5) (Chinnan & Park, 1996; Kaya & Kaya, 2000).

$$WVTR = m_1/A \quad (4)$$

$$WVP = L \times WVTR/(\rho_i - \rho_a) \quad (5)$$

where A (m^2) is the exposed film area, ρ_i (Pa) and ρ_a (Pa) are the vapor pressures of saturated air and air with 33% RH, respectively, at 25 ºC. L is the average film thickness (m).

2.4.5. Mechanical properties

Edible films were evaluated by tensile tests (elongation at break, EAB; and tensile strength, *TS*) and puncture tests (puncture force, *PF*) using a TA-TX2 texture analyzer (Stable Micro Systems, Goldaming, Surrey, U.K.). TS and EAB were determined by ASTM standard method D882-97 (ASTM, 1991). Rectangular strips (25 mm x 100 mm) were equilibrated into a cabin with a saturated solution of nitrate magnesium ($Mg(NO_3)_2$) (Fisher Scientific, U.K.) with HR 50 ± 5 % at 25 ºC during 5 days. After equilibration time, strips were placed in self-tightening roller grips and measurements were performed with an initial grip separation of 50 mm, a crosshead speed of 1 mm/s and using a load cell of 5 kg. TS and EAB were calculated by Eqs. (6) and (7):

$$TS = F_{max}/A \quad (6)$$

$$EAB = \left(L/L_o\right) \times 100 \quad (7)$$

where F_{max} is the maximum load for breaking films (N), A is the cross-sectional area of the sample (thickness x width). L_o represents the initial gage length (50 mm) of the sample, L the final length of the film before the moment of rupture.

Puncture analyses were determined by ASTM D6241-04 standard method (ASTM, 2004). The samples (30 mm x 30 mm) were equilibrated at the same conditions used for tensile tests. Films were placed on a film support ring adjusted to the texture analyzer. An aluminum circular plate with two screws was fitted on the film to avoid slippage. Then, a stainless steel spherical probe of 5 mm diameter scrolled perpendicularly to the film surface at a constant speed of 1 $mm.s^{-1}$ until cross the sample. PF was obtained from the force-displacement curves recorded by Texture Exponent 32 software (Stable Micro Systems, Goldaming, Surrey, U.K.).

2.4.6. Antimicrobial activity analysis

2.4.6.1. Inoculum preparation

A strain of *Escherichia coli* 1107 (Laboratoire de Répression des Fraudes (LRF), Montpellier, France) was provided from the culture collection of the Department of Food Technology of the University of Lleida, Spain. The *E. coli* culture was kept refrigerated at 5 ºC in slant tubes with Tryptone Soy Agar (TSA) (Biokar Diagnostics, France). The strain was then grown in Tryptone Soy Broth (TSB) (Biokar Diagnostics, France) at 37 ºC for 12 h, to obtain cells in stationary growth phase. The final concentration of the culture was 10^9 UFC.mL^{-1}.

2.4.6.2. Antimicrobial activity

Antimicrobial activity of edible films was determined according to their *E. coli* inactivation with a method described by other authors with some modifications (Kristo et al., 2008; Sánchez-González, Cháfer, et al., 2011). TSA containing NaCl 3% was used as a model of solid food system (TSA-NaCl) with high pH (∼6.5) and high a_w (∼0.98). Approximately 20 mL of TSA-NaCl medium was poured into petri dishes of 9 cm of diameter, solidified and stored under refrigeration. The *E. coli* culture was diluted to reach a concentration of 10^6 UFC/mL and aliquots of 1 µL were spread on the agar surface and coated with edible film circles of 9 cm diameter. TSA-NaCl plates inoculated and uncoated were used as control. Straightaway, coated and uncoated TSA-NaCl plates were left at room temperature for 12 h. During the first 4 h, antimicrobial activity of TSA-NaCl plates was evaluated hourly. Afterwards, essays were carried out every 2 h. For this purpose, 10 g of agar were carefully removed aseptically from Petri dishes and put in sterile stomacher bags with 90 mL of saline peptone (Biokar Diagnostics, France). Bags were homogenized for 2 min in a Stomacher blender. Serial dilutions were prepared and spread onto McConkey-Sorbitol Agar (Biokar Diagnostics, France). Plates were incubated at 37 ºC for 24 h and after colonies were counted.

2.5. Statistical analysis

Droplet size, ζ-potential, viscosity and whiteness index of EO-nanoemulsions, as well as color, thickness and WVP parameters of edible films were performed in triplicate. Antimicrobial activity was run in duplicate and

mechanical analyses were evaluated in ten samples per type of film. Two repetitions of each type of film were prepared for all the tests. The one-way analysis of variance (ANOVA) was applied to analyze data using the Statgraphics Plus 5.1 software package (Statistical Graphics Co., Rockville, MD, EE.UU). Fisher's least significant difference (LSD) procedure was applied to evaluate differences among average results with a significant level of 5%. Pearson's correlation coefficients were estimated to establish relationships between the physical properties of both nanoemulsions and edible films.

3. Results and discussion

3.1. Film-Forming Nanoemulsions properties

3.1.1. Droplet size and size distribution

The droplet size of nanoemulsions containing different EOs in sodium alginate solution were measured since they might have a relevant impact on features such as, color, permeability, or mechanical properties of edible films. The corresponding oil droplet size distribution expressed by intensity can be seen in Fig. 1. The size distributions were multimodal regardless the EO type, presenting several peaks corresponding to oil droplets of different size. In general, it was observed two major intensity peaks around 20 nm and 190 nm in the droplet size distributions, and a small peak around 6000 nm. The peak at 20 nm could be related to the presence of surfactant micelles that were not adsorbed at the oil/water interface of nanoemulsions, which are typically around 10 nm (Heydenreich, 2003; Rao & McClements, 2012a), or to oil droplets disrupted during the microfluidization process. The peak around 190 nm corresponded to EOs droplets (Cramer Flores et al., 2011; Liang et al., 2012). Residual intensity peaks close to the detection limit of the equipment (6000 nm) suggested the presence of larger oil droplets that were not disrupted or alginate colloidal structures. Nanoemulsions loaded with SG-EO presented the highest intensity peak at the 20 nm region indicating that most of the droplets had very small diameters after microfluidization. Nanoemulsions containing TH-EO showed the lowest peak at 20 nm, which could be due to the fact that surfactant molecules were mostly adsorbed at the oil/water interface compared to those formed with SG-EO or LG-EO, or the surfactant activity was affected by the presence of alginate molecules and did not adsorbed quickly enough during the formation of nanodroplets,

obtaining more droplets in the 190 nm region than in the 20 nm region. It is known that the surface activity of small molecule surfactants is determined by the oil polarity (Dickinson, 2009; Kralova & Sjöblom, 2009; Stang, Karbstein, & Schubert, 1994). TH-EO have shown a relatively high water solubility as it has been reported the need of ripening inhibitors, such as corn oil, in order to change EO polarity, thereby enabling its stabilization in nanoemulsions (Chang, McLandsborough, & McClements, 2012; Rao & McClements, 2012a). Salvia and co-workers (2013) reported narrow size distributions in nanoemulsions made with sodium alginate (1 % w/v) and LG-EO (1 % v/v) treated by microfluidization at the same processing conditions used in this study. Multimodal size distributions obtained in FFN prepared in the present work could be attributed to the high viscosity of the system due to the presence of sodium alginate at 3 % w/v in the continuous phase. The high viscosity of nanoemulsions could affect the efficacy of droplets disruption because the microfluidizer was not able to generate sufficiently intense disruptive forces at the pressure used (Jafari, Assadpoor, He, & Bhandari, 2008). Other authors have attributed the polydisperse behavior of nanoemulsions to the possible presence of instability phenomena after homogenization due to re-coalescence of oil droplets (Atarés, Bonilla, & Chiralt, 2010).

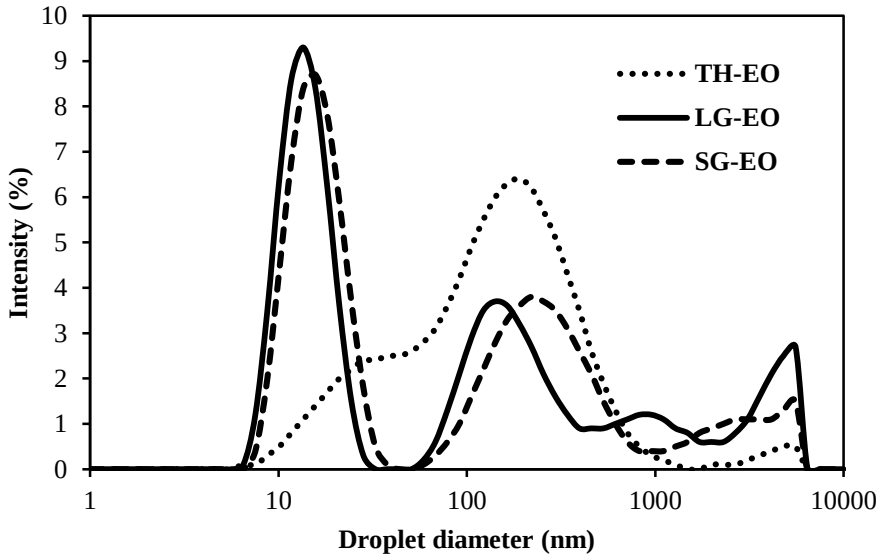

Fig. 1. Droplet size distributions expressed in intensity of film-forming EOs-loaded nanoemulsions, (TH-EO: thyme oil; LG-EO: lemongrass oil; SG-EO: sage oil).

On the other hand, the average droplet size of nanoemulsions of TH-EO, LG-EO and SG-EO were 82 ± 3 nm, 41 ± 9 nm, 35 ± 7 nm, respectively, showing

polydispersity indexes ranging from 0.65 to 0.52 (Table 1). In a preliminary study, the droplet size of coarse emulsions was measured presenting average droplet sizes above those obtained in nanoemulsions (TH: 236 ± 30 nm, LG: 591 ± 50 nm, SG: 113 ± 8 nm). The z-average size is a consistent parameter given for monodisperse systems measured by the DLS technique. This value is usually quite near to the peak of the particle size distribution. However, when samples present non-monodisperse distributions, interpretation of the z-average is more complicated and it is necessary to consider the size distributions regarding the mass and number of particles. Particle size measurements by the DLS technique are generated from the analysis of the fluctuations in scattered light intensity where large particles scatter light more strongly than small particles. In this sense, a small population of large droplets could be represented as a big intensity peak, whereas a similar population of small droplets is shown as a smaller intensity peak. Droplet size distributions presented in terms of volume of the particles were analyzed, in order to find relevant effects of peaks observed in the intensity distribution graph on the overall droplet size distribution of nanoemulsions. In all cases, it was found a major peak located below 100 nm, which could confirm that most of the EO droplets within nanoemulsions showed diameters in the nano-range, suggesting that the majority of oil droplets were disrupted by microfluidization.

In addition, the type of EO significantly affected ($p < 0.05$) average droplet size of nanoemulsions (Table 1). Incorporation of TH-EO led to larger droplet sizes than in nanoemulsions containing SG-EO, which suggests different grades of affinity between the oil and the alginate phases as well as the non-ionic surfactant used in the formulation. This particular effect can be related to the chemical composition of EOs, which is highly variable depending on their biological origin. The presence of surface-active substances in EO composition itself could increase their water solubility. EOs containing surfactant-like compounds may accumulate at the oil/water interface lowering the interfacial tension in emulsions and facilitating the droplet disruption during homogenization. In addition, other important properties such as oil polarity and viscosity can intervene on the resulting droplet size (Edris & Malone, 2012; Ziani, Fang, & McClements, 2012).

Table 1. Physicochemical characterization of the film-forming nanoemulsions loaded with different EOs.

Nanoemulsion	Z-average (nm)	PDI	ζ- potential (mV)	WI	Viscosity (mPa.s)
TH-EO	82 ± 3b	0.563 ± 0.024a	-44 ± 6a	27.95 ± 0.06a	452 ± 43a
LG-EO	41 ± 9a	0.52 ± 0.05a	-41 ± 3a	25.38 ± 0.14b	616 ± 62b
SG-EO	35 ± 7a	0.65 ± 0.04b	-70 ± 9b	23.53 ± 0.10c	473 ± 19a

TH-EO: thyme oil; LG-EO: lemongrass oil; SG-EO: sage oil. Z-average is the mean diameter droplet size, PDI refers to polydispersity index, WI is the whiteness index. Values were given as mean ± standard deviations. a.b,c mean values with same superscript within a column are not significantly different ($p < 0.05$).

3.1.2. ζ-potential

The electrical charge of TH-EO, LG-EO and SG-EO droplets in nanoemulsions are shown in Table 1. The ζ-potential values ranged between -41 mV and -70 mV. In general, electrical charge of droplets is governed by the charge of surfactants adsorbed around oil droplets, which can be of anionic, cationic or non-ionic nature. Nanoemulsions prepared in this study contained a non-ionic surfactant (Tween 80); then, one would expect an electrical charge close to zero. However, results showed oil droplets in nanoemulsions presented ζ-potentials highly negative. In this sense, it has been described that the incorporation of ionic biopolymers in the continuous phase of emulsions can change the ζ-potential of oil droplets (Dickinson, 2003). Although, most biopolymers work as thickening agents rather than surfactants in emulsions, they can be partially adsorbed to oil droplets by different types of interactions in certain conditions (Dickinson, 2009). Therefore, the negative electrical charge observed in EOs nanoemulsions stabilized with a non-ionic surfactant can be attributed to the adsorption of sodium alginate molecules dispersed in the continuous phase, due to their anionic nature. Choi, Kim, Cho, Hwang, and Kim (2011) previously observed negative electrical charge in multilayer nanoemulsions containing capsaicin and Tween 80 when they incorporated the oil-surfactant phase in alginate

solutions. It has been described that electrical charge of droplets plays an important role in nanoemulsions stability. When this charge is sufficiently large, droplets are prevented from aggregation because of the electrostatic repulsion among them. Droplets with electrical charge above 30 mV or below -30 mV are considered to be stable to within the nanoemulsion system (Heurtault, 2003). Therefore, nanoemulsions formed in the present study could be considered stable by electrostatic mechanisms.

Moreover, electrical charge of oil droplets was significantly ($p < 0.05$) influenced by the EO type. Nanoemulsions formed with SG-EO showed the largest ζ-potential in comparison with those containing LG-EO and TH-EO, which might be related with to the presence of ionizable groups in EOs composition that lead to different electrostatic interactions among oil, surfactant and biopolymer chains at the interface of the system. According to our results, Bonilla, Atarés, Vargas, and Chiralt (2012) found differences between the ζ-potentials of emulsions containing basil and thyme oil as disperse phase and chitosan in the continuous phase.

3.1.3. Whiteness index

Whiteness index values (WI) of EOs-loaded nanoemulsions are shown in Table 1. All nanoemulsions presented a visual appearance rather translucent; however, measurements of WI showed slight differences depending on EO type. For instance, SG-EO nanoemulsions presented the lowest WI with 23.53; whereas, LG-EO and TH-EO nanoemulsions showed the highest with 25.38 and 27.95, respectively. It is well known that emulsion appearance is mainly determined by the presence of oil droplets, therefore parameters such as droplet size, concentration and refractive index directly influence the overall emulsions optical properties (Chantrapornchai, Clydesdale, & McClements, 1998).

Nanoemulsions are described as slightly turbid systems, which it is attributed to the fact that small droplets scatter light weakly; therefore, as the droplet size increase, the light scattering is strong and emulsions tend to be opaque. In most of the cases, transparency of film-forming solutions is desirable in order to obtain films that scarcely modify the food color. In this study, it was observed that WI decreased as the droplet size lessened, thereby indicating

that optical properties of nanoemulsions were dependent on the particle size of nanoemulsions.

3.1.4. Viscosity

Table 1 shows viscosities of nanoemulsions including EOs as disperse phase and sodium alginate as continuous phase. Viscosity is one of the most relevant parameters in emulsions since it has a significant effect on system stability and depends on the rheology of emulsion phases. The viscosity of pure sodium alginate solutions was 800 mPa.s. However, nanoemulsions exhibited significantly lower viscosity values than sodium alginate solutions (Table 1). This behavior may be explained by the effect of microfluidization on biopolymer viscosity, since high-shear forces can induce conformational changes or degradation of polymer chains, changing their molecular weight. Previous authors have confirmed this trend by subjecting several types of biopolymer-based emulsions to high-shear homogenization (Bonilla et al., 2012; Salvia-Trujillo et al., 2013). Moreover, the EO type significantly ($p < 0.05$) affected viscosity of nanoemulsions, being those with LG-EO incorporated the most viscous (616 ± 62 mPa.s). Since EOs are complex mixtures of different components, this might lead to different adsorption kinetics between alginate molecules and oil droplets, thus changing the initial concentration of biopolymer in the continuous phase and thereby, changing the emulsion viscosity (Bonilla et al., 2012).

3.2. Edible films properties

3.2.1. Microstructure

Microstructure of edible films based on EOs nanoemulsions was examined to get some insights on nanodroplets organization along the biopolymer matrix, and its possible influence on the film properties. SEM images in Fig. 2 correspond to the surface of alginate films (ALG) and those containing TH-EO, LG-EO and SG-EO. Fig. 2A shows the film top that was dried against air, whereas Fig. 2B presents the film surface that was dried facing the support paper. As a general trend, microstructure of films made from nanoemulsions was rougher than ALG films (oil-free). The increase in surface coarseness with the presence of EOs have been previously observed by other authors (Norajit, Kim, & Ryu, 2010; Shojaee-Aliabadi et al., 2014). Sánchez-González and co-

workers (2011a) attributed this fact to the migration of oil droplets upwards the films and further volatilization during water evaporation, resulting in a holey structure. Moreover, it was observed different grades of roughness in the film side in contact with air according to the EO type (Fig. 2A). In the case of LG-EO films, noticeable oil body aggregates were observed suggesting that oil droplets were positioned at the film surface in contact with air during drying. On the other hand, edible films obtained from TH-EO or SG-EO nanoemulsions showed continuous surfaces with small circular protuberances, which indicated a better embedding of nanodroplets inside alginate matrix. It has been reported that films made from small droplet size emulsions have shown smoother surface than those obtained from large droplet size emulsions leading to a better stability of droplets within film structure (Fabra, Pérez-Masiá, Talens, & Chiralt, 2011).

In contrast, SEM images in Fig. 2B showed all film surfaces in contact to the support were rather uniform and absence of protuberances regardless of EO type, which suggested that alginate molecules were preferentially located near the plastic support during drying process. Generally, emulsion-based films experiment a reorganization of lipophilic and hydrophilic components originating a bilayer fashion structure. In concordance with the images observed in Fig. 2A and B, films formed in this study evidenced a structural arrangement of alginate molecules and EOs governed by their chemical affinity.

3.2.1. Color and opacity

The optical properties of edible films can change the overall appearance of food products, affecting the consumer acceptance. Table 2 shows optical properties of alginate films (ALG) and those formed from EOs nanoemulsions. The EO type significantly ($p < 0.05$) affected L^*, a^*, b^* parameters and difference of color (ΔE^*) in edible films. Lightness, expressed by coordinate L^* was higher in films based on LG-EO and SG-EO nanoemulsions, whereas ALG films and those including TH-EO showed the lowest values. Coordinate a^*, which negative values indicates a green color, significantly decreased to -0.83 ± 0.05 in films containing TH-EO, whereas the other films remained around -0.40. The coordinate b^*, which positive values refer to yellow color, showed a similar trend where the most positive value (6.9 ± 0.6) was observed in films containing TH-EO, thus indicating that these films had a light greenish-

yellowish tone. This could be explained by the presence of phenolic compounds in TH-EO, which might have light adsorption at low wavelength (Jouki, Mortazavi, Yazdi, & Koocheki, 2014). Furthermore, the difference of color (*ΔE**) was higher in edible films with TH-EO (58 ± 9), than in those containing SG-EO and LG-EO (11.9 ± 1.4 and 13 ± 3, respectively). In this particular case, we found a strong positive correlation between droplet size of nanoemulsions and *ΔE** values of the matching films, with r = 0.9424 (table 4). This means that *ΔE** of edible films was mainly influenced by the droplet size of their film-forming nanoemulsions, and difference of color decreased as the droplet size decreased.

We also have found strong relationship between *ΔE** of films and whiteness index of nanoemulsions (r = 0.9128). These two correlations let us stablish the robust effect of the optical properties of nanoemulsions on the color characteristics of films made from them.

Table 2. *L**, *a**, *b** values, color difference (*ΔE**) and opacity of alginate films and films made from EO nanoemulsions.

Film	*L**	*a**	*b**	Δ*E**	Opacity
ALG	89.61 ± 0.17^{a}	-0.47 ± 0.03^{b}	4.4 ± 0.4^{a}	24 ± 4^{a}	6.7 ± 0.4^{ab}
TH-EO	88.54 ± 0.25^{b}	-0.83 ± 0.05^{a}	6.9 ± 0.6^{b}	58 ± 9^{b}	7.4 ± 0.5^{b}
LG-EO	93.19 ± 0.19^{c}	-0.47 ± 0.12^{bc}	2.5 ± 0.4^{c}	13 ± 3^{c}	9.7 ± 1.9^{c}
SG-EO	92.72 ± 0.16^{d}	-0.42 ± 0.03^{c}	2.6 ± 0.3^{c}	11.9 ± 1.4^{c}	5.69 ± 0.25^{a}

ALG: alginate films; TH-EO: thyme essential oil films; SG-EO: sage essential oil films; LG-EO: lemongrass essential oil films. Data reported are mean values ± standard deviations. a,b,c values with the same superscript letters in the same column are not significantly different (p < 0.05).

Opacity of films was significantly different (p < 0.05) depending on EO type. Edible films based on LG-EO nanoemulsions showed the highest value (9.7 ± 1.9) compared with ALG films and those made of TH-EO and SG-EO nanoemulsions. This behavior could be explained by the differences in surface roughness observed in the films (Fig. 2A). LG-EO films presented a coarse surface caused by the presence of oil droplets that moved upwards the film in the drying process, which in turn, could have increased light scattering and

led to higher opacity values. On the contrary, films made from TH-EO and SG-EO presented homogenous surfaces due to a better entrapment of oil droplets within structure, and therefore, light scattering could have diminished.

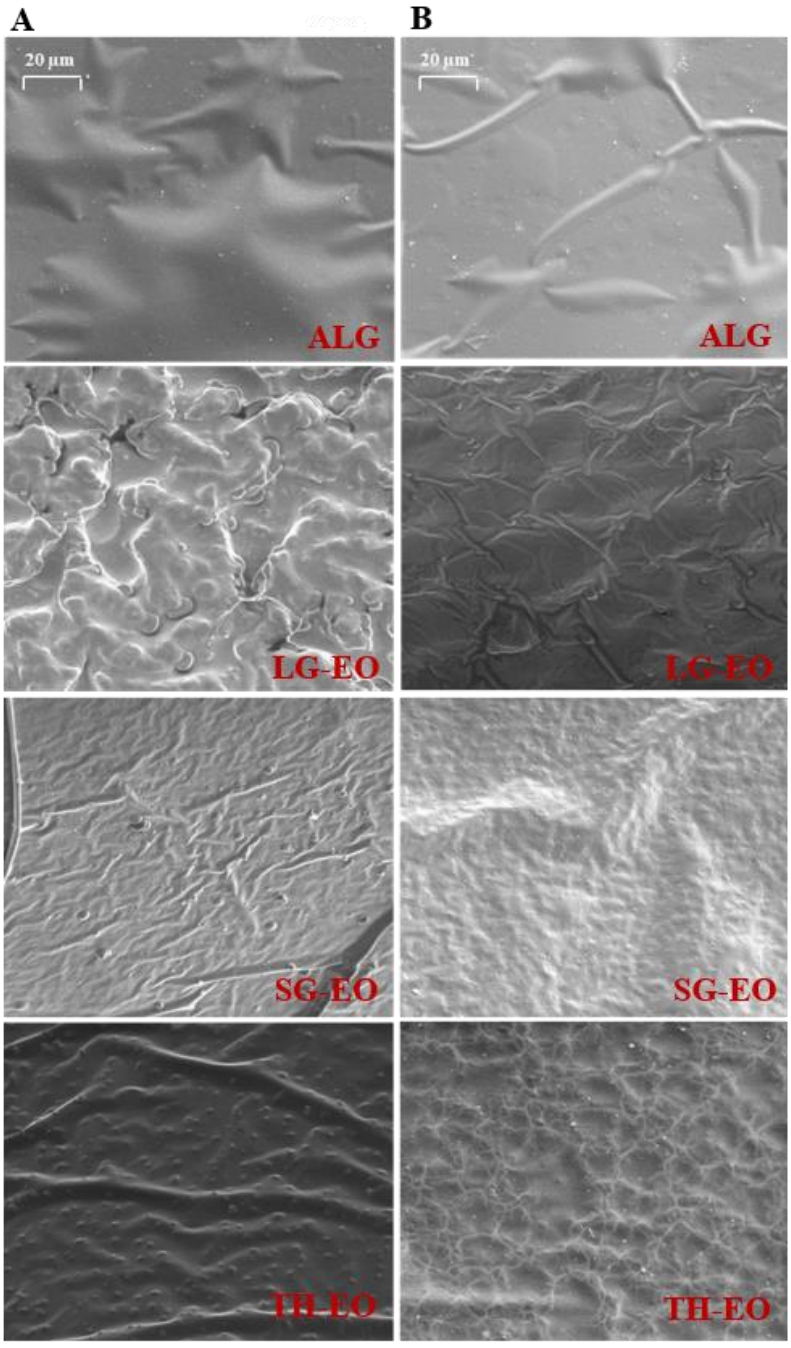

Fig. 2. SEM images of the surface of alginate films (ALG) and lemongrass (LG-EO), sage (SG-EO) or thyme (TH-EO) nanoemulsion-based films.

Furthermore, it was observed a positive relationship between ζ-potential of nanoemulsions and opacity of films, with a correlation coefficient of 0.7008 (Table 4). In other words, opacity of films decreased as the electrical charge

of nanoemulsions was more negative. Probably, the reason of this fact may be linked to the structural conformation of biopolymer chains regarding with their electrical charge; when biopolymers are strongly charged, chains should remain more extended. On the other hand, when the electrical charge is weak biopolymer chains tends to form globular structures, since inter-chain electrical repulsion is partially avoided. In both cases, the resulting film structure and hence, opacity should be fairly different.

3.2.2. Water vapor permeability and film thickness

Water vapor permeability (WVP) measures the diffusion of water molecules through the cross-section of the film and can give an estimation of its barrier property. To prevent or reduce the dehydration of foods, films used as packaging or coatings must control the moisture transport from the product to the environment, hence WVP of edible films should be as low as possible (Ma, Chang, & Yu, 2008). The transference of water vapor is carried out by the hydrophilic fraction of the film and permeability depends on its hydrophilic-lipophilic ratio (Hernandez, 1994). Therefore, the presence of lipid compounds in film structure enhances water barrier properties due to an increased tortuosity that creates a resistance to the water vapor through the film. It has been described that tortuosity is higher when oil phase ratio increases or oil particle size is reduced (Pérez-Gago & Krochta, 2001). EOs are known to decrease WVP of polysaccharide-based films due to their hydrophobic behavior. However, little differences were observed between ALG films and EO-containing films; probably due to the low oil content used in this study. Only films with SG-EO showed a significant reduction compared with ALG films ($p < 0.05$). It is possible that this small difference on WVP of films could have been favored by the small droplet size of the equivalent nanoemulsions, leading to a greater distribution of the oil phase in the film structure.

On the other hand, films cast from pure alginate solutions had a thickness of 50 ± 3 µm (Table 3). It was observed that films made from LG-EO and SG-EO nanoemulsions presented a significantly smaller thickness ($p < 0.05$). These results could be linked to the droplet size achieved in the nanoemulsions. Sánchez-González et al., (2011b) found a thickness reduction in edible films made from emulsions with small droplet size. They attributed this effect to possible losses of oil phase during film formation, which could decrease the total amount of solids concentration in the film matrix. Furthermore, film

thickness exhibited a significant relationship with droplet size of nanoemulsions with a correlation coefficient of 0.6919 (Table 4), supporting the dependence of this variables.

Table 3. Water vapor permeability (WVP) and thickness of alginate films and films made from EO-loaded nanoemulsions.

Film	WVP (g/m.s.Pa) $x10^{-10}$	Thickness (μm)
ALG	2.36 ± 0.21^{a}	50 ± 3^{a}
TH-EO	2.18 ± 0.23^{ab}	46 ± 5^{a}
LG-EO	2.12 ± 0.24^{ab}	42 ± 5^{b}
SG-EO	1.9 ± 0.4^{b}	38 ± 3^{b}

ALG: alginate films; TH-EO: thyme essential oil films; LG-EO: lemongrass essential oil films; SG-EO: sage essential oil films. Values were given as mean ± standard deviations. a,b,c Values with the same superscript letters within a column are not significantly different ($p < 0.05$).

3.2.3. Mechanical properties

The most common parameters that describes the mechanical properties of edible films are tensile strength (TS) and elongation at break (EAB), which are strongly related to the chemical structure of films (Dufresne & Vignon, 1998). TS indicates the resistance to tension forces and EAB is related to film stretching capacity. The mechanical properties of alginate-based films are shown in Fig. 3. Films made from EO nanoemulsions were as resistant as alginate films (ALG) without significant differences ($p < 0.05$) in TS values (Fig. 3B). Although several reports have mentioned that oil addition to film formulation tends to weaken the film by decreasing cohesion forces within the structure (Han & Gennadios, 2005; Zúñiga, Skurtys, Osorio, Aguilera, & Pedreschi, 2012), in this study we obtained nanoemulsion-based films rather resistant, probably due to the low oil content incorporated.

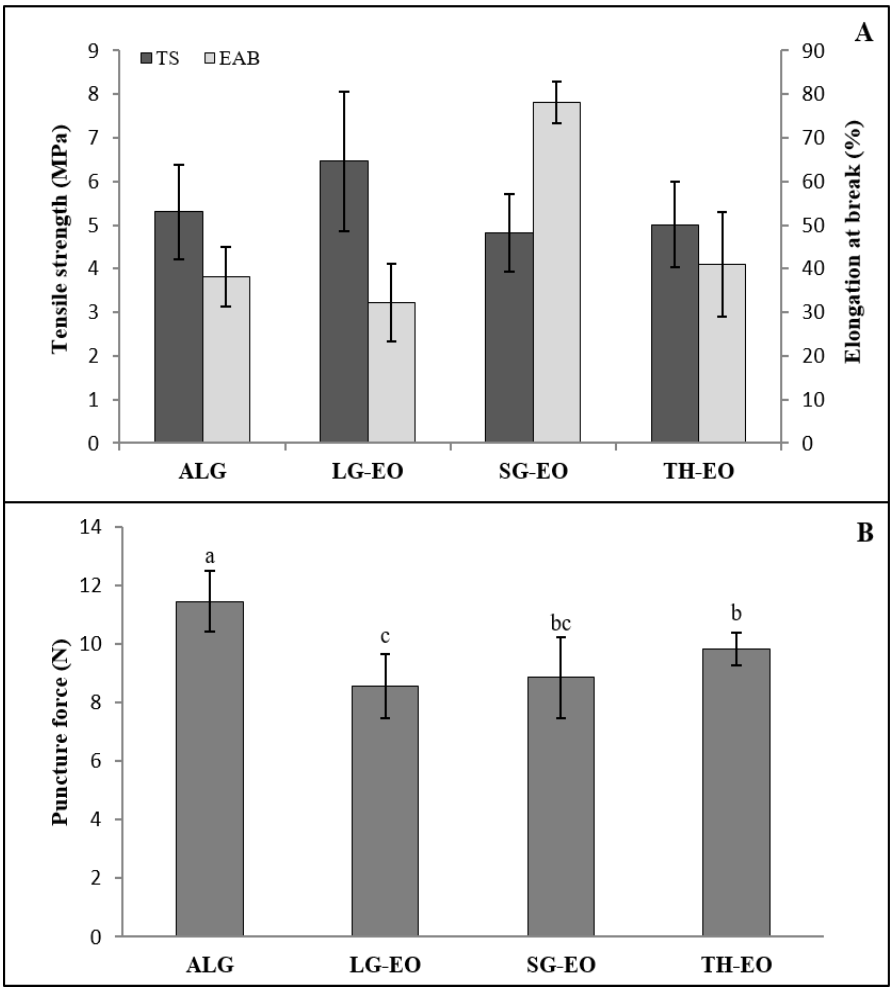

Fig. 3. (A) Tensile strength (TS) and elongation at break (EAB) of alginate films (ALG) and films based on nanoemulsions containing lemongrass (LG-EO), sage (SG-EO) and thyme (TH-EO) oils. (B) Puncture force (PF) of edible films. Error bars indicate standard deviations. Means with the same letter are not significantly different at $p < 0.05$.

On the other hand, edible films prepared from SG-EO nanoemulsions were the most stretchable (EAB: 78 ± 5 %), whereas films containing LG-EO and TH-EO (EAB: 32 ± 9 % and 41 ± 12 %, respectively) did not show significant differences ($p < 0.05$) regarding ALG films (38 ± 7 %) (Fig. 3A). These variations in film flexibility could be partially explained by the influence of the electrical charge of nanoemulsions in the film structure. The repulsive forces among molecules of the same charge can increase the distance between polymers, resulting in a plasticizing effect in the case of charged polymeric film structure (Han & Gennadios, 2005). In this sense, the pronounced difference between electrical charge of SG-EO nanoemulsions (-70 mV) and TH-EO or LG-EO nanoemulsions (-44 mV and -41 mV, respectively) could have led to

different grades of flexibility in edible films. In concordance, we observed a strong negative association between ζ-potentials of nanoemulsions and EAB of films, with a correlation coefficient of -0.8527 (Table 4). On the other hand, small droplet sizes also may influence film elasticity. As the surface area of oil droplets is larger in film structure, the biopolymer network become more heterogenous thus decreasing chain-chain interactions and increasing the plasticizing effect. In concordance with this, we found a moderate correlation between droplet size of nanoemulsions and EAB of edible films (r = 0.5383; Table 4).

Fig. 3B shows the puncture force (PF) of alginate films formed from EOs-loaded nanoemulsions. Puncture resistance is the maximum force required to cause the film break by a penetrating tip and describes film rigidity. Films made from nanoemulsions presented significantly lower values of PF compared with ALG films (11.47 ± 1.05 N). LG-EO films showed the lowest PF (8.58 ± 1.09 N) and the highest value was observed in TH-EO films (9.8 ± 0.5 N). The drop of PF values in films obtained from nanoemulsions could be related to the microfluidization effect on the molecular chains of alginate, which could decrease film rigidity. It has been described high pressure homogenization can affect molecular weight of biopolymers by changing their conformation, thereby, inducing an irreversible ordered-disordered conformation transition and molecular degradation (Lagoueyte & Paquin, 1998). This trend was also reported in biopolymer-based edible films treated by microfluidization (Jiménez, Fabra, Talens, & Chiralt, 2012; Vargas, Perdones, Chiralt, Cháfer, & González-Martínez, 2011).

Table 4. Pearson's correlation coefficients (*p*-value) between the physical properties of nanoemulsions containing EO and the physical and mechanical properties of their respective edible films.

		PHYSICAL PROPERTIES OF FILM-FORMING NANOEMULSIONS			
		Droplet size	ζ-potential	Whiteness index	Viscosity
PHYSICAL AND MECHANICAL PROPERTIES OF EDIBLE FILMS	*ΔE*	0.9424**	0.4377	0.9128**	-0.5198
		(0.0000)	(0.0900)	(0.0006)	(0.1515)
	Opacity	0.6846	0.7008**	0.2345	0.6159
		(0.8013)	(0.0025)	(0.5437)	(0.0774)
	WVP	0.3945	-0.1434	0.0282	0.2152
		(0.1305)	(0.5962)	(0.9425)	(0.5782)
	Thickness	0.6919**	0.2595	0.6332	-0.2852
		(0.0030)	(0.3319)	(0.0672)	(0.4569)
	Tensile Strength	-0.3389	0.2372	0.1306	0.4582
		(0.1991)	(0.3765)	(0.7377)	(0.2149)
	Elongation at break	-0.5383**	-0.8527**	-0.6317	-0.4449
		(0.0315)	(0.0000)	(0.0680)	(0.2302)
	Puncture Force	0.4233	0.1925	0.5019	0.1177
		(0.1023)	(0.4751)	(0.1686)	(0.7630)

** $p < 0.05$

3.2.4. Antimicrobial activity

The inhibitory effect against *Escherichia coli* of alginate films (ALG) and those prepared with EOs nanoemulsions is presented in Fig. 4. ALG films did not show any antimicrobial activity and the microorganism growth was similar to the TSA-NaCl plates without any film (CT). In line with these results, Pranoto and co-workers (2005) found that alginate films were not able to reduce the *E. coli* growth in 'in-vitro' tests. On the other hand, the type of EO significantly

affected antibacterial activity of edible films. In the case of films formed from TH-EO nanoemulsions, the inhibitory effect was significantly strong whereas LG-EO and SG-EO films did not show any growth reduction. In the case of TH-EO films, a dramatic decrease of bacteria population up to 3.97 Log reductions during the first contact hour was observed. Moreover, antibacterial effect was prolonged during the contact time between bacteria and antimicrobial films, reaching 4.71 Log reductions after 12 h. The strong inhibitory effect observed in TH-EO films is attributed to the presence of thymol molecules, which is the major compound in TH-EO. Thymol molecules can bind to membrane proteins of microbial cells by hydrophobic interactions, thus changing the membrane permeability. Moreover, thymol is able to disintegrate the outer membrane of gram-negative bacteria, hence releasing lipopolysaccharides and increasing the permeability of cytoplasmic membrane (Juven, Kanner, Schved, & Weisslowicz, 1994; Ultee, Bennik, & Moezelaar, 2002). The effectiveness of EOs is also influenced by the sensibility of the microorganism to EO. In this regard, *Escherichia coli* has been described as a sensitive bacteria to the action of TH-EO alone or incorporated in edible film (Emiroğlu, Yemiş, Coşkun, & Candoğan, 2010; Jouki et al., 2014).

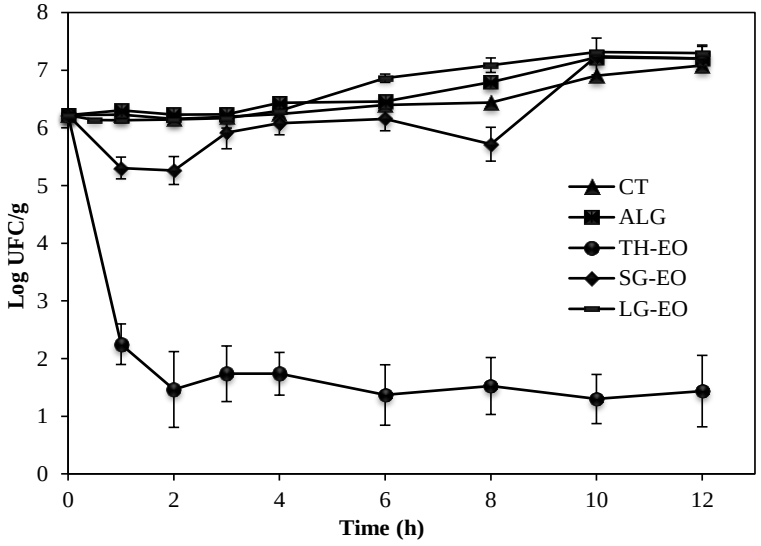

Fig. 4. Antimicrobial activity of alginate films containing EOs against *Escherichia coli* inoculated on TSA-NaCl plates. Data shown are a mean ± standard deviation. ▲ CT: Control without film; ■ ALG: alginate films; ● TH-EO: thyme essential oil film; ◆ SG-EO: sage essential oil film and ▪ LG-EO: lemongrass essential oil film. Data shown are a mean ± standard deviation.

In contrast, films based on SG-EO nanoemulsions presented less than 1 Log reduction of *E. coli* population during the first 2 h and microbial counts gradually increased until the end of experiments (12 h) (Fig. 4). This trend suggested a resistance mechanism of the microorganism to SG-EO as the time of exposure was longer. This results are in agreement with others reported previously, where the inhibitory effect of pure SG-EO was low in gram-negative bacteria such as *E.coli* (Gutierrez, Rodriguez, Barry-Ryan, & Bourke, 2008; Shirazi et al., 2008). Similarly, edible films including LG-EO did not show any effect against the *E. coli* growth along the contact time studied. Other authors have observed great antibacterial effect of LG-EO edible films against *E.coli* growth (Maizura, Fazilah, Norziah, & Karim, 2007; Rojas-Graü et al., 2007). Nevertheless, the absence of antimicrobial effect in LG-EO films found in this study could be partially attributed to volatilization of oil compounds during the film formation. We postulate LG-EO droplets migrated upwards during film drying due to the low density of their antimicrobial compounds (Citral: 0.856 kg/cm^3; limonene: 0.834 kg/m^3 (Rao & McClements, 2012b)). We could support the above mentioned assumption by examining the film microstructure, where surface of LG-EO films in contact with air exhibited a grainy appearance. This means that oil droplets were concentrated on the top of the film (Fig. 2A) and could evaporate faster due to the increase vapor pressure of nanometer size droplets (Nuchuchua et al., 2009). However, there are other crucial factors that could affect effectiveness of EOs, such as antagonistic interactions with other ingredients (e.g. proteins or carbohydrates), or the pH of the system (Pires et al., 2013; Raybaudi-Massilia, Mosqueda-Melgar, & Martin-Belloso, 2008).

4. Conclusions

The results obtained in the present study give some insights on the relevant effect of preparing edible films using nanoemulsions of EOs as film-forming dispersions. It was found that the most important factors of nanoemulsions affecting the physical properties of edible films were the droplet size and the electrical charge of oil droplets. A decrease on the droplet size and magnitude of the ζ-potential led to relevant changes in the barrier, color and mechanical properties of films. On the other hand, these parameters were not relevant in term of antimicrobial properties of edible films. Rather, the composition of EOs and the susceptibility of the bacteria to those compounds determined the

efficacy of films against the microbial growth. Therefore, this work confirms the feasibility of preparing nanoemulsions to enhance encapsulation of EOs and to obtain functional edible films, which might be useful to protect and preserve food products.

5. Acknowledgments

This research was supported by the Ministerio de Ciencia e Innovación (Spain) throughout projects ALG2009-11475 and ALG2012-35635. Author Acevedo-Fani also thanks to the University of Lleida for the pre-doctoral grant. Author Martín-Belloso acknowledges to the Institució Catalana de Recerca I Estudis Avançats (ICREA) for the Academia 2008 Award.

6. References

Alboofetileh, M., Rezaei, M., Hosseini, H., & Abdollahi, M. (2014). Antimicrobial activity of alginate/clay nanocomposite films enriched with essential oils against three common foodborne pathogens. *Food Control*, *36*(1), 1–7.

Atarés, L., Bonilla, J., & Chiralt, A. (2010). Characterization of sodium caseinate-based edible films incorporated with cinnamon or ginger essential oils. *Journal of Food Engineering*, *100*(4), 678–687.

Ayhan, Z., Cimmino, S., Esturk, O., Duraccio, D., Pezzuto, M., & Silvestre, C. (2015). Development of Films of Novel Polypropylene based Nanomaterials for Food Packaging Application. *Packaging Technology and Science*, *28*(7), 589–602.

Bech, L., Meylheuc, T., Lepoittevin, B., & Roger, P. (2007). Chemical surface modification of poly(ethylene terephthalate) fibers by aminolysis and grafting of carbohydrates. *Journal of Polymer Science, Part A: Polymer Chemistry*, *45*(11), 2172–2183.

Bhargava, K., Conti, D. S., da Rocha, S. R. P., & Zhang, Y. (2015). Application of an oregano oil nanoemulsion to the control of foodborne bacteria on fresh lettuce. *Food Microbiology*, *47*, 69–73.

Bieker, P., & Schönhoff, M. (2010). Linear and Exponential Growth Regimes of Multilayers of Weak Polyelectrolytes in Dependence on pH. *Macromolecules*, *43*(11), 5052–5059.

Bilbao-Sáinz, C., Avena-Bustillos, R. de J., Wood, D. F., Williams, T. G., & McHugh, T. H. (2010). Nanoemulsions prepared by a low-energy emulsification

method applied to edible films. *Journal of Agricultural and Food Chemistry*, *58*(22), 11932–8.

Boddohi, S., Killingsworth, C. E., & Kipper, M. J. (2008). Polyelectrolyte multilayer assembly as a function of pH and ionic strength using the polysaccharides chitosan and heparin. *Biomacromolecules*, *9*(7), 2021–2028.

Bonilla, J., Atarés, L., Vargas, M., & Chiralt, A. (2012). Effect of essential oils and homogenization conditions on properties of chitosan-based films. *Food Hydrocolloids*, *26*(1), 9–16.

Buranasuksombat, U., Kwon, Y. J., Turner, M., & Bhandari, B. (2011). Influence of emulsion droplet size on antimicrobial properties. *Food Science and Biotechnology*, *20*(3), 793–800.

Burt, S. (2004). Essential oils: their antibacterial properties and potential applications in foods—a review. *International Journal of Food Microbiology*, *94*(3), 223–253.

Carneiro-da-Cunha, M. G., Cerqueira, M. A., Souza, B. W. S., Carvalho, S., Quintas, M. A. C. C., Teixeira, J. A., & Vicente, A. A. (2010). Physical and thermal properties of a chitosan/alginate nanolayered PET film. *Carbohydrate Polymers*, *82*(1), 153–159.

Chang, Y., McLandsborough, L. A., & McClements, D. J. (2012). Physical properties and antimicrobial efficacy of thyme oil nanoemulsions: influence of ripening inhibitors. *Journal of Agricultural and Food Chemistry*, *60*(48), 12056–63.

Chantrapornchai, W., Clydesdale, F., & McClements, D. J. (1998). Influence of Droplet Size and Concentration on the Color of Oil-in-Water Emulsions. *Journal of Agricultural and Food Chemistry*, *46*, 2914–2920.

Chinnan, M. S., & Park, H. J. (1996). Effect of plasticizer level and temperature on water vapor transmission of cellulose-based edible films. *Journal of Food Process Engineering*, *18*(4), 417–429.

Cramer Flores, F., Fagundes Ribeiro, R., Ferreira Ourique, A., Bueno Rolim, C. M., De Bona Da Silva, C., Raffin Pohlmann, A., … Stanisçuaski Guterres, S. (2011). Nanostructured systems containing an essential oil: protection against volatilization. *Química Nova*, *34*(6), 968–972.

Davidov-Pardo, G., & McClements, D. J. (2015). Nutraceutical delivery systems: resveratrol encapsulation in grape seed oil nanoemulsions formed by spontaneous emulsification. *Food Chemistry*, *167*, 205–12.

de Oliveira Santos, R. P., Castro, D. O., Ruvolo-Filho, A. C., & Frollini, E. (2014). Processing and thermal properties of composites based on recycled PET, sisal fibers, and renewable plasticizers. *Journal of Applied Polymer Science*, *131*(12), 40386.

de Villiers, M. M., Otto, D. P., Strydom, S. J., & Lvov, Y. M. (2011). Introduction to nanocoatings produced by layer-by-layer (LbL) self-assembly. *Advanced Drug Delivery Reviews*, *63*(9), 701–715.

Deng, J., Liu, X., Ma, L., Cheng, C., Shi, W., Nie, C., & Zhao, C. (2014). Heparin-mimicking multilayer coating on polymeric membrane via LbL assembly of cyclodextrin-based supramolecules. *ACS Applied Materials & Interfaces*, *6*(23), 21603–14.

Dickinson, E. (2003). Hydrocolloids at interfaces and the influence on the properties of dispersed systems. *Food Hydrocolloids*, *17*(1), 25–39.

Dickinson, E. (2009). Hydrocolloids as emulsifiers and emulsion stabilizers. *Food Hydrocolloids*, *23*(6), 1473–1482.

Donsì, F., Cuomo, A., Marchese, E., & Ferrari, G. (2014). Infusion of essential oils for food stabilization: Unraveling the role of nanoemulsion-based delivery systems on mass transfer and antimicrobial activity. *Innovative Food Science & Emerging Technologies*, *22*, 212–220.

Dufresne, A., & Vignon, M. R. (1998). Improvement of starch film performances using cellulose microfibrils. *Macromolecules*, *31*(8), 2693–2696.

Edris, A. E., & Malone, C. F. R. (2012). Preferential solubilization behaviours and stability of some phenolic-bearing essential oils formulated in different microemulsion systems. *International Journal of Cosmetic Science*, *34*(5), 441–450.

Emiroğlu, Z. K., Yemiş, G. P., Coşkun, B. K., & Candoğan, K. (2010). Antimicrobial activity of soy edible films incorporated with thyme and oregano essential oils on fresh ground beef patties. *Meat Science*, *86*(2), 283–8.

Etienne, O., Schneider, A., Taddei, C., Richert, L., Schaaf, P., Voegel, J.-C., … Picart, C. (2005). Degradability of polysaccharides multilayer films in the oral environment: an in vitro and in vivo study. *Biomacromolecules*, *6*(2), 726–33.

Fabra, M. J., Pérez-Masiá, R., Talens, P., & Chiralt, A. (2011). Influence of the homogenization conditions and lipid self-association on properties of sodium caseinate based films containing oleic and stearic acids. *Food Hydrocolloids*, *25*(5), 1112–1121.

Farris, S., Introzzi, L., Biagioni, P., Holz, T., Schiraldi, A., & Piergiovanni, L. (2011). Wetting of Biopolymer Coatings: Contact Angle Kinetics and Image Analysis Investigation. *Langmuir*, *27*(12), 7563–7574.

Fu, J., Ji, J., Yuan, W., & Shen, J. (2005). Construction of anti-adhesive and antibacterial multilayer films via layer-by-layer assembly of heparin and chitosan. *Biomaterials*, *26*(33), 6684–6692.

Grant, C. A., Alfouzan, A., Gough, T., Twigg, P. C., & Coates, P. D. (2013). Nano-scale temperature dependent visco-elastic properties of polyethylene terephthalate (PET) using atomic force microscope (AFM). *Micron (Oxford, England : 1993)*, *44*, 174–8.

Gu, C.-H., Wang, J.-J., Yu, Y., Sun, H., Shuai, N., & Wei, B. (2013). Biodegradable multilayer barrier films based on alginate/polyethyleneimine and biaxially oriented poly(lactic acid). *Carbohydrate Polymers*, *92*(2), 1579–85.

Gutierrez, J., Rodriguez, G., Barry-Ryan, C., & Bourke, P. (2008). Efficacy of plant essential oils against foodborne pathogens and spoilage bacteria associated with ready-to-eat vegetables: Antimicrobial and sensory screening. *Journal of Food Protection*, *71*(9), 1846–1854.

Hammer, K. A., Carson, C. F., & Riley, T. V. (1999). Antimicrobial activity of essential oils and other plant extracts. *Journal of Applied Microbiology*, *86*(6), 985–990.

Han, J., & Gennadios, A. (2005). Edible films and coatings: a review. In *Innovations in Food Packaging* (pp. 239–262). Elsevier.

Harding, S. E. (1997). The intrinsic viscosity of biological macromolecules. Progress in measurement, interpretation and application to structure in dilute solution. *Progress in Biophysics and Molecular Biology*, *68*(2), 207–262.

Haynie, D. T., Zhang, L., Rudra, J. S., Zhao, W., Zhong, Y., & Palath, N. (2005). Polypeptide Multilayer Films. *Biomacromolecules*, *6*(6), 2895–2913.

Helander, I. M., Alakomi, H.-L., Latva-Kala, K., Mattila-Sandholm, T., Pol, I., Smid, E. J., … Von Wright, A. (1998). Characterization of the Action of Selected

Essential Oil Components on Gram-Negative Bacteria. *Journal of Agricultural and Food Chemistry*, *46*(9), 3590–3595.

Hernandez, R. J. (1994). Effect of water vapor on the transport properties of oxygen through polyamide packaging materials. *Journal of Food Engineering*, *22*(1-4), 495–507.

Heurtault, B. (2003). Physico-chemical stability of colloidal lipid particles. *Biomaterials*, *24*(23), 4283–4300.

Heydenreich, A. (2003). Preparation and purification of cationic solid lipid nanospheres—effects on particle size, physical stability and cell toxicity. *International Journal of Pharmaceutics*, *254*(1), 83–87.

Indest, T., Laine, J., Ribitsch, V., Johansson, L.-S., Stana-Kleinschek, K., & Strnad, S. (2008). Adsorption of chitosan on PET films monitored by quartz crystal microbalance. *Biomacromolecules*, *9*(8), 2207–14.

Irena, G., Jolanta, B., & Karolina, Z. (2009). Chemical modification of poly(ethylene terephthalate) and immobilization of the selected enzymes on the modified film. *Applied Surface Science*, *255*(19), 8293–8298.

Jafari, S. M., Assadpoor, E., He, Y., & Bhandari, B. (2008). Re-coalescence of emulsion droplets during high-energy emulsification. *Food Hydrocolloids*, *22*(7), 1191–1202.

Jiang, Bingbing Li, B. (2009). Tunable drug loading and release from polypeptide multilayer nano fi lms. *International Journal of Nanomedicine*, *4*, 37–54.

Jiménez, A., Fabra, M. J., Talens, P., & Chiralt, A. (2012). Influence of hydroxypropylmethylcellulose addition and homogenization conditions on properties and ageing of corn starch based films. *Carbohydrate Polymers*, *89*(2), 676–686.

Jouki, M., Mortazavi, S. A., Yazdi, F. T., & Koocheki, A. (2014). Characterization of antioxidant-antibacterial quince seed mucilage films containing thyme essential oil. *Carbohydrate Polymers*, *99*, 537–46.

Junka, K., Sundman, O., Salmi, J., Osterberg, M., & Laine, J. (2014). Multilayers of cellulose derivatives and chitosan on nanofibrillated cellulose. *Carbohydrate Polymers*, *108*, 34–40.

Juven, B. J., Kanner, J., Schved, F., & Weisslowicz, H. (1994). Factors that interact with the antibacterial action of thyme essential oil and its active constituents. *Journal of Applied Bacteriology*, *76*(6), 626–631.

Kaya, S., & Kaya, A. (2000). Microwave drying effects on properties of whey protein isolate edible films. *Journal of Food Engineering*, *43*(2), 91–96.

Kim, S. O., Ha, T. V. A., Choi, Y. J., & Ko, S. (2014). Optimization of homogenization-evaporation process for lycopene nanoemulsion production and its beverage applications. *Journal of Food Science*, *79*(8), N1604–10.

Klitzing, R. V, & V Klitzing, R. (2006). Internal structure of polyelectrolyte multilayer assemblies. *Physical Chemistry Chemical Physics : PCCP*, *8*(43), 5012–33.

Kralova, I., & Sjöblom, J. (2009). Surfactants used in food industry: a review. *Journal of Dispersion Science and Technology*, *30*(9), 1363–1383.

Kristo, E., Koutsoumanis, K. P., & Biliaderis, C. G. (2008). Thermal, mechanical and water vapor barrier properties of sodium caseinate films containing antimicrobials and their inhibitory action on Listeria monocytogenes. *Food Hydrocolloids*, *22*(3), 373–386. R

Krochta, J. M., Baldwin, E., & Nisperos-Carriedo, M. (1994). *Edible Coatings and Films to Improve Food Quality*. (J. Krochta, E. Baldwin, & M. Nisperos-Carriedo, Eds.). Lancaster, PA: Technomic.

Ladam, G., Schaad, P., Voegel, J. C., Schaaf, P., Decher, G., & Cuisinier, F. (2000). In Situ Determination of the Structural Properties of Initially Deposited Polyelectrolyte Multilayers. *Langmuir*, *16*(3), 1249–1255.

Lagoueyte, N., & Paquin, P. (1998). Effects of microfluidization on the functional properties of xanthan gum. *Food Hydrocolloids*, *12*(3), 365–371.

Lambert, R. J. W., Skandamis, P. N., Coote, P. J., & Nychas, G.-J. E. (2001). A study of the minimum inhibitory concentration and mode of action of oregano essential oil, thymol and carvacrol. *Journal of Applied Microbiology*, *91*(3), 453–462.

Liang, R., Xu, S., Shoemaker, C. F., Li, Y., Zhong, F., & Huang, Q. (2012). Physical and antimicrobial properties of peppermint oil nanoemulsions. *Journal of Agricultural and Food Chemistry*, *60*(30), 7548–55.

Lukomska, J., Malicka, J., Gryczynski, I., & Lakowicz, J. R. (2004). Fluorescence enhancements on silver colloid coated surfaces. *Journal of Fluorescence*, *14*(4), 417–23.

Lundin, M., Blomberg, E., & Tilton, R. D. (2010). Polymer dynamics in layer-by-layer assemblies of chitosan and heparin. *Langmuir*, *26*(5), 3242–3251.

Lundin, M., Solaqa, F., Thormann, E., MacAkova, L., & Blomberg, E. (2011). Layer-by-layer assemblies of chitosan and heparin: Effect of solution ionic strength and pH. *Langmuir*, *27*(12), 7537–7548.

Ma, X., Chang, P. R., & Yu, J. (2008). Properties of biodegradable thermoplastic pea starch/carboxymethyl cellulose and pea starch/microcrystalline cellulose composites. *Carbohydrate Polymers*, *72*(3), 369–375.

Maizura, M., Fazilah, A., Norziah, M. H., & Karim, A. A. (2007). Antibacterial activity and mechanical properties of partially hydrolyzed sago starch-alginate edible film containing lemongrass oil. *Journal of Food Science*, *72*(6), C324–30.

Martins, G. V, Mano, J. F., & Alves, N. M. (2011). Dual Responsive Nanostructured Surfaces for Biomedical Applications. *Langmuir*, *27*(13), 8415–8423.

McClements, D. J. (2005). *Food emulsions : principles, practices, and techniques*. (C. Press, Ed.). Boca Raton, Fla. : CRC Press.

McClements, D. J. (2011). Edible nanoemulsions: Fabrication, properties, and functional performance. *Soft Matter*, *7*(6), 2297–2316.

McClements, D. J., & Rao, J. (2011). Food-grade nanoemulsions: formulation, fabrication, properties, performance, biological fate, and potential toxicity. *Critical Reviews in Food Science and Nutrition*, *51*(4), 285–330.

Milani, J., & Maleki, G. (2012). Hydrocolloids in food industry. In B. Valdez (Ed.), *Food Idustrial Processes–Methods and Equipment* (pp. 17–38). Intech.

Morariu, S., Brunchi, C. E., & Bercea, M. (2012). The Behavior of Chitosan in Solvents with Different Ionic Strengths. *Industrial & Engineering Chemistry Research*, *51*(39), 12959–12966.

Norajit, K., Kim, K. M., & Ryu, G. H. (2010). Comparative studies on the characterization and antioxidant properties of biodegradable alginate films containing ginseng extract. *Journal of Food Engineering*, *98*(3), 377–384.

Nuchuchua, O., Sakulku, U., Uawongyart, N., Puttipipatkhachorn, S., Soottitantawat, A., & Ruktanonchai, U. (2009). In vitro characterization and mosquito (Aedes aegypti) repellent activity of essential-oils-loaded nanoemulsions. *AAPS PharmSciTech*, *10*(4), 1234–42.

Oriani, V. B., Molina, G., Chiumarelli, M., Pastore, G. M., & Hubinger, M. D. (2014). Properties of cassava starch-based edible coating containing essential oils. *Journal of Food Science*, *79*(2), E189–94.

Otoni, C. G., Moura, M. R. de, Aouada, F. A., Camilloto, G. P., Cruz, R. S., Lorevice, M. V., … Mattoso, L. H. C. (2014). Antimicrobial and physical-mechanical properties of pectin/papaya puree/cinnamaldehyde nanoemulsion edible composite films. *Food Hydrocolloids*, *41*, 188–194.

Otoni, C. G., Pontes, S. F. O., Medeiros, E. A. A., & Soares, N. de F. F. (2014). Edible films from methylcellulose and nanoemulsions of clove bud (Syzygium aromaticum) and oregano (Origanum vulgare) essential oils as shelf life extenders for sliced bread. *Journal of Agricultural and Food Chemistry*, *62*(22), 5214–9.

Pérez-Gago, M. B., & Krochta, J. M. (2001). Lipid particle size effect on water vapor permeability and mechanical properties of whey protein/beeswax emulsion films. *Journal of Agricultural and Food Chemistry*, *49*(2), 996–1002.

Picart, C. (2008). Polyelectrolyte multilayer film: From physico-chemical properties to the control of cellular processes. *Current Medicinal Chemistry*, *15*(7), 685–697.

Picart, C., Lavalle, P., Hubert, P., Cuisinier, F. J. G., Decher, G., Schaaf, P., & Voegel, J.-C. (2001). Buildup Mechanism for Poly(l -lysine)/Hyaluronic Acid Films onto a Solid Surface. *Langmuir*, *17*(23), 7414–7424.

Picart, C., Mutterer, J., Richert, L., Luo, Y., Prestwich, G. D., Schaaf, P., … Lavalle, P. (2002). Molecular basis for the explanation of the exponential growth of polyelectrolyte multilayers. *Proceedings of the National Academy of Sciences of the United States of America*, *99*(20), 12531–5.

Pinheiro, A. C., Bourbon, A. I., Medeiros, B. G. de S., da Silva, L. H. M., da Silva, M. C. H., Carneiro-da-Cunha, M. G., … Vicente, A. A. (2012). Interactions between κ-carrageenan and chitosan in nanolayered coatings—Structural and transport properties. *Carbohydrate Polymers*, *87*(2), 1081–1090.

Pires, C., Ramos, C., Teixeira, B., Batista, I., Nunes, L., & Marques, A. (2013). Hake proteins edible films incorporated with essential oils: Physical, mechanical, antioxidant and antibacterial properties. *Food Hydrocolloids*, *30*(1), 224–231.

Qian, C., & McClements, D. J. (2011). Formation of nanoemulsions stabilized by model food-grade emulsifiers using high-pressure homogenization: Factors affecting particle size. *Food Hydrocolloids*, *25*(5), 1000–1008.

Radeva, T., Kamburova, K., & Petkanchin, I. (2006). Formation of polyelectrolyte multilayers from polysaccharides at low ionic strength. *Journal of Colloid and Interface Science*, *298*(1), 59–65.

Rao, J., & McClements, D. J. (2012a). Food-grade microemulsions and nanoemulsions: Role of oil phase composition on formation and stability. *Food Hydrocolloids*, *29*(2), 326–334.

Rao, J., & McClements, D. J. (2012b). Impact of lemon oil composition on formation and stability of model food and beverage emulsions. *Food Chemistry*, *134*(2), 749–57.

Raybaudi-Massilia, R. M., Mosqueda-Melgar, J., & Martin-Belloso, O. (2008). Edible alginate-based coating as carrier of antimicrobials to improve shelf-life and safety of fresh-cut melon. *International Journal of Food Microbiology*, *121*(3), 313–327.

Rhim, J.-W., Lee, J.-H., & Hong, S.-I. (2006). Water resistance and mechanical properties of biopolymer (alginate and soy protein) coated paperboards. *LWT - Food Science and Technology*, *39*(7), 806–813.

Richert, L., Lavalle, P., Payan, E., Shu, X. Z., Prestwich, G. D., Stoltz, J.-F., … Picart, C. (2004). Layer by Layer Buildup of Polysaccharide Films: Physical Chemistry and Cellular Adhesion Aspects. *Langmuir*, *20*(2), 448–458.

Rojas-Graü, M. A., Avena-Bustillos, R. de J., Friedman, M., Henika, P. R., Martin-Belloso, O., & McHugh, T. H. (2006). Mechanical, barrier, and antimicrobial properties of apple puree edible films containing plant essential oils. *Journal of Agricultural and Food Chemistry*, *54*(24), 9262–7.

Rojas-Graü, M. A., Avena-Bustillos, R. de J., Olsen, C., Friedman, M., Henika, P. R., Martin-Belloso, O., … McHugh, T. H. (2007). Effects of plant essential oils and oil compounds on mechanical, barrier and antimicrobial properties of alginate-apple puree edible films. *Journal of Food Engineering*, *81*(3), 634–641.

Sæther, H. V., Holme, H. K., Maurstad, G., Smidsrød, O., & Stokke, B. T. (2008). Polyelectrolyte complex formation using alginate and chitosan. *Carbohydrate Polymers*, *74*(4), 813–821.

Salehi, A., Desai, P. S., Li, J., Steele, C. A., & Larson, R. G. (2015). Relationship between Polyelectrolyte Bulk Complexation and Kinetics of Their Layer-by-Layer Assembly. *Macromolecules*, *48*(2), 400–409.

Salvia-Trujillo, L., Rojas-Graü, M. A., Soliva-Fortuny, R. C., & Martín-Belloso, O. (2013). Effect of processing parameters on physicochemical characteristics of microfluidized lemongrass essential oil-alginate nanoemulsions. *Food Hydrocolloids*, *30*(1), 401–407.

Sánchez-González, L., Cháfer, M., Hernández, M., Chiralt, A., & González-Martínez, C. (2011a). Antimicrobial activity of polysaccharide films containing essential oils. *Food Control*, *22*(8), 1302–1310.

Sánchez-González, L., Chiralt, A., González-Martínez, C., & Cháfer, M. (2011b). Effect of essential oils on properties of film forming emulsions and films based on hydroxypropylmethylcellulose and chitosan. *Journal of Food Engineering*, *105*(2), 246–253.

Schoeler, B., Sharpe, S., Hatton, T. A., & Caruso, F. (2004). Polyelectrolyte Multilayer Films of Different Charge Density Copolymers with Synergistic Nonelectrostatic Interactions Prepared by the Layer-by-Layer Technique. *Langmuir*, *20*(7), 2730–2738.

Sessa, M., Tsao, R., Liu, R., Ferrari, G., & Donsì, F. (2011). Evaluation of the Stability and Antioxidant Activity of Nanoencapsulated Resveratrol during in Vitro Digestion. *Journal of Agricultural and Food Chemistry*, *59*(23), 12352–12360.

Severino, R., Ferrari, G., Vu, K. D., Donsì, F., Salmieri, S., & Lacroix, M. (2015). Antimicrobial effects of modified chitosan based coating containing nanoemulsion of essential oils, modified atmosphere packaging and gamma irradiation against Escherichia coli O157:H7 and Salmonella Typhimurium on green beans. *Food Control*, *50*, 215–222.

Shimoni, G., Shani Levi, C., Levi Tal, S., & Lesmes, U. (2013). Emulsions stabilization by lactoferrin nano-particles under in vitro digestion conditions. *Food Hydrocolloids*, *33*(2), 264–272.

Shiratori, S. S., & Rubner, M. F. (2000). pH-Dependent Thickness Behavior of Sequentially Adsorbed Layers of Weak Polyelectrolytes. *Macromolecules*, *33*(11), 4213–4219.

Shirazi, M. H., Ranjbar, R., Eshraghi, S., Amin, G., Nouri, M. S., & Bazzaz, N. (2008). Inhibitory Effects of Sage Extract on the Growth of Enteric Bacteria. *Pakistan Journal of Biological Sciences*, *11*(3), 487–489.

Shojaee-Aliabadi, S., Hosseini, H., Mohammadifar, M. A., Mohammadi, A., Ghasemlou, M., Hosseini, S. M., & Khaksar, R. (2014). Characterization of κ-

carrageenan films incorporated plant essential oils with improved antimicrobial activity. *Carbohydrate Polymers*, *101*, 582–91.

Solans, C., Izquierdo, P., Nolla, J., Azemar, N., & Garcia-Celma, M. J. (2005). Nano-emulsions. *Current Opinion in Colloid & Interface Science*, *10*(3), 102–110.

Stang, M., Karbstein, H., & Schubert, H. (1994). Adsorption kinetics of emulsifiers at oil—water interfaces and their effect on mechanical emulsification. *Chemical Engineering and Processing: Process Intensification*, *33*(5), 307–311.

Tokle, T., & McClements, D. J. (2011). Physicochemical properties of lactoferrin stabilized oil-in-water emulsions: Effects of pH, salt and heating. *Food Hydrocolloids*, *25*(5), 976–982.

Ultee, A., Bennik, M. H. J., & Moezelaar, R. (2002). The phenolic hydroxyl group of carvacrol is essential for action against the food-borne pathogen Bacillus cereus. *Applied and Environmental Microbiology*, *68*(4), 1561–1568.

Vargas, M., Cháfer, M., Albors, A., Chiralt, A., & González-Martínez, C. (2008). Physicochemical and sensory characteristics of yoghurt produced from mixtures of cows' and goats' milk. *International Dairy Journal*, *18*(12), 1146–1152.

Vargas, M., Perdones, Á., Chiralt, A., Cháfer, M., & González-Martínez, C. (2011). Effect of homogenization conditions on physicochemical properties of chitosan-based film-forming dispersions and films. *Food Hydrocolloids*, *25*(5), 1158–1164.

Vidyasagar, A., Sung, C., Losensky, K., & Lutkenhaus, J. L. (2012). pH-Dependent Thermal Transitions in Hydrated Layer-by-Layer Assemblies Containing Weak Polyelectrolytes. *Macromolecules*, *45*(22), 9169–9176.

Xu, J., Yang, L., Hu, X., Xu, S., Wang, J., & Feng, S. (2015). The effect of polysaccharide types on adsorption properties of LbL assembled multilayer films. *Soft Matter*, *11*(9), 1794–9.

Yoo, D., Shiratori, S. S., & Rubner, M. F. (1998). Controlling Bilayer Composition and Surface Wettability of Sequentially Adsorbed Multilayers of Weak Polyelectrolytes. *Macromolecules*, *31*(13), 4309–4318.

Yuan, W., Dong, H., Li, C. M., Cui, X., Yu, L., Lu, Z., & Zhou, Q. (2007). pH-Controlled Construction of Chitosan/Alginate Multilayer Film: Characterization and Application for Antibody Immobilization. *Langmuir*, *23*(26), 13046–13052.

Zhang, J., Senger, B., Vautier, D., Picart, C., Schaaf, P., Voegel, J.-C., & Lavalle, P. (2005). Natural polyelectrolyte films based on layer-by layer deposition of collagen and hyaluronic acid. *Biomaterials*, *26*(16), 3353–61.

Ziani, K., Fang, Y., & McClements, D. J. (2012). Fabrication and stability of colloidal delivery systems for flavor oils: Effect of composition and storage conditions. *Food Research International*, *46*(1), 209–216.

Zúñiga, R. N., Skurtys, O., Osorio, F., Aguilera, J. M., & Pedreschi, F. (2012). Physical properties of emulsion-based hydroxypropyl methylcellulose films: effect of their microstructure. *Carbohydrate Polymers*, *90*(2), 1147–58.

SECTION II: MULTILAYER EMULSIONS

CHAPTER II: FOOD-GRADE MULTILAYER EMULSIONS AS DELIVERY SYSTEMS OF RESVERATROL. PART I: FORMATION, STABILITY AND ANTIOXIDANT ACTIVITY

Acevedo-Fani, A., Silva, H. D., Soliva-Fortuny, R., Martín-Belloso, O., & Vicente, A. A

Food Hydrocolloids (sent)

ABSTRACT

Multilayer emulsions may be suitable delivery systems for active food ingredients. The addition of interfacial biopolymeric layers on oil droplets can enhance protection of encapsulated active ingredients and improve emulsion stability. Resveratrol has health-promoting benefits, however is poorly water-soluble and chemically unstable. The aim of this study was to formulate single-layer (lactoferrin) and multilayer (lactoferrin/alginate and lactoferrin/alginate/poly-L-lysine) emulsions, and to evaluate their physical stability and antioxidant activity during storage. All formulations of primary (single-layer) emulsions presented droplet sizes below 300 nm, which decreased by increasing lactoferrin concentration. The ζ-potentials of droplets were strongly positive (< 45 mV), allowing the electrostatic deposition of another layer. The droplet size in formulations of secondary (multilayer) emulsions increased from 187 nm up to 8700 nm using the lowest alginate concentration due to bridging flocculation. Higher alginate concentrations led to smaller droplet sizes in secondary emulsions. Tertiary emulsions formulated with low or high poly-L-lysine concentrations underwent increases in droplet size owing to different instability phenomena. The interfacial ζ-potential varied in sign and magnitude depending on the biopolymer concentration in emulsions, which is a clear indication of the presence of a new layer. Multilayer emulsions were more stable, in terms of droplet size and ζ-potential, than single-layer emulsions during storage. The antioxidant activity of all resveratrol-loaded emulsions did not change significantly during storage, whereas it decreased in non-encapsulated resveratrol oil from the third week onwards. These results demonstrate the advantages of using multilayer emulsions as delivery systems of resveratrol.

Keywords: Multilayer emulsions, emulsions, resveratrol, layer-by-layer, biopolymer concentration, antioxidant activity

1. Introduction

Encapsulating active food ingredients for their incorporation in food products is still a challenging task to the food industry. The use of nanostructured delivery systems, such as multilayer emulsions, might be a potential strategy to reach this goal. Multilayer emulsions are emulsions where oil droplets are coated by interfacial layers of charged emulsifiers and/or biopolymers (Bortnowska, 2015). These coatings are created by the stepwise electrostatic adsorption of oppositely charged materials on droplets' surfaces, thus producing a nanolaminated coating at the o/w interface. It has been described that the presence of a thick layer around oil droplets can increase emulsion stability to pH changes, high ionic strength, temperature (either heating or freezing) and dehydration (Fioramonti, Arzeni, Pilosof, Rubiolo, & Santiago, 2015; Liu, Wang, Sun, McClements, & Gao, 2016; Noshad, Mohebbi, Koocheki, & Shahidi, 2015). These characteristics might potentially enhance protection of functional compounds susceptible to degradation by their encapsulation within these systems. In addition, the composition of the interfacial coating on oil droplets can be modified, so that multilayers may respond to specific triggers and release the encapsulated functional compounds (Cerqueira et al., 2014; Guzey & McClements, 2006; Shchukina & Shchukin, 2012).

Proteins and polysaccharides are suitable to produce multilayer emulsions, acting either as emulsifiers in the initial emulsion or as polyelectrolytes to create nanolaminated coatings around droplets. For instance, lactoferrin is an iron-chelating glycoprotein present in large amounts in the breast milk of mammalian species. Lactoferrin plays an important biological role within the defense system due to its antimicrobial, antiviral and antioxidant properties (O'Regan, Ennis, & Mulvihill, 2009). From a technological point of view, lactoferrin has many zones with positively charged groups and high isoelectric point (p*I* ≈ 9), therefore it behaves as a cationic biopolymer at neutral pH (Bokkhim, Bansal, GrØndahl, & Bhandari, 2013). The great emulsifying capacity of lactoferrin during the formation of oil-in-water emulsions has been previously reported (Mao, Dubot, Xiao, & McClements, 2013; Pinheiro, Coimbra, & Vicente, 2016; Shimoni, Shani Levi, Levi Tal, & Lesmes, 2013). Alginate is a polysaccharide widely used as thickening agent in food products. However, since alginate exhibits anionic properties above its pK_a (≈ 3.6), it is

one of the polysaccharides mostly utilized to produce food nanostructures by the electrostatic interaction with cationic species (Bokkhim, Bansal, Grøndahl, & Bhandari, 2016; Chang, McLandsborough, & McClements, 2014; Choi, Kim, Cho, Hwang, & Kim, 2011; Hosseini, Emam-Djomeh, Sabatino, & Van der Meeren, 2015). Poly-L-lysine is a polypeptide with cationic characteristics within a wide range of pH values, as its isoelectric point is very high (p*I* ≈ 9). Among the most relevant properties ascribed to poly-L-lysine are the potent antimicrobial activity against a broad range of bacteria, which explains its importance in the food industry (Yoshida, Hiraki, & Nagasawa, 2005).

Phytochemicals, such as plant polyphenols, have received much attention from the scientific community, food industry and consumers because of their health-promoting benefits. Resveratrol is a naturally occurring phenolic compound mainly found in grapes' skin and berry fruits and belongs to the stilbenes family. The chemical structure of resveratrol consists of two aromatic rings joined by a methylene bridge (Xu & Si, 2012). Several investigations have evidenced important biological properties in resveratrol including antioxidant activity, anti-inflammatory, anti-carcinogenic, cardio-protective or neuro-protective effect (Brown et al., 2010; Kim, Jin, Choi, & Park, 2011; Park et al., 2012; Witte, Kerti, Margulies, & Flöel, 2014; Xu & Si, 2012). However, the most limiting factors that influence the incorporation of resveratrol in food and beverages is the poor-water solubility (Amri, Chaumeil, Sfar, & Charrueau, 2012; Zupančič, Lavrič, & Kristl, 2015) and high chemical instability to stressing conditions. In fact, resveratrol molecule shows extensive photo-isomerization under UV light exposure. The *–trans* conformation of resveratrol has been found to have a significant biological activity, whereas the *–cis* conformation formed after UV light exposure has shown less benefits to human health (Davidov-Pardo & McClements, 2014). Therefore, there is a need to design feasible delivery systems that can improve the protection of resveratrol and facilitate its further incorporation in food products. In this regard, multilayer emulsions could be an alternative to overcome these issues.

There are several factors influencing the formation and stability of multilayer emulsions such as droplet size, concentration of biopolymers or oil droplets in the emulsion and other processing parameters including pH, ionic strength, dielectric constant, temperature or stirring (Guzey & McClements, 2006).

For instance, the biopolymer concentration in aqueous phase plays an important role on the stability of emulsions and can lead to droplets flocculation (Bouyer, Mekhloufi, Rosilio, Grossiord, & Agnely, 2012). Finding an adequate biopolymer concentration in the aqueous phase of emulsions is crucial to form nanolaminated coatings on droplets leading to stable systems. The objective of the present work was to determine the influence of biopolymer concentration in the formation of primary (lactoferrin-coated droplets), secondary (lactoferrin/alginate-coated droplets) and tertiary (lactoferrin/alginate/poly-L-lysine-coated droplets) emulsions containing resveratrol. Moreover, the physical stability and antioxidant activity of single-layer and multilayer emulsions were examined throughout storage.

2. Materials and methods

2.1. Materials

Resveratrol extracted from grape skin (purity > 99%) was kindly supplied by Changsha Organic Herb Inc./ Phyto Nutraceutical Inc. (Changsha, China). Corn oil (Fula®, Sovena, Portugal) was purchased from a local supermarket. Lactoferrin was obtained from DMV International (Veghel, The Netherlands). The composition provided by the manufacturer and expressed as a dry weigh percentage was: 96% protein, 0.5% ash, 3.5% moisture and 120 ppm iron content. Sodium alginate was purchased from Kelco International, Ltd. (Aberdeen, UK) and poly-L-lysine hydrobromide (MW 1000–5000 Da) was purchased from Sigma-Aldrich (St. Louis, MO, USA). The 1,1-diphenyl-2-picrylhydrazyl radical (DPPH) was purchased from Sigma-Aldrich (Madrid, Spain). All emulsions and biopolymer solutions were prepared with deionized water extracted from a Milli-Q system (Millipore Corp., Massachusetts, USA).

2.2. Preparation of single-layer and multilayer emulsions

2.2.1. Primary emulsions

The oil phase of the emulsions was prepared by dissolving resveratrol powder in small amounts of absolute ethanol and incorporating the previous blend to corn oil, followed by mixing in a vortex for 2 min to ensure the complete resveratrol dispersion. Ethanol was used as a co-solvent to enhance dissolution of resveratrol crystals in oil (Sessa, Tsao, Liu, Ferrari, & Donsì,

2011). The concentration of ethanol in corn oil was 0.04 g/g. The lipid phase was homogenized with the aqueous phase containing the emulsifier agent (lactoferrin solutions at 1.0%, 1.5% and 2.0% w/w, pH ≈ 5.3) in a high-shear blender at 5000 rpm for 2 min (Ultra-turrax T25, IKA Werke, Staufen, Germany), so that the final systems contained 0.01% w/w resveratrol, 0.20% w/w ethanol, 5.00% w/w corn oil, and 0.95% w/w, 1.42% w/w or 1.90% w/w lactoferrin. Afterwards, a second homogenization was carried out in a high-pressure homogenizer (Nano DeBEE, BEE International, USA) at 22,000 psi and 5 cycles. In this case, the term 'primary emulsions' referred to emulsions in which oil droplets were coated by a single lactoferrin layer. Primary emulsions were adjusted to pH 5 using 0.1 M HCl. Formulations that obtained the smallest droplet size and sufficiently strong electrical charge (as measured by ζ-potential) were selected for the two-layer emulsions formation.

2.2.2. Secondary emulsions

To prepare secondary emulsions, 5 mL of sodium alginate solutions at different concentrations and 15 mL of water were added to 5 mL of primary emulsions under continuous stirring and at a drop rate of 10 mL/min, so that the resulting emulsions contained 0.002% w/w resveratrol, 1.00% w/w corn oil, 0.38% w/w lactoferrin, and from 0.02% to 0.28% w/w alginate. All components were previously adjusted to pH 5, since at this pH biopolymers would be sufficiently charged to form electrostatic complexes. Emulsions were stirred for 15 additional min at room temperature. Secondary emulsions were sonicated for 10 min to disrupt possible flocs formed during alginate adsorption. In this case, the term 'secondary emulsions' referred to emulsions in which oil droplets were coated by lactoferrin/alginate layers. The most stable formulation was used to prepare tertiary emulsions.

2.2.3. Tertiary emulsions

To form tertiary emulsions, 5 mL of poly-L-lysine solutions at different concentrations and 45 mL of water were added to 5 mL of secondary emulsions under continuous stirring and at a drop rate of 10 mL/min, so that the final composition of emulsions was 0.0002% w/w resveratrol, 0.090% corn oil, 0.038% w/w lactoferrin, 0.022% w/w alginate, and from 0.009% to 0.045% w/w poly-L-lysine. The pH of biopolymers, water and emulsions was adjusted to 5 before blending them to induce alginate/poly-L-lysine electrostatic

interactions. Mixtures were stirred for 15 additional min at room temperature. Finally, tertiary emulsions were sonicated as described in section 2.2.2. In this case, the term 'tertiary emulsions' referred to emulsions in which oil droplets were coated by lactoferrin/alginate/poly-L-lysine layers.

2.3. Droplet size and polydispersity index measurements

The droplet size of the emulsions was determined by dynamic light scattering using a laser diffractometer (Zetasizer NanoZS, Malvern Instruments, Worcestershire, U.K.) fitted with a laser at 633 nm and temperature of 25 ºC using a backscatter detector (173º). Primary and secondary emulsions were diluted prior to analysis with ultrapure water (pH 5) at a ratio of 1:100 (v/v) to avoid multiple scattering effects. Tertiary emulsions were analyzed at a ratio of 1:10 (v/v). Measurements were performed in triplicate.

2.4. ζ- potential measurements

The electrophoretic mobility of the droplets was analyzed by Laser Doppler Velocimetry (LDV) and converted into ζ-potentials using the Smoluchowski equation in a Zetasizer Nano ZS device (Malvern Instruments, Worcestershire, U.K.). Primary and secondary emulsions were diluted prior to analysis with ultrapure water (pH 5) at a ratio of 1:100 (v/v), whereas tertiary emulsions were analyzed 1:10 (v/v) by placing samples in plastic zeta cells (DTS 1061, Malvern, UK), and equilibrating them at 25 ºC during 60 s. Analyses were done in triplicate.

2.5. Short-term stability

The physical stability of single-layer and multilayer emulsions was analyzed through changes in the size and electrical charge of oil droplets. Analyses of droplet size and ζ-potentials were performed as described in sections 2.3 and 2.4. Emulsions were stored into conical centrifuge tubes of 15 mL (Falcon™, Fisher Scientific) during four weeks at room temperature (≈ 25 ºC) and lighting. Emulsions were examined every seven days. Two independent runs were carried out for each emulsion type.

2.6. Antioxidant activity

The scavenging effect of resveratrol-enriched corn oil, primary, secondary and tertiary emulsions on DPPH• radical was evaluated through a method described by Pinheiro et al., (2015) with some modifications. Briefly, 1 mL of each emulsion was blended with 4 mL of ethanol absolute to promote the emulsion leakage and release of encapsulated resveratrol. Then, an aliquot of 0.3 mL was mixed with 0.2 mL of ethanol absolute and 2.5 mL of DPPH• solution (60 µM in ethanol) in a 10 mL test tube, achieving a total volume of 3.0 mL. Solutions were kept under dark conditions during 30 min at room temperature to carry out the reaction. Absorbance was measured at 515 nm using a Multi-Detection Microplate Reader Synergy™ HT (Biotek, Winooski, USA). The scavenging effect of resveratrol-loaded emulsions was calculated through Eq. (1) as follows:

$$Scavenging\ Effect\ (\%) = \left(\frac{A_0 - A}{A_0}\right) \times 100 \quad (1)$$

where A_o is the absorbance of the DPPH• solution and A is the absorbance of the sample with DPPH•. Two independent experiments were carried out and samples were analyzed in triplicate.

2.7. TEM imaging

The morphology of single-layer emulsions and multilayer emulsions was evaluated by transmission electron microscopy (TEM) (EM 902A, ZEISS, Germany) operating at 80 kV. TEM samples were prepared by depositing the single-layer emulsions and multilayer emulsions suspensions on a carbon-coated copper grid, and negatively stained with 1 % (w/v) uranyl acetate for observation. Samples were air-dried before analyses.

2.8. Statistical analysis

Data were analyzed through a one-way analysis of variance (ANOVA) using the statistical and graphing software SigmaPlot 11.0 Windows package (Systat software Inc.). The Holm-Sidak method was used to determine significant differences among mean values at 5% of significance level. All results are presented as the average results and standard deviations.

3. Results and discussion

3.1. Effect of lactoferrin concentration on the formation of primary emulsions

Primary emulsions prepared with different concentrations of lactoferrin in the aqueous phase showed significant differences ($p < 0.05$) in their oil droplet properties (Table 1). Although all emulsions showed particle sizes below 300 nm, the lowest value was observed when the concentration of lactoferrin in the emulsion was 1.90% w/w (187 nm) with a polydispersity index of 0.15. From the particle size distributions graph (Fig. 1), it was confirmed that these emulsions had fairly similar nanometric droplet sizes using the highest concentration of lactoferrin in the aqueous phase. It has been described that emulsions with nano-sized droplets (between 20-200 nm) are relatively more stable to gravitational separation and particle aggregation than conventional emulsions with large droplets (McClements & Rao, 2011). This feature is especially important to produce stable multilayer emulsions.

Table 1. Droplet characteristics of primary emulsions containing different lactoferrin concentrations.

Final lactoferrin concentration in emulsion (% w/w)	Mean droplet size (nm)	PdI	ζ-potential (mV)
0.95	224 ± 4^{a}	0.29 ± 0.04^{a}	48.7 ± 2.1^{a}
1.42	289 ± 3^{b}	0.362 ± 0.004^{b}	44.4 ± 1.8^{b}
1.90	187 ± 4^{c}	0.153 ± 0.016^{c}	45.8 ± 0.5^{ab}

On the other hand, there were significant differences in the ζ-potentials of primary emulsions depending on the lactoferrin concentration in the aqueous phase ($p < 0.05$). The electrical charge of lactoferrin-coated droplets was strongly positive, ranging between 50 mV and 45 mV. This suggested that lactoferrin molecules were located at the o/w interface forming cationic interfacial layers around droplets, which favor their stabilization due to strong

electrostatic repulsive forces. However, no dependence between ζ-potential of droplets and lactoferrin concentration in the aqueous phase of emulsions was observed. A successful deposition of nanolaminated coatings on droplets is given by an initial strong droplet charge, thus it was considered that primary emulsions obtained in this study were suitable to produce multilayer emulsions. In a recent study, emulsions with 1.50% w/w lactoferrin in the aqueous phase obtained droplets sizes of ≈ 230 nm and ζ-potential values of ≈ 50 mV (Zhao, Wei, Wei, Yuan, & Gao, 2015), which is in agreement with the results found in the present work. The emulsion formulation that contained 1.90% (w/w) lactoferrin was selected for the formation of secondary emulsions.

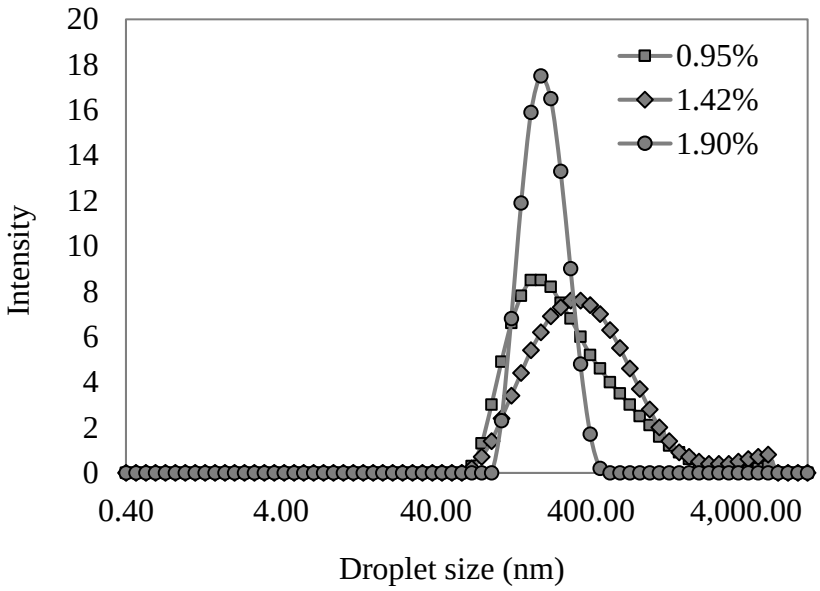

Fig. 1. Droplet size distributions of primary emulsions containing different concentrations of lactoferrin (% w/w) in the aqueous phase.

3.2. Effect of the alginate concentration on the formation of secondary emulsions

The formation of a second interfacial layer of alginate on lactoferrin-coated droplets was assessed by changes in droplet size and ζ-potentials of emulsions containing different biopolymer concentrations. In general, the alginate concentration in the aqueous phase significantly influenced the droplet size and ζ-potential of secondary emulsions, as can be seen in Fig. 2 ($p < 0.05$). First, there was an abrupt increase in the droplet size from 187 nm up to 8700 nm when the concentration of alginate increased to 0.02% w/w.

A visible phase separation could be observed in the emulsions 15 min after preparation (Fig. 2). The increase in droplet size at low alginate concentration was attributed to the bridging flocculation of droplets. If the concentration of charged species in the aqueous phase of emulsions is insufficient to saturate droplets surface, then a single molecular chain tends to adsorb to the surface of several droplets simultaneously, and hence flocculation occurs. However, bridging flocculation is reduced as the concentration of charged biopolymers in the continuous phase increases (Dickinson, 2003; Heurtault, 2003; McClements, 2005). In fact, this was also observed when alginate concentration increased in secondary emulsions. Droplet sizes gradually decreased from 1590 nm to 589 nm when alginate concentration increased from 0.04% to 0.16% w/w. However, these emulsions were also unstable after 24 h. At higher alginate concentrations (from 0.18% to 0.28% w/w), the droplet size decreased even more (249 nm). In this case, no signs of flocculation, precipitation or creaming were observed in emulsions after 24 h (Fig. 2), indicating that emulsions were fairly stable.

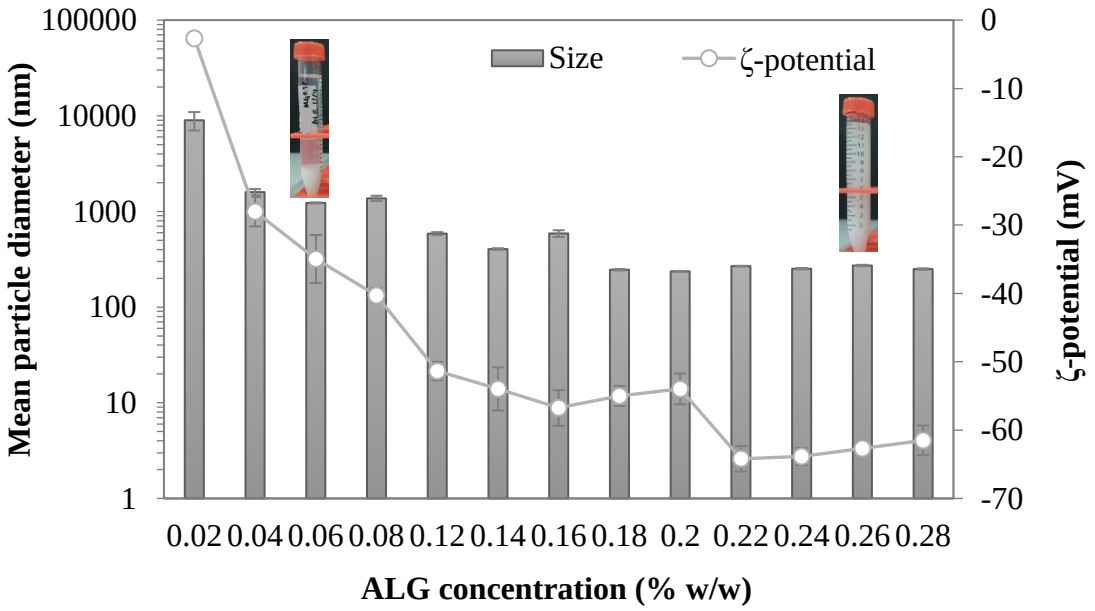

Fig. 2. Droplet size and ζ-potential values of secondary emulsions containing different concentration of alginate (ALG). The emulsions composition was 0.002% w/w resveratrol, 1% w/w oil, 0.38% w/w lactoferrin, and from 0.02% to 0.28% w/w alginate.

On the other hand, the initial ζ-potential of lactoferrin-coated droplets (46 mV) significantly decreased to -2.6 mV in emulsions that contained 0.02% w/w alginate. This suggests that lactoferrin-coated oil droplets were barely covered

by alginate molecules resulting in a weak negative ζ-potential. However, greater concentrations of alginate (from 0.04% to 0.20% w/w) led to more negative ζ-potentials (from -28 mV to -54 mV), and hence there were more alginate molecules available to be adsorbed onto lactoferrin-coated droplets. The ζ-potential remained stable in emulsions with alginate concentrations greater than 0.22% w/w, which suggested the complete saturation of droplets surface by alginate molecules and the formation of a new interfacial layer. It also means that some unbound alginate molecules were in the aqueous phase of emulsions in which the ζ-potential did not change in spite of the alginate concentration was increased. The emulsion containing 0.22% w/w alginate was selected as the most stable formulation to be used in tertiary emulsions. This formulation showed small droplet size and strong ζ-potential, without containing excessive unbound alginate chains in the aqueous phase.

3.3. Effect of the poly-L-lysine concentration on the formation of tertiary emulsions

A number of tertiary emulsions were obtained by incorporating different poly-L-lysine concentrations in secondary emulsions and the changes in droplets characteristics were evaluated. Fig. 3 shows the droplet sizes and ζ-potentials of tertiary emulsions. An increase in the initial diameter of lactoferrin/alginate-coated droplets (268 nm) was observed when the concentration of poly-L-lysine increased to 0.0018% w/w. Also, there was a visible phase separation in emulsions after 15 min of preparation. This was attributed to the bridging flocculation that led to emulsions instability, as observed in secondary emulsions that contained low biopolymer concentrations (section 3.2). However, a significant decrease in droplet size was observed when the poly-L-lysine concentration increased from 0.018% to 0.036% w/w. In this case, tertiary emulsions were visibly stable after 24 h. The further incorporation of poly-L-lysine in emulsions resulted in an increasing droplet size (more than 1 μm) and emulsions were highly unstable. Presumably, the high poly-L-lysine concentration in emulsions caused droplets aggregation by depletion interactions. This instability phenomenon occurs in the presence of excessive amounts of non-adsorbed biopolymers in the continuous phase of emulsions. This causes attractive interactions between droplets and their consequent aggregation (Benjamin, Silcock, Leus, & Everett, 2012; McClements, 2000).

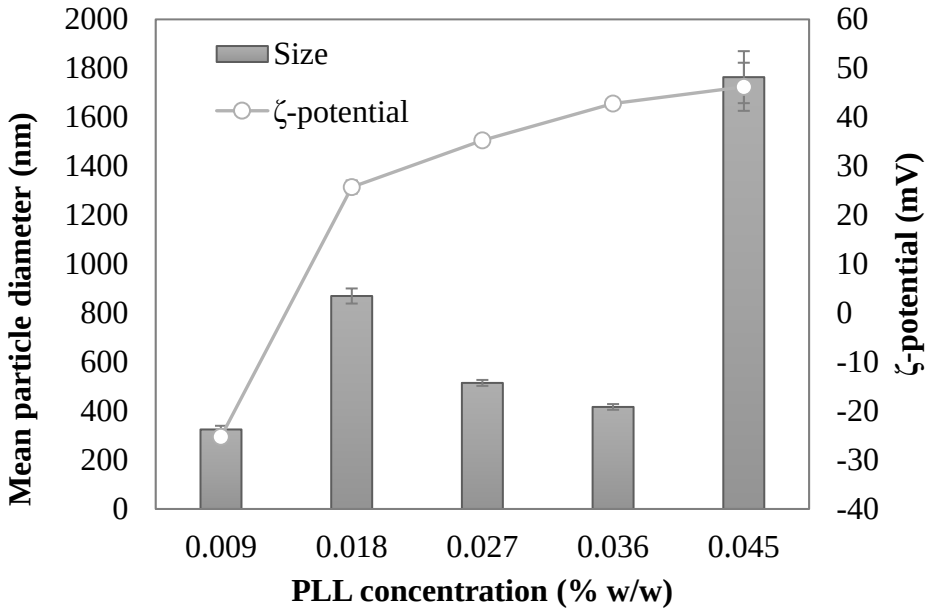

Fig. 3. Droplet size and ζ-potential values of tertiary emulsions containing different concentrations of poly-L-lysine (PLL). Emulsions were composed by 0.0002% w/w resveratrol, 0.090% w/w corn oil, 0.038% w/w lactoferrin, 0.022% w/w alginate, and from 0.009% to 0.045% w/w poly-L-lysine.

Moreover, the magnitude of the electrical charge of lactoferrin/alginate-coated droplets decreased from -64.2 mV to -25.6 mV, increasing the concentration of poly-L-lysine in emulsions to 0.009% (w/w). Although the net charge of particles was still negative, this decrease suggested that poly-L-lysine molecules adsorbed on droplets' surface were not sufficient to completely cover them. It is likely that the interfacial potential of droplets was the resulting contribution of uncoated negative alginate patches and positive poly-L-lysine patches adsorbed on the droplets' surface. Droplets in tertiary emulsions with 0.018% w/w poly-L-lysine had positive ζ-potentials (25.8 mV) and were more positive as the concentration increased to 0.045% w/w. At this point, the formation of a third poly-L-lysine layer on oil droplets was confirmed. Tertiary emulsions with 0.036% w/w poly-L-lysine were used in the subsequent experiments. These emulsions presented small droplet sizes and strong ζ-potential that corroborated the formation of tertiary emulsions.

3.4. Short-term stability of resveratrol-loaded emulsions

Once single-layer and multilayer emulsions were obtained, their physical stability was assessed by monitoring changes in droplet size and ζ-potential

during four weeks (Fig. 4). Emulsions were maintained at room temperature and lighting, simulating conventional storage conditions of non-perishable foods. The initial average droplet size of primary emulsions was 187 nm, and no significant changes were observed after four weeks ($p < 0.05$) (Fig. 4A). On the contrary, the droplet size of secondary emulsions slightly increased from 227 nm (just prepared) to 274 nm at the second week, though it remained stable until the fourth week. This increase may be caused by a subsequent adsorption of remaining *free* alginate molecules that were not bound to droplets surface initially, or by particle aggregation during storage. On the contrary, tertiary emulsions showed a decrease in the droplet diameter from 416 nm to 388 nm, which might be attributed to a rearrangement of the biopolymer chains adsorbed to oil droplets' surface, forming a denser molecular packing that result in a smaller hydrodynamic diameter of droplets. In fact, this behavior has been described for several multi-layered structures produced by the progressive adsorption of oppositely charged biopolymers. In a first moment, the molecular chains are rapidly adsorbed to the substrate and, in a second moment, changes in the conformation occur slowly in order to reach an energetic equilibrium (Marudova, Lang, Brownsey, & Ring, 2005). Despite of these events, droplet sizes of tertiary emulsions were similar from the second to the fourth week.

The ζ-potential values of primary, secondary and tertiary emulsions during four weeks were also assessed (Fig. 4B). The initial ζ-potential of primary emulsions decreased from 45.8 mV (just prepared) to 15.9 mV after four weeks. Lactoferrin molecules may change their conformation when they are located at an o/w interface, thus letting some of their most reactive groups exposed (originally protected inside of the globular protein). Therefore, the interaction of these functional groups with other molecules in the surrounding medium may result in protein degradation, hence changing electrical properties of droplets at storage conditions (pH 5, 25 ºC, lighting) (Tokle & McClements, 2011). In a previous work, the magnitude of positive ζ-potential of lactoferrin-coated droplets decreased in emulsions after 14 days of storage (Mao et al., 2013). The same behavior was observed in emulsions of citral stabilized with milk proteins after four weeks (Xiang, Liu, Fan, & Gao, 2015).

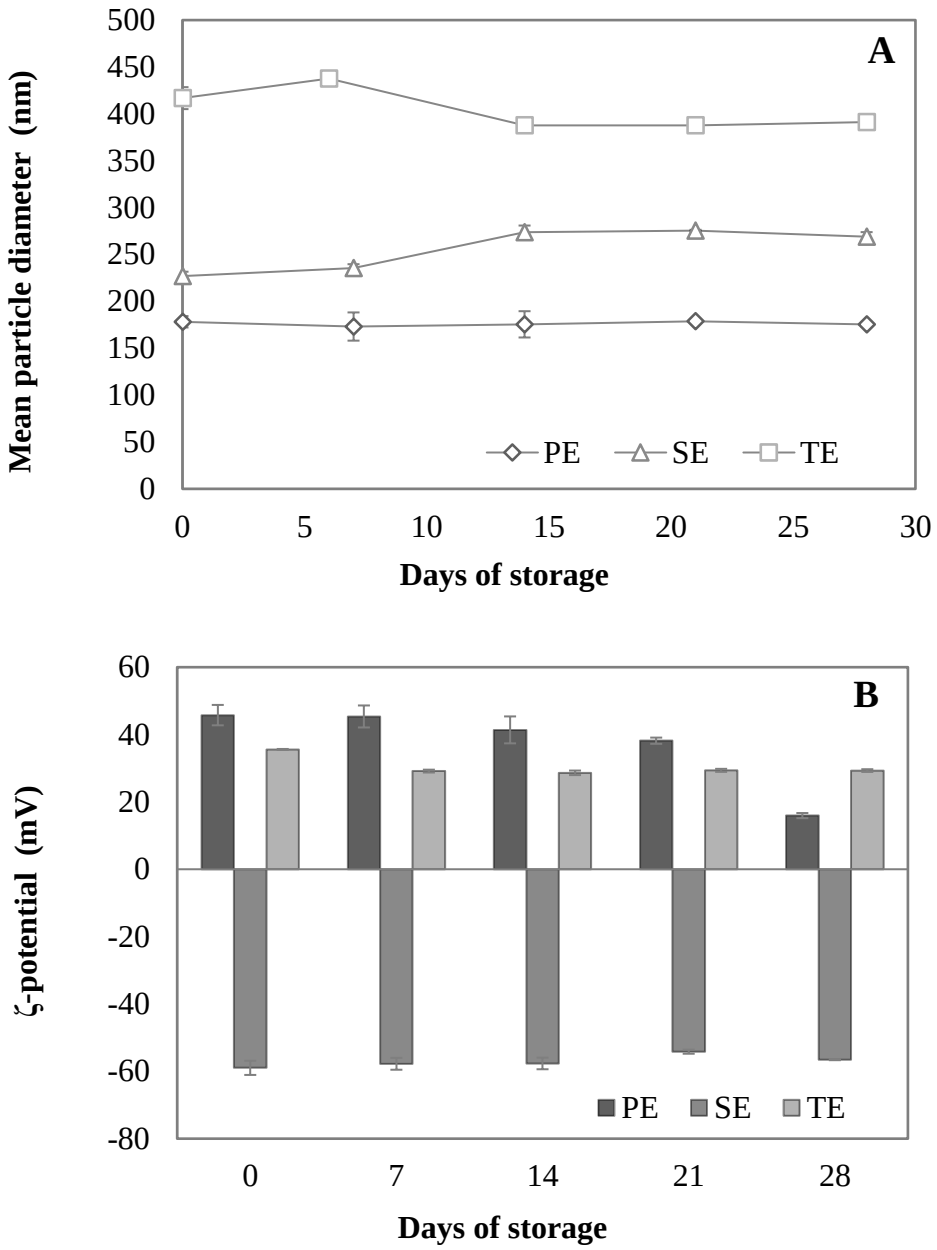

Fig. 4. (A) Mean droplet size and (B) ζ-potential values of primary emulsions (**PE**) (0.01% resveratrol, 5% corn oil and 1.90% lactoferrin), secondary emulsions (**SE**) (0.002% resveratrol, 1% corn oil, 0.38% lactoferrin and 0.22% alginate) and tertiary emulsions (**TE**) (0.0002% resveratrol, 0.090% corn oil, 0.038% lactoferrin, 0.022% alginate and 0.036% poly-L-lysine) during storage.

On the contrary, secondary emulsions did not show variations in their ζ-potential after four weeks. So, a change in the layer composition of oil droplets significantly enhanced emulsion stability, probably by protecting lactoferrin molecules from degradation. The ζ-potential of tertiary emulsions also remained stable during storage time, with only a slight decrease from

35.6 ± 0.15 mV to 29.2 ± 0.42 mV after 7 days. From the second to the fourth storage week, the ζ-potential of tertiary emulsions did not present significant differences. This confirmed that a tri-layered coating on droplets improved emulsions' stability during a short-term storage.

3.5. Changes in the antioxidant activity during storage

The DPPH$^{\bullet}$ radical scavenging activity of primary, secondary and tertiary emulsions with encapsulated resveratrol was studied during four weeks (Fig. 5). Also, the antioxidant activity of corn oil containing resveratrol was assessed. A significant decrease in the antioxidant activity of resveratrol-loaded oil was observed from 67.83% (day 0) to 52.99% after four weeks. This was attributed to the chemical instability of resveratrol under environmental conditions. Numerous studies have shown the high susceptibility of resveratrol to degradation by light, pH and temperature (Leiro et al., 2004; Zupančič, Lavrič, & Kristl, 2015). It has been described that resveratrol molecules can change rapidly from *trans*- to *cis*- isomers under UV light exposure, therefore reducing its biological activity (e.g. antioxidant activity). On the other hand, no significant differences were observed in the antioxidant activity of primary emulsions stored during four weeks ($p < 0.05$). In general, the antioxidant activities of the secondary and tertiary emulsions were lower than that of primary emulsions, which can be explained by the lower concentration of resveratrol in these emulsions. However, in both cases the antioxidant activity of the emulsions remained stable during storage. Interestingly, the DPPH$^{\bullet}$ radical scavenging activity of tertiary and secondary emulsions was very similar, although the concentration of resveratrol in tertiary emulsions was 10-fold lower than in secondary emulsions. This was probably attributed to the presence of other compounds, such as poly-L-lysine, that might have some antioxidant activity, thus contributing to the overall radical scavenging activity of the emulsions. Literature works support this statement, since it has been reported that poly-L-lysine molecules have certain antioxidant effect (Pan & Nitin, 2015; Tikekar, Hernandez, Land, & Nitin, 2013).

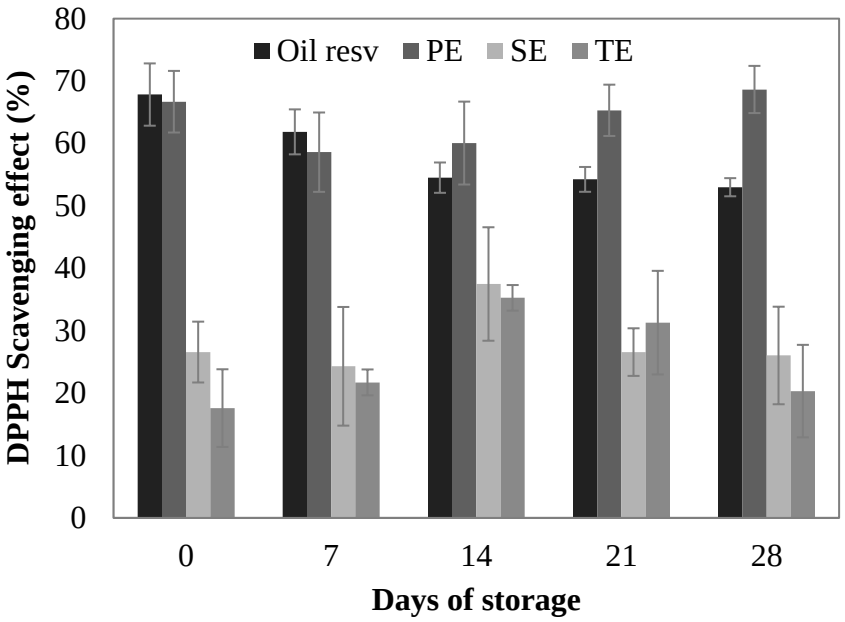

Fig. 5. Antioxidant activity of resveratrol-enriched corn oil (**oil-resv**), primary emulsions (**PE**), secondary emulsions (**SE**), and tertiary emulsions (**TE**) stored during four weeks.

3.6. Microstructure

The microstructure of single-layer and multilayer emulsions was observed by TEM (Fig. 6). The morphology of lactoferrin-coated oil droplets in primary emulsions showed a well-defined spherical shape surrounded by a discrete interface corresponding to lactoferrin layer (Fig. 6A). The droplet sizes observed by TEM are in concordance with those obtained by dynamic light scattering. The lactoferrin/alginate-coated droplets in secondary emulsions were also spherical with a light inner region and a slightly dark outer region conforming the shell, which is presumably the two-layer coating (Fig. 6B). In the third case, the oil droplets coated by three layers (lactoferrin, alginate and poly-L-lysine) were characterized by a light core and a visible intense black coating that corresponded to the nanolaminated coating (Fig. 6C). These results confirmed that emulsions showed different microstructures depending on the layer composition on droplets.

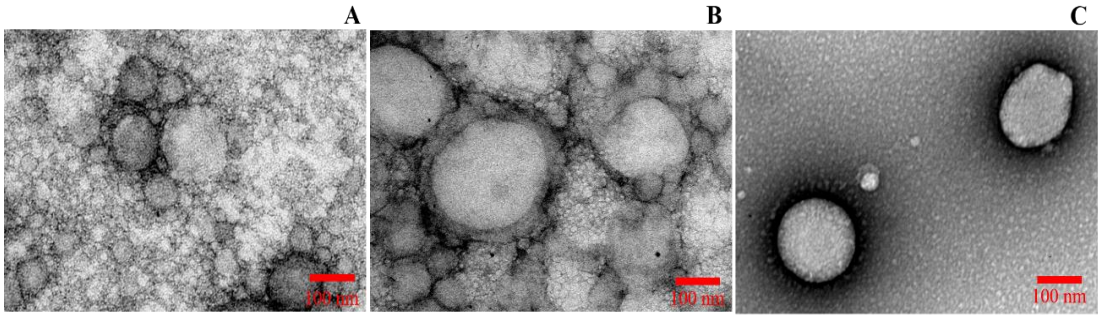

Fig. 6. Images obtained by Transmission Electron Microscopy of **(A)** primary emulsions, **(B)** secondary emulsions, and **(C)** tertiary emulsions. The magnification was 10.000x.

4. Conclusions

Multilayer emulsions were successfully obtained as a strategy to encapsulate resveratrol. Finding the effective biopolymer concentration was crucial to develop stable emulsions. For instance, bridging flocculation and depletion interactions were observed in emulsions when the biopolymer concentration was either too low or too high. The emulsion stability during storage was improved when oil droplets were coated by lactoferrin/alginate and lactoferrin/alginate/poly-L-lysine, leading to minimal changes in the droplet size and ζ-potential of emulsions during four weeks. The antioxidant activity of emulsions containing resveratrol remained stable during storage; however, the antioxidant activity of resveratrol-enriched oil decreased due to resveratrol degradation. TEM images revealed the presence of nanolaminated coatings around droplets. The current work confirms the feasibility of using multilayer emulsions as strategy to encapsulate resveratrol and presents relevant knowledge for designing nanostructured delivery systems of active ingredients for food applications.

5. Acknowledgments

This research was supported by the Ministerio de Ciencia e Innovación (Spain) throughout the projects AGL2009-11475 and ALG2012-35635, and by the Portuguese Foundation for Science and Technology (FCT) under the scope of the strategic funding of UID/BIO/04469/2013 unit and COMPETE 2020 (POCI-01-0145-FEDER-006684), Project RECI/BBB-EBI/0179/2012 (FCOMP-01-0124-FEDER-027462) and FCT Strategic Project of

UID/BIO/04469/2013 unit. The authors also thank the Project “BioInd - Biotechnology and Bioengineering for improved Industrial and Agro-Food processes, REF. NORTE-07-0124-FEDER-000028” Co-funded by the Programa Operacional Regional do Norte (ON.2 – O Novo Norte), QREN, FEDER. The author A. Acevedo-Fani thanks the University of Lleida for the pre-doctoral grant. The author H. D. Silva, (SFRH/BD/81288/2011) is the recipient of a fellowship from the Fundação para a Ciência e Tecnologia (FCT, Portugal). The authors would like to acknowledge to Rui Fernandes from IBMC, University of Porto, for assistance in taking the TEM microphotographs.

6. References

Benjamin, O., Silcock, P., Leus, M., & Everett, D. W. (2012). Multilayer emulsions as delivery systems for controlled release of volatile compounds using pH and salt triggers. *Food Hydrocolloids*, *27*(1), 109–118.

Bokkhim, H., Bansal, N., GrØndahl, L., & Bhandari, B. (2013). Physico-chemical properties of different forms of bovine lactoferrin. *Food Chemistry*, *141*(3), 3007–3013.

Bokkhim, H., Bansal, N., Grøndahl, L., & Bhandari, B. (2016). Characterization of alginate–lactoferrin beads prepared by extrusion gelation method. *Food Hydrocolloids*, *53*, 270–276.

Bortnowska, G. (2015). Multilayer Oil-in-Water Emulsions: Formation, Characteristics and Application as the Carriers for Lipophilic Bioactive Food Components – a Review. *Polish Journal of Food and Nutrition Sciences*, *65*(3), 157–166.

Bouyer, E., Mekhloufi, G., Rosilio, V., Grossiord, J.-L., & Agnely, F. (2012). Proteins, polysaccharides, and their complexes used as stabilizers for emulsions: alternatives to synthetic surfactants in the pharmaceutical field? *International Journal of Pharmaceutics*, *436*(1–2), 359–78.

Cerqueira, M. A., Pinheiro, A. C., Silva, H. D., Ramos, P. E., Azevedo, M. A., Flores-López, M. L., … Vicente, A. A. (2014). Design of Bio-nanosystems for Oral Delivery of Functional Compounds. *Food Engineering Reviews*, *6*(1–2), 1–19.

Chang, Y., McLandsborough, L. A., & McClements, D. J. (2014). Interaction of cationic antimicrobial (ε-polylysine) with food-grade biopolymers: Dextran, chitosan, carrageenan, alginate, and pectin. *Food Research International*, *64*, 396–401.

Choi, A.-J., Kim, C.-T. C.-J., Cho, Y.-J., Hwang, J.-K., & Kim, C.-T. C.-J. (2011). Characterization of Capsaicin-Loaded Nanoemulsions Stabilized with Alginate and Chitosan by Self-assembly. *Food and Bioprocess Technology*, *4*(6), 1119–1126.

Davidov-Pardo, G., & McClements, D. J. (2014). Resveratrol encapsulation: Designing delivery systems to overcome solubility, stability and bioavailability issues. *Trends in Food Science & Technology*, *38*(2), 88–103.

Dickinson, E. (2003). Hydrocolloids at interfaces and the influence on the properties of dispersed systems. *Food Hydrocolloids*, *17*(1), 25–39.

Fioramonti, S. A., Arzeni, C., Pilosof, A. M. R., Rubiolo, A. C., & Santiago, L. G. (2015). Influence of freezing temperature and maltodextrin concentration on stability of linseed oil-in-water multilayer emulsions. *Journal of Food Engineering*, *156*, 31–38.

Guzey, D., & McClements, D. J. (2006). Formation, stability and properties of multilayer emulsions for application in the food industry. *Advances in Colloid and Interface Science*, *128–130*, 227–248.

Heurtault, B. (2003). Physico-chemical stability of colloidal lipid particles. *Biomaterials*, *24*(23), 4283–4300.

Hosseini, S. M. H., Emam-Djomeh, Z., Sabatino, P., & Van der Meeren, P. (2015). Nanocomplexes arising from protein-polysaccharide electrostatic interaction as a promising carrier for nutraceutical compounds. *Food Hydrocolloids*, *50*, 16–26.

Leiro, J., Alvarez, E., Arranz, J. A., Laguna, R., Uriarte, E., & Orallo, F. (2004). Effects of cis-resveratrol on inflammatory murine macrophages: antioxidant activity and down-regulation of inflammatory genes. *Journal of Leukocyte Biology*, *75*(6), 1156–65.

Liu, F., Wang, D., Sun, C., McClements, D. J., & Gao, Y. (2016). Utilization of interfacial engineering to improve physicochemical stability of β-carotene emulsions: Multilayer coatings formed using protein and protein–polyphenol conjugates. *Food Chemistry*, *205*, 129–139.

Mao, Y., Dubot, M., Xiao, H., & McClements, D. J. (2013). Interfacial engineering using mixed protein systems: emulsion-based delivery systems for encapsulation and stabilization of β-carotene. *Journal of Agricultural and Food Chemistry*, *61*(21), 5163–9.

Marudova, M., Lang, S., Brownsey, G. J., & Ring, S. G. (2005). Pectin-chitosan multilayer formation. *Carbohydrate Research*, *340*(13), 2144–9.

McClements, D. J. (2000). Comments on viscosity enhancement and depletion flocculation by polysaccharides. *Food Hydrocolloids*, *14*(2), 173–177.

McClements, D. J. (2005). *Food emulsions : principles, practices, and techniques*. (C. Press, Ed.). Boca Raton, Fla. : CRC Press. Retrieved from t

McClements, D. J., & Rao, J. (2011). Food-grade nanoemulsions: formulation, fabrication, properties, performance, biological fate, and potential toxicity. *Critical Reviews in Food Science and Nutrition*, *51*(4), 285–330.

Noshad, M., Mohebbi, M., Koocheki, A., & Shahidi, F. (2015). Influence of Interfacial Engineering on Stability of Emulsions Stabilized with Soy Protein Isolate. *Journal of Dispersion Science and Technology*, *37*(1), 56–65.

O'Regan, J., Ennis, M. P., & Mulvihill, D. M. (2009). Milk Proteins. In G. Phillips & P. A. Williams (Eds.), *Handbook of hydrocolloids* (2nd ed., pp. 298–343). Boca ratón, FL: CRC Press and Woodhead Publishing.

Pan, Y., & Nitin, N. (2015). Effect of layer-by-layer coatings and localization of antioxidant on oxidative stability of a model encapsulated bioactive compound in oil-in-water emulsions. *Colloids and Surfaces. B, Biointerfaces*, *135*, 472–80.

Pinheiro, A. C., Bourbon, A. I., Cerqueira, M. A., Maricato, É., Nunes, C., Coimbra, M. A., & Vicente, A. A. (2015). Chitosan/fucoidan multilayer nanocapsules as a vehicle for controlled release of bioactive compounds. *Carbohydrate Polymers*, *115*, 1–9.

Pinheiro, A. C., Coimbra, M. A., & Vicente, A. A. (2016). In vitro behaviour of curcumin nanoemulsions stabilized by biopolymer emulsifiers – Effect of interfacial composition. *Food Hydrocolloids*, *52*, 460–467.

Shchukina, E. M., & Shchukin, D. G. (2012). Layer-by-layer coated emulsion microparticles as storage and delivery tool. *Current Opinion in Colloid & Interface Science*, *17*(5), 281–289.

Shimoni, G., Shani Levi, C., Levi Tal, S., & Lesmes, U. (2013). Emulsions stabilization by lactoferrin nano-particles under in vitro digestion conditions. *Food Hydrocolloids*, *33*(2), 264–272.

Tikekar, R. V., Hernandez, M., Land, D. P., & Nitin, N. (2013). "Click chemistry" based conjugation of lipophilic curcumin to hydrophilic ε-polylysine for enhanced functionality. *Food Research International*, *54*(1), 44–47.

Tokle, T., & McClements, D. J. (2011). Physicochemical properties of lactoferrin stabilized oil-in-water emulsions: Effects of pH, salt and heating. *Food Hydrocolloids*, *25*(5), 976–982.

Xiang, J., Liu, F., Fan, R., & Gao, Y. (2015). Physicochemical stability of citral emulsions stabilized by milk proteins (lactoferrin, α-lactalbumin, β-lactoglobulin) and beet pectin. *Colloids and Surfaces A: Physicochemical and Engineering Aspects*, *487*, 104–112.

Yoshida, T., Hiraki, J., & Nagasawa, T. (2005). ε-Poly-L-lysine. In A. Steinbüchel & S. K. Rhee (Eds.), *Polysaccharides and Polyamides in the Food Industry* (pp. 671–685). Weinheim: Wiley-VCH.

Zhao, J., Wei, T., Wei, Z., Yuan, F., & Gao, Y. (2015). Influence of soybean soluble polysaccharides and beet pectin on the physicochemical properties of lactoferrin-coated orange oil emulsion. *Food Hydrocolloids*, *44*, 443–452.

Zupančič, Š., Lavrič, Z., & Kristl, J. (2015). Stability and solubility of trans-resveratrol are strongly influenced by pH and temperature. *European Journal of Pharmaceutics and Biopharmaceutics : Official Journal of Arbeitsgemeinschaft Für Pharmazeutische Verfahrenstechnik e.V*, *93*, 196–204.

CHAPTER III: FOOD-GRADE MULTILAYER EMULSIONS AS DELIVERY SYSTEMS OF RESVERATROL. PART II: INFLUENCE OF LACTOFERRIN, ALGINATE AND POLY-L-LYSINE LAYERS ON THE GASTROINTESTINAL FATE

Acevedo-Fani, A., Pinheiro, A. C., Silva, H. D., Vilas Boas, D., Soliva-Fortuny, R., Martín-Belloso, O., & Vicente, A. A

Food Hydrocolloids (sent)

ABSTRACT

The influence of the interfacial layer composition on droplets stability during *in vitro* digestion and resveratrol bioaccessibility was investigated using resveratrol-enriched oil multilayer emulsions: Primary (lactoferrin layer), secondary (lactoferrin/alginate layers) and tertiary (lactoferrin/alginate/poly-L-lysine layers). Changes in the droplet size, ζ-potential and microstructure were monitored in the digestion stages, and resveratrol bioaccessibility of digested emulsions was also assessed. Primary and secondary emulsions were stable in the oral phase (pH 7), but underwent extensive droplet flocculation in the gastric phase (pH 3). On the contrary, tertiary emulsions were highly unstable incubated with salivary fluids, however, there was a reapportion of droplets under exposure with gastric fluids. Single-layer and multilayer emulsions presented particles of different sizes in the intestinal phase originated by the digestion products. Examinations of single-layer and multilayer emulsions by epifluorescence microscopy confirmed the aggregation, reapportion and digestion of droplets incubated with the simulated gastrointestinal fluids. The initial ζ-potential of primary (45 ± 3 mV), secondary (-64 ± 2 mV), and tertiary (42 ± 5 mV) emulsions became negative as advancing to the small intestine phase due to interactions between ionized groups on droplets' interface and electrolytes, enzymes or bio-surfactants within the simulated fluids. Resveratrol bioaccessibility increased as the number of interfacial layers increased, but the final resveratrol concentration in the mixed micelle phase was less than 1 ppm. These results contribute to shed light on the design of multilayer emulsions as delivery systems of resveratrol envisaged to be used in beverages or functional foods.

Keywords: resveratrol, multilayer emulsions, emulsions, layer composition, bioaccessibility, *in vitro* digestion

1. Introduction

Resveratrol is a naturally occurring polyphenol that belongs to the stilbenes family and is mainly present in grape skins, berry fruits and peanuts as well as in derived products such as wine or peanut butter (Kumar, Shankar, & Rao, 2009). It is widely recognized for a number of health-promoting benefits in humans, including antioxidant activity, anti-inflammatory, anti-carcinogenic, cardio-protective and neuro-protective properties. It has also been found to have a positive impact on the lipid and glucose metabolism (Cottart, Nivet-Antoine, & Beaudeux, 2014; Smoliga, Baur, & Hausenblas, 2011; Xu & Si, 2012). For such reasons, the presence of resveratrol in functional foods and beverages has a great interest. However, there are several challenges that have to be overcome in order to reach this goal.

Resveratrol is chemically unstable to oxygen, light, pH and high temperature, presenting isomerization from the *–trans* to *–cis* conformation, which reduces its biological properties (Amri, Chaumeil, Sfar, & Charrueau, 2012). The chemical stability of ingested resveratrol may be modified by the different gastrointestinal (GI) environments that involve changes in pH, ionic strength, as well as the presence of enzymes, surface-active substances or biopolymers (Ting, Jiang, Ho, & Huang, 2014; Zupančič, Lavrič, & Kristl, 2015). Moreover, resveratrol is scarcely water soluble (0.021 – 0.030 mg/mL) (Davidov-Pardo & McClements, 2014), which means that the vast majority of this compound tends to precipitate in the aqueous intestinal lumen, thus limiting adsorption through the intestinal epithelium (Delmas et al., 2011). The remaining resveratrol that can effectively be transported to the epithelial cells is rapidly metabolized by the enterocytes and hepatocytes to form glucuronide and sulfate derivatives, thus leading to a low bioavailability (Wenzel & Somoza, 2005). In fact, clinical investigations have shown that the oral bioavailability of resveratrol is less than 1% of the initial intake and around 75% is excreted by urine and feces (Walle, 2011). Therefore, food fortification with resveratrol is rather limited due to its low oral bioavailability. As a consequence, there is a need of designing food-grade delivery systems able to enhance resveratrol protection during the early stages of the gastrointestinal process and that allow the controlled delivery at the adsorption site.

Oil-in-water nanostructured systems are particularly suitable to increase the oral bioavailability of lipophilic active ingredients, since they can enhance their stability in the GI tract and in some cases, they may increase the bioavailability of encapsulated active ingredients by modulating the oil droplet size, composition or interfacial properties (McClements, 2015). In particular, multilayer emulsions are regarded as emulsions containing oil droplets

surrounded by a nanolaminated coating, which is formed by the electrostatic deposition of oppositely charged surfactants and/or biopolymers (layer-by-layer assembly technique) (Guzey & McClements, 2006). These emulsions allow loading poor-water soluble compounds, such as resveratrol, in the lipid core and hydrophilic substances in the coating shell. Their most important properties are the improved physical stability to pH, high ionic strength, temperature, dehydration or freezing, compared to conventional emulsions (Aoki, Decker, & McClements, 2005; Fioramonti, Arzeni, Pilosof, Rubiolo, & Santiago, 2015; Katsuda, McClements, Miglioranza, & Decker, 2008).

Interestingly, the layer composition of oil droplets can be prepared with different materials, such as polysaccharides, proteins or lipids, in order to achieve a controlled release of the encapsulated active ingredients or an specific behavior under trigger conditions (Beicht, Zeeb, Gibis, Fischer, & Weiss, 2013; Benjamin, Silcock, Leus, & Everett, 2012). It has been previously showed that emulsions in which oil droplets are surrounded by multilayer coatings are more stable in GI conditions than conventional emulsions (Zeeb, Lopez-Pena, Weiss, & McClements, 2015). The interfacial layer composition of oil droplets can also affect the lipid digestibility and bioaccessibility of nutraceuticals, such as β-carotene (Zhang et al., 2015). As far as we are concerned, the behavior of resveratrol-loaded multilayer emulsions under simulated gastrointestinal conditions to predict their biological fate has not yet been studied. Therefore, the objective of the current research work was to study the impact of the interfacial layer composition of oil droplets loaded with resveratrol and stabilized in oil-in-water emulsions on their physical and biological stability.

2. Materials and methods

2.1. Materials

Resveratrol extracted from grape skin (purity > 99%) was kindly supplied by Changsha Organic Herb Inc./ Phyto Nutraceutical Inc. (Changsha, China). Corn oil (Fula®, Sovena, Portugal) was purchased in a local supermarket. Powdered apo-lactoferrin was obtained from DMV International (Veghel, The Netherlands). The composition provided by the manufacturer and expressed as a dry weigh percentage was: 96% protein, 0.5% ash, 3.5% moisture and an iron content around 120 ppm. Powdered sodium alginate was provided by Kelco International, Ltd. (Aberdeen, U.K.) and poly-L-lysine hydrobromide (MW 1000–5000 Da) was purchased from Sigma-Aldrich (St. Louis, MO, USA). Pepsin from porcin gastric mucosa (600 U/mL), lipase from porcine pancreas (40 U/mL), pancreatin from porcine pancreas (8 × USP), porcine bile extract and hydrochloric acid and sodium bicarbonate were provided by

Sigma–Aldrich (St. Louis, MO, USA). Chloroform was acquired in Fisher Scientific (NJ, USA), acetone from Fisher Chemical (Loughborough, U.K.) and sodium hydroxide and phenolphthalein from Panreac (Barcelona, Spain). Emulsions and biopolymer solutions were prepared with deionized water extracted from a Milli-Q system (Millipore Corp., Massachusetts, USA).

2.2. Formation of single-layer and multilayer emulsions

2.2.1. Primary emulsions

The oil phase was prepared by dissolving powdered resveratrol in absolute ethanol, incorporating the previous blend in corn oil and mixing all together in a vortex for 2 min to ensure the complete dispersion of resveratrol. Ethanol was used as a co-solvent to enhance dissolution of resveratrol crystals in oil (Sessa, Tsao, Liu, Ferrari, & Donsì, 2011). The primary emulsions were prepared following the protocol developed by Pinheiro et al., (2016) with minor modifications. The oil phase and the aqueous phase containing the surfactant (lactoferrin solution 2% w/w, pH ≈ 5.3) were homogenized in a high-shear blender at 5000 rpm for 2 min (Ultra-turrax T25, IKA Werke, Staufen, Germany). Subsequently, emulsions were pumped into a high pressure homogenizer (Nano DeBEE, BEE International, USA) at 22.000 psi for 5 passes to produce primary emulsions, with a final concentration of 0.01% w/w resveratrol, 0.20% w/w ethanol, 5.00% w/w corn oil, and 1.90% w/w lactoferrin. The pH was adjusted to pH 5 using 0.1 M HCl.

2.2.2. Secondary emulsions

To prepare secondary emulsions, 5 mL of 1.1% (w/w) alginate solutions and 15 mL of water were added to 5 mL of primary emulsions under continuous stirring, at a drop rate of 10 mL/min. All components were adjusted to pH 5 separately before blending them, since at this pH biopolymers would be sufficiently charged to form electrostatic complexes. Emulsions were stirred for 15 additional min at room temperature. Secondary emulsions were sonicated for 10 min to disrupt possible flocs formed during alginate adsorption. In this case, secondary emulsions were referred to emulsions in which oil droplets were coated by lactoferrin/alginate layers. The final composition was 0.002% w/w resveratrol, 1% w/w corn oil, 0.38% w/w lactoferrin, and 0.22% w/w alginate.

2.2.3. Tertiary emulsions

To form tertiary emulsions, 5 mL of poly-L-lysine solution 0.4% (w/w) and 45 mL of water were added to 5 mL of secondary emulsions under continuous stirring, at a drop rate of 10 mL/min. The pH of the system was 5 to promote

electrostatic interactions between oppositely charged biopolymers. The mixtures were stirred for 15 min more, at room temperature. Finally, tertiary emulsions were sonicated as described in section 2.2.2. In this case, tertiary emulsions were referred to emulsions in which oil droplets were coated by lactoferrin/alginate/poly-L-lysine layers. The final composition was 0.0002% w/w resveratrol, 0.090% w/w corn oil, 0.038% w/w lactoferrin, 0.022% w/w alginate, and 0.036% w/w poly-L-lysine.

2.3. *In vitro* digestion

The gastrointestinal process was simulated using the harmonized static *in vitro* digestion protocol previously proposed by Minekus et al. (2014). In this model, the conditions of the mouth, stomach and small intestine were mimicked to study the biological fate of the single-layer and multilayer emulsions containing encapsulated resveratrol.

The simulated salivary fluid (SSF), simulated gastric fluid (SGF) and simulated intestinal fluid (SIF) solutions were prepared according to Table 1. Calcium chloride was added in every stage of the *in vitro* digestion rather than in the electrolyte solutions to avoid precipitation. The simulated digestion fluids were warmed up at 37 ºC in a water bath before starting the *in vitro* gastrointestinal process.

Oral phase: aliquots of 4 mL of SSF, 5 mL of the multilayer emulsions (primary, secondary or tertiary), 25 µL of $CaCl_2$ 0.3 M and 0.475 mL of ultrapure water were added to conical centrifuge tubes of 50 mL (Falcon™, Fisher Scientific, USA) to obtain a final ratio of emulsions and SSF of 50:50 (v/v). Tubes were incubated for 2 min at 37 ºC under agitation in a water bath. Afterwards, aliquots of 1 mL of sample were taken from the tubes.

Gastric phase: a porcine pepsin solution (3600 U/mL) was prepared in ultrapure water and left on ice. The “bolus” sample from the oral phase (9 mL) was mixed with 7.2 mL of SGF, 1 mL of pepsin (to obtain a final activity of 2000 U/mL) and 4.5 µL of $CaCl_2$, 0.3 M. The pH was adjusted to 3 by adding 1 M HCl and the volume required was recorded. The amount of ultrapure water needed to complete a volume of 18 mL was added, in order to reach a final ratio of bolus to SGF of 50:50 (v/v). The sample was incubated for 2 h at 37 ºC under agitation in a water bath. After incubation, an aliquot of 1 mL was removed from the sample and the pH was increased to 7 using 1 M NaOH and stored in ice to stop the enzymatic reactions.

Table 1. Composition of the simulated digestion fluids.

Salts added	SSF (pH 7)	SGF (pH 3)	SIF (pH 7)
	Salt concentration (mmol/L)	Salt concentration (mmol/L)	Salt concentration (mmol/L)
KCl	15.1	6.9	6.8
KH_2PO_4	3.7	0.9	0.8
$NaHCO_3$	13.6	25	85
NaCl	-	47.2	38.4
$MgCl_2(H_2O)_6$	0.15	0.12	0.33
$(NH_4)_2CO_3$	0.06	0.5	-
$CaCl_2(H_2O)_2$	1.5	0.15	0.6
HCl	1.1	15.6	8.4

SSF: simulated salivary fluid; SGF: simulated gastric fluid; SIF: simulated intestinal fluid

Intestinal phase: a pancreatin solution (680 U/mL) was prepared in SIF and left in ice. Bile salts (80 mg/mL) were solubilized in SIF under stirring until complete dissolution. The "chyme" sample from the gastric phase (17 mL) was mixed with 8.6 mL of SIF, 5 mL of pancreatin (to reach a final activity of 100 U/mL), 2.07 mL of bile (to reach 10 mM in the final mixture), and 34 µL of 0.3 M $CaCl_2$. The pH was adjusted to 7 adding 1 M NaOH and the volume required was recorded. The amount of ultrapure water necessary to complete a volume of 34 mL was added in order to obtain a final ratio of chyme to SIF of 50:50 (v/v). The sample was incubated for 2 h at 37 ºC under agitation in a water bath. Afterwards, an aliquot of 340 µL of 1 mM Pefabloc was added to the sample and stored in ice to inhibit enzymatic activities.

The *in vitro* digestion process was carried out in triplicate for each type of emulsion.

2.4. Physical stability of emulsions

The average droplet size and size distribution of single-layer and multilayer emulsions were measured in a laser diffractometer (Zetasizer NanoZS, Malvern Instruments, Worcestershire, UK) before and after every stage of the *in vitro* GI process. Digested emulsions were diluted prior to analysis with ultrapure water at the different pH conditions used during digestion (1:10) to avoid multiple scattering effects.

The ζ-potential of digested emulsions was also assessed by Laser Doppler Velocimetry (LDV) through the Smoluchowski equation, using a Zetasizer Nano ZS device (Malvern Instruments, Worcestershire, UK). Samples were diluted prior to analysis with ultrapure water as in the droplet size analyses (1:10) and placed in plastic zeta cells (DTS 1061, Malvern, UK). Analyses were carried out in triplicate.

2.5. Resveratrol bioaccessibility

The bioaccessibility of resveratrol encapsulated in primary, secondary and tertiary emulsions was assessed once the emulsions were subjected to the entire *in vitro* digestion, following the methodology described by Pinheiro et al. (2016). Briefly, an aliquot of 10 mL of digested emulsions was centrifuged at 6000 rpm for 60 min at 25 ºC. The supernatant was collected, assuming that it corresponded to the micelle fraction, where resveratrol was contained within mixed micelles. A standard extraction procedure was then carried out twice by mixing 5 mL of micelle phase and 5 mL of chloroform, vortexed and centrifuged at 1750 rpm for 10 min at 25 ºC. The chloroform containing the extracted resveratrol was quantified spectrophotometrically in a Multi-Detection Microplate Reader Synergy™ HT (Biotek, Winooski, USA) at 307 nm (absorbance peak). A cuvette containing pure chloroform was used as reference. The concentration of resveratrol was determined through a calibration curve in chloroform (0.5 – 7 μg/mL, R^2 = 0.9986). The bioaccessibility of resveratrol was determined by Eq. (1):

$$\%Bioaccessibility = \frac{C_m}{C_0} \times 100 \quad \textbf{(1)}$$

where C_m is the concentration of resveratrol in the micelle fraction after *in vitro* digestion, and C_0 is the initial concentration of resveratrol in the emulsions.

2.6. Microscope visualization

The microstructure of single-layer and multilayer emulsions in each phase (oral, gastric and intestinal) of the GI process was determined using an epifluorescence microscope (BX51 266 OLYMPUS, Tokyo, Japan) coupled with a DP71 digital camera and three sets of filters (DAPI-365-370/421, FITC-470-490/516e and TRITC-530-550/591) (Olympus Portugal SA, Porto, Portugal), and with an ×100 oil immersion objective lens. Samples were dyed with Nile Red (9-diethylamino-5H-benzo[α]phenoxazine-5-one, 0.25 mg/mL in dimethyl sulfoxide, 1:10 (dye:sample), v/v), which enabled the oil droplets to become visible. Slides were prepared by taking 10 μL of the dyed emulsion solution and placing in a glass microscope slide and covering with a glass cover slip. All images were acquired using the Olympus Cell-B software.

2.7. Statistical analysis

All analyses were performed in triplicate. Data were analyzed through a one-way analysis of variance (ANOVA) using the statistical and graphing software SigmaPlot 11.0 Windows package (Systat software Inc.). The Holm-Sidak method was used to determine significant differences among mean values at a level of significance of 5%. All results are presented as the average and standard deviation.

3. Results and discussion

3.1. Influence of the layer composition on physical stability of droplets during digestion

Single-layer emulsions and multilayer emulsions were subjected to *in vitro* digestion in order to evaluate their suitability as delivery systems of resveratrol. The physical stability of oil droplets within the GI tract has a significant impact on the efficacy of delivery systems (McClements, 2015). Therefore, mean particle size, size distribution, microstructure and interfacial electrical charge of oil droplets were examined in each stage of the *in vitro* digestion. In general, either single-layer or multilayer emulsions experimented great changes in their properties that mostly depended on their interfacial characteristics. The results supporting this statement are presented and discussed hereafter.

3.1.1. Particle size and size distributions

The average droplet size and size distributions of single-layer and multilayer emulsions after being exposed to simulated mouth, stomach and small intestine fluids are presented in Fig. 1 and Fig. 2. The droplet size of all

emulsions was affected by digestion, but the differences were governed by the polysaccharides and proteins forming the interfacial layer of droplets. For instance, the initial average droplet diameter of primary emulsions (181 ± 4 nm) was scarcely affected by the salivary fluids, indicating that lactoferrin-coated oil droplets were stable (Fig. 1). The particle size distributions also confirmed the emulsion monodispersity (Fig. 2). The composition of simulated salivary fluids used in this study was a mixture of different salts at pH 7. In some cases, simulated salivary fluids may contain enzymes (amylases) or biopolymers (mucins) that cause flocculation of oil droplets (Shimoni, Shani Levi, Levi Tal, & Lesmes, 2013). The absence of such compounds indicates that lactoferrin-coated droplets were stabilized by the electrostatic repulsive forces, since lactoferrin is positively charged at pH 7.

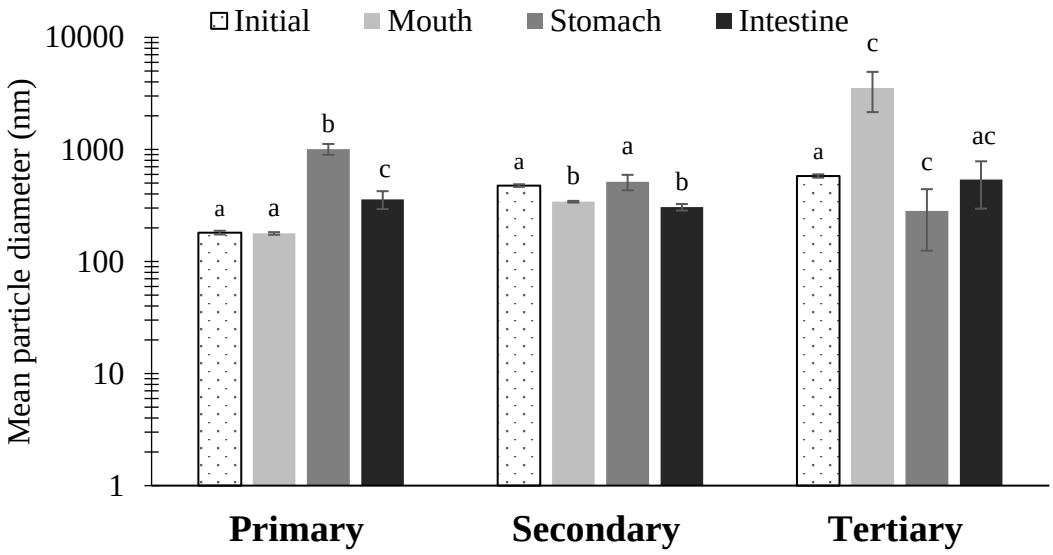

Fig. 1. Changes in average particle size of resveratrol-loaded primary (lactoferrin layer), secondary (lactoferrin/alginate layers), and tertiary (lactoferrin/alginate/poly-L-lysine layers) emulsions before and after being subjected to an *in vitro* gastrointestinal digestion. Different lowercase letters mean significant differences ($p < 0.05$) in the droplet size of a type of emulsion in a particular stage of the digestion.

Similarly, lactoferrin/alginate oil droplets were barely affected by the salivary fluids, presenting a decrease from 476 ± 13 nm (initially) to 342 ± 6 nm (Fig 1). In fact, the examination of droplet size distributions in this stage revealed a greater homogeneity compared to the initial emulsions. The decrease in the average droplet diameter could be caused by the disruption of some flocs initially present in secondary emulsions, induced by the dilution of the sample with SSF (reduction of positive depletion interactions that tend to aggregate alginate chains with oil droplets) and the increase of pH to 7 in

the oral phase (initial emulsion pH 5). Alginate chains are strongly charged at pH 7 (pK_a ≈ 3.65), which increase the electrostatic repulsion between droplets. This results is in concordance with previous studies reported for emulsions stabilized with proteins indicating a decrease in size after exposure to gastrointestinal fluids (Malaki Nik, Wright, & Corredig, 2011).

Moreover, when oil droplets were coated with lactoferrin/alginate/poly-L-lysine multilayers, the initial average droplet size (580 ± 20 nm) significantly increased above 3000 nm in simulated mouth conditions (Fig. 1), which suggests that droplets were unstable in salivary fluids. Particle size distributions of tertiary emulsions also confirmed this result, presenting great polydispersity that may be due to the aggregation of droplets (Fig. 2). The particles' flocculation might have occurred due to the presence of salts in the salivary fluid. Salt ions reduce electrostatic repulsion between droplets by screening the charged groups of poly-L-lysine forming the outermost layer on droplets. When the electrostatic repulsion is no longer strong enough to overcome the attractive interactions, then droplets instability occurs (Cosgrove, 2010).

It is known that some biopolymers (mucin) of the salivary fluid promote the formation of poly-L-lysine clusters by the electrostatic interaction between the positively charged polypeptide chains and the negatively charged salivary biopolymers (Lopez-Pena et al., 2016). However, the simulated salivary fluid used in this work was prepared in the absence of mucin, but it contained high concentrations of different salts that increase the overall ionic strength of the fluid. In addition, the amount of ionizable groups of the cationic poly-L-lysine at pH 7 (in the mouth) is reduced, as its p*I* is about 9, thus making it easier for counterions to screen the weakly charged poly-L-lysine chains located at the interface of oil droplets. Therefore, it was proposed that flocculation observed in tertiary emulsions at this stage was mainly induced by a combined effect of pH and high ionic strength of the simulated salivary fluid.

Interestingly, there was a steep increase in the droplet diameter of primary emulsions up to around 1000 nm under simulated gastric conditions (Fig. 1). This suggests that lactoferrin-coated droplets extensively flocculated, probably due to the hydrolysis of lactoferrin molecules located at the o/w interface in the presence of proteases (such as pepsin) of the gastric fluid. As a consequence, the protein interfacial layer of droplets can be reduced or even completely removed, as previously reported by other authors for emulsions stabilized with lactoferrin (Tokle, Mao, & McClements, 2013). Furthermore, droplet size distributions revealed the presence of a prominent intensity peak in the size region greater than 1000 nm and also a small peak in the nano-sized region (Fig. 2), which means that oil droplets were unstable to gastric conditions.

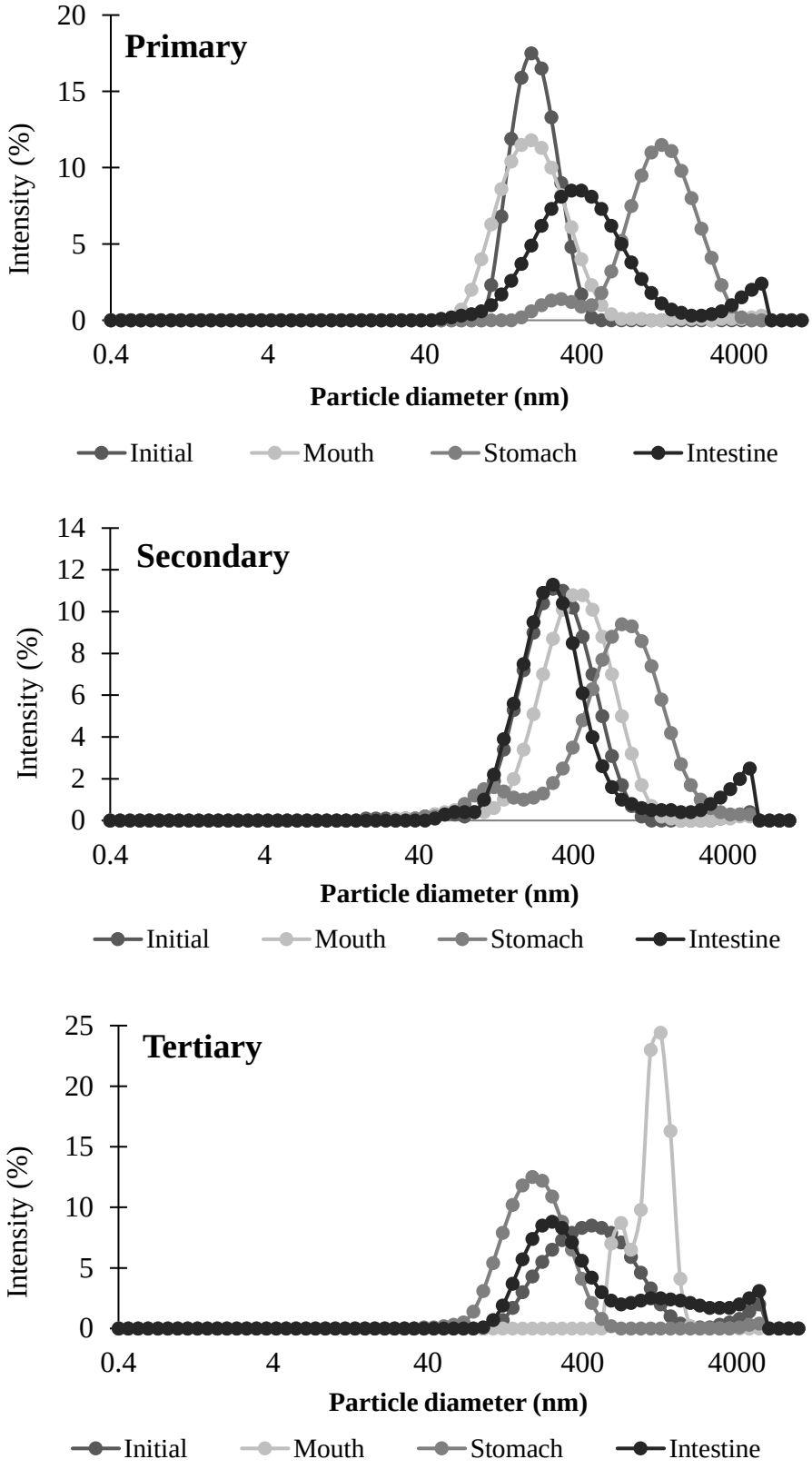

Fig. 2. Particle size distributions of resveratrol-loaded primary emulsions (lactoferrin layer) and multilayer emulsions (lactoferrin/alginate or lactoferrin/alginate/poly-L-lysine layers) before and after being subjected to an *in vitro* gastrointestinal digestion.

Secondary emulsions were more stable than primary emulsions, although some flocculation also occurred, leading to an increase in the particle diameter. The interfacial characteristics of droplets were affected by the acidic conditions of stomach, inducing their flocculation. Alginate molecules are weakly charged at pH 3, as the pK_a is ≈ 3.65, which causes the reduction of repulsive forces among droplets and the formation of clusters originated when attractive forces, such as van der Waals forces, take place. These results are in agreement with other studies of emulsions containing droplets coated by protein-polysaccharide layers and incubated with simulated gastric conditions, where the formation of droplets aggregates were reported (Pinheiro et al., 2016; Tokle, Lesmes, Decker, & McClements, 2012).

When lactoferrin/alginate/poly-L-lysine-coated droplets moved from the oral phase to gastric phase, there was a pronounced decrease in the particle size that suggests the reapportion of oil droplets (Fig. 1). The evaluation of droplet size distributions revealed that the vast majority of droplets presented fairly similar diameters under simulated gastric conditions (Fig. 2). This confirmed that the mechanism of instability occurring in the oral phase was droplets' aggregation and not coalescence. There are several processes happening during the different stages of digestion that may contribute to changes in the physical integrity of droplets, such as changes in pH, ionic composition, temperature, flow and forces profiles, the presence of surface active components or enzymatic activity (McClements & Li, 2010). It was hypothesized that the reapportion of droplets may have occurred by changes in the pH, continuous mechanical agitation and the dilution of emulsions with SGF. When tertiary emulsions passed from the oral to the gastric phase the pH decreased from 7 to 3, and cationic poly-L-lysine chains were then highly charged and the repulsive forces at the interface increases, which may have led to dissociation of big clusters formed in the oral phase. Likewise, the dilution of emulsions with gastric fluids may diminish some particles' aggregation mechanisms caused by depletion or bridging interactions. The reapportion of droplets in the gastric phase have been also indicated in previous studies of emulsions stabilized by surfactants (Golding et al., 2011; Salvia-Trujillo, Qian, Martín-Belloso, & McClements, 2013).

Surprisingly, it seems that gastric proteases did not destabilize the interfacial coating of droplets when the outermost layer was composed by poly-L-lysine; on the contrary, oil droplets were much more stable under gastric conditions. It has been reported that poly-L-lysine molecules are able to inhibit the proteolytic activity of gastric pepsins at very low pH, acting as competitive inhibitors due to their capacity to form electrostatic complexes (Katchalski, Berger, & Neumann, 1954; Lawton & Mekras, 1985). Therefore, the high

physical stability of tertiary emulsions in the stomach is likely to be explained by the inactivation of pepsin by the poly-L-lysine layer adsorbed at the interface of oil droplets.

When incubated under simulated intestinal conditions, primary and secondary emulsions exhibited a decrease in particle size, whereas the particle size of tertiary emulsions slightly increased (Fig. 1). However, the particle size distribution graphs of all emulsions show small peaks around 10000 nm, indicating the presence of bigger particles that were not detected by the equipment (Fig. 2). This could be attributed to the presence of digestion products of different sizes provoked by the hydrolytic activity of intestinal enzymes (pancreatin) on droplets and the further assembly of colloidal structures of big sizes, or by the presence of remaining non-digested polysaccharide-protein complexes. In this stage, the majority of the lipid fraction of emulsions is solubilized by the action of bile salts and these are believed to adsorb at the oil/water interface, displacing the existing interfacial layer on oil droplets. Then, the lipid phase is further converted into smaller molecules (such as free fatty acids, mono and/or di-acylglycerols) due to the enzymatic activity of intestinal lipases, releasing any encapsulated lipophilic nutraceutical. Finally, the assembly of mixed micelles that contain the lipolysis products and nutraceuticals takes place, which enhances transport across the epithelium walls. The typical size of mixed micelles ranges between 100 and 300 nm (Zou et al., 2016).

3.1.2. Particle microstructure

The changes in the physical stability of single-layer and multilayer emulsions were also examined by epifluorescence microscopy in order to obtain insights regarding the droplets microstructure during *in vitro* digestion (Fig. 3). Micrographs of all emulsions at the different simulated oral, gastric and intestinal stages are in good agreement with the results of particle sizes obtained by dynamic light scattering. The droplets microstructure presented significant differences depending on the interfacial layer composition. In the mouth, both lactoferrin-coated droplets and lactoferrin/alginate-coated droplets are shown as individual dots corresponding to a monodisperse droplet size distribution in the salivary fluid with no apparent signs of aggregation (Fig. $3A_1$ and $3B_1$). However, lactoferrin/alginate/poly-L-lysine-coated droplets are observed as notable clumps originated by flocculation (Fig. $3C_1$). In the stomach, lactoferrin-coated droplets flocculated forming appreciable clumps in the gastric fluid, being difficult to identify the spherical structure of oil droplets (Fig. $3A_2$). It seems that the alginate layer at the droplet interface somehow enhanced the physical stability of lactoferrin-coated droplets, probably by reducing the activity of pepsin in the gastric stage.

However, the presence of clusters formed by the agglomeration of well-defined tiny droplets is also evident (Fig. $3B_2$).

When an extra poly-L-lysine layer was adsorbed to the protein-polysaccharide layers, oil droplets were homogeneously distributed as singular structures within the gastric fluid, as can be confirmed in Fig. $3C_2$. In the intestinal phase, micrographs of all emulsions show structures of different morphologies and sizes ($3A_3$, $3B_3$, and $3C_3$). These could correspond to colloidal structures such as mixed micelles, vesicles, protein-polysaccharide complexes or small droplet aggregates that were not digested by the intestinal enzymes (pancreatin), or insoluble precipitates arising from the interaction between the components of emulsions (such as positively charged lactoferrin) and bile acids (negatively charged).

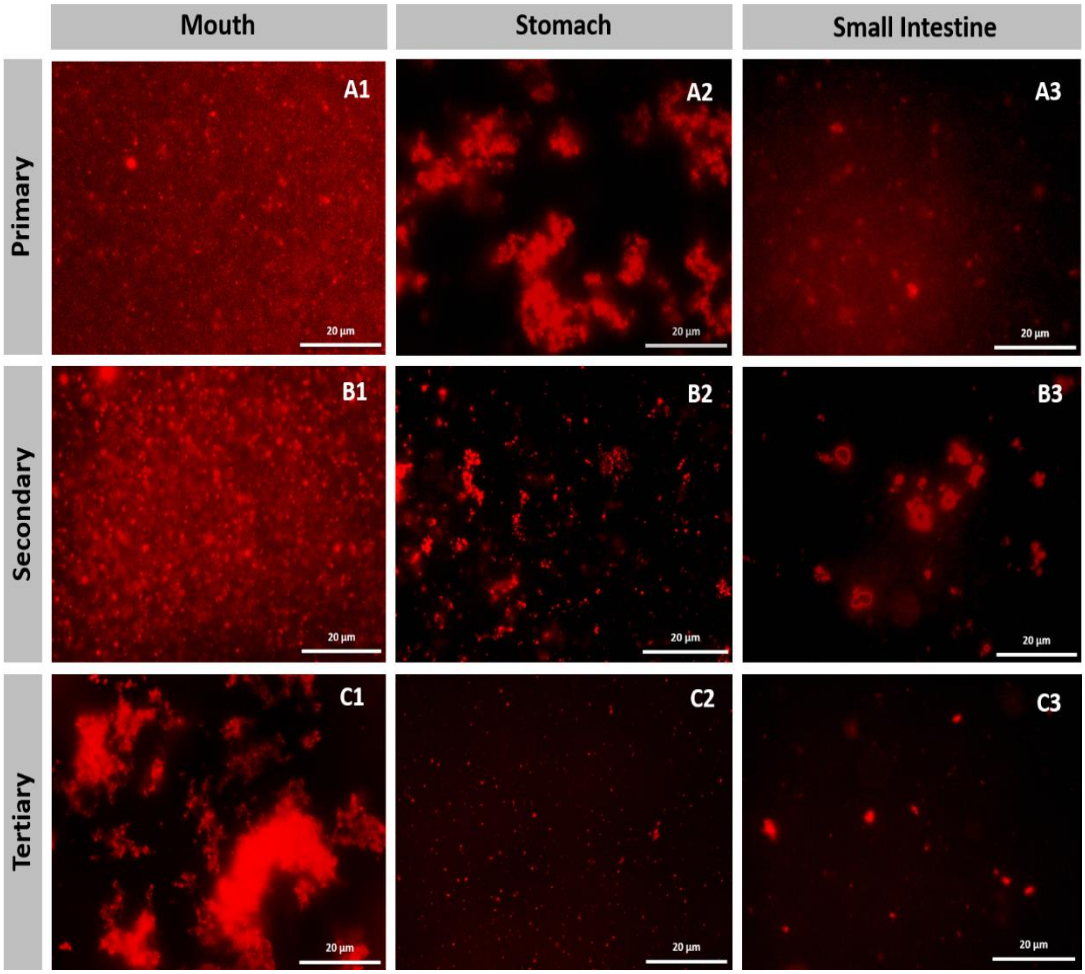

Fig. 3. Epifluorescence images showing changes in the microstructure of resveratrol-loaded primary (A), secondary (B) and tertiary (C) emulsions in different stages (columns) of a simulated gastrointestinal process (mouth, stomach and small intestinal).

3.1.3. Particles electrical charge

Changes in the electrical charge at the o/w interface of droplets in single-layer and multilayer emulsions were evaluated by measuring the ζ-potential during *in vitro* digestion. The initial electrical charge of lactoferrin-coated droplets was strongly positive (45 ± 3 mV), as expected due to the presence of a globular protein with a very high p*I*, and significantly decreased ($p < 0.05$) under simulated mouth conditions (12 ± 1.5 mV) (Fig. 4). The interfacial ζ-potential of droplets is highly influenced by the number of ionizable groups that can interact with ionic entities dispersed in the media. A change in the solution conditions (pH, ionic strength, the presence of surface active substances or enzymes) results in changes in the ζ-potential of droplets. Therefore, at the neutral conditions of salivary fluids (pH 7) lactoferrin molecules are less ionized, and hence the magnitude of the positive ζ-potential decreases. Despite of this fact, primary emulsions remained stable as confirmed by particle size analyses, probably due to steric stabilization. Globular proteins such as lactoferrin are known to create thick layers around oil droplets enhancing the emulsion stability, except when they are near to their isoelectric point (Lee, Choi, Li, Decker, & McClements, 2011).

On the other hand, the negative ζ-potential of lactoferrin/alginate-coated droplets slightly increased in simulated salivary fluids, indicating a decrease in the net charge of droplets. It has been reported that the surface ζ-potential of multilayer systems decreases as the amount of adsorbed material per layer diminishes, because there are less ionizable moieties that impart an electrical potential (Acevedo-Fani, Salvia-Trujillo, Soliva-Fortuny, & Martín-Belloso, 2015). Consequently, a less negative ζ-potential in the digested emulsions could be associated to a decrease in thickness of the alginate layer on oil droplets. On the contrary, the sign and magnitude of the electrical charge of lactoferrin/alginate/poly-L-lysine-coated droplets significantly changed from the initial conditions (42 ± 5 mV) to the simulated oral conditions (-3.4 ± 0.7 mV) ($p < 0.05$). It is likely that the high ionic strength of salivary fluids has led to electrostatic screening of the poly-L-lysine charged groups on droplets, causing significant changes in their electrical characteristics and also contributing to droplets' aggregation, as suggested by the particle size examinations (Fig. 1).

The particle ζ-potential was negative in the gastric phase regardless of the emulsion characteristics (Fig. 4). In particular, it was expected that primary emulsions exhibited positive ζ-potentials at pH 3; however, the negative electrical charge of emulsions could be due to the bonding of pepsin molecules to lactoferrin-coated droplets, since pepsin has a negative charge in acidic conditions. In addition, alginate chains are weakly charged in acid

media, which could also explain why the magnitude of negative ζ-potential of droplets in secondary emulsions decreased under simulated gastric conditions. Likewise, the ζ-potential of lactoferrin/alginate/poly-L-lysine-coated droplets was even more negative (-25 ± 9 mV) that in the mouth stage. It is presumed that pepsin binds to cationic poly-L-lysine molecules located as the outermost layer of droplets, creating an interfacial layer that leads to negative ζ-potential values.

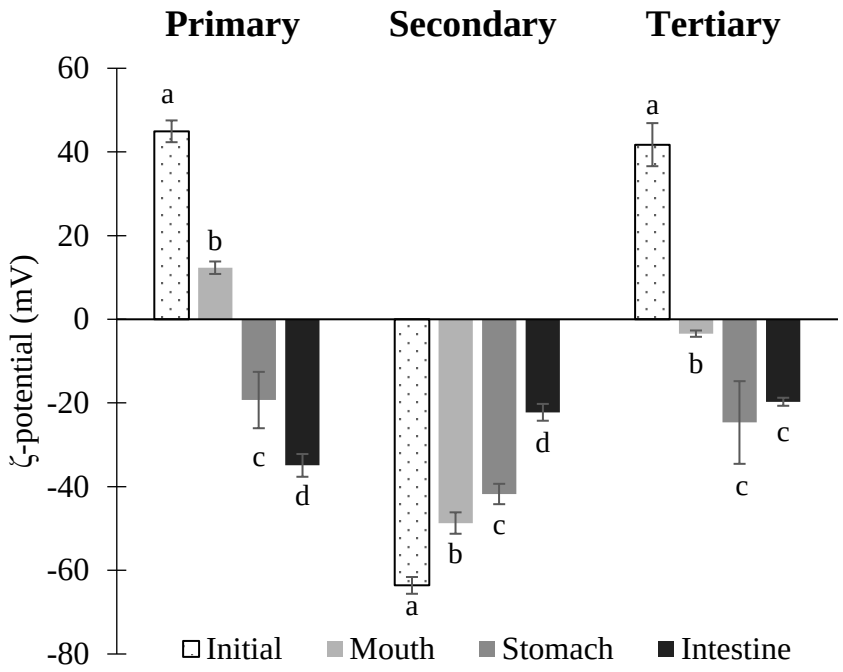

Fig. 4. Changes in the ζ-potential of resveratrol-loaded multilayer emulsions (primary, secondary and tertiary) under simulated gastrointestinal conditions. Different lowercase letters mean significant differences of an emulsion at a particular stage of digestion ($p < 0.05$).

In the intestinal stage, the ζ-potential values were negative regardless of the interfacial layer composition on droplets. In this stage, there are a number of lipolysis products that have a negative charge, for instance, i) free fatty acids and di-acylglycerols are negatively charged due to ionization of the carboxyl groups at the pH of the intestine; ii) some oil droplets surrounded by bile acids, which have a negative charge, or iii) mixed micelles that are composed by many surface active substances (e.g. bile salts, phospholipids, cholesterol, and fatty acids) (Reis, Holmberg, Watzke, Leser, & Miller, 2009; Singh, Ye, & Horne, 2009). As a result, particles dispersed in the intestinal fluids may have a significant negative net charge.

3.2. Effect of layer composition on resveratrol bioaccessibility

The bioaccessibility of resveratrol in single-layer and multilayer emulsions was also assessed once the digestion process was concluded. The amount of resveratrol released from emulsions in the intestinal stage of the *in vitro* digestion and solubilized in the mixed micelles fraction was assumed as the resveratrol available for adsorption (Carbonell-Capella, Buniowska, Barba, Esteve, & Frígola, 2014). The behavior of resveratrol emulsions under simulated intestinal conditions depended on the layer composition at the o/w interface of oil droplets ($p < 0.05$) (Fig. 5). The resveratrol bioaccessibility of emulsions increased following this order: primary (0.32%) > secondary (2.70%) > tertiary (25%). In an attempt to explain the behavior of single-layer and multilayer emulsions under simulated intestinal conditions, it was postulated that the physical stability of oil droplets in the gastric phase was the main factor that influenced the resveratrol bioaccessibility in the intestinal phase. This is based on the fact that primary and secondary emulsions were rather unstable under gastric conditions, whereas tertiary emulsions were much more stable. It has been described that the lipid digestion, and hence nutraceutical bioaccessibility, increases as the surface area of the lipid phase increases, due to a greater interaction of bile salts and enzymes with oil droplets (Salvia-Trujillo et al., 2013). Thereby, the big droplet aggregates may not be completely digested, hence precipitating in the intestinal lumen and carrying some nutraceutical content with them, which is thus unavailable to be solubilized into the mixed micelles. Conversely, the tiny oil droplets exposed to intestinal conditions can be rapidly digested increasing the nutraceutical concentration in the micelle fraction, and hence its bioaccessibility.

It is noteworthy that the final resveratrol concentration in the micelle fraction was less than 1 ppm regardless the initial content in the emulsions. Since emulsions had different initial oil concentrations, and therefore different resveratrol quantities, the bioaccessibility might be also influenced by some other reasons. First, the initial concentration of oil and resveratrol was greater in single-layer emulsions than in multilayer emulsions. In the latter case, the lipolysis and formation of mixed micelles could have been accelerated by the presence of less substrate for the reactions. The opposite can be true in the case of a greater oil concentration. Second, it is possible that at high oil concentrations, bile salts preferably form mixed micelles with the free fatty acids instead of resveratrol molecules, and at low oil concentration the resveratrol solubilization in the micelles could be favored. Previous studies establish that some types of bile acids are capable of solubilizing greater amounts of resveratrol than others (Atanacković, Poša, Heinle, Gojković-Bukarica, & Cvejić, 2009). Thereby, the composition of bile salts is likely to have an important impact on resveratrol solubilization. However, further

studies should be proposed to clarify these hypotheses. Compared with results obtained in this study, previous works reported greater percentages of bioaccessibility in pterostilbene-enriched oil nanoemulsions using two carrier oils (olive oil and flaxseed oil). Pterostilbene is a methylated analog of resveratrol with greater lipid-solubility than resveratrol, which might have increased the pterostilbene bioaccessibility (Sun et al., 2015).

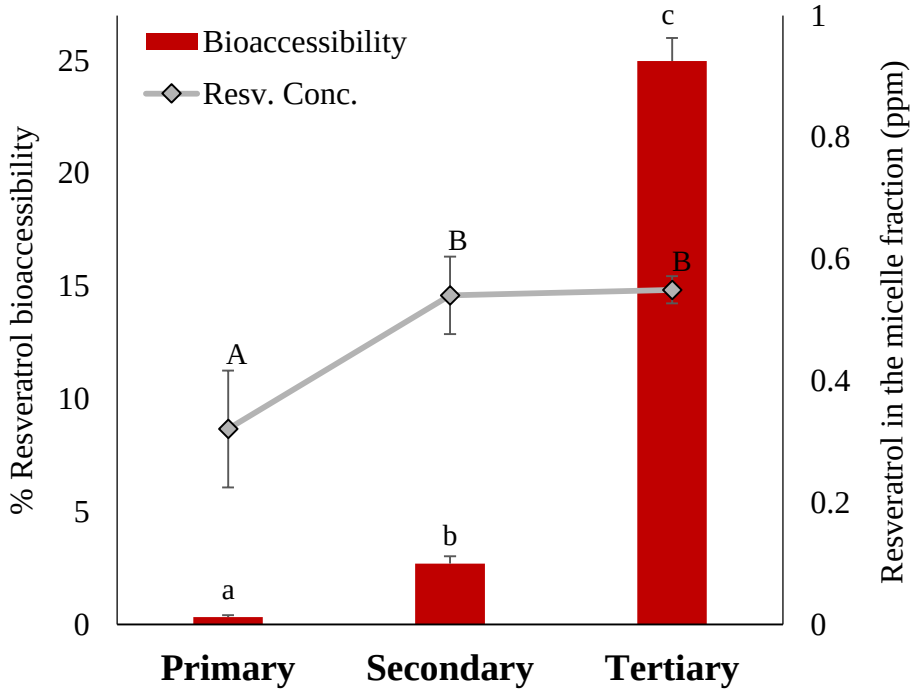

Fig. 5. Bioaccessibility and concentration of resveratrol in the micelle fraction after digestion of primary and multilayer emulsions. The initial resveratrol concentration in primary, secondary and tertiary emulsions was 100 ppm, 20 ppm and 2.2 ppm, respectively. Different capital letters means significant differences among the resveratrol concentration of emulsions. Different lowercase letters means significant differences among resveratrol bioaccessibility of emulsions (p <0.05).

4. Conclusions

The current work has demonstrated the important impact of the interfacial layer composition of droplets in emulsions on their potential fate within a simulated gastrointestinal tract. There were significant changes in the physical integrity of droplets exposed to the different stages of an *in vitro* digestion (mouth, stomach and small intestine). Changes in particle size, droplet charge and microstructure were found to be dependent on the outermost layer adsorbed onto droplets surfaces. The primary and secondary emulsions were unstable under gastric conditions presenting extensive flocculation. On the

contrary, the tertiary emulsions containing droplets coated by lactoferrin/alginate/poly-L-lysine layers were highly susceptible to aggregation in simulated mouth conditions, but this behavior was reversed in the gastric phase, probably due to the inhibitory effect of poly-L-lysine on the enzymatic activity of gastric pepsin. On the other hand, the interfacial layer composition of oil droplets in emulsions had a significant impact on resveratrol bioaccessibility, increasing with the number of layers adsorbed on droplets surface. The results obtained from this study have relevance in the design of nanostructured delivery systems of nutraceuticals such as resveratrol to be used in food systems or beverages. Finally, it is important to point out that further experiments using *in vivo* models should be done in order to confirm these findings.

5. Acknowledgments

This research was supported by the Ministerio de Ciencia e Innovación (Spain) throughout the projects AGL2009-11475 and ALG2012-35635, and by the Portuguese Foundation for Science and Technology (FCT) under the scope of the strategic funding of UID/BIO/04469/2013 unit and COMPETE 2020 (POCI-01-0145-FEDER-006684), Project RECI/BBB-EBI/0179/2012 (FCOMP-01-0124-FEDER-027462) and FCT Strategic Project of UID/BIO/04469/2013 unit. The authors also thank the Project “BioInd - Biotechnology and Bioengineering for improved Industrial and Agro-Food processes, REF. NORTE-07-0124-FEDER-000028” Co-funded by the Programa Operacional Regional do Norte (ON.2 – O Novo Norte), QREN, FEDER. Author A. Acevedo-Fani also thanks to the University of Lleida for the pre-doctoral grant. The authors A. C. Pinheiro and H. D. Silva are recipient of a fellowship from the Fundação para a Ciência e Tecnologia (FCT, Portugal) through grants SFRH/BPD/101181/2014 and SFRH/BD/81288/2011.

6. References

Acevedo-Fani, A., Salvia-Trujillo, L., Soliva-Fortuny, R., & Martín-Belloso, O. (2015). Modulating Biopolymer Electrical Charge to Optimize the Assembly of Edible Multilayer Nanofilms by the Layer-by-Layer Technique. *Biomacromolecules*, *16*(9), 2895–2903.

Amri, A., Chaumeil, J. C., Sfar, S., & Charrueau, C. (2012). Administration of resveratrol: What formulation solutions to bioavailability limitations? *Journal of Controlled Release : Official Journal of the Controlled Release Society*, *158*(2), 182–93.

Aoki, T., Decker, E. A., & McClements, D. J. (2005). Influence of environmental stresses on stability of O/W emulsions containing droplets stabilized by multilayered membranes produced by a layer-by-layer electrostatic deposition technique. *Food Hydrocolloids*, *19*(2), 209–220.

Atanacković, M., Poša, M., Heinle, H., Gojković-Bukarica, L., & Cvejić, J. (2009). Solubilization of resveratrol in micellar solutions of different bile acids. *Colloids and Surfaces B: Biointerfaces*, *72*(1), 148–154.

Beicht, J., Zeeb, B., Gibis, M., Fischer, L., & Weiss, J. (2013). Influence of layer thickness and composition of cross-linked multilayered oil-in-water emulsions on the release behavior of lutein. *Food & Function*, *4*(10), 1457.

Benjamin, O., Silcock, P., Leus, M., & Everett, D. W. (2012). Multilayer emulsions as delivery systems for controlled release of volatile compounds using pH and salt triggers. *Food Hydrocolloids*, *27*(1), 109–118.

Carbonell-Capella, J. M., Buniowska, M., Barba, F. J., Esteve, M. J., & Frígola, A. (2014). Analytical Methods for Determining Bioavailability and Bioaccessibility of Bioactive Compounds from Fruits and Vegetables: A Review. *Comprehensive Reviews in Food Science and Food Safety*, *13*(2), 155–171.

Cosgrove, T. (2010). *Colloid Science: Principles, Methods and Applications*. John Wiley & Sons.

Cottart, C.-H., Nivet-Antoine, V., & Beaudeux, J.-L. (2014). Review of recent data on the metabolism, biological effects, and toxicity of resveratrol in humans. *Molecular Nutrition & Food Research*, *58*(1), 7–21.

Davidov-Pardo, G., & McClements, D. J. (2014). Resveratrol encapsulation: Designing delivery systems to overcome solubility, stability and bioavailability issues. *Trends in Food Science & Technology*, *38*(2), 88–103.

Delmas, D., Aires, V., Limagne, E., Dutartre, P., Mazué, F., Ghiringhelli, F., & Latruffe, N. (2011). Transport, stability, and biological activity of resveratrol. *Annals of the New York Academy of Sciences*, *1215*, 48–59.

Fioramonti, S. A., Arzeni, C., Pilosof, A. M. R., Rubiolo, A. C., & Santiago, L. G. (2015). Influence of freezing temperature and maltodextrin concentration on stability of linseed oil-in-water multilayer emulsions. *Journal of Food Engineering*, *156*, 31–38.

Golding, M., Wooster, T. J., Day, L., Xu, M., Lundin, L., Keogh, J., & Clifton, P. (2011). Impact of gastric structuring on the lipolysis of emulsified lipids. *Soft Matter*, *7*(7), 3513.

Guzey, D., & McClements, D. J. (2006). Formation, stability and properties of multilayer emulsions for application in the food industry. *Advances in Colloid and Interface Science*, *128–130*, 227–248.

Katchalski, E., Berger, A., & Neumann, H. (1954). Reversible Inhibition of Pepsin by Polylysine. *Nature*, *173*(4412), 998–999.

Katsuda, M. S., McClements, D. J., Miglioranza, L. H. S., & Decker, E. A. (2008). Physical and oxidative stability of fish oil-in-water emulsions stabilized with beta-lactoglobulin and pectin. *Journal of Agricultural and Food Chemistry*, *56*(14), 5926–31.

Kumar, D. S., Shankar, P., & Rao, G. U. (2009). Health Benefits of Resveratrol, *2*(1), 407–412.

Lawton, J. B., & Mekras, C. I. (1985). The effect of polycations on the activity of pepsin. *Journal of Pharmacy and Pharmacology*, *37*(6), 396–400.

Lee, S. J., Choi, S. J., Li, Y., Decker, E. A., & McClements, D. J. (2011). Protein-stabilized nanoemulsions and emulsions: Comparison of physicochemical stability, lipid oxidation, and lipase digestibility. *Journal of Agricultural and Food Chemistry*, *59*(1), 415–427. JOUR.

Lopez-Pena, C. L., Zheng, B., Sela, D. A., Decker, E. A., Xiao, H., & McClements, D. J. (2016). Impact of ε-polylysine and pectin on the potential gastrointestinal fate of emulsified lipids: In vitro mouth, stomach and small intestine model. *Food Chemistry*, *192*, 857–64.

Malaki Nik, A., Wright, A. J., & Corredig, M. (2011). Impact of interfacial composition on emulsion digestion and rate of lipid hydrolysis using different in vitro digestion models. *Colloids and Surfaces B: Biointerfaces*, *83*(2), 321–330.

McClements, D. J. (2015). Nanoscale Nutrient Delivery Systems for Food Applications: Improving Bioactive Dispersibility, Stability, and Bioavailability. *Journal of Food Science*, *80*(7), N1602-11.

McClements, D. J., & Li, Y. (2010). Structured emulsion-based delivery systems: Controlling the digestion and release of lipophilic food components. *Advances in Colloid and Interface Science*, *159*(2), 213–228.

Minekus, M., Alminger, M., Alvito, P., Ballance, S., Bohn, T., Bourlieu, C., … Brodkorb, A. (2014). A standardised static in vitro digestion method suitable for food - an international consensus. *Food & Function*, *5*(6), 1113–24.

Pinheiro, A. C., Coimbra, M. A., & Vicente, A. A. (2016). In vitro behaviour of curcumin nanoemulsions stabilized by biopolymer emulsifiers – Effect of interfacial composition. *Food Hydrocolloids*, *52*, 460–467.

Reis, P., Holmberg, K., Watzke, H., Leser, M. E., & Miller, R. (2009). Lipases at interfaces: a review. *Advances in Colloid and Interface Science*, *147–148*(C), 237–50.

Salvia-Trujillo, L., Qian, C., Martín-Belloso, O., & McClements, D. J. (2013). Influence of particle size on lipid digestion and β-carotene bioaccessibility in emulsions and nanoemulsions. *Food Chemistry*, *141*(2), 1472–80.

Sessa, M., Tsao, R., Liu, R., Ferrari, G., & Donsì, F. (2011). Evaluation of the Stability and Antioxidant Activity of Nanoencapsulated Resveratrol during in Vitro Digestion. *Journal of Agricultural and Food Chemistry*, *59*(23), 12352–12360.

Shimoni, G., Shani Levi, C., Levi Tal, S., & Lesmes, U. (2013). Emulsions stabilization by lactoferrin nano-particles under in vitro digestion conditions. *Food Hydrocolloids*, *33*(2), 264–272.

Singh, H., Ye, A., & Horne, D. (2009). Structuring food emulsions in the gastrointestinal tract to modify lipid digestion. *Progress in Lipid Research*, *48*(2), 92–100.

Smoliga, J. M., Baur, J. A., & Hausenblas, H. A. (2011). Resveratrol and health--a comprehensive review of human clinical trials. *Molecular Nutrition & Food Research*, *55*(8), 1129–41.

Sun, Y., Xia, Z., Zheng, J., Qiu, P., Zhang, L., McClements, D. J., & Xiao, H. (2015). Nanoemulsion-based delivery systems for nutraceuticals: Influence of carrier oil type on bioavailability of pterostilbene. *Journal of Functional Foods*, *13*, 61–70.

Ting, Y., Jiang, Y., Ho, C. T., & Huang, Q. (2014). Common delivery systems for enhancing in vivo bioavailability and biological efficacy of nutraceuticals. *Journal of Functional Foods*, *7*(1), 112–128.

Tokle, T., Lesmes, U., Decker, E. A., & McClements, D. J. (2012). Impact of dietary fiber coatings on behavior of protein-stabilized lipid droplets under simulated gastrointestinal conditions. *Food & Function*, *3*(1), 58–66.

Tokle, T., Mao, Y., & McClements, D. J. (2013). Potential biological fate of emulsion-based delivery systems: lipid particles nanolaminated with lactoferrin and β-lactoglobulin coatings. *Pharmaceutical Research*, *30*(12), 3200–13.

Walle, T. (2011). Bioavailability of resveratrol. *Annals of the New York Academy of Sciences*, *1215*, 9–15.

Wenzel, E., & Somoza, V. (2005). Metabolism and bioavailability of trans-resveratrol. *Molecular Nutrition & Food Research*, *49*(5), 472–81.

Xu, Q., & Si, L.-Y. (2012). Resveratrol role in cardiovascular and metabolic health and potential mechanisms of action. *Nutrition Research*, *32*(9), 648–658.

Zeeb, B., Lopez-Pena, C. L., Weiss, J., & McClements, D. J. (2015). Controlling lipid digestion using enzyme-induced crosslinking of biopolymer interfacial layers in multilayer emulsions. *Food Hydrocolloids*, *46*, 125–133.

Zhang, C., Xu, W., Jin, W., Shah, B. R., Li, Y., & Li, B. (2015). Influence of anionic alginate and cationic chitosan on physicochemical stability and carotenoids bioaccessibility of soy protein isolate-stabilized emulsions. *Food Research International*, *77*, 419–425.

Zou, L., Zheng, B., Zhang, R., Zhang, Z., Liu, W., Liu, C., … McClements, D. J. (2016). Enhancing the bioaccessibility of hydrophobic bioactive agents using mixed colloidal dispersions: Curcumin-loaded zein nanoparticles plus digestible lipid nanoparticles. *Food Research International*, *81*, 74–82.

Zupančič, Š., Lavrič, Z., & Kristl, J. (2015). Stability and solubility of trans-resveratrol are strongly influenced by pH and temperature. *European Journal of Pharmaceutics and Biopharmaceutics : Official Journal of Arbeitsgemeinschaft Für Pharmazeutische Verfahrenstechnik e.V*, *93*, 196–204.

SECTION III. NANOLAMINATES

CHAPTER IV: LAYER-BY-LAYER ASSEMBLY OF FOOD-GRADE ALGINATE/CHITOSAN NANOLAMINATES: FORMATION AND PHYSICOCHEMICAL CHARACTERIZATION

Acevedo-Fani, A., Salvia-Trujillo, L., Soliva-Fortuny, R., & Martín-Belloso, O

Food Biophysics (sent)

ABSTRACT

The alternate deposition of oppositely charged materials (layer-by-layer technique) is an effective approach to functionalize materials. Biopolymer-based nanolaminates obtained by the layer-by-layer technique can also be used to change the surface properties of food products or food contact materials. However, the final properties of nanolaminates may be affected by the conditions of the adsorbing solutions. The objective of this study was to form and characterize the physicochemical properties of nanolaminates assembled from alginate and chitosan solutions. The effect of pH, ionic strength and polysaccharide concentration on the properties of the absorbing solutions was also evaluated. The ζ-potential, viscosity and whiteness index of the solutions were assessed before the assembly. Alginate/chitosan nanolaminates were characterized in terms of UV-visible spectroscopy, surface ζ-potential, contact angle, DSC analysis and SEM. The absorbance increased as a function of the number of polysaccharide layers on the substrate, suggesting an increase in the mass adsorbed. The surface ζ-potential of nanolaminates changed depending on the last polysaccharide deposited. Alginate layers were negatively charged, whereas chitosan layers were positively charged. Contact angles obtained in alginate layers were ≈ 10º, being mostly hydrophilic. Chitosan layers showed higher contact angle values (80º), indicating a more hydrophobic behavior. Microscopic examinations revealed the presence densely packed structures that corresponded to alginate/chitosan nanolaminates, having an estimated thickness of 700 nm. The results obtained in this work lay the basis for the rational design of polysaccharide-based nanolaminates in the food sector.

Keywords: alginate; chitosan; layer-by-layer; nanolaminates, food-grade coatings and films

1. Introduction

Nowadays, the use of nanomaterials in the food field is becoming rather important since it can offer remarkable prospects to design innovative products and applications in many industrial sectors, ranging from food processing, novel foods, food additives and food contact materials [1]. In particular, nanolaminates have been recently proposed as a potential strategy to modify the surface properties of either food contact materials (e.g. plastics films, paper, and aluminum) or foodstuffs (e.g. fruits, vegetables, meats, and candies). These modifications can improve the material properties.

Nanolaminates are defined as thin coatings formed on a substrate by the sequential deposition of at least two layers of different materials, wherein the typical thickness is less than 100 nm per layer. The final thickness depends on the number of layers deposited [2,3]. These nanolaminate structures are obtained by the well-known layer-by-layer assembly technique, which consists on the alternate adsorption of species (normally, polyelectrolytes) using different chemical interactions. Electrostatic bonding, hydrogen bonding, hydrophobic interactions, charge-transfer interactions, covalent bonding are among the mostly explored [4].

So far, the most commonly approach used to produce nanolaminates is the electrostatic interactions between oppositely charged species [4]. The layer-by-layer assembly method has been widely explored for several applications in different science fields (e.g. material science, pharmacology or biomedicine) due to its simplicity, high adaptability and low-cost [7,8]. However, its application in the food sector is still incipient. The major advantage of this procedure is the possibility to fine-tune the characteristics of nanolaminates by simply controlling the processing parameters, such as polyelectrolyte type, molecular weight, charge density, the conditions of adsorbing solutions (pH, ionic strength, polyelectrolyte concentration, and temperature), adsorption and rinse times, drying between layers, number of layers deposited and washing steps, or the terminal layer [4,5,9].

Polysaccharides have been playing an important role within the food industry, working as additives to improve, modify and stabilize food texture properties, but also to produce edible food packaging systems (e.g. films and coatings for solid foods), and more recently, for the nanoencapsulation of food ingredients

[10,11]. Polysaccharides are biodegradable, present good gas barrier properties and high compatibility with foods [12]. Nevertheless, when functional groups with charged moieties are present in the backbone, polysaccharides behave as polyelectrolytes, which enable their use as building blocks for assembling food-grade nanolaminates by electrostatic interactions [13]. For instance, alginate is a natural linear copolymer extracted from marine brown algae, consisting of 1-4 linked β-D-mannuronic acid and α-L-guluronic acid [14]. The negative charge of alginate is provided by ionized carboxyl functional groups (COO^-) of mannuronic and guluronic acid monomers whose dissociation constants (pK_a) are 3.3 and 3.6, respectively [15].

Chitosan, a deacetylated form of chitin, is a naturally-occurring polysaccharide found in the exoskeleton of crustaceans and fungi. Chitosan is formed by *N*-acetylglucosamine and glucosamine residues, being soluble in acidic media because of the protonation of -NH_2 groups of D-glucosamine residues [16,17]. Then, the positive charge of chitosan is given by the protonated amine groups (NH_3^+), with a pK_a around ≈ 6.3 [18]. On the other hand, polyethylene terephthalate (PET) has been extensively used as a versatile food contact material [19]. PET has also been reported as a suitable substrate to produce polysaccharide-based nanolaminates [20,21], since its properties are well described, allowing to characterize the physical and chemical characteristics of nanolaminates. Quartz is another type of substrate commonly used for monitoring the layer-by-layer build-up when using spectrophotometric techniques, such as UV-visible spectroscopy [22].

The conditions of preparation of the absorbing solutions, including the pH, ionic strength or concentration may affect the layer-by-layer assembly with weak polyelectrolytes, such as alginate and chitosan [13,23]. Therefore, knowledge on polysaccharides behavior is crucial to determine adequate experimental conditions for designing nanolaminates. The main objective of this work was to form and characterize food-grade nanolaminates by the layer-by-layer technique, as well as assess the effect on the conditions of preparation on the electrical charge and physical stability of polysaccharide solutions. This was necessary to find the suitable experimental conditions to prepare the nanolaminates.

2. Materials and methods

2.1. Materials

Food grade sodium alginate (MANUCOL® DH) was purchased from FMC Biopolymers (Scotland, UK). Chitosan (High molecular weight ≈ 310000 - 375000 Da; deacetylate degree: > 75 %) was acquired in Sigma-Aldrich (Steinheim, Germany). Lactic acid (88 – 90 %) and sodium hydroxide were obtained from Sharlau Chemie (Barcelona, Spain). Sodium chloride (POCH, Poland) was purchased from Afora (Barcelona, Spain). Quartz slides (Suprasil® 300) and polyethylene terephthalate (PET) sheets were obtained from Hellma Analytics (Müllhein, Germany) and Isovolta (Barcelona, Spain), respectively. All polysaccharide solutions were prepared in deionized water obtained from a Milli-Q filtration system (18.2 mΩ, Merck Millipore, Madrid, Spain).

2.2. Preparation of polysaccharide solutions

2.2.1. Effect of pH

Powdered alginate and chitosan solutions were prepared at different concentrations (0.1- 1% w/v) by dispersing them into water or lactic acid solution (1% v/v), respectively, under continuous stirring overnight. Then, both solutions were adjusted to pH 3 to 11, using either lactic acid (1 M) or NaOH (1 M) solutions. Finally, polysaccharide solutions were transferred into plastic bottles, closed and stored at room temperature (≈ 25º C) for the subsequent analysis as described in section 2.3.

2.2.2. Effect of ionic strength

Alginate and chitosan was dissolved in water and lactic acid (1% v/v) respectively, at different concentrations (0.1 – 1% w/v). Then, different amounts of sodium chloride (NaCl) were added to polysaccharide solutions under continuous stirring until complete dissolution to obtain concentrations from 0.1 M to 0.5 M. Finally, alginate and chitosan were adjusted to pH 5 and 4, respectively. Solutions were transferred into plastic bottles, closed and stored at room temperature (≈ 25º C) for the subsequent analysis as described in section 2.3.

2.3. Polysaccharide solutions properties

2.3.1. ζ-Potential

Changes in the electrical charge of polysaccharide chains in aqueous solutions were performed with a laser diffractometer (Zetasizer Nano ZS, Malvern Instruments, Worcestershire, UK) operating at 633 nm. The ζ-potential was measured by Laser Doppler Velocimetry (LDV) and calculated by the Smoluchowski approximation. Alginate and chitosan solutions without previous dilution were placed into a clear plastic zeta cell (DTS 1061, Malvern, UK) to carry out measurements. Two independent runs with three repetitions of each sample were performed. The measurement consists on placing two gold paddles inside the liquid that then vibrates, stimulated by an electromagnetic drive at a constant amplitude. The shear waves imparted to the liquid are damped at a rate that is a function of the viscosity of the liquid. The power required to maintain a constant amplitude is proportional to the viscosity of the fluid, and is measured and transformed to a value of viscosity [27].

2.3.2. Viscosity measurements

The viscosity of polysaccharide solutions was analyzed in a sine-wave vibro viscometer (SV-10, A&D Company, Tokyo, Japan), with a range from 0.3 mPa.s to 10000 mPa.s operating at 30 Hz and a constant amplitude (less than 1 mm). Alginate and chitosan solutions were analyzed at ≈ 25ºC and this parameter was monitored by the same device. Two independent runs with four repetitions of each sample were performed. The instrument was calibrated with distilled water as a standard solution.

2.3.3. Whiteness index

The optical properties of polysaccharide solutions were analyzed using a colorimeter Minolta CR-400, working with an illuminant D_{65} and 10° observer angle (Konica Minolta Sensing Inc., Osaka, Japan). A crystal flat-faced cuvette was filled with the solutions and put in the measuring device to obtain the CIE Lab parameters. Measurements were performed at room temperature (≈ 25 ºC). The colorimeter was calibrated with a white standard plate (Y = 94, x = 0.3158, y = 0.3222) prior to analyses. Whiteness index (WI) of

alginate and chitosan solutions was calculated with the following equation [28]:

$$WI = 100 - \sqrt{(100 - L^*)^2 + \left(a^{*2} + b^{*2}\right)} \qquad \textbf{Eq. (1)}$$

Two independent runs with four repetitions were performed for each sample.

2.4. Layer-by-layer assembly procedure

Alginate/chitosan nanolaminates were formed on quartz slides and PET sheets (2 x 6 cm). As a previous step, both substrates were cleaned and grafted with amino groups to provide an initial positive charge to the substrates' surface. The procedure for substrate pre-treatment was described in great detail in a previous work of our group [29]. Briefly, quartz slides were cleaned in Hellmanex® solution (2%) for 2 h. Then, substrates were immersed in an APTS solution (1% v/v) for 30 min to induce grafting of amino groups, and this was followed by a rinse step with deionized water. The PET sheets were cleaned using a water/propanol solution 50:50, for 3 h. Cleaned sheets were immersed in 1,6-hexanodiamine/methanol solution 1 M, at 50 ºC and 4 h. Afterwards, substrates were washed with methanol and dried for 12 h. Finally, PET substrates were positively charged by submerging them into an HCl 0.1 M solution for 3 h at room temperature.

Both quartz and PET slides (positively charged) were submerged in alginate solutions (negatively charged) at pH 5 for 20 minutes, followed by two rinse steps in water at pH 5 for 5 minutes. Afterwards, substrates were immersed in chitosan solutions (positively charged) at pH 4 for 20 minutes, and two rinse steps with water at pH 4 for 5 min were carried out. The alginate and chitosan adsorption cycles were repeated in order to produce 10-layer nanolaminates. Finally, these assemblies were dried using gas nitrogen when the layer-by-layer process was ended.

2.5. Characterization of nanolaminates

2.5.1. Buildup

The assembly process of alginate and chitosan layers on quartz slides was monitored by measuring the increase in absorbance of the substrate after an adsorption step. Dried substrates containing different number of layers were

analyzed in a UV-visible-NIR spectrometer (V-670, Jasco Corporation, Tokyo, Japan), using a film holder accessory (FLH-740, Jasco Corporation, Tokyo, Japan). Absorbance spectra were recorded from 190 nm to 700 nm.

2.5.2. Surface ζ-potential

The surface ζ-potential of alginate and chitosan layers after each adsorption was measured in a laser diffractometer Zetasizer NanoZS (Malvern Instruments Ltd, Worcestershire, UK) equipped with a surface ζ-potential cell unit (ZEN1020) specially designed to measure the ζ-potential in planar surfaces. Rectangles (5 x 4 mm) of alginate/chitosan nanolaminates assembled on PET sheets were attached to a sample holder with glue (Araldite®) and then dried for 12 h. Sample holders with samples were placed between two electrodes into the surface ζ-potential cell unit using a screwdriver. Then, the cell unit was put into a disposable polystyrene cuvette (DTS0012, Malvern Instruments) previously filled with 1 mL of a suspension containing negative tracer particles, (polystyrene latex particles in buffer solution pH 9, DTS1235, Malvern instruments) or positive tracer particles (quaternary ammonium salts from fragrance-free fabric conditioner solutions in a ratio of 1:100). The surface ζ-potential of alginate layers was analyzed using negative tracer particles, whereas the surface charge of chitosan layers was assessed with positive tracer particles to avoid particle adsorption. The apparent mobility of the tracer particles was determined at five vertical distances from the sample surface (125, 250, 375, 500 and 625 microns). Five measurements were performed in each distance point. The ζ-potential of tracer particles was measured at 1500 microns from the sample surface. The surface ζ-potential of alginate and chitosan layers was calculated by extrapolating the ‘zero’ distance from the ζ-potential vs displacement graphs using the Zetasizer Software version 7.11 (Malvern Instruments). Four readings were carried out per sample.

2.5.3. Wetting properties

The contact angle measurements of nanolaminates assembled on PET sheets were measured after each layer formation, using a goniometer (DSA25, Krüss GmbH, Hamburg, Germany). The water contact angle was carried out with the sessile drop method, in which a deionized water drop (1 μL) is created at the tip of the syringe and then placed onto the

nanolaminate surface at room temperature. Immediately, the contact angle formed by the water drop onto the surface was recorded using the Drop Shape Analysis System software (Krüss GmbH) and calculated through the Young-Laplace fit. Six measurements were performed for each sample.

2.5.4. Thermal properties

The influence of a nanolaminate coating on the thermal properties of PET sheets (used as substrate) was examined by Differential Scanning Calorimetry (DSC) using a DSC822e system (Mettler Toledo, Barcelona, Spain). PET sheets and PET coated by alginate/chitosan nanolaminates were studied in a temperature range of 0-400 ºC at a scanning rate of 10 ºC/min under an atmosphere of inert nitrogen. Samples of ≈ 5 mg were put into aluminum pans (1/8 ME-51119872 aluminum crucibles 100 µl without pin) for analysis. An empty aluminum pan was used as reference and measurements were performed in duplicate. Thermograms were analyzed by the StartE v.11 software (Mettler Toledo). Thermal properties such as the glass transition temperature (T_g), the melting temperature (T_m) and the enthalpy of melting (ΔH_m) were determined from the thermograms. The enthalpy of meting was calculated by integrating the peak area, drawing a baseline from the onset to the end of the thermal transition.

2.5.5. SEM imaging

SEM micrographs of nanolaminates assembled on PET sheets were obtained with a Scanning Electron Microscope (J-6510, JEOL Ltd, Tokyo, Japan). PET sheets coated by 10-layer nanolaminates were placed onto aluminum stubs, coated with carbon and metalized with evaporated gold in a sputter coater (SCD050, Balzers Union AG, Liechtenstein). Treated samples were analyzed by SEM with an acceleration voltage of 5 kV.

2.6. Statistics

Data obtained from measuring the properties of alginate and chitosan solutions were analyzed by two-way ANOVA using the Statgraphics Plus 5.1 statistical package (Statistical Graphics Co., Rockville, MD, EE.UU). Fisher's least significant difference (LSD) procedure was used to determine differences among means at a 5% significance level. Data obtained from the

nanolaminates characterization was reported as the average ± standard deviation of the repetitions.

3. Results and discussion

Initially, polysaccharide solutions used to prepare alginate/chitosan nanolaminates were characterized in terms of electrical charge, viscosity and optical properties varying the solvent composition (pH, ionic strength) and polysaccharide concentration. Preliminary analysis of the behavior of polysaccharides was used to set out the experimental parameters for the layer-by-layer assembly of nanolaminates.

3.1. Changes in the electrical charge of polysaccharides

The ζ-potential of alginate and chitosan molecules was evaluated as a function of pH, ionic strength and polysaccharide concentration of the solution (Fig. 1). Alginate solutions had rather negative ζ-potentials (< -70 mV) from pH 5 to 11, but increased at pH 3 (≈ -40 mV). The decrease in the magnitude of the electrical charge at pH 3 was attributed to the protonation of the carboxyl groups of alginate (pK_a ≈ 3.65). The polysaccharide concentration also affected the electrical charge of alginate chains. Higher alginate concentration resulted in more negative ζ-potential values.

The electrical charge of chitosan solutions was strongly positive in acidic conditions. The greatest ζ-potential values at pH 3 (45 mV, 0.1 %). Nevertheless, an increase in the pH to more alkaline conditions decreased the electrical charge of chitosan molecules. This indicated that chitosan chains were less ionized. Chitosan solutions with pH values above 7 or with 1% w/w of concentration could not be analyzed. Polysaccharides were insoluble, presenting clumps of great size that could not be placed in the measurement cell. These results are in good agreement with those reported by other authors, where the increase in pH of polysaccharide solutions, including alginate and chitosan, led to a decrease of the magnitude of the positive ζ-potential [33,34].

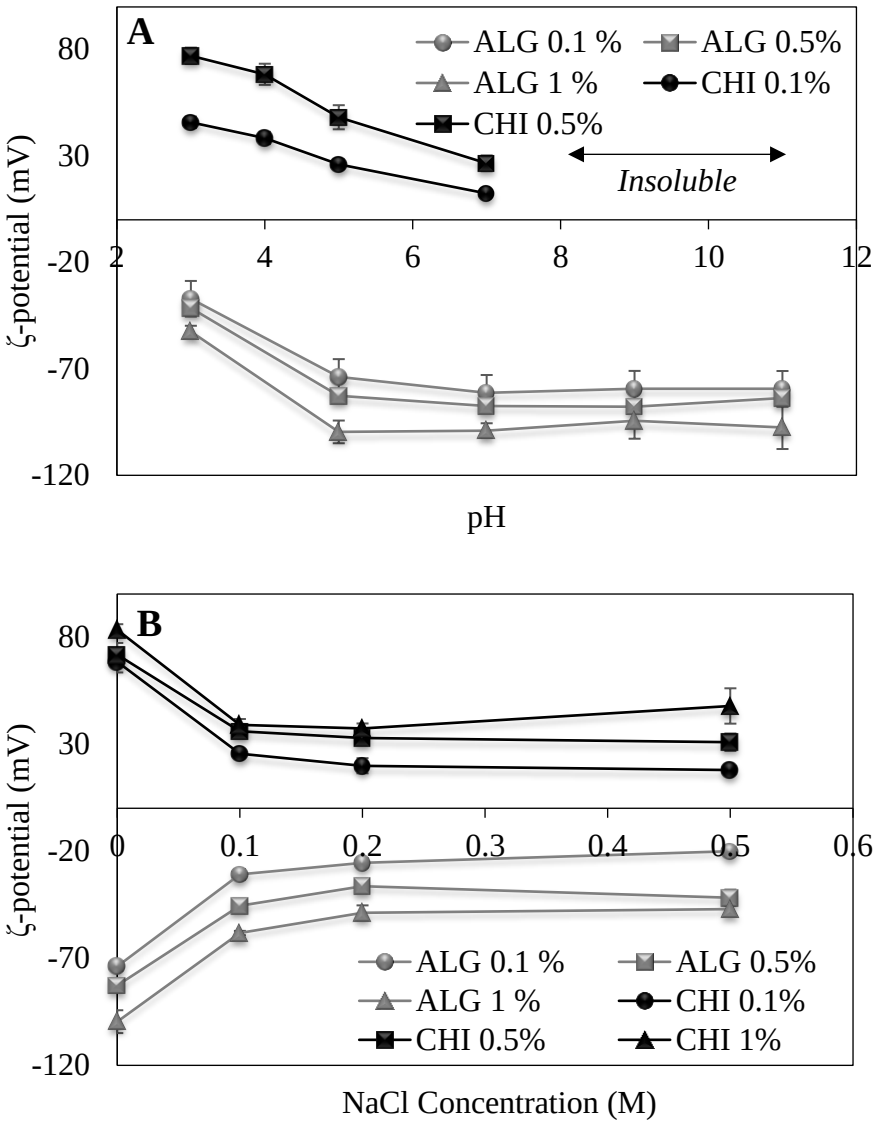

Fig. 1. Influence of (A) pH and (B) NaCl concentration on ζ-potential of alginate (ALG) and chitosan (CHI) solutions at different concentrations. The pH of biopolymer solutions with NaCl was 5 and 4, respectively

On the other hand, the presence of NaCl in the solution decreased the magnitude of ζ-potential values for both polysaccharides (Fig. 1B). For instance, the ζ-potentials of alginate and chitosan without NaCl were -83 mV and 72 mV at 0.5 %, respectively. At 0.2 M NaCl, the magnitude of the ζ-potential decreased to -37 mV and 33 mV in alginate and chitosan solutions, respectively. The effect of the ionic strength on the ζ-potential was less pronounced at higher NaCl concentrations (0.5 M). Previous studies demonstrated a reduction of the net charge in alginate and chitosan solutions as the ionic strength increased [33,35]. This predictable behavior of polysaccharides may be governed by a compression of the electrical double

layer due to the interactions with Na^+ and Cl^- ions dispersed in the solvent [36], or by electrostatic screening effects induced by the accumulation of sodium ions around the charged moieties of polysaccharides [37,38].

3.2. Changes in the viscosity of polysaccharide solutions

The conformation and chain dimensions of polyelectrolytes in the adsorbing solutions has a strong influence on the growth behavior, structure and properties of the resulting nanolaminates [39]. The viscosity of the solution, may give valuable information about the conformations of macromolecules in different conditions. Therefore, the effect of pH, ionic strength and polysaccharide concentration on the viscosity of adsorbing solutions was investigated (Fig. 2).

The viscosity increased with the concentration of polysaccharide, due to the greater entanglement of chains [40]. On the other hand, with the exception of pH 3, the viscosity of alginate solutions was not affected by the pH. A decrease in viscosity was observed in alginate solutions at pH 3 (Fig. 2A). This is reasonable since the ζ-potential values of alginate solutions were weaker at this pH value. Hence, alginate chains could have adopted coiled conformations induced by the protonation of the carboxylic acid groups (COO^-) thereby reducing their hydrodynamic size and solvation. It has been stated that linear and stiff polymers (fully charged polyelectrolytes) have a larger hydrodynamic size than highly flexible polymers (weakly charged polyelectrolytes) of the same molecular mass, resulting in a higher viscosity of the solution [41].

In the case of chitosan solutions, an increase in the pH led to a decrease in viscosity. This effect was less pronounced at low polysaccharide concentrations (Fig. 2A). It is worth mentioning that chitosan solutions at pH above 7 presented insoluble clumps, indicating that solutions were not physically stable within this pH range (>7). This behavior is understandable since these pH values are closer to the pK_a of the glucosamine residues in chitosan (≈ 6-6.5), where most of the amino groups were not ionized. The decrease in viscosity of chitosan from acidic to alkaline pH values also indicated changes in the conformation of chitosan chains and the degree of entanglement. The amino groups of glucosamine residues are highly ionized (NH_3^+) at acidic conditions and the hydrodynamic size of chitosan chains is

greater. However, at low polysaccharide concentration the effect of pH was less pronounced. In diluted solutions, polymer chains are isolated with no chain-chain interactions and their conformational changes may have less effect on the solution viscosity [40].

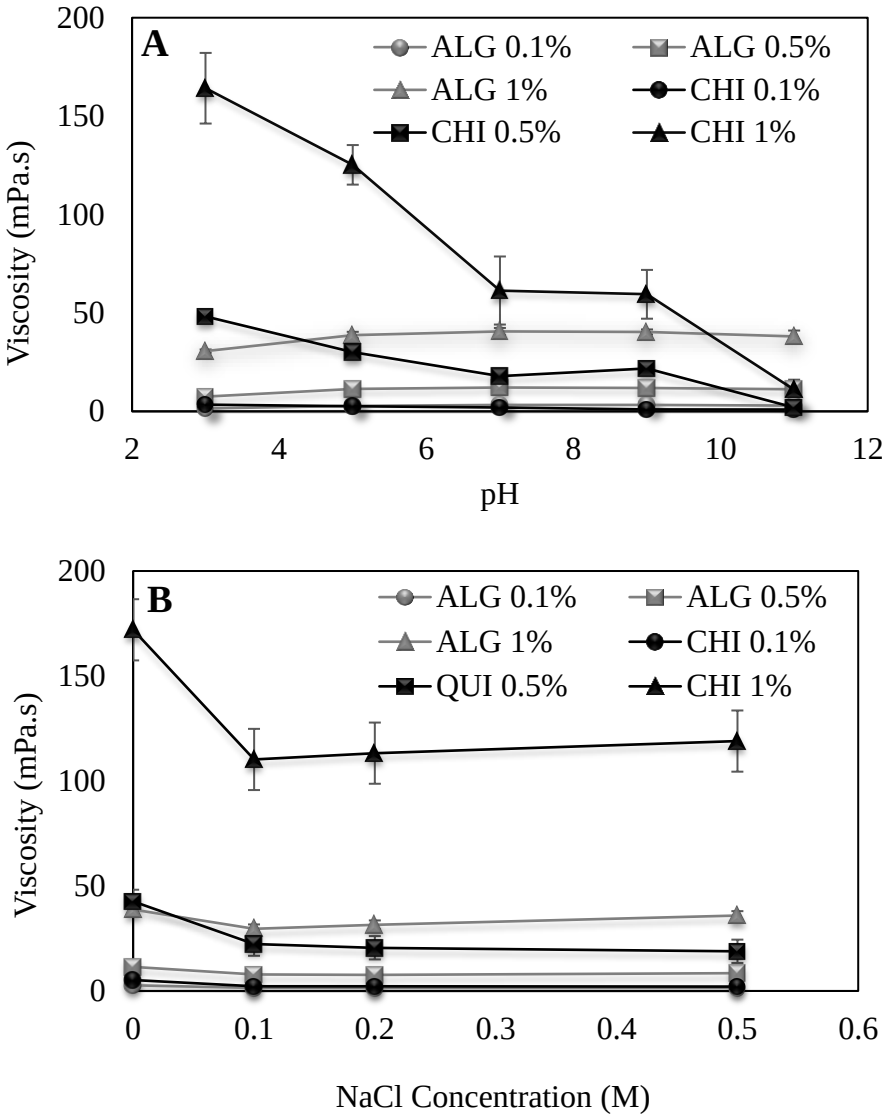

Fig. 2. Influence of pH (A) and (B) NaCl concentration on apparent viscosity of alginate (ALG) and chitosan (CHI) solutions at different concentrations. The pH of biopolymer solutions with NaCl was set to 5 and 4, respectively.

The viscosity decreased by increasing the NaCl concentration to 0.1 M of both polysaccharide solutions. This behavior was less evident at low concentration and at very high ionic strength (Fig. 2B). The greatest change was observed in chitosan solutions at 1%, where the viscosity was 172 mPa.s without NaCl and decreased to 110 mPa.s at 0.1 M NaCl.

The low effect of ionic strength in alginate solutions was probably related to the high residual Na^+ ions concentration coming from the sodium alginate dissociation in aqueous media. The viscosity of polyelectrolyte solutions is strongly affected by the ionic strength, since the dissolved ions in the solvent interact with chains causing charge screening, which in turn, induces the coiling of chains and reduces the degree of solvation [38,42].

3.3. Changes in the whiteness index of polysaccharide solutions

The whiteness index (WI) of polysaccharide solutions was used to determine the presence of insoluble aggregates, which may have an effect on the optical properties of nanolaminates. WI of alginate and chitosan solutions was evaluated as a function of pH, ionic strength and polysaccharide concentration (Fig. 3). Alginate solutions did not present significant differences in WI, neither by increasing the polysaccharide concentration nor by changing the pH of solutions (Fig. 3A). This suggests the absence of insoluble aggregates.

On the other hand, WI of chitosan solutions at acidic conditions (pH 3-5) was similar regardless the polysaccharide concentration. At pH values greater than 5, an abrupt increase could be appreciated. This is reasonable due to the presence of insoluble clumps that could be observed with the naked eye, which tend to scatter the light more strongly and increase the luminosity (L^*) of the solutions. This was attributed to the folding of chitosan molecules as the solution pH was near to the pK_a value (6.3 - 7.5), causing molecular aggregation and increasing the whiteness index. Moreover, a further increase of the ionic strength did not cause changes in WI of both alginate and chitosan solutions, at least within the range of NaCl concentrations used in this work (Fig.3B). This confirmed that the polysaccharide solutions were physically stable in the presence of sodium ions.

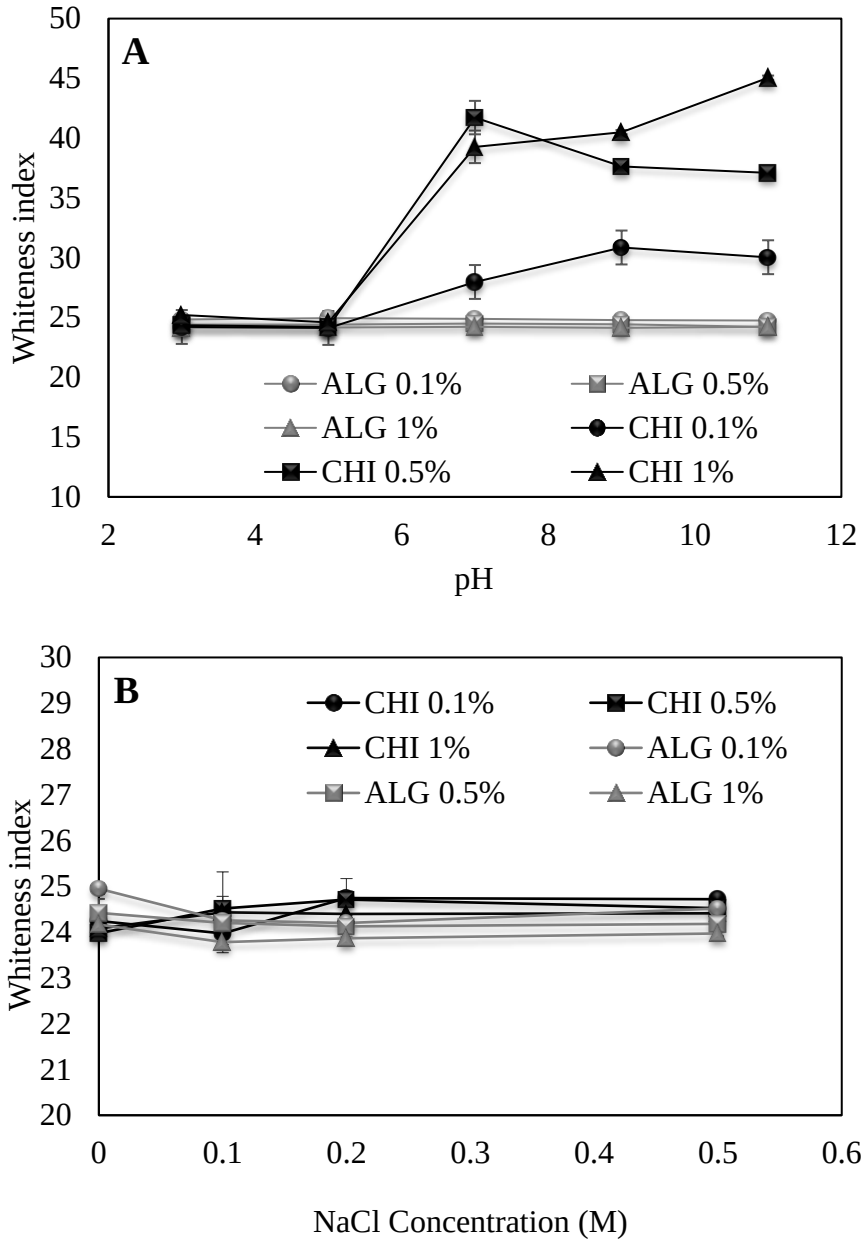

Fig. 3. Effect of (A) pH and (B) NaCl concentration on whiteness index of alginate (ALG) and chitosan (CHI) solutions at different concentrations. The pH of biopolymer solutions with NaCl was set to 5 and 4, respectively.

3.4. Buildup mechanism of alginate/chitosan nanolaminates

Nanolaminates were assembled in quartz slides for the analysis of absorbance. The conditions of preparation of the adsorbing solutions were fixed, so that polysaccharides were equally charged at medium ionic strength. Therefore, nanolaminates were assembled using alginate and chitosan solutions at 0.5%, 0.2 M NaCl and pH 5 and 4, respectively. The high ionic strength can increase layer thickness of the assemblies [43]. Moreover, the

formation of stable nanolaminates has been demonstrated when both polysaccharides have a similar charge density [44].

UV-visible spectra of five bilayers (alginate/chitosan) are shown in Fig. 4A. Absorbance increased as a function of the number of layers deposited. This behavior confirms the sequential formation of layers after an adsorption process. The UV-visible spectroscopy is a practical and reliable technique that allows monitoring the buildup of nanolaminates by increases in the optical mass [45], and although the mass adsorbed cannot be quantified, information about the growth regime of nanolaminates can be obtained.

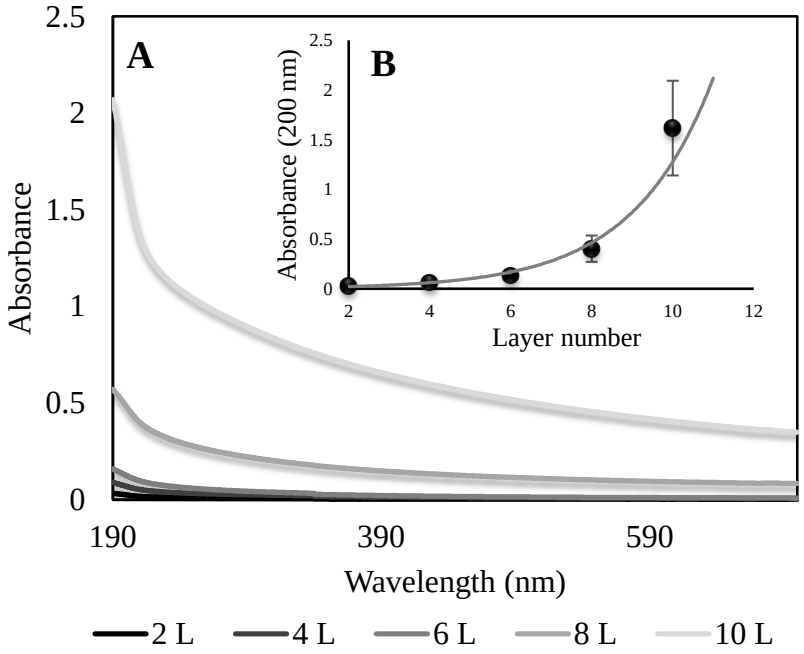

Fig, 4. (A) UV-visible spectra and (B) Absorbance at 200 nm as a function of layers (L) deposited. Nanolaminates were obtained from alginate and chitosan 0.5 % (w/w), 0.2 M NaCl and pH 5 and 4, respectively.

The experimental conditions of the adsorbing solutions may affect the kinetic of adsorption of the polysaccharides, resulting in different growth regimes [46]. Therefore, the type of growth regime was evaluated by plotting the absorbance at 200 nm vs the number of layers. At this wavelength, alginate solutions present the maximum absorption peak, whereas chitosan solutions does not show adsorption within the UV-visible range (data not shown). Interestingly, alginate peak could not be observed in the nanolaminates spectra, probably due to a change in the molar absorptivity of the

chromophore groups of alginate interacting with chitosan. In fact, it has been observed that nanolaminates composed by two polyelectrolytes can form molecular *blends* with intermediate spectrum [47].

The type of growth observed in alginate/chitosan nanolaminates was exponential, which is characterized by an increasing rate of mass deposition with each additional layer. This could be explained by the capacity of certain polyelectrolytes to diffuse in/out of the structure; this *free* chains can interact with oppositely-charged molecules of the absorbing solution [46,48]. Other authors have demonstrated that chitosan chains are able to diffuse vertically (out of the plane), interacting with oppositely-charged adsorbing species in the solution. This behavior was observed in chitosan/heparin assemblies [43].

It is also known that an increase in ionic strength of the adsorbing solutions results in exponential growth nanolaminates, since polyelectrolyte chains are deposited in a coiled conformation [23]. Therefore, the exponential growth of alginate/chitosan nanolaminates could be probably explained by the combined effect of high ionic strength and the diffusion of chitosan and not alginate in the structure of nanolaminates.

3.5. Surface ζ-potential

The surface ζ-potential of the nanolaminates is useful for monitoring changes in the electrical charge after a new layer formation. Surface ζ-potential values changed in terms of sign and magnitude of the electrical charge after a layer deposition (Fig. 5). Initially, the surface ζ-potential of the bare substrate (PET sheets) was 49 mV, and the first alginate layer led to a negative ζ-potential (≈ -32 mV). After the adsorption of the second chitosan layer, surface ζ-potentials changed to positive (≈ 52 mV). These results confirmed the charge reversal of the surface, which is the principle of the layer-by-layer technique. These results are in concordance with those previously reported for polypeptide-polysaccharide assemblies [49]. The charge inversion on the surface after a new layer has been observed also in later-by- systems formed on spherical templates, such as liposomes or nanoparticles [50,51].

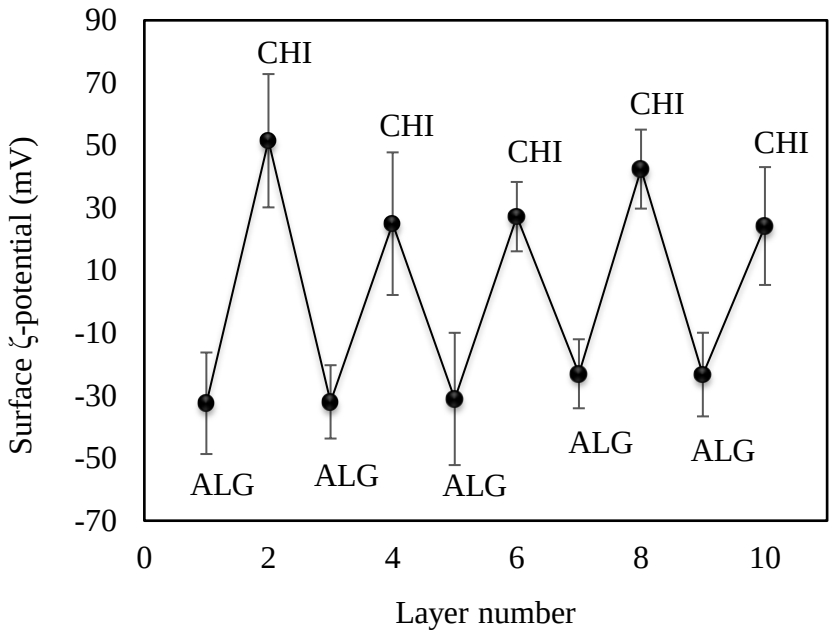

Fig. 5. Surface ζ-potentials as a function of the number of alginate (ALG) and chitosan (CHI) layers deposited in a nanolaminate system. ALG and CHI were prepared at 0.5 % (w/v), 0.2 M NaCl and pH 5 and 4, respectively.

It is worth mentioning that the magnitude of surface ζ-potential values of chitosan layers (between 24 and 51 mV) were slightly superior to those observed in alginate layers (between -23 and -32 mV) although the initial electrical charge of both polysaccharides in solution were similar (ζ-potentials: -36 mV, alginate; 37 mV, chitosan). These differences might be related to different adsorption rates of both polysaccharides during the assembly of layers, or to the ability of chitosan free chains to diffuse toward the surface, probably increasing the surface ζ-potential. Another important factor influencing the surface electrical charge of nanolaminates is the ionic strength, since the coiled conformation adopted by polyelectrolytes favors a greater material deposition on the forming layer, which might also increase the magnitude of the electrical charge in the surface. These results are of great interest when designing nanolaminates for food applications, thus offering the possibility to control attractive or repulsive interactions between the coated food surface and other charged food ingredients.

3.6. Wetting properties

Wettability is one of the most important properties of solid surfaces and describes the ability of a liquid to spread over a certain surface, giving rise to

a continuous film (spontaneous spreading) or discrete droplets (partial wetting) [52]. Interactions between a surface and a liquid depend on the free energies at the solid/liquid interface. The most common approach to discuss the wetting properties is through the contact angle. This parameter is governed by the competition between cohesion of a liquid to itself and adhesion of a liquid to a solid, this indicating the degree of hydrophilicity or hydrophobicity of the surface [53].

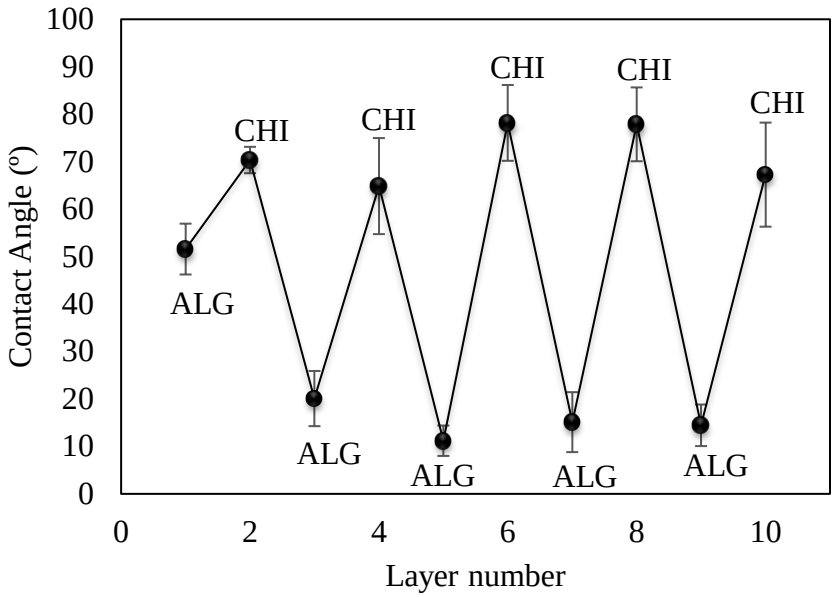

Fig. 6. Water contact angles of the surface of nanolaminates as a function of the number of alginate (ALG) and chitosan (CHI) layers. ALG and CHI solutions were prepared at 0.5 % (w/v), 0.2 M NaCl and pH 5 and 4, respectively.

Water contact angles of nanolaminates created on PET were evaluated after a layer deposition (Fig. 6). The contact angle (θ) of bare PET was 85º, as reported by other authors [26]. After an alginate layer assembly, there was a decrease in θ to ≈52º that further increased to ≈70º with the subsequent deposition of a chitosan layer. These results are in concordance with other studies in alginate/polyethyleneimine and κ-carrageenan/chitosan nanolaminates that reported changes in the contact angle as a function of the number of layers [54,55]. Moreover, greater contact angle values were observed as the number of layers increased in nanolaminates, reaching θ of 14º in alginate layers and 75º in chitosan layers. Chitosan has more hydrophobic features than alginate, which has been attributed to the non-polar impurities contained in all commercial chitosan samples, rather than to the

possible orientation of acetyl moieties at the solid/air interface [56]. These observations highlight the feasibility of the layer-by-layer technique as a strategy to modify the wetting properties of food surfaces, being interesting to design systems that can control the humidity of food products.

3.7. Thermal properties

DSC profiles of uncoated and coated substrate (PET sheets) by alginate/chitosan nanolaminates were examined (Fig. 8). In general, the presence of nanolaminates did not change the glass transition temperature (T_g) and the melting temperature (T_m) of the substrate. Probably, the mass ratio between PET and nanolaminates was too large, and hence the thermal properties of the composite material was governed by the PET. The results obtained in this study for the T_g and T_m of PET are in concordance with previous studies [56,57].

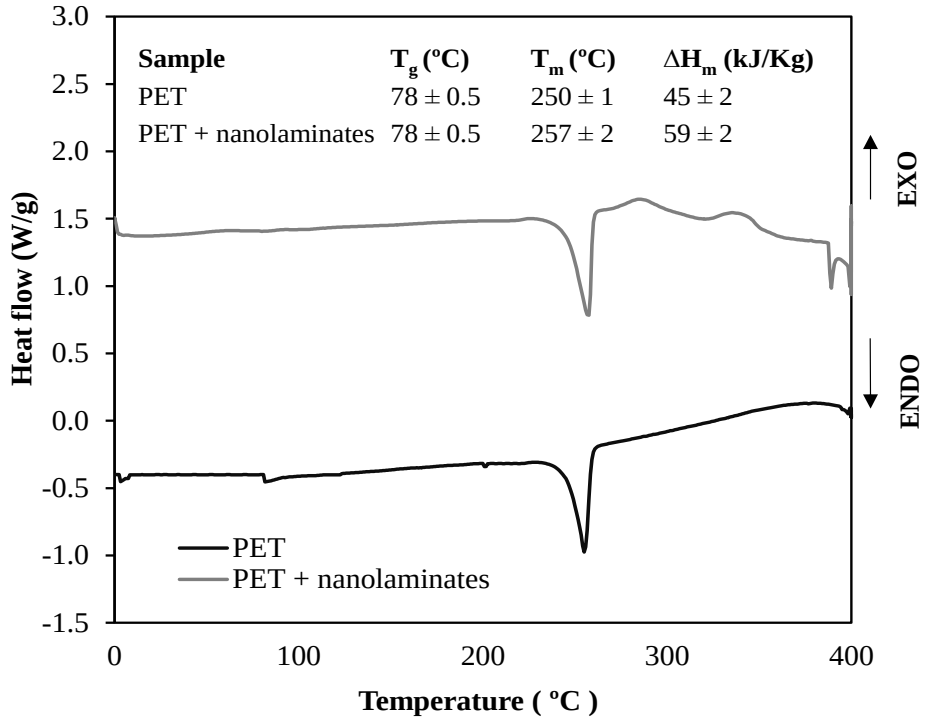

Fig. 7. DSC profile of bare PET and PET containing alginate/chitosan nanolaminates.

On the other hand, a slight increase in the enthalpy of melting (ΔH_m) was observed in coated PET by alginate/chitosan nanolaminates, compared to uncoated PET. This increase could be related with a barrier effect of nanolaminates against the gases generated during the polymer degradation, thus slowing down the process [58]. Another possibility is that the great

accumulation of alginate and chitosan chains on the surface could increase in polymer crystallinity, changing the enthalpy of melting, as suggested previously for alginate/chitosan nanolaminates assembled on PET [26].

3.8. Microstructure

The microstructure and topography of alginate/chitosan nanolaminates are presented in Fig. 8. Experimental parameters including pH, ionic strength, deposition time or temperature of polyelectrolyte solutions have an important impact on the final morphology of nanolaminates, originating different structures such as stratified or solid, as well as different degrees of porosity. In this study, nanolaminates exhibited a dense architecture, being difficult to detect the stratified inner layers. However, it was possible to estimate the average thickness, being around 700 nm for 10-layer assemblies. It has been reported that 20-layer nanolaminates growing exponentially can reach thicknesses > 10 μm, whereas assemblies with a linear growth are typically around 100 nm thick, having equal number of layers [59].

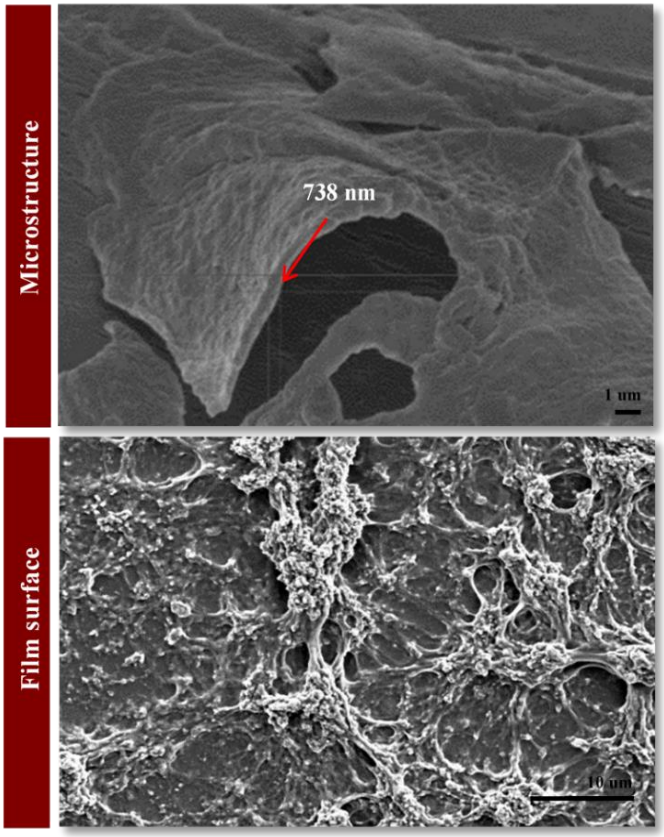

Fig. 8. Microstructure and surface of alginate/chitosan nanolaminates examined by SEM microscopy.

Other authors reported that thickness of exponential growing chitosan/hyaluronan assemblies containing 24 layers was about 6 μm thick [60]. The topography was characterized by the presence of big clusters connected in a net of polysaccharide chains, which could be attributed to the electrostatic interactions between alginate and chitosan molecules. These observations are in line with those reported previously about the topography of chitosan-grafted/alginate assemblies [61].

4. Conclusions

Food-grade alginate and chitosan were assembled into nanolaminates using the layer-by-layer technique. The analysis of the properties of polysaccharide solutions before deposition revealed changes in the ζ-potential, viscosity and whiteness index influenced by changes in the molecular conformation of polysaccharides under different conditions. From this study, it was found that the conditions where alginate and chitosan were physically stable, with a medium electrical charge at high ionic strength was 0.5%, 0.2 M NaCl and pH 5 and 4, respectively. The build-up of nanolaminates assembled under these experimental parameters could be confirmed by the absorbance increase of the substrate with an additional layer, and it presented an exponential growth regime induced by the ability of chitosan to diffuse throughout the structure and the adsorption of polysaccharides at high ionic strength. The surface ζ-potential of nanolaminate was affected by the type of polysaccharide in the terminal layer, being positive for chitosan layers and negative for alginate layers. Charge reversal on the surface also indicated that the assembly process was carried out successfully. The wetting properties of nanolaminates also varied as a function of the number of layers, observing partially hydrophilic or hydrophobic surfaces when alginate or chitosan was the terminal layer, respectively. Regarding the thermal properties, no changes were observed in the thermal properties of the substrate coated by 10-layer assemblies. Results obtained from this study are relevant in the design of food-grade nanolaminates and get specific features, simply by controlling the experimental conditions. In addition, the information generated elucidates the great potential of nanolaminates made from food-grade materials as a strategy for modifying food surfaces or food contact materials, for example, inducing attractive or repulsive interactions between food ingredients, or controlling the moisture of a certain food surface.

5. Acknowledgments

This research was supported by the Ministerio de Ciencia e Innovación (Spain) (project AGL2009-11475). Author Acevedo-Fani also thanks to the University of Lleida for the pre-doctoral grant.

6. References

1. R. J. B. Peters, H. Bouwmeester, S. Gottardo, V. Amenta, M. Arena, P. Brandhoff, H. J. P. Marvin, A. Mech, F. B. Moniz, L. Q. Pesudo, H. Rauscher, R. Schoonjans, A. K. Undas, M. V. Vettori, S. Weigel, and K. Aschberger, Trends in Food Science & Technology **54**, 155 (2016).

2. S. L. Clark and P. T. Hammond, Advanced Materials **10**, 1515 (1998).

3. J. Weiss, P. Takhistov, and D. J. McClements, Journal of Food Science **71**, R107 (2006).

4. J. Borges and J. F. Mano, Chemical Reviews **114**, 8883 (2014).

5. M. M. de Villiers, D. P. Otto, S. J. Strydom, and Y. M. Lvov, Advanced Drug Delivery Reviews **63**, 701 (2011).

6. R. V Klitzing and R. V Klitzing, Physical Chemistry Chemical Physics : PCCP **8**, 5012 (2006).

7. M. A. Cerqueira, A. C. Pinheiro, H. D. Silva, P. E. Ramos, M. A. Azevedo, M. L. Flores-López, M. C. Rivera, A. I. Bourbon, Ó. L. Ramos, and A. A. Vicente, Food Engineering Reviews **6**, 1 (2014).

8. G. Decher, J. D. Hong, and J. Schmitt, Thin Solid Films **210**–**211**, 831 (1992).

9. K. Ariga, M. McShane, Y. M. Lvov, Q. Ji, and J. P. Hill, (2011).

10. M. Fathi, Á. Martín, and D. J. McClements, Trends in Food Science & Technology **39**, 18 (2014).

11. A. Stephen and G. Phillips, *Food Polysaccharides and Their Applications* (CRC Press, Boca Ratón, FL, 2006).

12. A. Ferreira, V. Alves, and I. Coelhoso, Membranes **6**, 22 (2016).

13. T. Crouzier, T. Boudou, and C. Picart, Current Opinion in Colloid & Interface Science **15**, 417 (2010).

14. S. N. Pawar and K. J. Edgar, Biomaterials **33**, 3279 (2012).

15. O. Draget, Kurt Ingar; Moe, Storker T; Skjak-Braek, Gudmund; Smidsrod, in *Food Polysaccharodes and Their Applications*, edited by P. A. Stephen, Alistair M; Phillips, Glyn O; Williams, Second edi (CRC Press, Boca Ratón, FL, 2006), pp. 289–334.

16. M. Rinaudo, Progress in Polymer Science **31**, 603 (2006).

17. C. K. S. Pillai, W. Paul, and C. P. Sharma, Progress in Polymer Science **34**, 641 (2009).

18. G. O. Phillips and P. A. Williams, *Handbook of Hydrocolloids* (Woodhead Pub., Oxford :, 2009).

19. American Chemistry Council, Plastics 1 (2013).

20. J. Fu, J. Ji, W. Yuan, and J. Shen, Biomaterials **26**, 6684 (2005).

21. W. Graisuwan, O. Wiarachai, C. Ananthanawat, S. Puthong, S. Soogarun, S. Kiatkamjornwong, and V. P. Hoven, Journal of Colloid and Interface Science **376**, 177 (2012).

22. H.-Y. Zhang, A.-J. Miao, and M. Jiang, Materials Chemistry and Physics **141**, 482 (2013).

23. S. Boddohi, C. E. Killingsworth, and M. J. Kipper, Biomacromolecules **9**, 2021 (2008).

24. C. Eiras, A. C. Santos, M. F. Zampa, A. C. F. Se Brito, C. J. Leopoldo Constantino, V. Zucolotto, and J. R. Dos Santos Jr., Journal of Biomaterials Science, Polymer Edition **21**, 1533 (2010).

25. J. Xu, L. Yang, X. Hu, S. Xu, J. Wang, and S. Feng, Soft Matter **11**, 1794 (2015).

26. M. G. Carneiro-da-Cunha, M. A. Cerqueira, B. W. S. Souza, S. Carvalho, M. A. C. C. Quintas, J. A. Teixeira, and A. A. Vicente, Carbohydrate Polymers **82**, 153 (2010).

27. M. C. Bourne and M. C. Bourne, in *Food Texture and Viscosity* (2002), pp. 235–256.

28. L. Salvia-Trujillo, M. A. Rojas-Graü, R. C. Soliva-Fortuny, and O. Martín-Belloso, Food Hydrocolloids **30**, 401 (2013).

29. A. Acevedo-Fani, L. Salvia-Trujillo, R. Soliva-Fortuny, and O. Martín-Belloso, Biomacromolecules **16**, 2895 (2015).

30. S. a. Sukhishvili, E. Kharlampieva, and V. Izumrudov, Macromolecules **39**, 8873 (2006).

31. H. Espinosa-Andrews, K. E. Enríquez-Ramírez, E. García-Márquez, C. Ramírez-Santiago, C. Lobato-Calleros, and J. Vernon-Carter, Carbohydrate Polymers **95**, 161 (2013).

32. D. Guzey and D. J. McClements, Food Hydrocolloids **20**, 124 (2006).

33. M. G. Carneiro-da-Cunha, M. A. Cerqueira, B. W. S. Souza, J. A. Teixeira, and A. A. Vicente, Carbohydrate Polymers **85**, 522 (2011).

34. Y.-H. Hong and D. J. McClements, Journal of Agricultural and Food Chemistry **55**, 5653 (2007).

35. A. Abodinar, A. M. Smith, and G. A. Morris, Carbohydrate Polymers **112**, 6 (2014).

36. X. He, F. Meng, A. Lin, J. Li, and C. Y. Tang, AIChE Journal **62**, 2501 (2016).

37. M. G. Semenova, L. E. Belyakova, Y. N. Polikarpov, A. S. Antipova, and E. Dickinson, Food Hydrocolloids **23**, 629 (2009).

38. S. Morariu, C. E. Brunchi, and M. Bercea, Industrial & Engineering Chemistry Research **51**, 12959 (2012).

39. Peng Zhang, * Jinwen Qian, Quanfu An, * Binyang Du, and Xiaoqin Liu, and Q. Zhao, (2008).

40. D. L. B. Wetzel and G. Charalambous, *Instrumental Methods in Food and Beverage Analysis* (Elsevier, 1998).

41. J. Milani and G. Maleki, in *Food Idustrial Processes–Methods and Equipment*, edited by B. Valdez (Intech, 2012), pp. 17–38.

42. S. E. Harding, Progress in Biophysics and Molecular Biology **68**, 207 (1997).

43. M. Lundin, F. Solaqa, E. Thormann, L. MacAkova, and E. Blomberg, Langmuir **27**, 7537 (2011).

44. T. Radeva, K. Kamburova, and I. Petkanchin, Journal of Colloid and Interface Science **298**, 59 (2006).

45. D. T. Haynie, L. Zhang, J. S. Rudra, W. Zhao, Y. Zhong, and N. Palath, Biomacromolecules **6**, 2895 (2005).

46. P. Bieker and M. Schönhoff, Macromolecules **43**, 5052 (2010).

47. P. Lavalle, J.-C. Voegel, D. Vautier, B. Senger, P. Schaaf, and V. Ball, Advanced Materials (Deerfield Beach, Fla.) **23**, 1191 (2011).

48. C. Picart, J. Mutterer, L. Richert, Y. Luo, G. D. Prestwich, P. Schaaf, J. C. Voegel, and P. Lavalle, Proceedings of the National Academy of Sciences of the United States of America **99**, 12531 (2002).

49. C. Picart, P. Lavalle, P. Hubert, F. J. G. Cuisinier, G. Decher, P. Schaaf, and J.-C. Voegel, Langmuir **17**, 7414 (2001).

50. J. Zhang, B. Senger, D. Vautier, C. Picart, P. Schaaf, J.-C. Voegel, and P. Lavalle, Biomaterials **26**, 3353 (2005).

51. J.-Y. Chun, M.-J. Choi, S.-G. Min, and J. Weiss, Food Hydrocolloids **30**, 249 (2013).

52. T. Cosgrove, *Colloid Science: Principles, Methods and Applications* (John Wiley & Sons, 2010).

53. E. M. Baba, C. E. Cansoy, and E. O. Zayim, Applied Surface Science **350**, 115 (2015).

54. C.-H. Gu, J.-J. Wang, Y. Yu, H. Sun, N. Shuai, and B. Wei, Carbohydrate Polymers **92**, 1579 (2013).

55. A. C. Pinheiro, A. I. Bourbon, B. G. de S. Medeiros, L. H. M. da Silva, M. C. H. da Silva, M. G. Carneiro-da-Cunha, M. A. Coimbra, and A. A. Vicente, Carbohydrate Polymers **87**, 1081 (2012).

56. R. P. de Oliveira Santos, D. O. Castro, A. C. Ruvolo-Filho, and E. Frollini, Journal of Applied Polymer Science **131**, 40386 (2014).

57. C. A. Grant, A. Alfouzan, T. Gough, P. C. Twigg, and P. D. Coates, Micron (Oxford, England : 1993) **44**, 174 (2013).

58. Z. Ayhan, S. Cimmino, O. Esturk, D. Duraccio, M. Pezzuto, and C. Silvestre, Packaging Technology and Science **28**, 589 (2015).

59. L. Richert, P. Lavalle, E. Payan, X. Z. Shu, G. D. Prestwich, J.-F. Stoltz, P. Schaaf, J.-C. Voegel, and C. Picart, Langmuir **20**, 448 (2004).

60. O. Etienne, A. Schneider, C. Taddei, L. Richert, P. Schaaf, J.-C. Voegel, C. Egles, and C. Picart, Biomacromolecules **6**, 726 (2005).

61. G. V Martins, J. F. Mano, and N. M. Alves, Langmuir **27**, 8415 (2011).

CHAPTER V: MODULATING BIOPOLYMER ELECTRICAL CHARGE TO OPTIMIZE THE ASSEMBLY OF EDIBLE MULTILAYER NANOFILMS BY THE LAYER-BY-LAYER TECHNIQUE

Acevedo-Fani, A., Salvia-Trujillo, L., Soliva-Fortuny, R., & Martín-Belloso, O

Biomacromolecules (2015); 16: 2895 – 2903

ABSTRACT

The aim of this work was to study the influence of biopolymer (alginate, ALG; chitosan, CHI) charge on the formation of multilayer nanofilms by the layer-by-layer (LbL) technique. The electrical charge of ALG and CHI (*high, medium* or *low*) was modulated by adjusting the pH of biopolymer solutions. The amount of biopolymer deposited in multilayers depended on the charge of ALG and CHI solutions. The lower the charge the higher the deposition rate due to the higher number of biopolymer molecules needed to neutralize the previous layer. *Medium* and *low* charge biopolymers led to a drastic change in the wettability of multilayers, with ALG layers being strongly hydrophilic and CHI layers strongly hydrophobic. The surface ζ-potential alternatively changed from negative to positive using ALG or CHI. This effect was more pronounced using highly charged biopolymers. Results obtained in this study evidenced that the multilayers properties can be tuned by controlling the biopolymer electrical charge.

Keywords

Layer-by-layer, sodium alginate, chitosan, multilayers, electrostatic deposition

1. Introduction

Over the past few years, there has been a growing interest in nanotechnology as a versatile tool to design new types of materials. Multilayer nanofilms formed by the layer-by-layer (LbL) electrostatic deposition have been extensively used as a simple strategy to coat and functionalize the surface of materials with different applications in biomedicine, pharmacology and biomaterials science, among others. In the food sector, multilayer nanofilms offer a wide range of interesting applications such as thin edible coatings, functionalization of food packaging surfaces or encapsulation of food bioactive compounds with controlled release under certain conditions.[1–3]

The LbL technique is based on the assembly of several thin layers by alternating the adsorption of oppositely charged polyelectrolytes on a charged substrate. The LbL process is mainly driven by electrostatic forces, although other interactions such as hydrogen bounding, hydrophobic and van der Waals forces may intervene.[4] Each deposited layer leads to a charge overcompensation that has two important consequences: (i) the repulsion of equally charged molecules and thus self-regulation of the adsorption and restriction to a single layer and; (ii) the formation of a new layer by the adsorption of oppositely charged molecules on the top of the previous layer.[5] This process results in the formation of multilayer nanofilms of 10-100 nm per layer, and the average thickness is determined by the number of layers of the film.

A variety of polysaccharides could be used to form edible multilayer nanofilms. Alginates are unbranched polysaccharides extracted from marine brown algae consisting of (1→4) linked β-D-mannuronic acid and α-L-guluronic acid residues. In aqueous solutions, alginates behave as polyanions (pK_a ≈ 3.6) due to the presence of -COOH groups along the molecular chains that can be deprotonated to confer negative charges.[6] Chitosan is a copolymer naturally abundant in the exoskeleton of crustaceans, fungal cell walls and in other biological materials. It is mainly composed by β-(1-4)-2-acetamido-D-glucose and β-(1-4)-2-amino-D-glucose units and it is generally described in terms of degree of deacetylation. Chitosan acts as a cationic biopolymer (pK_a ≈ 6.26) in acidic conditions due to the protonation of -NH_2 groups in the chemical structure. The formation of stable complexes between alginate and chitosan through electrostatic interactions has been described by other authors.[7,8]

In spite of the simplicity of the LbL technique, processing parameters such as coating material concentration, washing and drying steps, ion concentration, and pH of solutions may influence the adsorption kinetics of the films.[4,9] The solution pH is an important factor to be considered since its variation alters the dissociation of charged polysaccharides and thereby, the magnitude of the electrical charge. This fact directly affects the electrostatic interactions between polysaccharides, changing the adsorption process and the film properties. The assembly of alginate and chitosan through the layer-by-layer technique has been previously described for biomedical approaches.[10–12] However, scarce systematic studies have reported the effect of the electrical charge of both biopolymers modulated by pH for food purposes. The study of the deposition during the LbL process is crucial to understand the assembly mechanism and optimize the conditions for the use of nanofilms in practical applications. The objective of this work was to obtain multilayer nanofilms based on natural polymers such as alginate and chitosan and evaluate the effect of the electrical charge of the biopolymers solutions on the formation and film properties of multilayers through the layer-by-layer assembly method.

2. Materials and methods

2.1. Materials

Quartz slides (Suprasil® 300) were purchased from Hellma analytics (Müllhein, Germany) and polyethylene terephthalate (PET) sheets were obtained from Isovolta (Barcelona, Spain). Reactives for substrate aminolization such as, 3-aminopropyltriethoxysilane (APTS, 99%), N,N-dimethylformamide (DMF, 99,8%) and 1,6-hexanediamine (99,5%) were purchased from Acros Organics (Geel, Belgium). Piperidine (99%) was purchased from Sigma-Aldrich (Madrid, Spain). Methanol and bromophenol blue (BPB) were obtained from Fisher Scientific (Loughborough, U.K.). Ethanol absolute and 1-propanol were purchased from Scharlau (Barcelona, Spain). Hydroclorhidric acid (HCl, 35-38%) was purchased from POCH (Gliwice, Poland). Chitosan (CHI, high molecular weight, deacetylation degree > 75%) and sodium alginate (ALG; manucol® DH) were purchased from Sigma-Aldrich (Madrid, Spain) and FMC Biopolymers (Scotland, U.K.), respectively. The pH of the polysaccharide solutions was adjusted with lactic acid (88-90%) and sodium hydroxide (NaOH) purchased from Scharlau

(Barcelona, Spain). Deionized water (18.2 mΩ, Milli-Q ultrapure water system, Millipore) was used in all film-forming solutions and washing steps for the nanofilms fabrication.

2.2. Substrates pre-treatment

Quartz slides were cleaned with a Hellmanex solution 2% (v/v) for 2 h. Substrates were immersed in APTS (1% v/v) at 25 ºC during 30 min to induce a positive charge on the quartz surface, and rinsed with copious deionized water in order to remove reactive excess.[13] Quartz slides were left in a desiccator containing silica gel until nanofilms were assembled.

PET sheets were functionalized according to a method described by Bech et al.[14] with some modifications. PET rectangles (6 cm x 2 cm) were cleaned in propanol/water 1:1 solution during 3 h. Briefly, the sheets were submerged in tubes containing 10 mL of 1,6-hexanediamine/methanol solution (1 M) at 50 ºC during 4 h to induce the aminolysis reaction, giving a positive charge to the PET surface. PET substrates were removed from the tubes and washed with methanol, and then dried in vacuum at room temperature (25 ºC) for 12 h. The PET sheets were treated with HCl 0,1 M during 3 h at 25ºC to protonate amine groups attached to the material surface. After this process the rectangles were left in vacuum for at least 12 h and 25 ºC.

2.3. Polyelectrolyte solution preparation

Sodium alginate and chitosan solutions were prepared at a concentration of 0.5% w/w. Sodium alginate was dissolved in ultrapure water and chitosan was prepared in lactic acid solution (1% v/v) to promote protonation of amino groups in the biopolymer molecule and therefore increase its solubility. Polysaccharide solutions were left under agitation during 5 h. Alginate and chitosan solutions with different electrical charges (*high*, *medium*, and *low*) were prepared by adjusting the pH of the solutions using lactic acid or NaOH solutions (Table 1).

2.4. ζ- potential

The electrical charge of ALG and CHI solutions was evaluated by phase-analysis light scattering using a laser diffractometer (Zetasizer NanoZS, (Malvern Instruments Ltd, U.K.).

2.5. Layer-by-layer assembly

Nanofilms were assembled on two types of substrates. Quartz slides were used to obtain the UV-visible spectra and PET rectangles were used for the other determinations. The previously cleaned and positively charged substrates were submerged in alginate solutions in order to form the first layer. Substrates remained in this solution during 20 min. After the adsorption process, samples were rinsed twice in ultrapure water at the same pH of alginate solutions for 5 min. This step was necessary to remove the sodium alginate molecules that were not bound to the substrate. Straightaway, substrates were immersed in chitosan solutions for 20 min to obtain the second layer. In this step, the positively charged chitosan molecules were adsorbed to the previous negatively charged alginate layer by means of electrostatic interactions. After this, the process was followed by two rinse steps with ultrapure water at the pH of chitosan solutions for 5 min. Alternate deposition of layers was repeated to obtain a multilayered structure film.

For the purpose of this work, 10 layers was considered as a reasonable number to study the buildup process and the differences in film architecture according to the pH used during the assembly. When the deposition of layer was complete the nanofilms were dried using a nitrogen gas flow.

2.6. Characterization of substrates

2.6.1. Determination of the concentration of amine groups

After the aminolysis reaction, the concentration of amine groups introduced to the PET sheets and quartz slides were analyzed with a method previously reported by Irena et al.[15] The substrates were immersed in 25 mL of BPB/DMF solution (0.1 mg/mL) for 30 min. Then rectangles were removed from the previous solution and washed with copious ethanol to remove unbounded dye. PET sheets were treated with 10 mL of piperidine/DMF solution (20%), and the absorbance of the solution obtained was measured at λ = 605 nm. The surface concentration of amine groups was calculated from Lambert-Beer law following Eq. (1):

$$A=\varepsilon l c \qquad (1)$$

where A is the absorbance of the sample, ε is the molar extinction coefficient ($BPB_{\varepsilon 605}$ = 91,800 $L.mol^{-1}.cm^{-1}$), *l* is the path length (1 cm), and *c* is the sample concentration. The concentration of amine groups found in untreated PET and quartz slides was 0.04 ± 0.01 $nmol/cm^2$, and after being treated the final concentrations increased up to 0.63 $nmol/cm^2$ and 0.11 ± 0.01, respectively (Fig. 1). In both cases it could be confirmed that $–NH_2$ groups were incorporated onto the substrates.

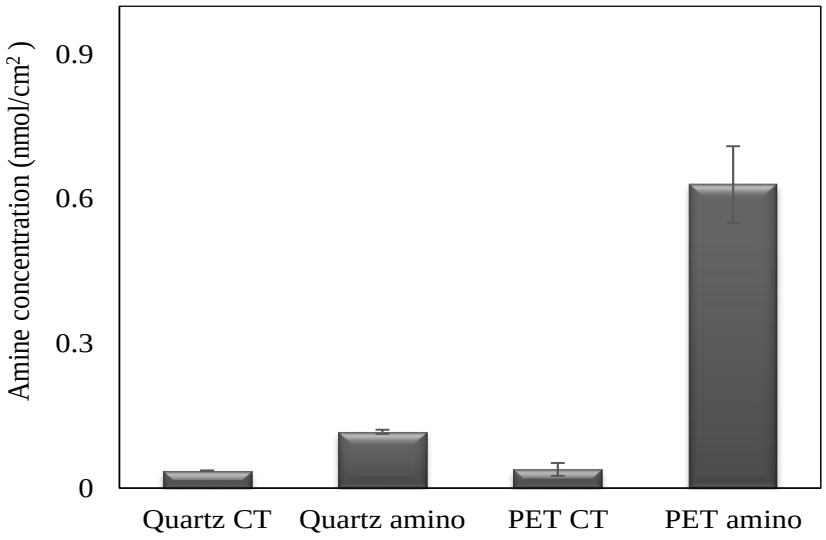

Fig. 1. Surface concentration of amine groups on untreated PET or quartz substrates (PET CT and Quartz CT) and after aminolization (PET amino and Quartz amino). Characterization of edible nanofilms

2.6.2. Spectrophotometric measurements

The layer-by-layer assembly of ALG and CHI on quartz slides was monitored using a UV-visible-NIR spectrometer (V670, Jasco Corporation, Tokio, Japan). The absorption spectra of bilayers were obtained. The absorbance of ALG in aqueous solutions is increased as a function of the biopolymer concentration (Fig. 2). ALG (0.5%) presented a bell-shaped absorption peak at 200 nm, whereas CHI does not show appreciable absorbance at that wavelength range (Fig. 2), thus multilayer deposition was assessed using 200 nm.

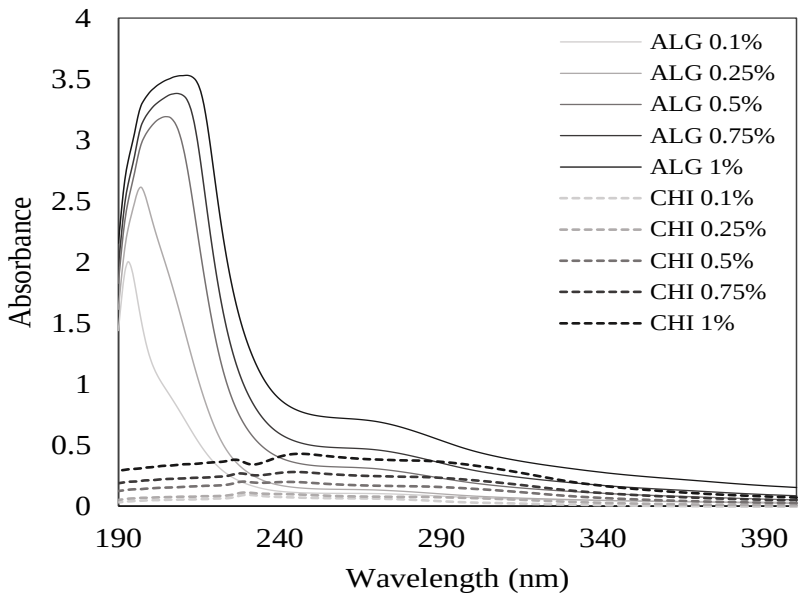

Fig. 2. (A) Absorption spectra of ALG and CHI in aqueous phase at different concentrations (0.1–1%).

2.6.3. Surface ζ-potential analysis

The ζ-potential is an important and useful indicator of the electrical charge at the film surface. The zeta potential of nanofilms after each deposition of layers was determined using the Zetasizer NanoZS laser diffractometer, (Malvern Instruments Ltd., Worcestershire, U.K) equipped with a surface ζ-potential cell unit (ZEN1020), specially designed for zeta potential analysis in flat surfaces. Nanofilms formed on PET and attached to a sample holder were placed between two electrodes of the surface ζ-potential cell. After that, samples were immersed in an appropriated aqueous solution containing tracer particles. The negative and positive particles were polystyrene latex particles in buffer solution pH 9 (DTS1235, Malvern instruments) and quaternary ammonium salts in solution (obtained from fragrance-free fabric conditioner), respectively. The electrical charge of these tracer particles was opposite to the charge of the surface to be analyzed. The tracer ζ-potential was measured by phase-analysis light scattering (PALS) at 5 distances from the sample surface. By plotting the zeta potential as a function of displacement from the surface, the software equipment extrapolated this relationship to zero displacement to obtain the surface ζ-potential of nanofilms.

2.6.4. Water contact angle measurements

The contact angle of the nanofilms after each layer deposition was determined using a DSA25 Krüss goniometer (Krüss GmbH, Hamburg, Germany) equipped with image analysis software (Drop Shape Analysis System, Krüss GmbH, Germany). By applying the sessile drop method, five deionized water drops of 1 µL were created at the tip of the syringe and carefully placed along the PET sheet covered with nanofilms. Measurements were conducted immediately after drop deposition and tests were carried out at room temperature. The contact angle was calculated using the Young-Laplace fit.

2.6.5. SEM imaging

SEM imaging measurements were performed using a J-6510 scanning electron microscope (JEOL Ltd., Tokio, Japan). Aluminum stubs containing PET covered with nanofilms were treated with carbon and metalized with evaporated gold, using a SCD 050 sputter coater (Balzers Union AG, Liechtenstein). This step was necessary to confer electrical conductive properties to the substrate with nanofilms. Samples were analyzed with an acceleration voltage of 5 kV.

2.6.6. Thermal properties

The thermal properties of ALG and CHI nanofilms fabricated on PET substrates were determined using a differential scanning calorimeter (DSC822e, Mettler Toledo S.A.E., Barcelona, Spain). Samples were heated from 0 ºC to 400 ºC at a rate of 10 ºC/min under an atmosphere of inert nitrogen. The glass transition temperature (T_g), the melting temperature (T_m) and the enthalphy of melting (ΔH_m) were reported from the thermograms. The melting curve was integrated using StartE v.11 software (Mettler Toledo S. A. E., Barcelona, Spain), in order to obtain the enthalpy of melting.

2.7. Statistics

Experiments were repeated twice and samples were analyzed by triplicate. The average and standard deviations of data were presented. ANOVA analysis was performed using Statgraphics plus 5.1 software (Statistical Graphics Co., Rockville, MD, EE.UU), and differences among average results were assessed using Fisher's least significant difference (LSD) method with a significance level of 5%.

3. Results and discussion

3.1. Effect of the biopolymer charge on the buildup

The pH of the biopolymer solution determines the ionization of the surface groups on a macromolecule and therefore the final surface charge density.[17] ALG and CHI are weak polyelectrolytes, and thus, the degree of dissociation of their functional groups, and in turn, the electrical charge can be controlled by changing the pH of the solutions. In this study, three combined pH settings for ALG and CHI were selected in order to obtain polysaccharide solutions with a *low*, *medium* and *high* electrical charge during the formation of multilayers. Table 1 shows the electrical charge expressed by ζ-potential of ALG and CHI solutions at different pH conditions corresponding to three different levels of charge. In the case of ALG, the ζ-potential values of *high*, *medium* and *low* charge polysaccharides used for the formation of nanofilms were -87.4, -77.3 and -41.3 mV at pH 7, 5 and 3, respectively. Similarly, the ζ-potential of *high*, *medium* and *low* charge CHI chains in aqueous solutions were 77, 68 and 27 mV at pH 3, 4 and 7, respectively. The change in the degree of ionization of both biopolymers can be explained by the protonation or deprotonation of the charged moieties, such as -COOH and $-NH_2$, under the presence of different concentrations of H^+ and OH^- ions in the surrounding media.

Table 1. Electrical properties of biopolymer solutions at different pH conditions.

Levels of electrical charge	Polysaccharide, pH	ζ-potential (mV)
High	ALG, 7	-87.4 ± 2.1
	CHI, 3	77.0 ± 4.0
Medium	ALG, 5	-77.3 ± 1.4
	CHI, 4	68.0 ± 4.0
Low	ALG, 3	-41.4 ± 1.6
	ALG, 7	27.0 ± 4.0

Results are presented as the average ± standard deviation. ALG: alginate solutions, and CHI: chitosan solutions.

To study the effect of the biopolymer electrical charge on the buildup of multilayers, absorbance spectra in the UV-visible range were obtained

(Fig. 3). Absorbance is, in principle, directly proportional to the amount of material deposited on the substrate after the formation of multilayers. The spectra of $(ALG\text{-}CHI)_5$ multilayer nanofilms showed absorbance around 200 nm, although, there is not a bell-shape peak at this absorbance, probably due to the formation of molecular complexes between ALG and CHI during the LbL procedure that could have influenced the optical properties. In fact, it is known that layers of oppositely charged polyelectrolytes form molecular *blends* that might present an intermediate molecular spectrum.[17]

The absorbance increased as a function of the number of layers, regardless of the electrical charge of the polysaccharides chains (Fig. 3A - 3C). This fact evidenced the deposition of material onto the substrate, thus confirming the effective buildup of nanolayers with the LbL technique by oppositely charged biopolymers. Nevertheless, the electrical charge of polysaccharides significantly affected the amount of material deposited in nanofilms. When multilayers were assembled with *low* charge ALG and CHI chains, the absorbance was significantly higher after each layer formation compared to the multilayers formed from *medium* or *high* charged biopolymers (Fig. 3D). After 10-layers, nanofilms assembled with *high*, *medium* and *low* charge ALG and CHI chains exhibited significant differences in absorbance values of 0.2690 ± 0.016, 1.3 ± 0.4 and 1.55 ± 0.05, respectively. The differences observed in the absorbance of multilayer nanofilms depending on the electrical charge of the polysaccharide might be due to the different molecular conformations of the biopolymers under pH conditions selected. ALG presented a high electrical charge at pH 7 whereas CHI presented a high charge at pH 3. At these pH conditions, carboxylic groups of ALG and amino groups of CHI had a strong intra molecular repulsion exhibiting a well-extended molecular conformation. When the net charge is rather *high*, less amount of material is required to overcompensate surface charge during the adsorption process. On the contrary, when ALG and CHI have relatively *low* charge, at pH 3 and 7, respectively, most of the carboxylic groups of ALG and amino groups of CHI become neutral and the molecules tend to fold, adopting loopy conformations. In consequence, greater amounts of material are required to achieve the charge reversal during the assembly process, thus increasing absorbance. In fact, this is what is typically observed when the multilayers assemblies are carried out with weak polyelectrolytes at different pH conditions.[18,19]

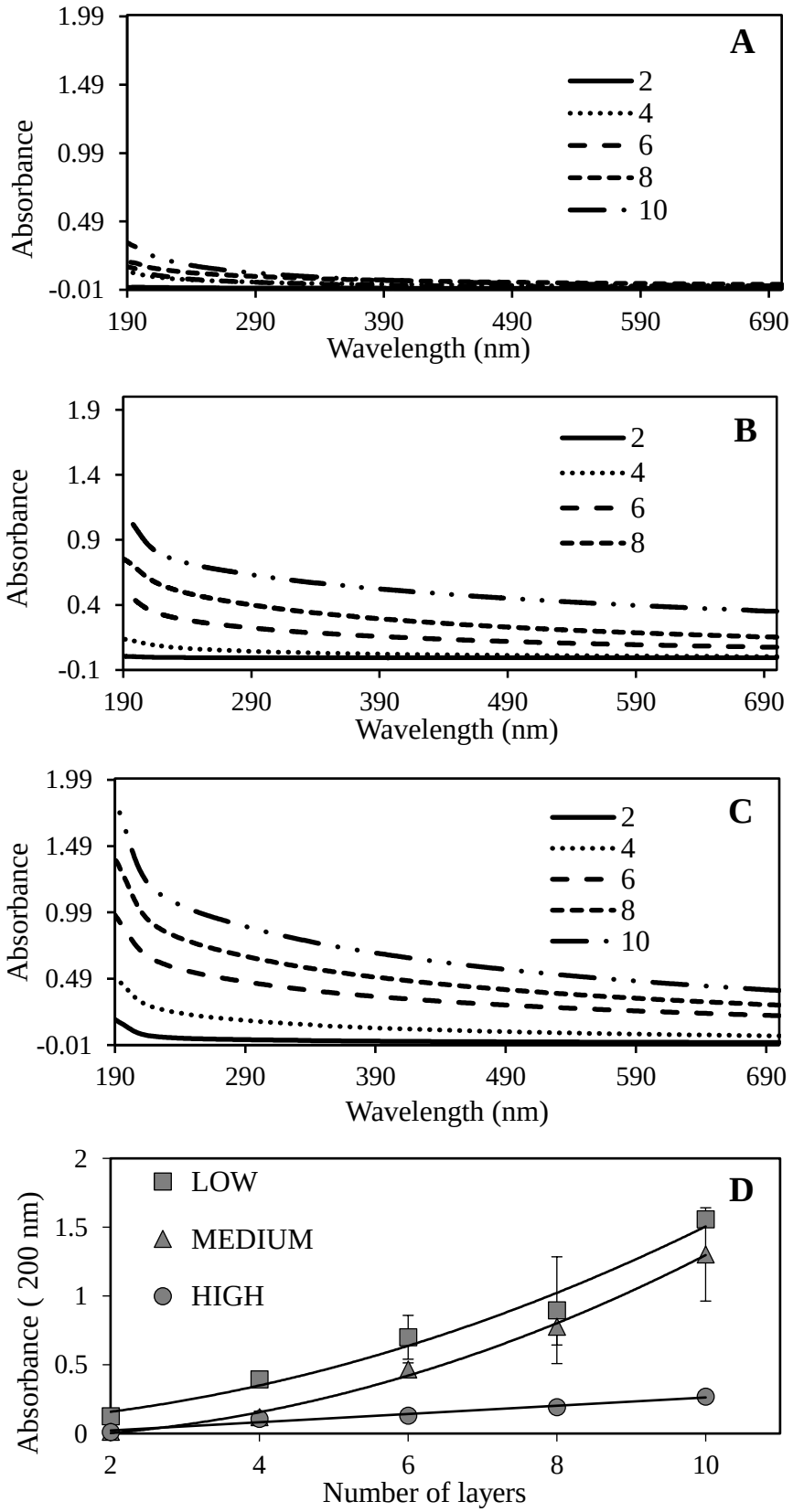

Fig. 3. UV-visible spectra of sequential adsorptions of bilayers (2, 4, 6, 8 or 10 layers) at (A) *low*, (B) *medium* and (C) *high* electrical charge, according to Table 1. (D) Absorbance at 200 nm of nanofilms as a function of the number of layers.

For poly(allylamine hydrochloride) and poly(acrylic) acid multilayers, the film thickness dramatically decreases when the pH is between 6.5 and 7.5, and both polyelectrolytes are fully charged. However, if one of the two polyelectrolytes is partially charged at certain pH the film thickness is increased. Moreover, Pargaonkar et al.[20] and Ai et al.[21] observed that the thickness of multilayers made of poly(dimethyldiallyl ammonium chloride), sodium poly(styrenesulfonate) and gelatin on drug particles increased when gelatin in acidic pH was incorporated, and that behavior was attributed to changes in its molecular conformation. Other authors have described that thickness of the adsorbing layer can be modulated by changing the pH of the polyelectrolyte solution.[11]

Additionally, the growth rate of nanofilms was evaluated (Fig. 3D). Multilayers assembled with *high* charge polysaccharides exhibited a linear trend, meaning that absorbance at 200 nm increased uniformly in each bilayer. Conversely, multilayers formed from *medium* and *low* charge polysaccharides exhibited an exponential growth trend, which is characterized by an increasing rate of mass deposition for each additional layer with the number of layer depositions. A polyanion/polycation system that grows exponentially under certain conditions can also grow linearly when deposition conditions are modified.[22] A linear growth indicates that charged molecules in the solution interact exclusively with the outer layer of the multilayer film. However, when exponential growth occurs one of the polyelectrolytes is able to diffuse within the film structure toward the outer layer, and these free chains can interact with the adsorbing solution contributing to the film growth.[23] Therefore the results observed in the present work are in agreement with other studies, confirming that the charge density of the polysaccharide solution plays a key role in their capacity to form multilayers by the LbL technique.[24] Furthermore, changes in the growth type as a function of pH have been observed in multilayers made with polymers that behave as weak polyelectrolytes.[25]

3.1. Effect of the biopolymer charge on the surface ζ-potential

An important property of multilayers formed by electrostatic interactions is the ζ-potential, which is defined as the potential at the hydrodynamic slipping plane adjacent to the boundary phase.[26] To assess the effect of the polysaccharide charge on the electrical properties of nanofilms, the surface

ζ-potential (SZP) was measured after each layer deposition (Fig. 4). Initially, the aminolyzed PET was positively charged (49 ± 7 mV). After the first layer formation, the charge magnitude switched to negative in assemblies formed with *high* and *medium* charge ALG chains, suggesting that surface was completely saturated by the adsorbing molecules. Nevertheless, the first layer formed from *low* charge ALG chains did not show a change in SZP sign, although the magnitude decreased down to 5.0 ± 2.4 mV, which can be associated with a sparse coverage of the substrate. In this case, the positive SZP value may result from contributions of the low residual charge of ALG chains and the PET surface. Literature reports that a minimum charge density is required for the formation of multilayers and below this threshold, the charge reversal is not sufficient to achieve charge overcompensation.[4,9] However, despite the low charge of the first ALG layer, the results evidence that the formation of multilayers is possible and even presents an increased deposition when using *low* charge biopolymers as discussed earlier. In this line, the electrostatic interactions were not necessarily the main driving force responsible for the multilayers formation. The non-Coulombic interactions such as hydrogen bonding between neutral molecules, van der Waals forces or steric interactions, play an important role on the process of adsorption of multilayers. The impact of non-electrostatic interactions on the deposition of multilayer systems of cellulose and chitosan have been recently described in detail by other authors.[27] Moreover, the formation of multilayers from *low* charge polyelectrolytes have been reported, attributing this fact to the presence of synergistic non-electrostatic interactions that contribute to the layer formation.[28,29]

After the consecutive addition of new layers of the oppositely charged biopolymers, the SZP of the subsequent layer presented a positive charge (CHI layers) or negative charge (ALG layers). This supports the fact that each layer adsorption leads to a charge reversal, providing a new opposite charge required to continue further adsorption steps. These results are consistent with the ζ-potential measured by Richert et al.,[30] on biopolymer-based (hyaluronan/chitosan) multilayers and by Ladam et al.,[31] on synthetic polymer-based (poly(allylamine hydrochloride)/poly(sodium 4-styrenesulfonate)) multilayers, deposited on flat surfaces and determined by streaming potential measurements.

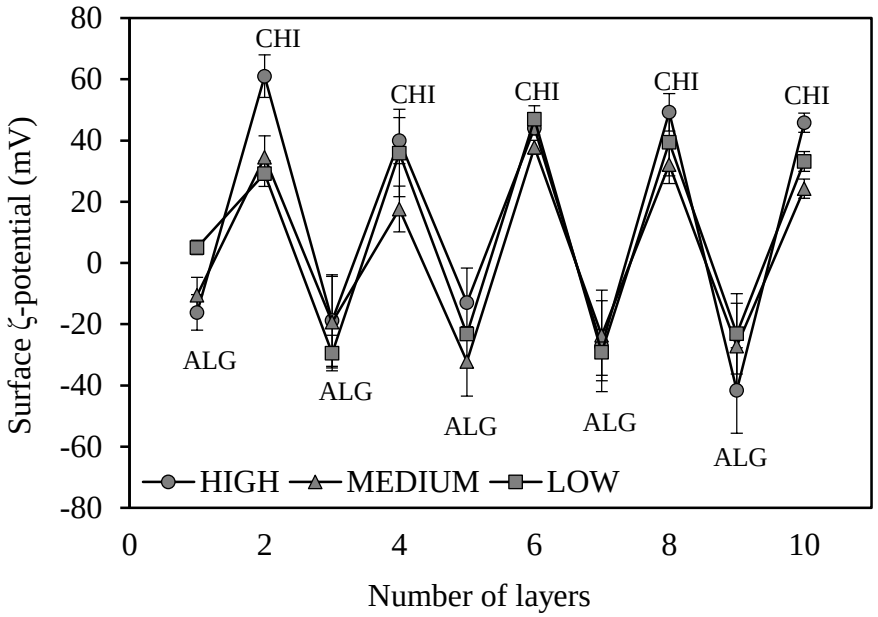

Fig. 4. Surface ζ-potential (SZP) of multilayer nanofilms assembled from alginate (ALG) and chitosan (CHI) at *high*, *medium* and *low* electrical charge (according to Table 1).

The charge of the biopolymer solution significantly affected the SZP of the successive layers formed. When *high* and *low* charge ALG and CHI solutions were used, the ALG layers (odd) and CHI layers (even) showed significantly more negative or more positive SZP, respectively, at increasing number of layers. However, this pattern was not observed for the medium charge biopolymer solutions, where the SZP of increasing number of ALG or CHI layers was significantly lower ($p < 0.05$). These results are in concordance with those previously discussed in this work. The layers formed with high charge polysaccharides may present a greater number of ionizable groups on the surface that can increase the magnitude of electrical charge. In the case of layers formed with *low* charge polysaccharides, the high surface charge may be attributed to the greater amount of polysaccharides chains needed to form the nanolayers that, in turn, increase the number of charged groups on the surface. In all the assemblies the charge magnitude of even layers was greater than the charge magnitude of the odd layers suggesting a higher contribution of CHI to the electrical properties of nanofilms. The pH of solutions containing biopolymers with ionizable groups could lead to irregular behaviors on the charge reversal during the LbL deposition. According to Zhang et al.,[32] the multilayers composed by hyaluronic acid and collagen followed a similar trend regarding the SZP. However, the magnitude of SZP remained relatively

constant from the eighth layer at the different levels of charge, suggesting the stability of the system after the deposition of a certain amount of layers.

3.2. Effect of biopolymer charge on the contact angle

The contact angle is often used to describe the wetting behavior of films. It is defined as the angle formed at the intersection of the liquid, gas and solid phases.[33] There is a balance between the cohesion forces within a liquid and adhesion of a liquid to a solid.[34] The contact angle that creates a drop of water on the surface of the multilayers provides meaningful information to describe the hydrophilic or hydrophobic behavior of the nanofilm. The greater the contact angle value the more hydrophobic the film surface. Fig. 5 shows the contact angles of the multilayers assembled from biopolymers with different electrical charge. Water contact angles showed a zigzag trend when nanofilms passed from ALG-ending layers to CHI-ending layers with *low* and *medium* charge, indicating a pronounced change in the wetting properties of the multilayers. CHI layers were more hydrophobic, whereas ALG layers presented a strong hydrophilic behavior. This effect was more pronounce in multilayers formed with *low* charge biopolymers. Results are in good agreement with those found by other authors.[35,36] Conversely, no remarkable differences were observed in the results obtained from multilayers assembled with *high* charge polysaccharides ($p < 0.05$), which could be correlated with the results of absorbance previously discussed (Fig. 3). This means that the strong hydrophobic/hydrophilic interactions observed in multilayers made of *medium* and *low* charge biopolymers can be due to a greater amount of material deposited in each layer during the assembly process, originating more uniform and structured layers. On the contrary, the assemblies obtained from *high* charge polysaccharides did not show differences in the wetting properties during the sequential formation of new layers and presented the lower mass adsorption rate as well. This behavior suggests that the hydrophilic or hydrophobic character of the nanofilms is highly dependent on the experimental conditions used during the assembly of multilayers.

For instance, Fu et al.[37] have reported the strong effect of the film thickness on the wettability of multilayers made of two natural polyelectrolytes (heparin and chitosan). In thinner layers, the oppositely charged polysaccharides establish strong interactions originating well-interpenetrated structures in

which the surface properties will be governed by the properties of the polysaccharide blend resulting in a less stratified multilayer structure.

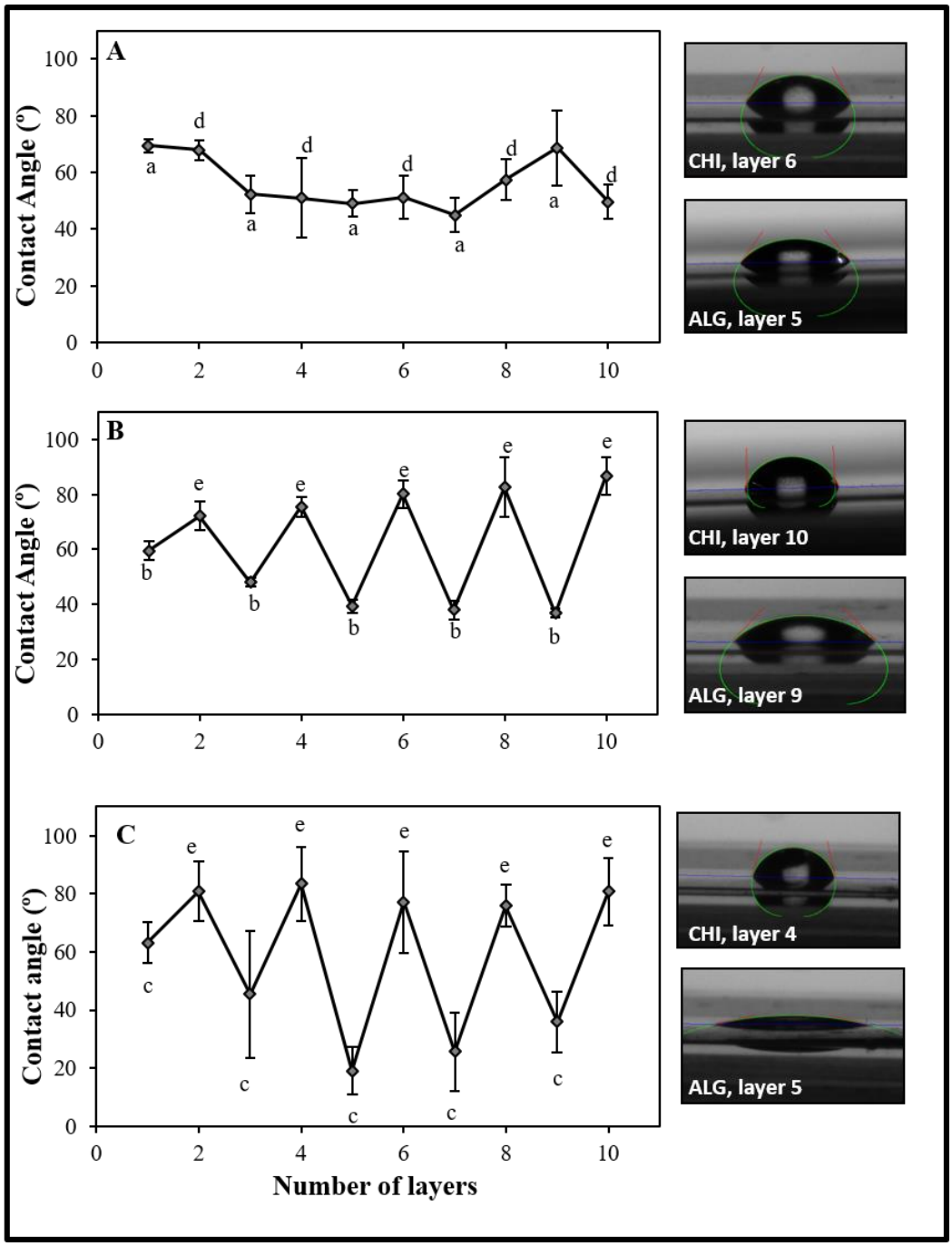

Fig. 5. Water contact angle of multilayer nanofilms assembled from polysaccharides with different electrical charge (A) *high*, (B) *medium*, and (C) *low*, according to Table 1. Different letters means significant differences between layers ($p < 0.05$).

In thicker layers, the surface composition is rich in the last polysaccharide adsorbed and the chain segments of the outermost layer dominate the film

wetting properties.[31,38] Thus, water contact angles observed in this study are strongly related with the differences in the amount of polyanion/polycation mass adsorbed during the LbL procedures. Other factors including the microstructure of multilayers might have an influence on the wettability. For example, in the work of Deng et al.,[39] the notable decrease in water contact angles of star-shaped supramolecule-deposited surface regarding to pristine polymeric surface coated by multilayers was attributed to a greater porosity of the first-mentioned surface, thus increasing its hydrophilicity.

On the other hand, contact angles of the outermost layers (CHI) increased as the electrical charge decreased, indicating an increase in surface hydrophobicity. Similarly, when the outermost layer was ALG significant differences were observed among assemblies at *low*, *medium,* or *high* electrical charge ($p < 0.05$). Contact angles tended to decrease as the polysaccharide electrical charge decreased, indicating that film surface increased their water affinity. These results indicate that the outermost layer and the thickness of the individual layers govern the wettability of multilayer nanofilms. This has important implications in the food sector, since multilayer nanofilms can be designed to provide strong hydrophobic properties in the case of dry food products sensitive to moisture effects, whereas hydrophilic multilayers can be used in products that need certain water activity to maintain their freshness.

3.3. Microstructure

To study the film microstructure, multilayers fabricated from polysaccharides with *medium* electrical charge were selected, since the most uniform deposition was observed based on previous analyses of absorbance, SZP and contact angles. Fig. 6A shows the uncoated PET substrate, where the surface present a smooth appearance. However, the micrographs taken after the coating of PET with ten layers reveal the presence of a thin film, thus confirming the formation of multilayers by the layer-by-layer method. According to the image in Fig. 6B, multilayer nanofilms present film thickness of 297 nm in ten layers. The structure shows an appreciably grainy appearance. Additionally, the cross section of nanofilms (Fig. 6C) reveals that layers present a solid structure, but it is not possible to distinguish a nanolayered structure. The topography of the 10-layer nanofilm was also

evaluated (Fig. 6D). The film surface was characterized by the presence of small clusters with a globule-like appearance connected between them, probably due to formation of polyelectrolyte complexes of ALG/CHI onto the surface during the LbL assembly process.[8]

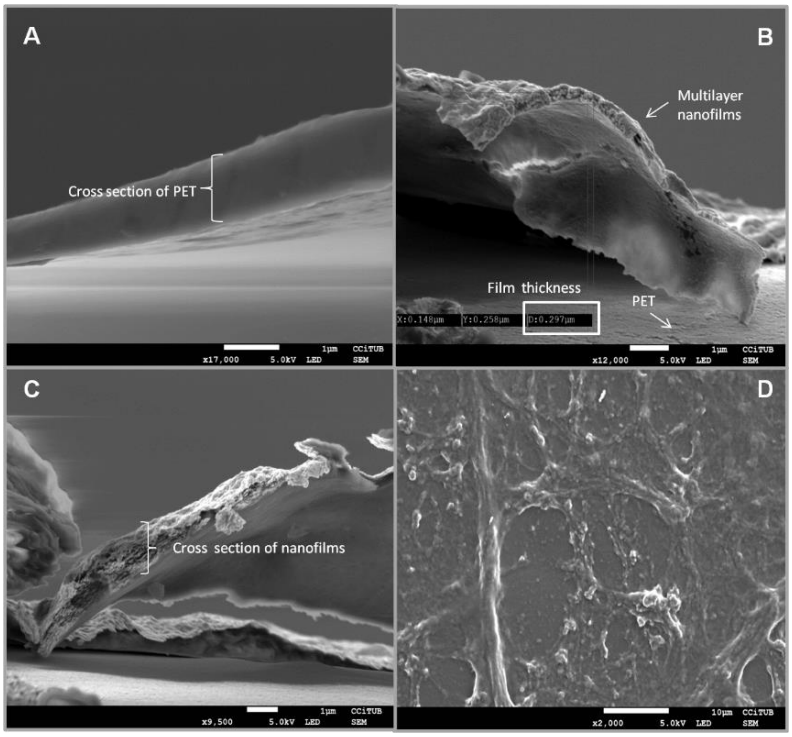

Fig. 6. SEM images obtained from multilayers formed from ALG and CHI solutions at *medium* electrical charge. (A) Cross-sectional view of PET without coating. (B) 10-layer nanofilms formed onto PET, film thickness = 297 nm. (C) Cross section of multilayer nanofilms. (D) The topography of films at x2000.

3.4. Thermal properties

Thermal properties were evaluated in assemblies formed with *medium* charge polysaccharides considering the same criteria used for SEM analyses. Thermograms of uncoated and coated PET containing 10-layer nanofilms are presented in Fig. 7. The thermal profile of PET coated by the alginate and chitosan multilayers showed a similar behavior regarding to uncoated PET. The glass transition temperature (T_g) and melting temperature (T_m) were 78 ºC and 257 ºC; whereas the T_g and T_m found for uncoated PET was 78 ºC and 255 ºC, respectively. The latter results of uncoated PET are in good agreement with those reported by other authors.[40–42] The presence of multilayers on the PET film did not significantly affect the T_g and T_m obtained

in the DSC analysis, probably due to differences in the mass ratio between the PET film and multilayer nanofilms, predominating the PET thermal properties. The glass transition temperature is reversible and occurs when an amorphous material is heated or cooled in a certain temperature range. Furthermore, the melting temperature is the point where the material changes from solid to liquid phase due to an increase in molecular mobility.[43] These thermal properties are especially relevant from a practical point of view in materials coated with biopolymer-based multilayers because they greatly determine the mechanical behavior of the material.

Moreover, the melting enthalpy (ΔH_m) of coated PET with multilayers slightly increased compared to the melting enthalpy of uncoated PET. This could be related to the ability of multilayers of acting as barrier to the diffusion of gases originated by the thermal degradation process, from the bulk to the surface of the film, contributing to slow down the polymer degradation.[44] In addition, the surface modification by the carboxylic groups and amino groups from CHI and ALG, or an increase in the polymer crystallinity may have a contribution to the enthalpy changes, as it was previously discussed in the thermal properties of PET coated with five multilayers of alginate and chitosan.[45]

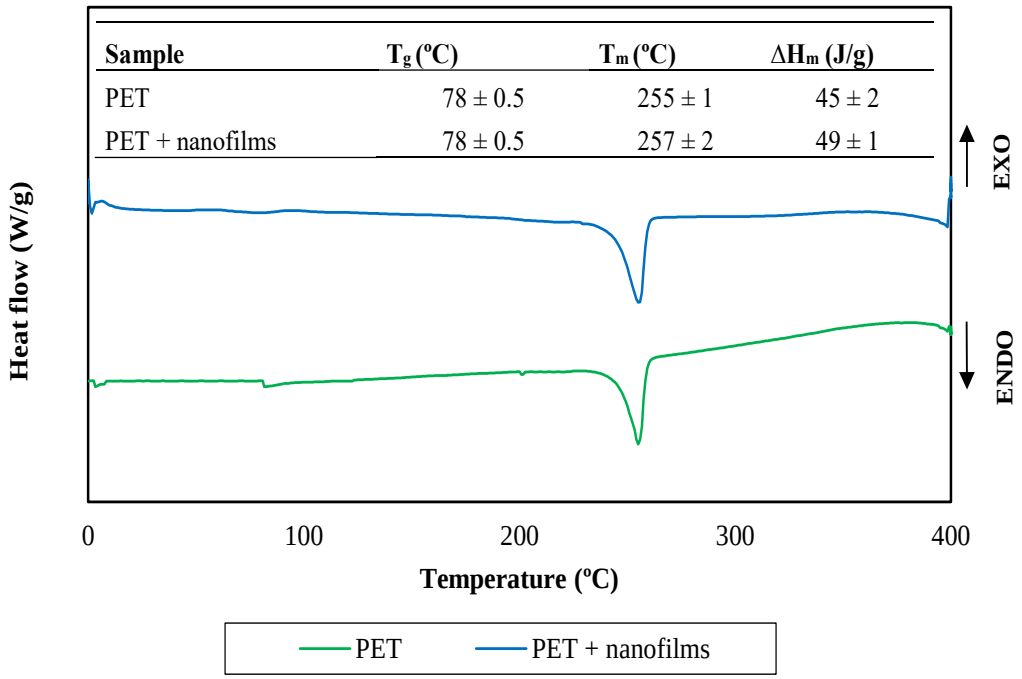

Fig. 7. DSC thermograms and thermal properties of PET uncoated and PET coated with $(ALG\text{-}CHI)_5$ multilayer nanofilms formed from *medium* charged biopolymers, according to Table 1.

4. Conclusions

The effect of the electrical charge of ALG and CHI on the formation of multilayer nanofilms was investigated. A linear growth type was characteristic of nanofilms assembled from highly charged ALG and CHI layers, however, as the polysaccharides charge diminished nanofilms exhibited an exponential growth type, which was associated with the different electrostatic and nonelectrostratic interactions between polysaccharides under the pH conditions selected in this study. The amount of material adsorbed substantially increased when *low* charge polysaccharides were used, and conversely, mass adsorption was lower when the polysaccharides were fully charged. SZP of multilayers switched from negative (in ALG layers) to positive (in CHI layers), confirming the LbL deposition. Differences in SZP with regard to the charge of polysaccharides were also found. Wetting properties were affected by the electrical charge of ALG and CHI. A correlation between the water contact angles and the amount of material absorbed was observed. From these results, it can be concluded that the buildup of multilayers can be easily modulated by controlling the electrical charge of the oppositely charged polysaccharides to reach specific properties. In addition, this study provides valuable knowledge for the rational selection of the experimental conditions needed to obtain multilayers from food-grade ingredients, and could represent a starting point for further applications in food products.

5. Acknowledgments

This research was supported by the Ministerio de Ciencia e Innovación (Spain) throughout projects ALG2009-11475. A.A.-F. also thanks the University of Lleida for the pre-doctoral grant. O.M.-B. acknowledges to the Institució Catalana de Recerca I Estudis Avançats (ICREA) for the Academia 2008 Award.

6. References

(1) Guzey, D.; McClements, D. J. Adv. Colloid Interface Sci. 2006, 128, 227–248.

(2) Weiss, J.; Takhistov, P.; McClements, D. J.; Brunswick, N. J. Food Sci. 2006, 71, R107–R116.

(3) Fabra, M. J.; Busolo, M. A.; Lopez-Rubio, A.; Lagaron, J. M. Trends Food Sci. Technol. 2013, 31, 79–87.

(4) De Villiers, M. M.; Otto, D. P.; Strydom, S. J.; Lvov, Y. M. Adv. Drug Deliv. Rev. 2011, 63, 701–715.

(5) Decher, G. Science. 1997, 277, 1232–1237.

(6) Pawar, S. N.; Edgar, K. J. Biomaterials 2012, 33, 3279–3305.

(7) Lawrie, G.; Keen, I.; Drew, B.; Chandler-Temple, A.; Rintoul, L.; Fredericks, P.; Grøndahl, L. Biomacromolecules 2007, 8, 2533–2541.

(8) Sæther, H. V.; Holme, H. K.; Maurstad, G.; Smidsrød, O.; Stokke, B. T. Carbohydr. Polym. 2008, 74, 813–821.

(9) Klitzing, R. V. Phys. Chem. Chem. Phys. 2006, 8, 5012–5033.

(10) Alves, N. M.; Picart, C.; Mano, J. F. Macromol. Biosci. 2009, 9, 776–785.

(11) Yuan, W.; Dong, H.; Li, C. M.; Cui, X.; Yu, L.; Lu, Z.; Zhou, Q. Langmuir 2007, 23, 13046–13052.

(12) Caridade, S. G.; Monge, C.; Gilde, F.; Boudou, T.; Mano, J. F.; Picart, C. Biomacromolecules 2013, 14, 1653–1660.

(13) Lukomska, J.; Malicka, J.; Gryczynski, I.; Lakowicz, J. R. J. Fluoresc. 2004, 14, 417–423.

(14) Bech, L.; Meylheuc, T.; Lepoittevin, B.; Roger, P. J. Polym. Sci. Part A Polym. Chem. 2007, 45, 2172–2183.

(15) Irena, G.; Jolanta, B.; Karolina, Z. Appl. Surf. Sci. 2009, 255, 8293–8298.

(16) Choi, J.; Rubner, M. F. Macromolecules 2005, 38, 116–124.

(17) Lavalle, P.; Voegel, J.-C.; Vautier, D.; Senger, B.; Schaaf, P.; Ball, V. Adv. Mater. 2011, 23, 1191–1221.

(18) Shiratori, S. S.; Rubner, M. F. Macromolecules 2000, 33, 4213–4219.

(19) Vidyasagar, A.; Sung, C.; Losensky, K.; Lutkenhaus, J. L. Macromolecules 2012, 45, 9169–9176.

(20) Pargaonkar, N.; Lvov, Y. M.; Li, N.; Steenekamp, J. H.; de Villiers, M. M. Pharm. Res. 2005, 22, 826–835.

(21) Ai, H.; Jones, S. A.; de Villiers, M. M.; Lvov, Y. M. J. Control. Release 2003, 86, 59–68.

(22) Picart, C. Curr. Med. Chem. 2008, 15, 685–697.

(23) Crouzier, T.; Boudou, T.; Picart, C. Curr. Opin. Colloid Interface Sci. 2010, 15, 417–426.

(24) Xu, J.; Yang, L.; Hu, X.; Xu, S.; Wang, J.; Feng, S. Soft Matter 2015, 11, 1794–1799.

(25) Bieker, P.; Schönhoff, M. Macromolecules 2010, 43, 5052–5059.

(26) Kirby, B. J.; Hasselbrink, E. F. Electrophoresis 2004, 25, 203–213.

(27) Junka, K.; Sundman, O.; Salmi, J.; Osterberg, M.; Laine, J. Carbohydr. Polym. 2014, 108, 34–40.

(28) Schoeler, B.; Sharpe, S.; Hatton, T. A.; Caruso, F. Langmuir 2004, 20, 2730–2738.

(29) Salehi, A.; Desai, P. S.; Li, J.; Steele, C. A.; Larson, R. G. Macromolecules 2015, 48, 400–409.

(30) Richert, L.; Lavalle, P.; Payan, E.; Shu, X. Z.; Prestwich, G. D.; Stoltz, J.-F.; Schaaf, P.; Voegel, J.-C.; Picart, C. Langmuir 2004, 20, 448–458.

(31) Ladam, G.; Schaad, P.; Voegel, J. C.; Schaaf, P.; Decher, G.; Cuisinier, F. Langmuir 2000, 16, 1249–1255.

(32) Zhang, J.; Senger, B.; Vautier, D.; Picart, C.; Schaaf, P.; Voegel, J.-C.; Lavalle, P. Biomaterials 2005, 26, 3353–3361.

(33) Allen, K. W. Contact angle, wettability and adhesion. International Journal of Adhesion and Adhesives, 1994, 14, 69.

(34) Kwok, D. Y.; Neumann, A. W. Adv. Colloid Interface Sci. 1999, 81, 167–249.

(35) Wu, T.; Sun, Y.; Li, N.; de Villiers, M. M.; Yu, L. Langmuir 2007, 23, 5148–5153.

(36) Almodóvar, J.; Place, L. W.; Gogolski, J.; Erickson, K.; Kipper, M. J. Biomacromolecules 2011, 12, 2755–2765.

(37) Fu, J.; Ji, J.; Yuan, W.; Shen, J. Biomaterials 2005, 26, 6684–6692.

(38) Yoo, D.; Shiratori, S. S.; Rubner, M. F. Macromolecules 1998, 31, 4309–4318.

(39) Deng, J.; Liu, X.; Ma, L.; Cheng, C.; Shi, W.; Nie, C.; Zhao, C. ACS Appl. Mater. Interfaces 2014, 6, 21603–21614.

(40) De Oliveira Santos, R. P.; Castro, D. O.; Ruvolo-Filho, A. C.; Frollini, E. J. Appl. Polym. Sci. 2014, 131, 40386.

(41) Grant, C. A.; Alfouzan, A.; Gough, T.; Twigg, P. C.; Coates, P. D. Micron 2013, 44, 174–178.

(42) Lee, C. S.; Yoon, K. H.; Park, J. C.; Kim, H.-U.; Park, Y.-B. Fibers Polym. 2014, 15, 1493–1499.

(43) Braun, D.; Cherdron, H.; Ritter, H. Polymer Synthesis: Theory and Practice: Fundamentals, Methods, Experiments; Springer Science & Business Media, 2013.

(44) Ayhan, Z.; Cimmino, S.; Esturk, O.; Duraccio, D.; Pezzuto, M.; Silvestre, C. Packag. Technol. Sci. 2015, 28, 589–602.

(45) Carneiro-da-Cunha, M. G.; Cerqueira, M. A.; Souza, B. W. S. S.; Carvalho, S.; Quintas, M. A. C. C.; Teixeira, J. A.; Vicente, A. A. Carbohydr. Polym. 2010, 82, 153–159.

CHAPTER VI: *PHOTO-PROTECTION AND CONTROLLED RELEASE OF FOLIC ACID USING FOOD-GRADE ALGINATE/CHITOSAN NANOLAMINATES*

Acevedo-Fani, A., Soliva-Fortuny, R., & Martín-Belloso, O

Colloids and Interfaces B: Biointerfaces (sent)

ABSTRACT

The formation, characterization, photo-protective properties and release profiles of folic acid-loaded nanolaminated films were investigated by UV-visible spectroscopy, FTIR, Raman and SEM microscopy. Food-grade alginate/chitosan nanolaminates were obtained by the layer-by-layer technique and folic acid (FA) was encapsulated by post-diffusion. The amount of FA loaded within nanolaminates increased as a function of the FA concentration and immersion time of adsorbing solutions. The maximum loading in nanolaminates was reached using FA solutions at 10 mg/mL for 30 min (54.4 μg/cm^2), or 12.5 mg/mL for 120 min (≈ 70 μg/cm^2). Nanolaminates containing FA were more stable under ultraviolet light exposure than non-encapsulated FA. The rate and concentration of FA released from nanolaminates were greater at buffer pH 7 than at pH 3, which might play a key role in the delivery and bioavailability of nutraceuticals. These results provide important information for the design of nanolaminates containing hydrophilic active compounds for food applications.

Keywords: nanolaminates, layer-by-layer, folic acid, nutraceuticals, delivery systems, edible films, controlled release, photo-stability.

1. Introduction

Folic acid is a water soluble vitamin of the group B, essential for human health that has to be obtained through diet or supplementation. The use of folic acid in food fortification is widely extended due to its better stability and bioavailability, compared to naturally occurring folates [1]. This micronutrient plays a crucial co-factor role in one-carbon metabolism, participating in the formation of DNA and maintaining the rate of cell division. Research works support that an inadequate folate status increases the risk of neural tube birth defects (such as spina bifida), megaloblastic anemia, cardiovascular diseases and some types of cancer [2,3]. Absorption of folates mainly occurs in the small intestine, where the proton-coupled folate transporter allows the pass across epithelium cells. Then, folates are metabolized into the polyglutamate form in the liver in order to be used by cells, stored or released into the blood system [4].

Chemically, folic acid consists of a pteridine ring bound to a *para*-aminobenzoic acid with a glutamate tail. It has been reported that folic acid is highly soluble and stable in alkaline solutions [5]. However, the degradation of the folic acid molecule takes place during the UV light exposure, causing the breakdown of the structure into a pteridine ring and a *p*-aminobenzoic acid linked to the polyglutamate tail. This photoproducts have been found to be biologically inactive [1]. This means that the incorporation of folic acid into foodstuffs is restricted to certain applications, and generally, large concentrations have to be used in foods in order to assure a health-promoting effect. Therefore, the use of effective delivery systems able to encapsulate, protect and transport nutraceuticals into food products may be a favorable alternative to improve their physicochemical stability and it would allow a more rational use of food ingredients.

Over the past few years, there has been paid great attention to the application of the layer-by-layer assembly technique with promising applications in the pharmaceutical, biomedical and food packaging field [6,7]. The assembly technique is a simple and effective strategy to functionalize any type of substrate including food surfaces or food contact materials. Most common applications in foods are in highly perishable foods to extend the shelf life [8,9], or in smart active packaging [10]. Nanolaminates can be defined as very thin

films formed by the alternate electrostatic deposition of oppositely charged polyelectrolytes (e.g. polysaccharides or proteins) on a charged substrate [11,12]. The driven forces governing the layer-by-layer assembly is the charge reversal occurring in the surface's substrate after the adsorption of anionic or cationic polyelectrolytes [13]. Among the most interesting advantages of nanolaminates is the possibility of fine-tune the final properties and film thickness by controlling aspects such as the number of layers deposited, the type of polyelectrolyte, the adsorbing solution conditions, or the terminal layer composition [14]. On the other hand, nanolaminates might be used for encapsulation and delivery of active food ingredients including, nutraceutical compounds, antimicrobials, antioxidants, anti-browning agents, enzymes, flavors or colorants, to the foods surface [11]. Importantly, the rate of encapsulated ingredients release from nanolaminates may be controlled by changing external triggers conditions such as pH, ionic strength or temperature [15,16], which is particularly useful for achieving the release of the active ingredient to the targeted site.

Alginate is a copolymer of 1→4 linked *β*-D-mannuronic acid and α-L-guluronic acid residues obtained from marine brown algae. In the presence of divalent cations (e.g. Ca^{+2}), alginates form hydrogels induced by ionic crosslinking [17,18]. Among the features ascribed to alginates are thickening, gelling and film-forming properties. They also behave as anionic polyelectrolytes in aqueous media owing to the ionizable carboxyl groups located in the backbone. Chitosan, a cationic linear polymer composed of β-(1−4)-2-acetamido-D-glucose and β-(1−4)-2-amino-D-glucose units, is the deacetylated form of chitin, which is mostly extracted from the exoskeleton of crustaceans and fungal wall cells [19]. The importance of chitosan in the food industry lies on the antimicrobial, antioxidant, oxygen barrier and thickening properties [20]. It has been extensively used in edible films and coatings as well [21] The solubility of chitosan occurs in acidic media, where amino groups are protonated and the polysaccharide is converted into a cationic polyelectrolyte [22]. Nanolaminates assembled from food-grade alginate and chitosan was demonstrated in a previous study released from our group [23]. This systems might be also a suitable alternative to encapsulate hydrophilic nutraceuticals, such as folic acid, envisaged to be applied on food matrices that need to be enriched or fortified. The assessment of the loading and release process of the active ingredient from nanolaminates using a substrate

can give a close approximation of their behavior in real foods. As far as we are concerned, the encapsulation of hydrophilic nutraceuticals into food-grade nanolaminates have not been study so far. Therefore, the objective of this research work was to form and characterize alginate/chitosan nanolaminates containing folic acid and to evaluate their loading and release behavior, as well as their ability to protect the encapsulated ingredient from degradation under stressing conditions, such as UV lighting.

2. Materials and methods

2.1. Materials

Sodium alginate Manucol® DH was purchased from FMC Biopolymers Ltd. (Scotland, U.K.). Chitosan of high molecular weight with deacetylate degree > 75%, and powdered folic acid (FA) were obtained from Sigma Aldrich (Steinheim, Germany). Lactic acid (80–90%) and sodium hydroxide (NaOH) were purchased from Sharlau Chemie (Barcelona, Spain). Sodium chloride (NaCl) was obtained from Afora (Barcelona, Spain). Film substrates, Quartz slides (Suprasil® 300) and polyethylene terephthalate (PET) sheets (6 x 2 cm) were obtained from Hellma Analytics (Müllhein, Germany) and Isovolta (Barcelona, Spain), respectively. All solutions were prepared with deionized water obtained from a Milli-Q system (18,2 mΩ, Millipore).

2.2. Preparation of polysaccharide solutions

Alginate solutions were prepared by dissolving 0.5% w/v of powdered sodium alginate in deionized water overnight to ensure complete hindrance. Chitosan, at 0.5% w/v was dissolved in lactic acid solution (1% v/v) by stirring overnight. Then, both polysaccharide solutions were mixed with the amount of NaCl required to reach a concentration of 0.2 M. Finally, alginate and chitosan solutions were adjusted to pH 5 and 4, respectively, using 1 M of lactic acid or NaOH. These parameters were set out from preliminary experiments that proved the successful formation of nanolaminates by electrostatic interactions. Rinse solutions consisted of 0.2 M NaCl solutions at pH 5 (for alginate) or 4 (for chitosan).

2.3. Alginate/chitosan nanolaminates buildup

First, the surface of PET sheets and quartz slides was positively charged by aminolysis, following the procedure described in a previous work [23]. For the layer-by-layer buildup, positively charged substrates were firstly dipped in anionic alginate solution for 10 min. This was followed by two washing steps with water for 2 min, to remove the excess of unbound polysaccharide chains. The pH and ionic strength of washing solutions matched with the previous polysaccharide solution. Negatively charged substrates were further submerged in cationic chitosan solutions for 10 min, and then washed twice with water at the same solution conditions of the previous polysaccharide. All solutions remained under agitation at 30 rpm. This procedure was repeated alternating the polysaccharides deposition to a final number of 20 layers. The resulting nanolaminates were then dried at room temperature (25ºC) and stored in a desiccator with silica.

The buildup of alginate/chitosan layers in quartz slides was monitored using a V-670 UV-visible-NIR spectrophotometer (Jasco Corporation, Tokyo, Japan) containing a film holder accessory (FLH-740, Jasco Corporation, Tokyo, Japan). Absorbance spectra of quartz slides were collected after deposition of a pair of layers. Infrared spectroscopy (FTIR) was used to assess the presence of alginate and chitosan functional groups in the coated PET sheets. Spectra were collected on a FT/IR-6600 spectrophotometer (Jasco Corporation, Tokyo, Japan) fitted with an ATR cell. All measurements were performed in triplicate.

2.4. Loading of folic acid to nanolaminates

The FA loading into nanolaminates was performed using the post-diffusion method, as described in a previous study for drug loading in layer-by-layer assemblies [24]. To study the effect of the solution concentration on the FA loaded to nanolaminates, coated quartz slides were submerged in FA solutions at different concentrations (1-12.5 mg/mL) during 30 min, and then washed with water to remove the compound excess on the surface. Samples were dried at room temperature. The loading process of FA to nanolaminates was confirmed by measuring the absorbance in the UV-Visible range. To determine the total FA loading, samples were sonicated in a pH 9 phosphate buffer solution for 30 min. This procedure was repeated until absorption peaks

of FA disappeared from spectra. Absorbance of sonicated solutions (with the FA extracted from nanolaminates) was measured at 364 nm, and the concentration of FA was calculated from a calibration curve (0.5-10 μg/mL - R^2 0.995126). The effect of immersion time on the loading process of FA to nanolaminates was carried out dipping coated substrates in FA solutions at a fixed concentration (12.5 mg/mL) for different times (1-240 min). The total FA loading was analyzed following the above-mentioned procedure. Measurements were carried out in triplicate.

2.5. Release of folic acid from nanolaminates

The release profiles of FA from nanolaminates were assessed using a modified method previously reported by other authors [25]. Nanolaminates assembled in PET sheets (0.7 x 2 cm) were loaded in 12.5 mg/mL FA solutions for 30 min for the release experiments. Each PET sheet was immersed in 2 ml of phosphate-citrate buffer solutions at pH 3 or 7, for 7 h at 37ºC. These pH values were selected in order to mimic the alkaline and acid conditions in the gastrointestinal tract. At predetermined times, buffer solutions were removed and stored in ice under darkness for further analysis, and 2 ml of fresh buffer were added. The buffer solutions containing FA released at pH 7 were directly analyzed by UV-visible spectroscopy at 347 nm. The buffer solutions with FA released at pH 3 were adjusted to pH 7 using 1.2 ml of 1 M sodium phosphate, and absorbance was then measured at 347 nm. The FA concentration released at each time was quantified through a calibration curve of FA solutions at pH 7 (0.5-10 μg/mL - R^2 0.991046). Each sample extracted from a vial represents the FA released from nanolaminates at a particular time rather than a cumulative amount released during the entire release period. Measurements were performed in triplicate.

2.6. Photo-stability of folic acid-loaded nanolaminates

The stability of FA encapsulated into nanolaminates was evaluated under UV lighting exposure using a method previously published, with some modifications [26]. PET sheets (0.7 x 2 cm) coated by FA-loaded nanolaminates (FA concentration ≈ 91 μg/ml) and FA solutions (91 μg/ml) at pH 9 were placed below an UV light lamp (Osram Ultra-vitalux, 300 W) for 120 min, to accelerate folic acid degradation. The distance between lamp and

samples was 20.5 cm. At certain irradiation times, FA-loaded nanolaminates were taken off from the lamp and submerged in 2 ml of phosphate buffer solution pH 9. Samples were sonicated for 30 min at room temperature. Degradation of folic acid was determined by changes in absorbance spectra of FA solutions using a UV-Visible-NIR spectrophotometer (Jasco Corporation, Tokyo, Japan). Measurements were carried out in triplicate.

2.7. Microstructure

Microstructural examinations were performed using a J-6510 Scanning Electron Microscope (JEOL Ltd., Tokyo, Japan). PET sheets coated by nanolaminates were placed on aluminum stubs and treated with carbon prior to microscopic observations. Samples were analyzed with an acceleration voltage of 5 kV.

2.8. Raman Analysis

Micro-Raman determinations of powdered FA and FA-loaded nanolaminates were carried out in a Jobin-Yvon LabRam H800 system (HORIBA Scientific, Kyoto, Japan), equipped with an Olympus BXFM optical microscope (objective 50x) and a CCD detector cooled at -70 ºC. The excitation source was a diode laser at 785 nm. The focused laser beam diameter was about 2 μm and the spectral resolution 2.5 cm^{-1}. Measurements were performed in duplicate.

2.9. Statistical analysis

One-way analysis of variance (ANOVA) was performed using the statistical and graphing software SigmaPlot 11.0 Windows package (Systat software Inc.). The Holm-Sidak method was applied to determine significant differences among mean values at 5% of significance level. All results are presented as the average results and standard deviations.

3. Results and discussion

3.1. Alginate/chitosan nanolaminates buildup

The layer-by-layer assembly of polysaccharide layers on quartz slides are shown in Fig. 1. Absorbance was measured in every bilayer since chitosan

has two chromophore groups (*N*-acetyl-glucosamine and glucosamine residues) in the far-UV region [27]. The optical density increased with the number of assemblies, suggesting that the amount of material adsorbed was proportional to the number of layers. This confirmed the successful formation of alginate/chitosan nanolaminates. Interestingly, spectra did not exhibit any absorption peak from the second to the eighth layer, whereas a further increase in the number of layers revealed a peak at 195 nm that corresponded to *N*-acetyl-glucosamine and glucosamine. It is likely that the concentration of these molecules in nanolaminates was below the limit of detection in assemblies of less than twelve layers, thus explaining the absence of adsorption peaks.

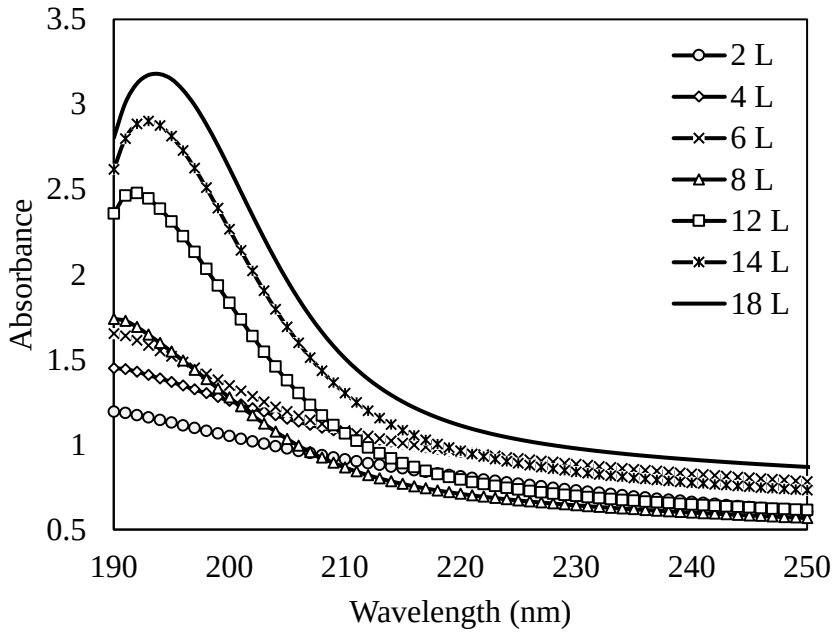

Fig. 1. UV spectra of alginate-chitosan nanolaminates as a function of the number of deposited layers (L).

On the other hand, the formation of nanolaminates on PET sheets was also confirmed by infrared spectroscopy (Fig. 2). The bands observed in PET spectra were in good agreement with results previously reported by other authors, where polyesters have three intense bands [28]. These bands were located at 1721 cm^{-1}, 1245 cm^{-1} and 1100 cm^{-1}, owing to the C=O, C-C-O and O-C-C stretching vibrations of aromatic ester groups, respectively. After assembling alginate and chitosan layers on PET sheets, these bands disappeared resulting in new ones mostly located at the fingerprint zone. For instance, the band at 1410 cm^{-1} corresponds to the symmetric stretching

vibrations of carboxyl (COO^-) groups of alginate molecules [29]. Two intense bands characteristics of the skeletal vibrations of saccharine rings in both chitosan and alginate molecules were observed at 1030 cm^{-1} and 1080 cm^{-1}, corresponding to C-O and C-O-C asymmetric stretching vibrations, respectively [30,31]. Some distinctive bands of chitosan were also found in nanolaminates spectrum. Bands at 1650 cm^{-1} (N-H-C=O stretching vibrations of amide I), 1515 cm^{-1} (amide II stretching, N-H bending vibrations or symmetric NH_3^+ deformation) and 1150 cm^{-1} (asymmetric C-O-C and C-N stretching vibrations) were particular of chitosan molecules [32]. Changes in the PET infrared spectra containing the alginate/chitosan assemblies indicated the surface modification of the substrate, and hence the presence of nanolaminates.

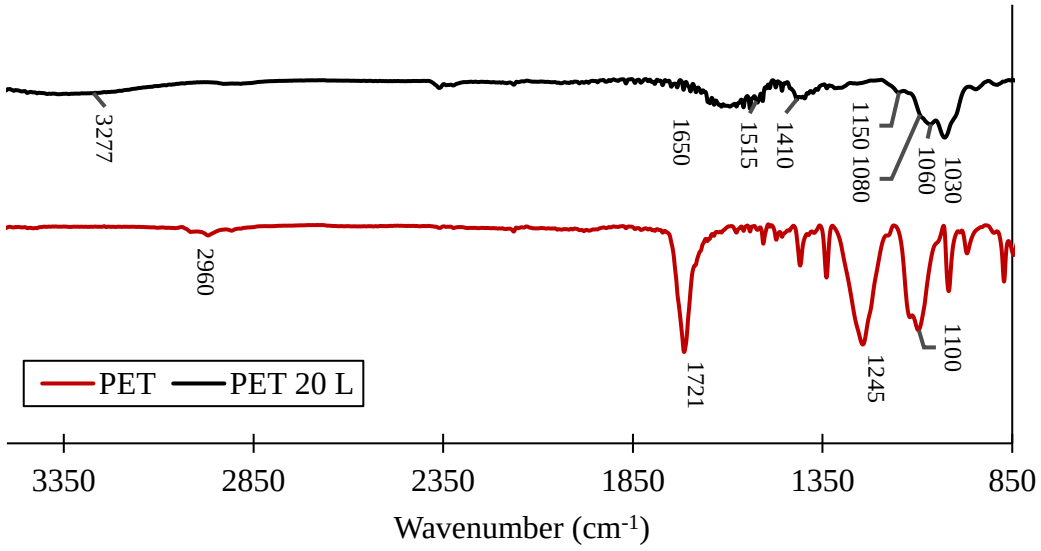

Fig. 2. Infrared spectra of bare PET sheets (PET) and PET coated by alginate-chitosan nanolaminates of 20 layers (PET 20 L).

3.2. Loading capacity of folic acid in nanolaminates

The encapsulation of FA molecules into nanolaminates was carried out by post-diffusion. UV-visible spectra of alginate/chitosan assemblies before and after FA encapsulation are shown in Fig. 3. Inset plot presents the UV-visible spectrum of a FA solution at pH 9. Before submerging nanolaminates in FA solutions, a single absorption peak at 195 nm was observed corresponding to chitosan molecules. After FA was loaded in nanolaminates, two new absorption peaks were observed at 295 nm and 373 nm. These peaks were distinctive of the FA solution, but appeared at 283 nm and 364 nm due to the

presence of the heteroaromatic pterine chromophore, as reported previously by other authors [5,33]. New peaks in the spectrum indicated the presence of FA and the swift toward greater wavelength might be probably ascribed to the presence of FA aggregates formed in nanolaminates during drying [34]. After FA loading process, nanolaminates became yellowish and this color remained even after numerous washes with water, which suggest that FA was encapsulated.

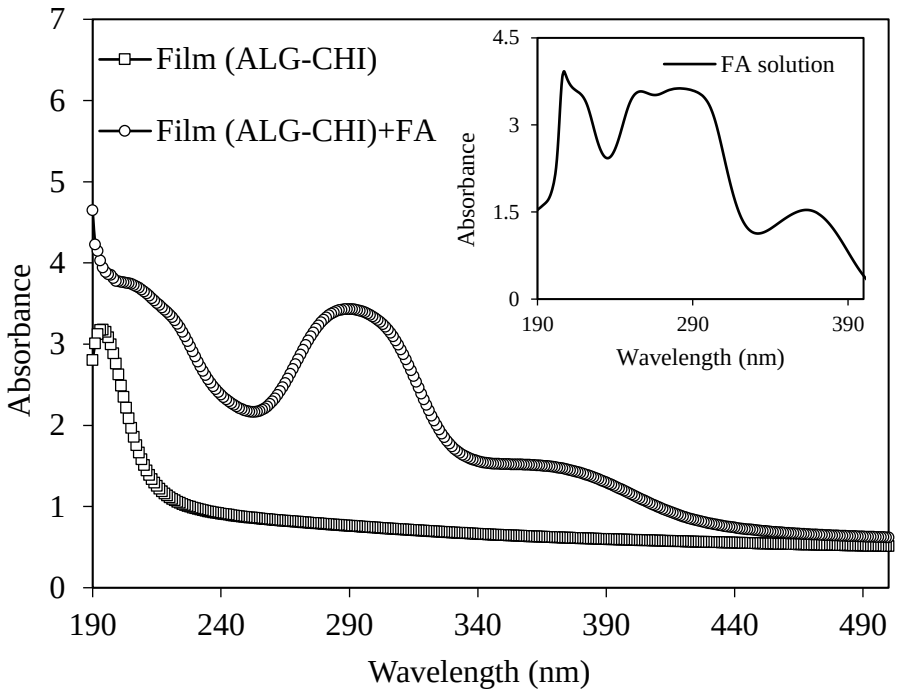

Fig. 3. UV-visible spectra of 20-layer alginate-chitosan nanolaminates before and after FA encapsulation, using loading solutions at 5 mg/mL. Inset plot corresponds to the absorbance spectrum of FA solution at pH 9.

The loading process of small molecules (e.g. folic acid) to layer-by-layer assemblies is governed by a number of intrinsic properties, including the degree of swelling, hydrophilic/hydrophobic balance, dissociation constants, surface charge density and pore size of nanolaminates. Properties of small molecules, such as size, charge and hydrophilicity play an important role [35]. In this study, encapsulation of FA was performed under alkaline conditions (buffer pH 9). In this environment, free amino groups in chitosan chains are less ionized ($pK_a \approx 6.3$) within the nanolaminated structure, whereas the carboxyl groups in alginate molecules have a strong electrical charge ($pK_a \approx 3.65$). Moreover, FA molecules behave as weak acids in alkaline solutions, having a negative charge (ζ-potential ≈ -34 mV, pH 9). Therefore, it

was postulated that the mechanism of FA loading may have been governed by hydrogen bounding rather than ionic crosslinking between the active compound and polysaccharide layers. At alkaline conditions, there is not sufficient electrostatic interactions between cationic chitosan and anionic FA to promote ionic binding. The fact that polysaccharide-based nanolaminates have a great swelling capacity play a key role in the loading of small molecules induced by H-H bounds. The presence of a large hydrogen binding sites in nanolaminates creates more free volume for storage. This also allow small molecules moving within the structure, thus avoiding undesirable electrostatic forces and finding sites for more favorable non-electrostatic interactions [35]. In fact, a previous study have demonstrated the high swelling capacity of alginate/chitosan nanolaminates, where the film thickness in wet state can be two times greater than in dried state [36]. Thereby, the great loading capacity of FA in alginate/chitosan nanolaminates could be associated to the high degree of swelling in aqueous solutions. In concordance with this postulation, the loading mechanism of small molecules to alginate/chitosan assemblies has been previously reported using hydrophilic small drug molecules [37].

Moreover, the kinetics of FA absorption in nanolaminates were evaluated as a function of the FA concentration in loading solutions as well as the immersion time (Fig. 4). The FA concentration obtained after the complete extraction from nanolaminates is shown in Fig. 4A. When the concentration of FA in the immersion solutions was 1 mg/mL and 2.5 mg/mL, only a slight increase from 9.8 to 11.6 μg/cm^2 in the FA concentration encapsulated in nanolaminates was observed. However, a logarithmic upsurge in the concentration of encapsulated FA up to 53.3 μg/cm^2 was found when increasing the concentration of FA to 7.5 mg/mL in immersion solutions. Interestingly, when the loading process was carried out using more concentrated FA solutions, the amount of FA encapsulated did not increase significantly (54.4 μg/cm^2). Therefore, the initial concentration of the immersion solution has a remarkable impact on the final amount of active ingredient encapsulated within the nanolaminated structure.

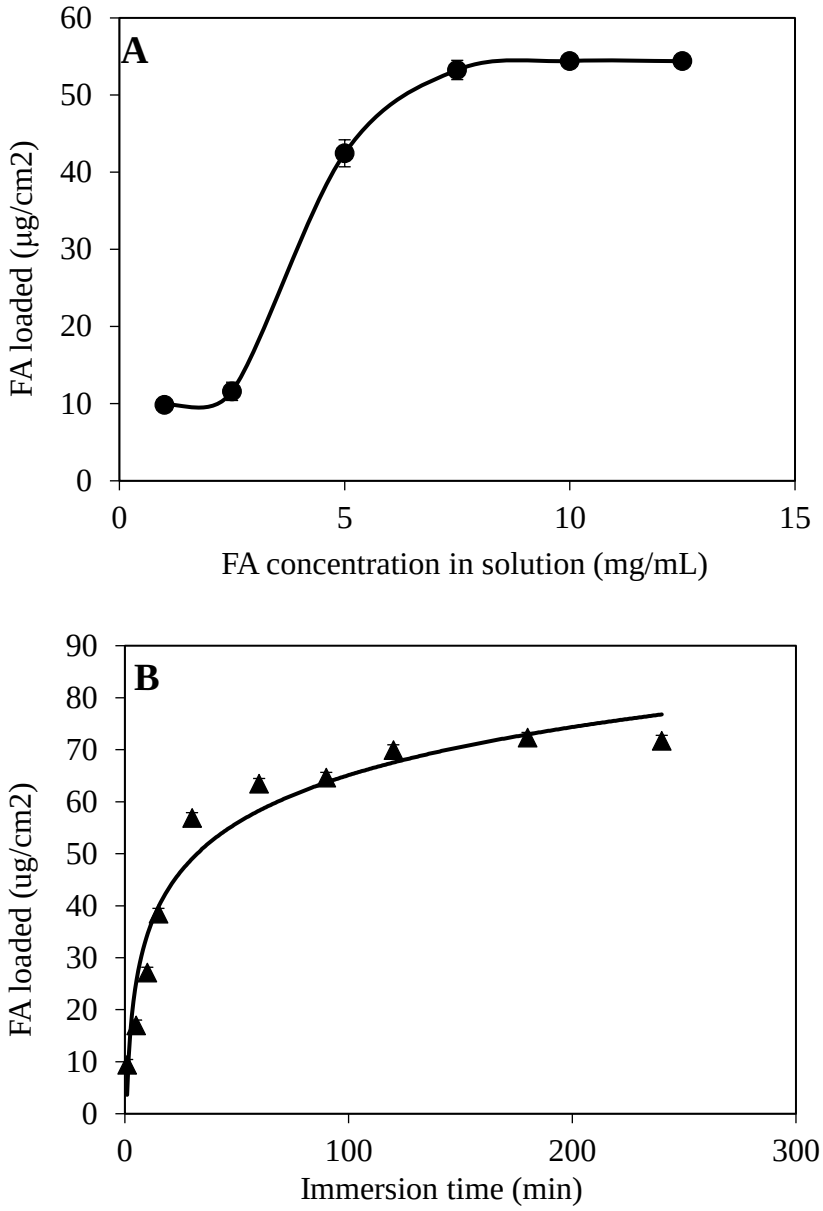

Fig. 4. (A) Effect of the concentration of FA in immersion solutions (1-12.5 mg/mL) on the final concentration of FA encapsulated into nanolaminates; and B) Effect of the immersion time (1-240 min) on FA concentration encapsulated.

The impact of increasing the immersion time in the loading capacity of nanolaminates was investigated using FA solutions with a fixed concentration (12.5 mg/mL). Results can be observed in Fig. 4B. The FA loading rate to nanolaminates exhibited a logarithmic behavior characterized by a fast rise in the FA concentration (≈ 57 µg/cm^2) during the first 30 min, and then a slow loading process reaching 70 µg/cm^2 after 120 min. The process followed a plateau until 240 min. This result indicates that the maximum loading capacity of FA to nanolaminates is achieved at 120 min.

3.3. Microstructure of nanolaminates

Changes in the morphology of alginate/chitosan assemblies incorporating FA were examined by SEM (Fig. 5). The topography dramatically changed in nanolaminates with or without FA, as shown in Fig. 5A and 5B. Nanolaminates' surface without FA exhibited a pronounced roughness, which was attributed to globular structures mostly composed of chitosan as it was the outermost layer assembled in the nanolaminates. In addition, this surface also presents uncoated zones identified by their smoother appearance that were ascribed to the alginate layer located below the outer chitosan layer. Highly irregular surfaces may contribute to increase the loading of small molecules to nanolaminates, since a rough topography has greater surface area than an even one. Hence, a large surface area results in more binding sites potentially available to encapsulate small molecules, such as FA [38]. Therefore, it is likely that the microstructure of alginate/chitosan nanolaminates may have intervened in the process of loading of folic acid.

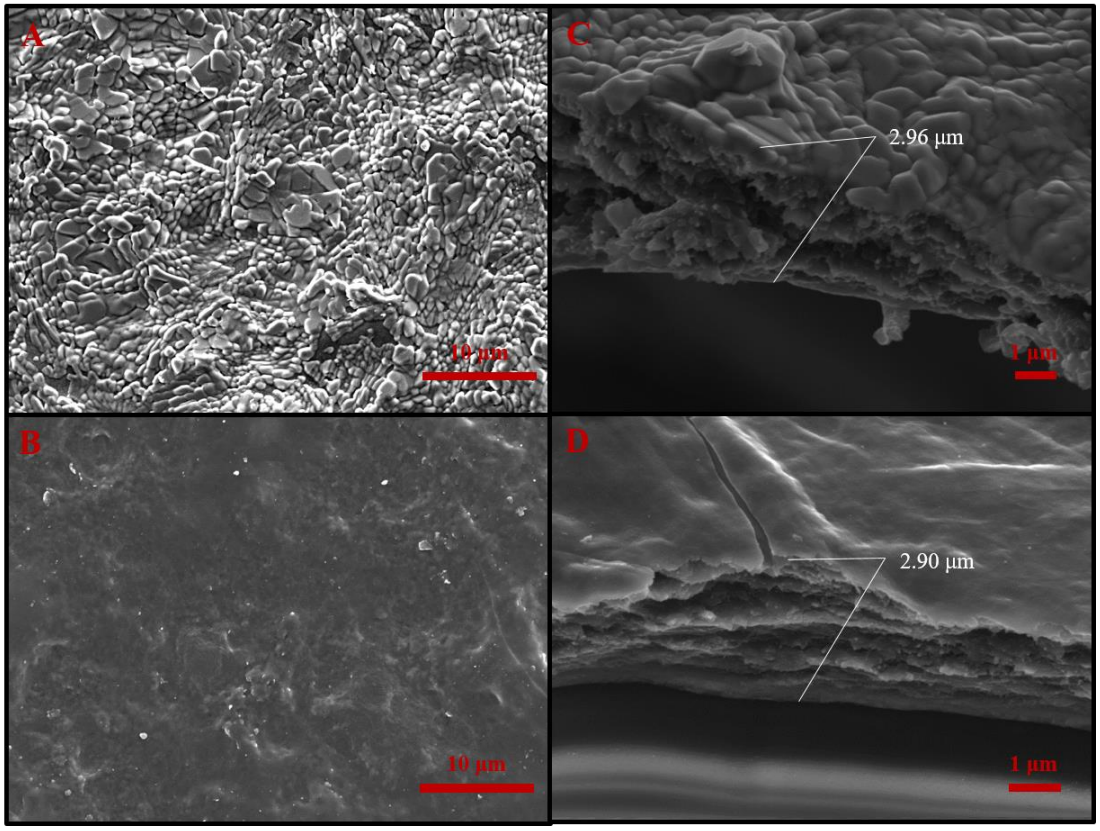

Fig. 5. A, B) Topography and C, D) cross-sectional view of alginate-chitosan nanolaminates before and after FA encapsulation.

These peculiar topography completely changed once nanolaminates were submerged in FA solutions, presenting a quite regular and smooth surface (Fig. 5B). This change suggests a molecular reorganization phenomenon provoked by the incorporation of FA in nanolaminates as well as their swelling during the loading process. SEM images also revealed a stratified structure in the internal section of nanolaminates, which was much more defined in the presence of FA (Fig. 5C and 5D). The estimated film thickness obtained was around 2.96 μm in nanolaminates without FA, whereas the incorporation of FA apparently led to a slight reduction of thickness (2.9 μm). This is reasonable considering that the overall structure of nanolaminates was more homogeneous when it contained encapsulated FA.

3.4. Raman analysis

The presence and distribution of FA along the nanolaminated structure was examined by Raman Spectroscopy and results are shown in Fig. 6A. The spectrum of alginate/chitosan nanolaminates containing FA presented a small peak at 680 nm that it was also typical in the spectrum of powdered FA. This peak was attributed to the C-N and C-C stretching vibrations of the pteridine ring and *p*-aminobenzoic acid fragment in the FA molecule, respectively [39]. Therefore, the presence of FA in alginate/chitosan assemblies could be also confirmed by this technique.

The distribution of FA along the nanolaminate structure was also studied. A cross section of a PET sheet coated by 20-layer nanolaminates that contained FA was examined by Raman spectroscopy monitoring changes in the intensity peak at 680 nm (Fig. 6B). Measurements were recorded linearly from a zero point to 1000 μm far. The measurement points were located in the middle of the nanolaminate area analyzed, in order to minimize the influence of PET in the spectrum. Results indicated that the intensity patterns scarcely changed, suggesting that FA was distributed homogeneously within nanolaminate in this particular section.

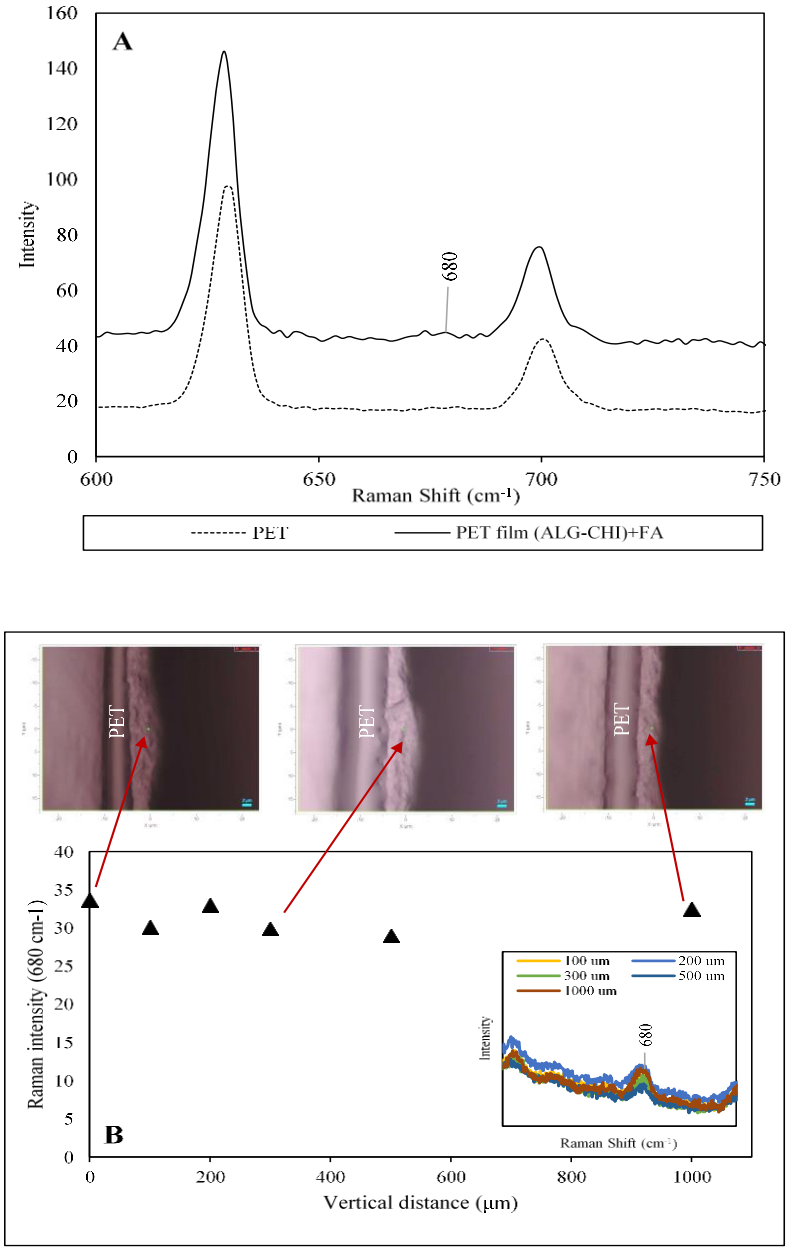

Fig. 6. A) Raman spectra of a PET sheet (PET) and PET coated by 20-layer nanolaminates containing FA. Inset plot corresponds to the Raman spectra of powdered FA. B) Changes in intensity of the FA band at 680 cm^{-1} along the cross-sectional area of nanolaminates. Inset plot indicates Raman spectra recorded in the cross-sectional area of nanolaminates at different measurement distance.

3.5. Photo-stability of the encapsulated folic acid

Fig. 7 shows absorbance spectra of FA in solution and encapsulated within nanolaminates after UV irradiation. Initially, FA solutions were characterized by two main narrow peaks at 283 nm and 364 nm owing to the pteridine moieties and *p*-aminobenzoic glutamate moieties. This adsorption profile

partially changed after 20 min of irradiation, observing a broad peak between 310 nm and 374 nm. Moreover, the FA spectrum dramatically changed after 120 min, being the most representative absorption peaks eliminated, and hence suggesting a chemical degradation of the vitamin.

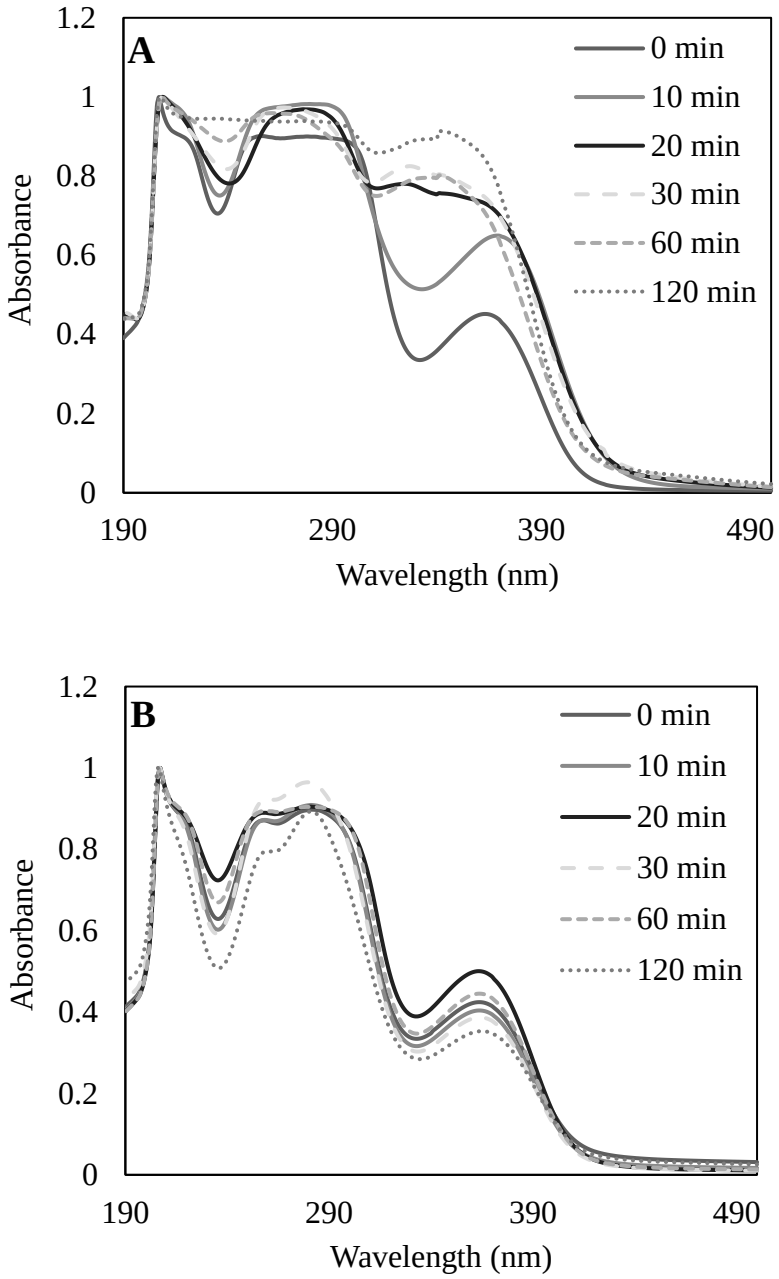

Fig. 7. (A) Normalized absorbance spectra of folic acid (FA) solutions and (B) alginate-chitosan nanolaminates containing FA irradiated with UV-light at different exposure times (0-120 min).

These results are in good agreement with published studies regarding the photo-stability of FA, where the vitamin was very light sensitive [40]. The FA

molecule is decomposed by UV light into biologically inactive products. The main photoproducts found after UV irradiation are 6-formylpterin (FPT) and pterine-6-carboxylic acid (PCA) [41]. FPT has adsorption peaks at 278, 310 and 365 nm, whereas PCA is identified by two peaks at 290 and 350 nm. The increasing concentration of PCA and FPT in FA solutions gives rise to wider peaks in the absorbance spectrum. On the other hand, UV-visible spectra of nanolaminates containing FA did not exhibit remarkable changes, preserving the distinctive peak of FA after being irradiated during 120 min. Therefore, it could be confirmed that FA was more stable encapsulated in alginate/chitosan assemblies than in the non-encapsulated form when it was exposed to UV lighting. This feature may be particularly important in foods fortification with FA and for the design of functional foods.

3.6. Release behavior of folic acid from nanolaminates

The FA released from nanolaminates was investigated by UV-visible spectroscopy and results are shown in Fig. 8. To assess the possible influence of pH on the vitamin release, nanolaminates were incubated under different pH conditions that would mimic those found in the gastrointestinal tract (GIT). Most nutraceuticals including FA, are mainly adsorbed in the small intestine where pH values are alkaline. However, to achieve a successful nutraceutical delivery, several hurdles along the GIT should be surpassed, such as acidic pH conditions, temperature, interactions with enzymes, etc. This factors may compromise the nutraceutical stability before reaching the adsorption site where it should be eventually released. In this study, it was observed that nanolaminates have photo-protective properties with the encapsulated FA. Therefore, it may be expected that nanolaminates would also exhibit a protective effect in GIT, or that somehow they could be able to control the FA release changing the environmental conditions. To evaluate these assumptions, nanolaminates were incubated at pH 3 (stomach) and pH 7 (intestine) and 37 ºC (body temperature), which closely simulate some of the most important conditions found in an *in vitro* digestion.

At pH 3, only 22 % of FA was released after 7 h, whereas a complete release was observed at pH 7. This suggests that nanolaminates present different pH stimuli-responsive properties that allow controlling FA release. In the latter case, the profile was characterized by a faster release of 88 % during the first

hour, followed by a slower release until the seventh hour of incubation. To a lesser degree, release profiles at pH 3 also exhibited a fast FA release initially, and then it reached a plateau. Previous findings demonstrated that changes in pH conditions have an impact in the release of small molecules. The release is normally biphasic. During the first hour, an initial burst release occurs driven by an excess of encapsulated compound on the nanolaminates' surface. After this stage, the concentration of compound within alginate/chitosan assemblies decreases, reducing the concentration gradient, and hence the FA release [42].

The greater FA release from nanolaminates at pH 7 than at pH 3 can be attributed to the high solubility of FA in alkaline media owing to its low pK_a (3.46) [43]. In concordance with our results, it has been previously described that pH greatly affects the release of the drug dipyridamole, loaded in poly(methacrylic acid) microspheres and protected with alginate/chitosan coatings, which was attributed to a greater solubility of the targeted compound under acidic conditions [37]. Therefore, these results indicate that solubility of encapsulate compounds may determine their release rate from nanolaminates, which represent a promising advantage to control the delivery of nutraceuticals in the gastrointestinal tract.

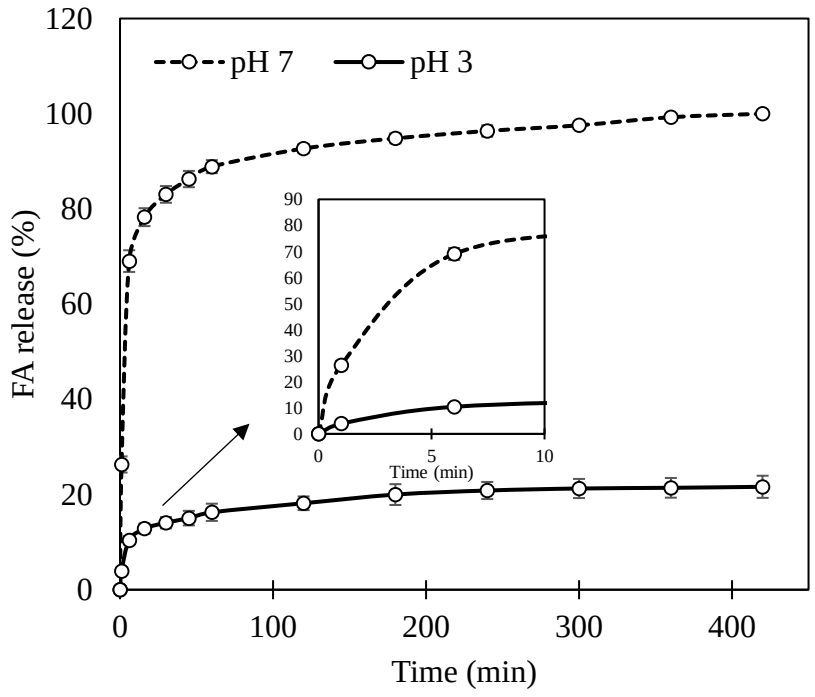

Fig. 8. Folic acid release from 20-layer nanolaminates under pH conditions of an *in vitro* digestion (pH 3 and pH 7).

4. Conclusions

The results obtained in this work demonstrate the feasibility of alginate/chitosan nanolaminates obtained by the layer-by-layer technique as delivery systems of FA. It was established that FA loading is highly dependent on the initial concentration of FA solutions as well as the immersion time. The maximum loading in films was observed at 10 mg/mL FA solution and after 120 min of immersion. The FA encapsulation in nanolaminates could also be confirmed by Raman spectroscopy and suggested a homogeneous distribution of the vitamin. Alginate/chitosan nanolaminates were also able to protect FA from degradation by UV irradiation and the release profiles were affected by pH conditions, showing a greater release at pH 7. This suggests that FA-loaded nanolaminates might exhibit a controlled release in the gastrointestinal tract, presenting a scarce release at the stomach, but a burst released in the pH conditions of small intestine, where it is supposed to be adsorbed. However, further research should be carried out using *in vitro* or *in vivo* digestion models and apply nanolaminates on food matrices. The results of the current study may contribute to shed light on the suitability of food-grade nanolaminates as delivery systems of nutraceuticals with relevance in the food and nutrition field.

5. Acknowledgments

This research was supported by the Ministerio de Ciencia e Innovación (Spain) throughout the projects AGL2009-11475 and MINECO ALG2012-35635. Author Acevedo-Fani also thanks to the University of Lleida for the pre-doctoral grant.

6. References

[1] N. Delchier, A.-L. Herbig, M. Rychlik, C.M.G.C. Renard, Folates in Fruits and Vegetables: Contents, Processing, and Stability, Comprehensive Reviews in Food Science and Food Safety. 15 (2016) 506–528.

[2] B.A. Jennings, G. Willis, How folate metabolism affects colorectal cancer development and treatment; a story of heterogeneity and pleiotropy, Cancer Letters. 356 (2015) 224–230.

[3] S.J. Moat, D. Lang, I.F.. McDowell, Z.L. Clarke, A.K. Madhavan, M.J. Lewis, et al., Folate, homocysteine, endothelial function and cardiovascular disease, The Journal of Nutritional Biochemistry. 15 (2004) 64–79.

[4] M. Visentin, N. Diop-Bove, R. Zhao, I.D. Goldman, The Intestinal Absorption of Folates, Annual Review of Physiology. 76 (2014) 251–274.

[5] R. Matias, P.R.S. Ribeiro, M.C. Sarraguça, J.A. Lopes, A UV spectrophotometric method for the determination of folic acid in pharmaceutical tablets and dissolution tests, Analytical Methods. 6 (2014) 3065.

[6] S. Boddohi, J. Almodóvar, H. Zhang, P.A. Johnson, M.J. Kipper, Layer-by-layer assembly of polysaccharide-based nanostructured surfaces containing polyelectrolyte complex nanoparticles., Colloids and Surfaces. B, Biointerfaces. 77 (2010) 60–8.

[7] J. Hernandez-Montelongo, E.G. Lucchesi, I. Gonzalez, W.A.A. Macedo, V.F. Nascimento, A.M. Moraes, et al., Hyaluronan/chitosan nanofilms assembled layer-by-layer and their antibacterial effect: a study using Staphylococcus aureus and Pseudomonas aeruginosa, Colloids and Surfaces B: Biointerfaces. 141 (2016) 499–506.

[8] M.P. Souza, A.F.M. Vaz, M.A. Cerqueira, J.A. Texeira, A.A. Vicente, M.G. Carneiro-da-Cunha, Effect of an Edible Nanomultilayer Coating by Electrostatic Self-Assembly on the Shelf Life of Fresh-Cut Mangoes, Food and Bioprocess Technology. 8 (2015) 647–654.

[9] B.G. de S. Medeiros, M.P. Souza, A.C. Pinheiro, A.I. Bourbon, M.A. Cerqueira, A.A. Vicente, et al., Physical Characterisation of an Alginate/Lysozyme Nano-Laminate Coating and Its Evaluation on “Coalho” Cheese Shelf Life, Food and Bioprocess Technology. 7 (2014) 1088–1098.

[10] A. Denis-Rohr, L.J. Bastarrachea, J.M. Goddard, Antimicrobial efficacy of N-halamine coatings prepared via dip and spray layer-by-layer deposition, Food and Bioproducts Processing. 96 (2015) 12–19.

[11] N. Durán, P.D. Marcato, Nanobiotechnology perspectives. Role of nanotechnology in the food industry: a review, International Journal of Food Science & Technology. 48 (2013) 1127–1134.

[12] M.A. Cerqueira, A.C. Pinheiro, H.D. Silva, P.E. Ramos, M.A. Azevedo, M.L. Flores-López, et al., Design of Bio-nanosystems for Oral Delivery of Functional Compounds, Food Engineering Reviews. 6 (2014) 1–19.

[13] J. Borges, J.F. Mano, Molecular Interactions Driving the Layer-by-Layer Assembly of Multilayers, Chemical Reviews. 114 (2014) 8883–8942.

[14] R. V Klitzing, R. V Klitzing, Internal structure of polyelectrolyte multilayer assemblies., Physical Chemistry Chemical Physics : PCCP. 8 (2006) 5012–33.

[15] K. Ariga, M. McShane, Y.M. Lvov, Q. Ji, J.P. Hill, Layer-by-layer assembly for drug delivery and related applications, (2011).

[16] J.T. Martins, Ó.L. Ramos, A.C. Pinheiro, A.I. Bourbon, H.D. Silva, M.C. Rivera, et al., Edible Bio-Based Nanostructures: Delivery, Absorption and Potential Toxicity, Food Engineering Reviews. 7 (2015) 491–513.

[17] K.I. Draget, Alginates, in: G.O. Phillips, P.A. Williams (Eds.), Handbook of Hydrocolloids, Second, CRC Press and Woodhead Publishing, Boca ratón, FL, 2009: pp. 807–825.

[18] S.N. Pawar, K.J. Edgar, Alginate derivatization: A review of chemistry, properties and applications, Biomaterials. 33 (2012) 3279–3305.

[19] S.K. Shukla, A.K. Mishra, O.A. Arotiba, B.B. Mamba, Chitosan-based nanomaterials: A state-of-the-art review, International Journal of Biological Macromolecules. 59 (2013) 46–58.

[20] F. Shahidi, J.K.V. Arachchi, Y.-J. Jeon, Food applications of chitin and chitosans, Trends in Food Science & Technology. 10 (1999) 37–51.

[21] A. Cagri, Z. Ustunol, E.T. Ryser, Antimicrobial edible films and coatings, Journal of Food Protection. 67 (2004) 833–848.

[22] M. Rinaudo, Chitin and chitosan: Properties and applications, Progress in Polymer Science. 31 (2006) 603–632.

[23] A. Acevedo-Fani, L. Salvia-Trujillo, R. Soliva-Fortuny, O. Martín-Belloso, Modulating Biopolymer Electrical Charge to Optimize the Assembly of Edible Multilayer Nanofilms by the Layer-by-Layer Technique, Biomacromolecules. 16 (2015) 2895–2903.

[24] B. Jiang, Bingbing Li, Tunable drug loading and release from polypeptide multilayer nano fi lms, International Journal of Nanomedicine. 4 (2009) 37–54.

[25] A. Shukla, J.C. Fang, S. Puranam, P.T. Hammond, Release of vancomycin from multilayer coated absorbent gelatin sponges., Journal of Controlled Release : Official Journal of the Controlled Release Society. 157 (2012) 64–71.

[26] M. Aceituno-Medina, S. Mendoza, J.M. Lagaron, A. López-Rubio, Photoprotection of folic acid upon encapsulation in food-grade amaranth (Amaranthus hypochondriacus L.) protein isolate – Pullulan electrospun fibers, LWT - Food Science and Technology. 62 (2015) 970–975.

[27] J. Kumirska, M. Czerwicka, Z. Kaczyński, A. Bychowska, K. Brzozowski, J. Thöming, et al., Application of Spectroscopic Methods for Structural Analysis of Chitin and Chitosan, Marine Drugs. 8 (2010) 1567–1636.

[28] P. Roger, L. Renaudie, C. Le Narvor, B. Lepoittevin, L. Bech, M. Brogly, Surface characterizations of poly(ethylene terephthalate) film modified by a carbohydrate-bearing photoreactive azide group, European Polymer Journal. 46 (2010) 1594–1603.

[29] S. Kumar, N. Chauhan, M. Gopal, R. Kumar, N. Dilbaghi, Development and evaluation of alginate–chitosan nanocapsules for controlled release of acetamiprid, International Journal of Biological Macromolecules. 81 (2015) 631–637.

[30] G. Lawrie, I. Keen, B. Drew, A. Chandler-Temple, L. Rintoul, P. Fredericks, et al., Interactions between alginate and chitosan biopolymers characterized using FTIR and XPS, Biomacromolecules. 8 (2007) 2533–2541.

[31] N.M. Alves, C. Picart, J.F. Mano, Self assembling and crosslinking of polyelectrolyte multilayer films of chitosan and alginate studied by QCM and IR spectroscopy., Macromolecular Bioscience. 9 (2009) 776–85.

[32] R. Aston, M. Wimalaratne, A. Brock, G. Lawrie, L. Grøndahl, Interactions between Chitosan and Alginate Dialdehyde Biopolymers and Their Layer-by-Layer Assemblies., Biomacromolecules. 16 (2015) 1807–17.

[33] J.-H. Choy, J.-S. Jung, J.-M. Oh, M. Park, J. Jeong, Y.-K. Kang, et al., Layered double hydroxide as an efficient drug reservoir for folate derivatives, Biomaterials. 25 (2004) 3059–3064.

[34] K.K. Karukstis, L.A. Perelman, W.K. Wong, Spectroscopic Characterization of Azo Dye Aggregation on Dendrimer Surfaces, Langmuir. 18 (2002) 10363–10371.

[35] S.E. Burke, C.J. Barrett, pH-Dependent Loading and Release Behavior of Small Hydrophilic Molecules in Weak Polyelectrolyte Multilayer Films, Macromolecules. 37 (2004) 5375–5384.

[36] S.G. Caridade, C. Monge, F. Gilde, T. Boudou, J.F. Mano, C. Picart, Free-standing polyelectrolyte membranes made of chitosan and alginate., Biomacromolecules. 14 (2013) 1653–60.

[37] X. Li, P.C. Du, P. Liu, I. d'Angelo, C. Conte, A. Miro, et al., Layer-by-layer polyelectrolyte complex coated poly(methacrylic acid) nanogels as a drug delivery system for controlled release: structural effects, RSC Adv. 4 (2014) 56323–56331.

[38] L. Zhang, B. Li, Z. Zhi, D.T. Haynie, Perturbation of Nanoscale Structure of Polypeptide Multilayer Thin Films, Langmuir. 21 (2005) 5439–5445.

[39] J.J. Castillo, T. Rindzevicius, K. Wu, C.E. Rozo, M.S. Schmidt, A. Boisen, Silver-capped silicon nanopillar platforms for adsorption studies of folic acid using surface enhanced Raman spectroscopy and density functional theory, Journal of Raman Spectroscopy. 46 (2015) 1087–1094.

[40] L. Liang, J. Zhang, P. Zhou, M. Subirade, Protective effect of ligand-binding proteins against folic acid loss due to photodecomposition., Food Chemistry. 141 (2013) 754–61.

[41] M.K. Off, A.E. Steindal, A.C. Porojnicu, A. Juzeniene, A. Vorobey, A. Johnsson, et al., Ultraviolet photodegradation of folic acid., Journal of Photochemistry and Photobiology. B, Biology. 80 (2005) 47–55.

[42] S. Anandhakumar, P. Gokul, A.M. Raichur, Stimuli-responsive weak polyelectrolyte multilayer films: A thin film platform for self triggered multi-drug delivery, Materials Science and Engineering: C. 58 (2016) 622–628.

[43] A.M. Gazzali, M. Lobry, L. Colombeau, S. Acherar, H. Azaïs, S. Mordon, et al., Stability of folic acid under several parameters, European Journal of Pharmaceutical Sciences. 93 (2016) 419–430.

GENERAL DISCUSSION

SECTION I: NANOEMULSIONS AND EDIBLE FILMS

Consumers are demanding safe, high-quality and 'label-friendly' food products. In consequence, new trends toward the progressive substitution of synthetic additives by natural alternatives are emerging in the food industry. Essential oils, being plant-derived compounds, are promising candidates for enhance safety and quality of foods, because of their notable antimicrobial effect against spoilage and pathogenic microorganisms. Nonetheless, essential oils exhibit poor-water solubility and instability, compromising their efficacy as antimicrobials. Oil-in-water nanoemulsions have been conceived as delivery systems of active lipophilic substances; the small droplet size of these systems may increase emulsion stability and biological activity of entrapped ingredients. Additionally, nanoemulsions might work as film-forming solutions, opening new alternatives to obtain edible packaging materials.

The first study submitted in this Doctoral thesis consist on evaluate the viability of using essential oil nanoemulsions for developing antimicrobial edible films was explored.

1. Physicochemical properties of essential oil nanoemulsions

Firstly, the properties of nanoemulsions formulated with thyme (TH-EO), lemongrass (LG-EO) and sage (SG-EO) oils as disperse phase, and sodium alginate solutions as continuous phase were characterized. This allowed elucidating the possible impact of nanoemulsions characteristics on the physical properties of the resulting edible films.

The initial mean droplet size of coarse emulsions decreased after microfluidization, resulting in nanoemulsions with droplet sizes below 100 nm. However, size distributions were always multimodal, which indicated the presence of different droplet sizes in the system. In general, three intensity peaks were observed in the size distributions plots. The peak found at 20 nm was ascribed to micellar structures of the small molecule surfactant used in the formulation (Tween 80), with typical diameters of 10 nm. The other peak located at around 190 nm could correspond to nano-sized oils droplets. The last peak observed around 6000 nm was attributed to the presence of large oil droplets or alginate colloidal structures. Contrarily, other authors have reported narrow size distributions in nanoemulsions formulated with 1% of

alginate in the continuous phase and 1% of lemongrass oil in the disperse phase, using similar homogenization conditions (Salvia-Trujillo, Rojas-Graü, Soliva-Fortuny, & Martín-Belloso, 2013). The nanoemulsions produced in the present study were highly viscous due to the incorporation of sodium alginate in the continuous phase. The concentration of alginate used in the formulation was much higher (3%) than that reported in previous studies. One of the factors affecting the droplet size disruption is the viscosity of both disperse and continuous phase. In this case, it was proposed that the elevated viscosity of essential oil emulsions could have diminished the efficacy of the microfluidizer in breaking up oil droplets.

The mean droplet size measured by dynamic light scattering is normally quite consistent in monodisperse systems, representing the average value obtained from the unique intensity peak in the particle sizes distribution plot. However, in non-monodisperse emulsions, the mean droplet size is less precise due to the presence of several intensity peaks. Therefore, the mean droplet diameters in non-monodisperse systems should be interpreted considering their size distributions in terms of volume and number of droplets, since large particles have the ability to scatter light more strongly than small particles. In this study, size distributions either in volume or number of particles confirmed that nano-sized emulsions were effectively created with microfluidization.

On the other hand, the oil type significant influenced particle size of nanoemulsions. For instance, the incorporation of TH-EO led to bigger droplet sizes than when SG-EO was used. The degree of affinity between essential oil and surfactant, and interactions with other components in the system (e.g. alginate) may change, depending on the chemical composition of oil. In particular, essential oils could contain variable concentrations of surface-active molecules that decrease the oil/water interfacial tension, originating nanoemulsions with different droplet sizes. Important properties of oils, such as polarity or viscosity, also play a key role in the resulting droplet sizes of nanoemulsions.

The interfacial charge of oil droplets was always negative. In fact, the ζ-potential values were between -41 mV and -70 mV, despite the presence of a non-ionic surfactant (Tween 80) at the oil/water interface. Theoretically, non-ionic surfactants should originate uncharged interfaces. However, the incorporation of an anionic polysaccharide in the continuous phase, such as

alginate, can modify the interfacial electrical charge conferring rather negative ζ-potentials to droplets (Dickinson, 2003). Although, most polysaccharides work as thickening agents rather than emulsifiers, they can also be partially adsorbed at the oil/water interface by different interactions in certain conditions (Dickinson, 2009). Therefore, the negative electrical charge of droplets can be attributed to the presence of alginate in the formulation of nanoemulsions.

A strong droplet charge may improve colloidal stability by increasing the repulsive forces between droplets and reducing the attractive forces that lead to flocculation, creaming, sedimentation or coalescence phenomena. It is known that nanoemulsions with ζ-potentials above 30 mV or below -30 mV are considered to be physically stable (Heurtault, 2003). In this regard, the obtained essential oil nanoemulsions were highly stable to gravitational forces. The oil type also had an influence on the ζ-potential of nanoemulsions. Namely, the most negative ζ-potential was observed in SG-EO nanoemulsions. It is possible that some ionizable groups in the essential oil were located at the oil/water interface, thus increasing the overall charge of droplets. In concordance with this result, other authors have also found differences in the ζ-potential of emulsions containing different essential oils and ionic polysaccharides (Bonilla, Atarés, Vargas, & Chiralt, 2012).

On the other hand, all nanoemulsions were rather translucent to the naked eye, but there were slight differences among them. In general, the whiteness index decreased as the droplet size lessened in nanoemulsions. Those containing SG-EO exhibited the lowest whiteness index values, whereas nanoemulsions of TH-EO presented the highest. This behavior agrees with the fact that nanoemulsions are optically transparent systems, since droplets scatter the light weakly, and their diameters are smaller than the wavelength of visible light (McClements & Rao, 2011). The point that essential oil nanoemulsions are translucent systems represents a major advantage for their application in foods because it may have negligible effect on food appearance.

Furthermore, the viscosity of nanoemulsions was strongly influenced by the presence of alginate in the continuous phase. The high viscosity values observed (452-600 mPa.s) indicated that alginate conferred texturizing properties to nanoemulsions. However, viscosity of alginate solutions used as

continuous phase (3%) was greater (800 mPa.s) than in nanoemulsions. These differences suggested that the viscosity reduction could have occurred after microfluidization process, affecting the polysaccharide characteristics. Previous studies have demonstrated changes in the viscosity of polysaccharide solutions treated with high-shear forces. The strong disruptive forces generated during microfluidization may cause conformational changes in polysaccharide chains or even induce degradation (Bonilla et al., 2012; Salvia-Trujillo et al., 2013). It was also found that the oil type affected viscosity of nanoemulsions. Probably, interactions among compounds contained in essential oils and other components of the system (e.g. alginate) may lead to different adsorption kinetics, affecting the initial polysaccharide concentration in the continuous phase, and thus decreasing or increasing viscosity.

2. Influence of nanoemulsion properties on the physical features of edible films

The surface of nanoemulsion-based edible films containing essential oils was evaluated by microscopy and compared with alginate films without oil. Surface examinations were carried out in both sides of the films: the one dried facing the air, and the other dried facing the support (Mylar® paper). In general, nanoemulsion-based edible films with essential oils presented a topography much more uneven than the surface of alginate films without oil. This result was consistent with others reported previously, where these changes were attributed to the migration of oil droplets upwards the film, hence resulting in a holey structure (Sánchez-González et al., 2011).

However, the degree of roughness in the film surface also varied with the oil type incorporated. In fact, the surface of LG-EO films was rather irregular, whereas TH-EO and SG-EO films exhibited a smooth surface. This suggests that different degrees of embedment of droplets inside the film matrix could have occurred during drying. In general, edible films prepared from emulsions of small droplet size tend to be more homogeneous than those obtained from emulsions of big oil droplets. This is because nanoemulsions can be more stable during film drying (Fabra, Pérez-Masiá, Talens, & Chiralt, 2011). However, nanoemulsions may suffer destabilization during film formation, resulting in uneven topographies or bilayer structures.

Regarding to the optical properties, the color difference (*ΔE*)* between a particular film and a white background, as well as their CIE $L^* a^* b^*$ parameters were affected by the type of essential oil encapsulated within nanoemulsions. Namely, there was a significant increase in lightness (L^*) when films contained LG-EO and SG-EO, compared with those with TH-EO. In fact, these films had a light greenish-yellowish tone. As a result, the color difference (*ΔE*)* of TH-EO films was greater than in the others. In this particular parameter, it was found a strong positive correlation between oil droplet size of nanoemulsions and *ΔE** values of the corresponding edible films (r = 0.9424). This means that *ΔE** of edible films was mainly influenced by the droplet size of their film-forming nanoemulsions. Therefore, *ΔE** decreased as the droplet size decreased. A strong relationship between whiteness index of nanoemulsions and *ΔE** of the resulting films and was also found (r = 0.9128), which indicated that the emulsion color determines the optical characteristics of the edible films. These results demonstrate that the optical properties of edible films can be enhanced by controlling the physicochemical properties of the film-forming nanoemulsions.

On the other hand, the water vapor permeability of films was little affected by the presence of essential oils, compared to alginate films without oil. It is known that the incorporation of essential oils may reduce the path of water molecules through the film, having certain hydrophobic character. However, the low oil content used in nanoemulsions could have hindered the perception of this effect. Only films with SG-EO exhibited a slight reduction of the water vapor permeability, being ascribed to the small droplet size obtained in their equivalent nanoemulsions that could lead to a better oil distribution inside the film.

The thickness of nanoemulsion-based films significantly decreased, compared to alginate films without oil. Those obtained from LG-EO and SG-EO nanoemulsions were the thinnest. It has been described that films prepared from small droplet size emulsions can undergo changes in the total solids concentration of films during drying, since tiny volatile oil droplets, such as essential oils, can evaporate more rapidly (Sánchez-González et al., 2011). This assumption was also supported by the significant correlation found between droplet size of nanoemulsions and film thickness (r = 0.6919).

Finally, nanoemulsion-based films were as resistant as alginate films without oil in terms of tensile strength. Several reports have demonstrated that incorporating oil to the formulation of film-forming solutions may weaken the film resistance, decreasing cohesion forces within the structure (Han & Gennadios, 2005; Zúñiga, Skurtys, Osorio, Aguilera, & Pedreschi, 2012). Nevertheless, nanoemulsion-based films obtained in this study were rather resistant, probably due to the low oil content incorporated. Interestingly, SG-EO films were much more elastic (EAB: 78% ± 5) than LG-EO (EAB: 32% ± 9) and TH-EO (41% ± 12) films, or even alginate films (38% ± 7). In this case, the electrical charge of nanoemulsions might have an important impact on the film flexibility. The repulsive forces among macromolecules chains (e.g. alginate) of the same charge can increase the distance between polymers originating a plasticizing effect within the film (Han & Gennadios, 2005). In particular, edible films prepared from SG-EO nanoemulsions presented the greatest elongation capacity, but also the strongest electrical charge of droplets (ζ-potential: -70 mV) among all nanoemulsions obtained. In fact, a marked negative correlation between ζ-potentials of nanoemulsions and EAB of films was found (r = -0.8527). The droplet size may also affect film flexibility, since large surface area of oil droplets increases the heterogeneity of film structure. In line with the above-mentioned statement, a moderate correlation between droplet size and EAB of edible films was observed (r = 0.5383).

3. Antimicrobial properties of nanoemulsion-based films

The efficacy of essential oil films in inactivating *Escherichia coli* inoculated on a model surface was affected by the oil type. First, it was also confirmed that alginate films without oil did not exhibit any antimicrobial effect. Then, the antimicrobial efficacy of films was discussed considering the differences in composition of the essential oils. The most effective films were those that contained TH-EO, being able to reduce 4.71 logarithmic units of the microbial population after 12 h. This strong inhibitory effect was explained by the presence of thymol molecules as the major active compound of TH-EO. It has been proposed that the mechanism of action of thymol in microbial cells is based on the destabilization of cytoplasmic membrane. Thymol binds to proteins located in the membrane, altering its selective permeability properties. Gram-negative bacteria, such as *Escherichia coli*, are especially susceptible to thymol molecules due to its ability of disintegrate the outermost

lipopolysaccharide membrane (Juven, Kanner, Schved, & Weisslowicz, 1994; Ultee, Bennik, & Moezelaar, 2002).

The SG-EO films exhibited certain antimicrobial effect, but it was only significant during the first 2 h. After that period, a progressive increase in the microbial population was observed. This result suggests that *E.coli* was rather resistant to SG-EO. In fact, other authors have pointed out that this essential oil is little effective with gram-negative bacteria, such as *E. coli.* (Gutierrez, Rodriguez, Barry-Ryan, & Bourke, 2008; Shirazi et al., 2008).

Similarly, the LG-EO films did not inhibited *E. coli* growth, although a strong antimicrobial activity has been proved previously (Maizura et al., 2007; Rojas-Graü et al., 2007). In this particular study, it was hypothesized that the absence of antimicrobial effect of LG-EO films could be partially attributed to the oil volatilization induced by the nanometric size of droplets in the film-forming solution. Most of the active compounds responsible of the antimicrobial activity of LG-EO are volatile, and thus they may be easily eliminated during film drying. It is known that the major active compounds in LG-EO have low density (Citral: 0.856 kg/cm^3; limonene: 0.834 kg/m^3 (Rao & McClements, 2012)), which could have promoted the rapid migration of droplets upwards the film and their fast evaporation due to the high vapor pressure of nano-sized droplets (Nuchuchua et al., 2009).

In relation with this statement, microscopic examinations confirmed that the surface of LG-EO films exhibited the most irregular appearance. Other factors, such as antagonistic interactions between oil compounds and proteins or carbohydrates in foods, as well as the pH may compromise the antimicrobial activity of essential oils (Pires et al., 2013; Raybaudi-Massilia et al., 2008).

SECTION II: MULTILAYER EMULSIONS

Nowadays, the pursuit of a healthier lifestyle among consumers has increased the interest for the intake of food components able to provide health-promoting properties beyond its nutritional value. Food fortification and food enrichment with nutraceutical compounds is becoming a common practice in the food industry. Nonetheless, most nutraceuticals are poor water-soluble, highly unstable to environmental conditions, and also present low bioavailability.

Their encapsulation into emulsion-based systems may allow a better protection, while preserving their functional properties. In this regard, multilayer emulsions are a promising alternative to encapsulate and deliver hydrophobic active ingredients, enhancing their physicochemical stability and dispensability into water-based foods. Moreover, the possibility of changing the interfacial properties of oil droplets may have an important impact in their behavior under gastrointestinal conditions.

Consequently, the study of the feasibility multilayer emulsions to be used as delivery systems of hydrophobic nutraceuticals (resveratrol) was investigated.

1. Formulation of multilayer emulsions: Effect of biopolymer concentration on droplets stability

Primary emulsions

All formulations of single-layer (primary) emulsions presented average droplet sizes below 300 nm, depending on the concentration of lactoferrin incorporated. The smallest droplet size (187 nm) was found in the formulation prepared with the highest concentration of lactoferrin (1.90%), exhibiting monomodal droplet size distributions. The surface-active properties of lactoferrin (a globular protein) have been previously described, as well as its ability to form emulsions with nanometric droplet sizes (Tokle & McClements, 2011). To obtain a stable multilayer emulsions, the stability of primary emulsions must be ensured. Therefore, emulsions with nano-sized droplets (between 20-200 nm) are good candidates, since they are relatively more stable to creaming, sedimentation, flocculation and coalescence than emulsions containing bigger droplets (McClements & Rao, 2011).

The interfacial droplet charge also changed with the lactoferrin concentration incorporated in primary emulsions. Nevertheless, there was not a clear

relationship between the ζ-potential values of droplets and the lactoferrin concentration. In general, the ζ-potentials found in all formulations were strongly positive (between 50 and 45 mV), confirming that lactoferrin molecules were located at the oil/water interface forming cationic interfacial layers. This fact has two important consequences: i) the emulsion stabilization by strong repulsive forces, and ii) the possibility of forming another interfacial layer using oppositely charged biopolymers added in a second step.

In concordance with this result, other authors have reported droplets sizes of ≈ 230 nm and ζ-potential values of ≈ 50 mV in emulsions with 1.50% lactoferrin (Zhao et al., 2015). The formulation that contained 1.90% lactoferrin was selected for the formation of secondary emulsions, based on their smallest droplet size and strong positive electrical charge.

Secondary emulsions

The incorporation of different alginate concentrations in the continuous phase led to remarkable changes in the droplet size of single-layer emulsions (lactoferrin coated droplets). In effect, there was an abrupt increase from 187 nm up to 8700 nm using the lowest alginate concentration (0.02%). The resulting secondary emulsions presented phase separation that could be visibly appreciated. This increase in droplet size was attributed to the bridging flocculation of droplets.

If the biopolymer concentration in the continuous phase is insufficient to saturate droplets surface, a single molecular chain tends to adsorb to the surface of several droplets simultaneously, and hence flocculation occurs. However, bridging flocculation tend to be reduced when the biopolymer concentration increases (Dickinson, 2003; Heurtault, 2003; McClements, 2005). This effect could be observed in secondary emulsions containing higher alginate concentrations, decreasing the droplet size down to 249 nm at 0.28 %. In this case, emulsions remained visibly stable without signs instability.

On the other hand, important changes were observed regarding the ζ-potential, changing from strongly positive (lactoferrin coated droplets) to neutral in emulsions containing the lowest alginate concentration (0.02%). This result indicated that most droplets were partially coated by polysaccharide chains. However, the ζ-potential of droplets changed to

strongly negative by increasing the alginate concentration in the emulsion. In this case, it was indicative of the complete saturation of the droplets interface with alginate molecules, leading to the formation of a new interfacial layer.

This assumption was confirmed by the fact that ζ-potential values followed a plateau from a certain biopolymer concentration. Higher alginate concentrations did not affect the droplet charge, meaning that unbounded chains remained in the continuous phase of the emulsion. The formulation containing 0.22% alginate was selected as the most stable formulation to be used in tertiary emulsions. This formulation showed small droplet size and strong ζ-potential, without containing excessive unbound alginate chains in the continuous phase.

Tertiary emulsions

The poly-L-lysine concentration significantly changed the droplet size in tertiary emulsions, following a similar pattern to that observed in secondary emulsions. The initial diameter of lactoferrin/alginate-coated droplets (268 nm) abruptly increased using the lowest poly-L-lysine concentration (0.0018%). A fast emulsion destabilization was observed in the first 15 min, which was attributed to the bridging flocculation. However, stable emulsions with rather small droplet sizes were obtained by increasing the poly-L-lysine concentration up to 0.036%.

Interestingly, emulsions containing higher biopolymer concentrations were unstable and the droplet size was greater than 1μm. This could be explained by the positive depletion interactions between unbounded alginate molecules and oil droplets, promoting droplets aggregation (Benjamin et al., 2012; McClements, 2000).

Moreover, the magnitude of the interfacial electrical charge decreased when poly-L-lysine was incorporated to the formulation at the lowest concentration (0.009%). However, a change in the sign of the interfacial electrical charge could not be appreciated. This behavior indicates that poly-L-lysine molecules in the continuous phase were not sufficient to cover all droplets in the emulsion. In this case, it is likely that the ζ-potential of lactoferrin/alginate/poly-L-lysine-coated droplets was the resulting contribution of uncoated negative alginate patches and positive poly-L-lysine patches adsorbed on the droplets' surface. The oil droplets in tertiary emulsions containing 0.018% poly-L-lysine

had positive ζ-potentials (25.8 mV), and were more positive as the concentration increased to 0.045% w/w. At this point, the formation of a third poly-L-lysine interfacial layer on droplets was confirmed. The formulation containing 0.036% w/w poly-L-lysine was used in the subsequent experiments. These systems presented small droplet sizes and strong ζ-potential, confirming the formation of tertiary emulsions.

Furthermore, the microstructure of oil droplets contained in single-layer and multilayer emulsions was examined using the optimal formulations. Lactoferrin-coated oil droplets (primary emulsions) presented a well-defined spherical structure surrounded by a discrete interface, which corresponded to the lactoferrin layer. The droplet size calculated from micrographs was in concordance with those obtained by dynamic light scattering.

Lactoferrin/alginate-coated droplets (secondary emulsions) were identified as core/shell structures, having a light inner region (core) coated by a thin grey layer (shell). Similarly, lactoferrin/alginate/poly-L-lysine-coated droplets (tertiary emulsions) appeared as spherical structures that consisted of a white inner region surrounded by an intense black coating, corresponding to the multilayer coating. These results confirmed the successful formation of single-layer and multilayer emulsions, and also demonstrated the structural differences in emulsions depending on the interfacial layer composition.

2. Short-term physical and chemical stability of single-layer and multilayer emulsions

Changes in the droplet size of resveratrol-loaded single-layer emulsions and multilayer emulsions were examined during 4 weeks of storage. It was found that the initial particle size of primary emulsions did not change significantly, which confirmed that droplets were stable to gravitational separation mechanisms, such as creaming, sedimentation, coalescence and flocculation.

On the other hand, there was a 20.7% increase in the initial droplet size of secondary emulsions during the first two weeks of storage. Nonetheless, droplet size did not further increased until the fourth week. This change suggests a subsequent adsorption of some remaining *free* alginate molecules that were not bound to droplets' surface initially, or could be caused by a partial aggregation of droplets during storage. However, it is noteworthy that

these emulsions were visibly stable, with no evident signs of phase separation, creaming or sedimentation during storage.

Conversely, tertiary emulsions suffered a decrease in their droplet size of 6.7% of their initial size. This fact could be attributed to the rearrangement of the poly-L-lysine chains adsorbed to the droplets interface, thus forming a denser molecular packing and decreasing the hydrodynamic diameter of oil droplets. This behavior has been described for several multilayered structures produced by the progressive adsorption of oppositely charged biopolymers. In a first moment, the molecular chains are rapidly adsorbed to the substrate, and then changes in the conformation occur slowly in order to reach an energetic equilibrium (Marudova et al., 2005). Despite of these events, droplet sizes of tertiary emulsions were similar from the second to the fourth week, which suggests the stability of the system.

Regarding the interfacial droplet charge in emulsions, important changes were observed during storage. In effect, positive ζ-potentials of primary emulsions decreased abruptly, reaching values near to the neutrality after 4 weeks. The same behavior was observed in citral emulsions stabilized with milk proteins after 4 weeks (Xiang et al., 2015), and in emulsions stabilized with lactoferrin after 14 days (Mao et al., 2013). Lactoferrin molecules tend to change their conformation in order to be adsorbed at the oil/water interface, letting exposed highly reactive functional groups that were originally contained in the lobules of globular protein. These reactive moieties may interact with other compounds, such as metal ions or free oxygen molecules, inducing degradation reactions at the oil/water interface and changing the ζ-potential of droplets (Tokle & McClements, 2011).

On the contrary, secondary emulsions did not present variations in the ζ-potential values after 4 weeks. An additional interfacial alginate layer could have avoided changes in the droplet charge, probably acting as a protective shield against degradation reactions occurring at the oil/water interface. The ζ-potential of tertiary emulsions also remained stable during storage time, with only a slight decrease after 7 days. From the second to the fourth storage week, the ζ-potential of tertiary emulsions did not present significant differences. This confirmed that a multilayer coating on droplets may improve the emulsion stability during storage.

On the other hand, the chemical stability of resveratrol-loaded single-layer and multilayer emulsions was also examined under lighting conditions at room temperature. Resveratrol is a stilbenoid highly unstable to the incidence of UV light, which is rapidly transformed from its biologically active *trans*- isomer to the inactive *cis*- isomer. Therefore, it was important to elucidate the effect of interfacial layer composition of droplets on the antioxidant activity of encapsulated resveratrol, compared to non-encapsulated resveratrol.

A significant 22% decrease in the initial antioxidant activity of resveratrol-loaded oil (non-encapsulated compound) was observed after 4 weeks, which was ascribed to the isomerization of resveratrol due to the constant light exposure (Leiro et al., 2004; Zupančič et al., 2015). However, a greater retention of the antioxidant activity was observed in primary emulsions, exhibiting scarce changes during storage. Secondary and tertiary emulsions initially presented lower antioxidant activity than primary emulsions, which could be explained by the lower concentration of encapsulated resveratrol in these systems. Nonetheless, significant changes in the antioxidant activity of both systems were not observed during storage, and therefore multilayer emulsions may also offer a better protection to resveratrol under stressing conditions.

Remarkably, antioxidant activity of tertiary and secondary emulsions was comparable, although the concentration of resveratrol in tertiary emulsions was 10-fold lower than in secondary emulsions. This could be probably explained by the presence of other components, such as poly-L-lysine, which might exhibit some antioxidant activity, contributing to the overall radical scavenging capacity of emulsions. Literature works support this statement, since poly-L-lysine has shown certain antioxidant effect (Pan & Nitin, 2015; Tikekar et al., 2013).

Although further analysis are required to confirm the role of multilayer emulsions on resveratrol chemical stability, these results can be a starting point that suggests their potential positive impact. Anyhow, previously published studies regarding resveratrol-loaded nanoemulsions have demonstrated their outstanding protective properties for the encapsulated ingredient (Davidov-Pardo & McClements, 2015; Sessa et al., 2011), being an alternative to improve the incorporation of light-sensitive lipophilic compounds in foods.

3. Influence of the interfacial layer composition of oil droplets on their physical stability during *in vitro* digestion

Changes in the droplets integrity

The physical stability of single-emulsions and multilayer emulsions in terms of droplet size, microstructure and droplet charge under simulated mouth, stomach and intestine fluids was evaluated. There were remarkable differences in the behavior under gastrointestinal conditions that depended on the interfacial layer composition of droplets in the emulsions. In fact, the droplet size of primary emulsions (lactoferrin coated droplets) in the oral phase remained similar to the mean droplet size initially obtained before digestion (181 nm). Primary emulsions presented monomodal particle size distributions, which was in concordance with the microscopic examinations carried out by confocal microscopy; oil droplets appeared as separated small red dots, corresponding to a monodisperse emulsion. In this case, emulsions could be stabilized by the repulsive forces coming from lactoferrin molecules adsorbed at the oil/water interface, which were positively charged (p*I* ≈ 9) in the simulated salivary fluids (pH 7).

It has been reported the remarkable aggregation of lactoferrin coated droplets incubated with simulated salivary fluids. This effect has been mostly attributed to the presence of enzymes or biopolymers that interact with oil droplets promoting their destabilization (Shimoni et al., 2013). In the present study, the simulated salivary fluids were a mixture of different salts at pH 7. This explains the high stability of primary emulsions observed in the oral phase, since other digestion components did not induce droplets aggregation.

Similarly, lactoferrin/alginate oil droplets were affected by simulated salivary fluids, observing a 28 % reduction in their initial size. Although the particle size distributions of secondary emulsions before and after being exposed to salivary fluids were always monomodal, a greater droplets homogeneity was found in the oral phase. This result was also confirmed by microscopic examinations. Likely, the size decrease of lactoferrin/alginate coated droplets in the oral phase could have been attributed to the disruption of some flocs initially present in secondary emulsions. The sample dilution with simulated salivary fluids may decrease the positive depletion interactions between alginate chains with oil droplets. In addition, with the pH of emulsions

increasing from 5 (non-digested) to 7 (oral phase), alginate chains are more charged ($pK_a \approx 3.65$), thus increasing electrostatic repulsion between droplets. This result was in good agreement with previous studies that reported a decrease in droplet size of emulsions stabilized with proteins incubated with gastrointestinal fluids (Malaki Nik et al., 2011).

Lactoferrin/alginate/poly-L-lysine coated droplets were highly unstable in the oral phase, increasing their average diameters from 580 nm up to more than 3000 nm. Particle size distributions and microscopic examinations also confirmed an extensive droplets aggregation forming noticeable clumps. In contrast with the results obtained in this study, other authors have reported that emulsions containing poly-L-lysine-coated droplets were rather stable being incubated with simulated salivary fluids that did not contain mucin (Lopez-Pena et al., 2016).

Nevertheless, although salivary fluids used in this study were also prepared without mucin, the electrolytes concentration was much higher than that reported previously. Therefore, the extensive droplets aggregation in the oral phase was ascribed to the screening of the charged groups in poly-L-lysine adsorbed at the droplet's interface, due to the high electrolyte concentration in the media. The pH conditions in the oral phase might have contributed to droplets destabilization, since poly-L-lysine molecules at pH 7 (mouth) are weakly charged ($pI \approx 9$), thus making it easier for counterions to screen the ionizable groups of poly-L-lysine chains located at the droplet's interface.

On the other hand, the droplet size of primary emulsions under gastric conditions increased abruptly up to about 1000 nm, and the particle size distributions were multimodal. Additionally, microscopic evaluations confirmed the presence of appreciable clumps, being difficult to identify the spherical structures of droplets. This indicates that lactoferrin coated droplets were highly unstable in the gastric phase, probably due to the hydrolysis of lactoferrin molecules located at the oil/water interface in the presence of proteases (such as pepsin) of the gastric fluid. As a consequence, the protein interfacial layer of droplets can be damaged or even completely removed. This behavior was previously reported in other works dealing with emulsions stabilized by lactoferrin (Tokle et al., 2013).

Secondary emulsions were more stable in the gastric phase than primary emulsions, although some flocculation also occurred. This led to an increase

in the particle diameter, which was confirmed by the multimodal particle size distributions of digested emulsions. The microscopic analysis also revealed the presence of clusters constituted by agglomerations of well-defined tiny droplets, which suggests a flocculation process rather than coalescence of droplets. These results are comparable to those reported by other authors, where the emulsions containing protein/polysaccharide interfacial membranes were also unstable under simulated gastric conditions (Pinheiro et al., 2016; Tokle et al., 2012). In fact, alginate molecules are weakly charged ($pK_a \approx 3.65$) at the acidic pH conditions of the gastric phase (pH 3). Therefore, repulsive forces among droplets decrease and attractive forces (e.g. van der Waals) take place, leading to the formation of clusters.

Tertiary emulsions experimented a noticeable decrease in their droplet size in contact with the simulated gastric fluids, and the particle size distribution graphs became monomodal. Additional microscopic examinations corroborated that lactoferrin/alginate/poly-L-lysine coated droplets were homogeneously distributed as singular structures within the gastric fluid. This suggests a possible reapportion of droplets when these passed from the oral to the gastric phase.

It was hypothesized that this behavior could have occurred by two reasons. First, the pH changes in the digesta from 7 (oral phase) to 3 (gastric phase). Poly-L-lysine molecules adsorbed at the oil/water interface are strongly charged under acidic conditions, hence the repulsive forces between droplets are greater, helping to dissociate big clusters already existing. Second, the effect of diluting emulsions with the simulated gastric fluid, which could have reduced the attractive interactions that originated droplets aggregation in the oral phase. In concordance with this result, it has been described a droplet size decrease in emulsion-based systems when particles moved from the oral to the gastric phase during an *in vitro* digestion (Golding et al., 2011; Salvia-Trujillo et al, 2013).

Surprisingly, this decrease in droplet size seems to indicate that gastric proteases did not destabilize the interfacial coating of droplets when the outermost layer was composed of poly-L-lysine (a polypeptide); on the contrary, oil droplets were much more stable under gastric conditions. It has been described that poly-L-lysine molecules are able to inhibit the proteolytic activity of gastric pepsins at very low pH, acting as competitive inhibitors due

to their capacity to form electrostatic complexes (Katchalski et al., 1954; Lawton & Mekras, 1985). Therefore, the high physical stability of tertiary emulsions in the gastric phase may be probably explained by the presence of the poly-L-lysine in the interfacial membranes of droplets, being able to inhibit the proteases activity.

Finally, the average particle size of primary and secondary emulsions decreased in the intestinal phase, whereas tertiary emulsions exhibited a slight increase. Nonetheless, particle size distributions of all emulsions were multimodal, presenting intensity peaks above the detection limit of the equipment that suggested the presence of bigger particles. In the micrographs, different structures of variable morphologies and sizes could be appreciated. These structures may be ascribed to the presence of digestion products (e.g. mixed micelles or vesicles) as a result of the hydrolytic activity of intestinal enzymes (pancreatin) in the digesta, or to the presence of remaining non-digested oil droplets and polysaccharide/protein complexes.

In the intestinal stage, the majority of the lipid fraction of emulsions is solubilized by the action of bile salts and these are believed to adsorb at the oil/water interface, displacing the existing interfacial layer on oil droplets. Then, the lipid phase is further converted into smaller molecules (such as free fatty acids, mono and/or di-acylglycerols) due to the enzymatic activity of intestinal lipases, releasing any encapsulated lipophilic nutraceutical. Finally, the assembly of mixed micelles that contain the lipolysis products and nutraceuticals takes place, which enhances transport across the epithelium walls.

Changes in the droplet charge

Lactoferrin coated droplets in primary emulsions experienced a decrease of their initial ζ-potentials (≈ 45 mV) in the oral phase (≈12 mV). This behavior can be expected since lactoferrin molecules have a strong positive charge in acidic pH conditions, but is weaker at pH values near to the isoelectric point of the protein (p*I* ≈ 9). At the neutral conditions of salivary fluids (pH 7), lactoferrin molecules located at the oil/water interface are less ionized than in the non-digested emulsions (pH 5) and the positive ζ-potentials of droplets tend to decrease. In spite of this fact, primary emulsions remained stable as particle size analyses confirmed, probably due to steric stabilization. It has

been described that globular proteins, such as lactoferrin, provide high physical stability to emulsions by creating thick layers around oil droplets, excepting when the pH of the media is near to the isoelectric point of the protein (Lee et al., 2011).

Contrarily, initial negative ζ-potentials found in non-digested secondary emulsions (lactoferrin/alginate coated droplets) slightly increased in the oral phase, indicating a decrease in the net charge of droplets. Changes in the magnitude of the interfacial electrical charge may be associated with changes in the thickness of the interfacial layer around droplets. In fact, a previously published study in biopolymer-based multilayer systems proved that the magnitude of the ζ-potential decreases as the amount of material adsorbed per layer decreases. Hence, there are less ionizable functional groups providing an electrical charge to the surface (Acevedo-Fani et al., 2015). Consequently, changes in the droplet ζ-potential might be associated with a reduction in thickness of the alginate layer forming interfacial coating in droplets.

Furthermore, initial positive ζ-potentials of lactoferrin/alginate/poly-L-lysine droplets (tertiary emulsions) were neutralized in the oral phase. This effect could probably be explained by the high electrolyte concentration in the salivary fluids, which may have screened most of ionized groups of poly-L-lysine molecules located at the oil-water interface of droplets.

When all emulsions moved to the gastric phase at pH 3, the ζ-potential became negative. Namely, lactoferrin coated droplets (primary emulsion) should have exhibited positive ζ-potentials at pH 3, due to the presence of lactoferrin at the oil/water interface of droplets. However, the negative ζ-potential observed in these emulsions could be explained by the adsorption of pepsin molecules to droplets' surface. This enzyme is negatively charged in acidic conditions, being able to interact with positive lactoferrin molecules by electrostatic binding.

The lactoferrin/alginate coated droplets (secondary emulsions) presented a decrease in the magnitude of the negative ζ-potential in the gastric phase. In this case, alginate molecules were weakly charged in acid media. Regarding lactoferrin/alginate/poly-L-lysine coated droplets (tertiary emulsions), the ζ-potential was strongly negative under simulated gastric conditions. It is likely that pepsin molecules contained in the gastric fluid may have formed

electrostatic complexes with poly-L-lysine molecules located in the droplets' surface, changing the particles ζ-potential.

On the other hand, the particles ζ-potential remained negative in the intestinal phase, regardless the interfacial layer composition of oil droplets in the emulsions. Assuming that most of the oil droplets were completely digested in the intestinal phase, the negative charge of particles might be attributed to the intrinsic properties of the digestion products (e.g. free fatty acids and di-acylglycerols), some oil droplets surrounded by bile acids, or mixed micelles composed by many surface active substances (e.g. bile salts, phospholipids, cholesterol, and fatty acids) (Reis et al., 2009; Singh et al., 2009). As a result, all these particles dispersed in the simulated intestinal fluids may have a significant negative net charge.

4. Effect of the interfacial layer composition of oil droplets on resveratrol bioaccessibility

Finally, resveratrol bioaccessibility of the single-layer and multilayer emulsions was assessed once *in vitro* digestion concluded. The resveratrol solubilized in mixed micelles during intestinal digestion was assumed as the resveratrol fraction available for absorption in the small intestine. It has been proposed that poor-water soluble substances, such as resveratrol, tend to be solubilized into micelles to extend the transport to intestinal epithelium (Joye, Davidov-Pardo, & McClements, 2014). Resveratrol had a very low bioaccessibility when it was encapsulated in primary emulsions and secondary emulsions (0.32% and 2.70%, respectively), but it significantly increased for tertiary emulsions (25%).

Based on the results obtained from the physical stability assessment of the emulsions during digestion, it was firstly proposed that the differences in the percentages of bioaccessibility might be associated to the instability of droplets in the gastric phase.

It has been described that intestinal digestion of emulsion-based systems depended on the droplet size. Oil droplets containing the active ingredient may be rapidly hydrolyzed by enzymes when the surface area is larger (small droplet size), hence releasing the encapsulated ingredient in a great extent (Salvia-Trujillo et al., 2013). In this study, both primary and secondary emulsions presented extensive droplets aggregation in the gastric phase,

while tertiary emulsions were significantly more stable. Thereby, the big clumps found in primary and secondary emulsions may not be completely digested in the small intestine; this non-digested aggregates with part of the resveratrol content can precipitate in the intestinal lumen, being unavailable to be solubilized into mixed micelles. Contrarily, tiny oil droplets of tertiary emulsions coming from the gastric digestion could have been rapidly digested in the intestinal phase, and in turn, increasing the resveratrol concentration in the micelle fraction.

Nonetheless, the final resveratrol concentration in the micelle fraction was less than 1 ppm in all emulsions, although the initial resveratrol concentration incorporated was rather different in each system. It was then proposed that the initial oil content in emulsions might also have had some influence in the resveratrol bioaccessibility.

Firstly, primary and secondary emulsions had greater oil and resveratrol content than tertiary emulsions. In the latter case, the lipolysis and formation of mixed micelles could have been accelerated by the presence of less substrate for the reactions. The opposite can be true in the case of a greater oil concentration. Secondly, it is possible that bile salts preferably form mixed micelles with the free fatty acids instead of resveratrol molecules at high oil concentrations, but resveratrol solubilization in the micelles could be favored at low oil concentration.

Previous studies have demonstrated that some types of bile acids can solubilize resveratrol molecules more efficiently than others (Atanacković et al., 2009). Thereby, the composition of bile salts likely has an important impact on resveratrol solubilization. Nevertheless, further studies should be carried out to clarify these hypotheses.

SECTION III: NANOLAMINATES

The effective fortification of food products with hydrophilic nutraceutical compounds is still a challenge, in spite of the variety of strategies currently existent. Namely, the incorporation of water-soluble vitamins in foods is not always successful owing to their high chemical instability to environmental conditions. In addition, many water-soluble vitamins have low stability in the gastrointestinal tract and little residence time in the adsorption site, which results in a low bioavailability.

Therefore, the encapsulation of these substances into nanostructured systems may help to maintain their functional properties and provide a controlled release of encapsulated compounds. Albeit delivery systems have been mostly thought for fortification of liquid foods, this is also possible in solid foods through a nanostructured edible coating. Nanolaminates, defined as thin coatings created by the alternative deposition of oppositely charged polyelectrolytes, may be good candidates. The simplicity of manufacture, low cost and versatility of coating materials are among the most relevant advantages of nanolaminates. In comparison with conventional edible coatings, their final characteristics can be fine-tuned with a precise control of the coating thickness, which would imply less impact on the visual characteristics of coated foods.

To address this topic, the most important factors affecting the formation and physicochemical properties of nanolaminates were investigated in this Doctoral Thesis. Then, their ability of to encapsulate water-soluble nutraceuticals (folic acid), increase the chemical stability and modulate the vitamin release from nanolaminates was explored.

1. Effect of the experimental parameters on the physicochemical properties of polysaccharide solutions

In the design of stable nanolaminates by electrostatic deposition, the properties of the oppositely charged building blocks play an important role. In effect, controlling the conditions of the absorbing solution for the layer-by-layer assembly is the most practical way to modulate the final nanolaminates properties. Therefore, changes in the electrical charge and physical stability of alginate and chitosan dissolved in aqueous media were assessed at

different pH (3-11), ionic strength (0-0.5 M NaCl) and polysaccharide concentrations (0.1-1%).

The negative electrical charge of alginate molecules, measured in terms of ζ-potential, was rather strong (< -70 mV) from pH 5 to 11, but became significantly weaker at pH 3 (≈ -40 mV). The pK_a of mannuronic acid and guluronic acid monomers are 3.30 and 3.65, respectively. Therefore, it is expected that alginate molecules were less charged in acidic conditions. The pH also had relevance in the viscosity values of polysaccharide solutions. Alginate solutions experimented a slight drop at pH 3, which can be explained by the fact that polysaccharide chains, being weakly charged, adopt a coiled conformation that reduces the hydrodynamic size and their ability to hold water molecules. It has been reported that linear and stiff molecules have larger hydrodynamic size than highly branched and flexible molecules of the same molecular mass (Milani & Maleki, 2012); this has an important influence of the rheological properties of the system. On the other hand, the whiteness index of alginate solutions was not affected by pH changes.

Chitosan molecules had a strong positive charge (80 mV) in the most acidic pH conditions evaluated (pH 3). In alkaline conditions (pH 7), chitosan molecules were weakly charged due to the proximity to its pK_a value (≈ 6.3); then deprotonation of amino groups of chitosan occurred. Furthermore, the apparent viscosity of chitosan solutions decreased abruptly from pH 3 to 11, observing noticeable insoluble clumps above pH 7. This was associated to the scarce electrical charge of the chitosan molecules, which leads to conformational changes induced by extensive intramolecular H-H bonding that reduce the entanglement of chitosan chains.

However, the pH effect on the solution viscosity was less pronounced using low concentrations of the chitosan; this indicates the strong relationship of these two parameters with the rheological properties of polysaccharide solutions. Regarding the optical features, chitosan solutions presented a marked change in the whiteness index at pH values above 7, which agree with the presence of insoluble clumps able to scatter the light strongly.

The upsurge of ionic strength (up to 0.2 M NaCl) in the media resulted in weaker charged polysaccharide chains, compared to low ionic strength conditions (0 M NaCl). The screen of charged carbonyl groups of alginate and amino groups of chitosan by dissolved ions might explain this behavior.

However, the ζ-potential of both polysaccharides was barely affected increasing ionic strength from 0.2 to 0.5 M NaCl. In addition, alginate and chitosan solutions were less viscous when NaCl concentration increased from 0 M to 0.1 M, and this effect was more pronounced in solutions with the highest polysaccharide concentration (1%). Nevertheless, a further increase in the ionic strength of solutions did not affect the viscosity.

The lessening of viscosity values were linked to the reduction of the electrical charge of polysaccharides. In consequence, weakly charged polysaccharides tend to adopt a coiled conformation, being less capable of attracting water molecules that result in a decrease of the solution viscosity (Harding, 1997; Morariu, Brunchi, & Bercea, 2012) Concerning the whiteness index, no changes were observed in both polysaccharide solutions, suggesting that both systems remained physically stability under these conditions.

The increase in polysaccharide concentration led to stronger electrical charge of alginate and chitosan molecules, and higher viscosity values in the solutions. In this case, a greater entanglement of polysaccharide chains allow water molecules to be sequestered within the polysaccharide net in a greater extent. Moreover, the whiteness index increased as a function of the polysaccharide concentration in both alginate and chitosan solutions. This is presumable since the large number of polysaccharide colloidal structures in the aqueous media tend to increase the light scattering, thus affecting the optical properties of the solution.

2. Buildup of alginate/chitosan nanolaminates

In the former study it was observed that the physicochemical properties of alginate and chitosan solutions depended on pH, ionic strength and polysaccharide concentration. The criteria to select the experimental conditions of the adsorbing solutions used in the layer-by-layer assembly was based in the results obtained previously, and information found in the literature.

It has been reported that the high ionic strength increases the film thickness of layer-by-layer assemblies, owing to the deposition of coiled polymer chains (Lundin, Solaqa, Thormann, MacAkova, & Blomberg, 2011). Moreover, polyelectrolytes with similar charge density tend to form more stable nanolaminates (Radeva, Kamburova, & Petkanchin, 2006). Consequently,

alginate and chitosan solutions were fixed at a pH, ionic strength and concentration in which polysaccharides were equally charged and highly stable. Therefore, 10-layer nanolaminates were assembled from alginate and chitosan solutions at 0.5%, pH 5 and 4 (respectively) and containing 0.2 M NaCl.

The buildup of alginate/chitosan nanolaminates was assessed by UV-visible spectroscopy, and the spectra revealed a marked increase in the absorbance as the number of layers increased. This indicates an upsurge of the mass deposited onto the substrate with the formation of a new layer. Hence, the alternative adsorption of oppositely charged polysaccharides could be confirmed. The UV-visible spectroscopy is a practical and reliable technique that allows monitoring the buildup of nanolaminates by measuring the increases in the optical mass (Haynie et al., 2005). Although the mass adsorbed cannot be quantified, it is possible to get insights about the growth regime of nanolaminates. The experimental parameters of adsorbing solutions may affect the adsorption kinetic of the polysaccharides, resulting in different growth regimes (Bieker & Schönhoff, 2010).

To evaluate the growth type in alginate/chitosan nanolaminates, absorbance at 200 nm vs the number of bilayers was plotted. This wavelength was chosen based on the fact that alginate solutions exhibit the maximum absorbance peak in this region, whereas chitosan solutions do not present absorbance in the UV-visible range. Interestingly, when both polysaccharides were combined in nanolaminated structures the absorption peak of alginate was overlapped. Probably, the formation of electrostatic complexes led to changes in the molar absorptivity of the chromophore groups of alginate, even though the major absorption region was still observed in the UV range.

Therefore, the wavelength of 200 nm was used as reference for evaluating the growth regime of the nanolaminates. This was characterized by an exponential trend, meaning that the rate of mass accumulation occurred rather rapid as the number of layers increased in nanolaminates. It has been reported that an exponential growth in nanolaminates happens when *free* chains are able to diffuse in and out of the structure during layer formation, interacting with the polyelectrolytes of the adsorbing solutions, where electrostatic interactions take place (Bieker & Schönhoff, 2010; Picart et al., 2002). In fact, some authors have demonstrated that chitosan chains are able

to diffuse vertically (out of the plane) to interact with the oppositely charge adsorbing species in the solution, during the assembly of chitosan/heparin layers (Lundin, Blomberg, & Tilton, 2010). It is also known that an increase in ionic strength of the adsorbing solutions results in assemblies that grow exponentially, since polyelectrolyte chains are deposited in a coiled conformation (Boddohi, Killingsworth, & Kipper, 2008).

Hence, the exponential growth of alginate/chitosan nanolaminates could be probably explained by the combined effect of high ionic strength and the diffusion of chitosan molecules in the nanolaminates structure.

3. Physicochemical properties of nanolaminates

One of the properties evaluated in nanolaminates was the surface electrical charge, since the layer-by-layer assembly was driven by electrostatic interactions. Hence, a change in the sign of the electrical charge should take place after with the formation of a new layer. In this regard, changes in the surface ζ-potential of alginate/chitosan nanolaminates were observed with the number of layers deposited. In particular, there was a swift in the positive ζ-potential of bare aminolyzed substrate (polyethylene terephthalate (PET) sheets: 49 mV) after depositing the first alginate layer (≈ -32 mV), turning into negative.

Moreover, a second chitosan layer changed the surface ζ-potentials to positive (≈ 50 mV), and this pattern was repeated along the assembly. Therefore, the charge reversal of the surface and the layer-by-layer process could be confirmed. This results are in good agreement with others previously published for polypeptide/polysaccharide assemblies, where the surface ζ-potential varied with the number of layers deposited (Picart et al., 2001).

Interestingly, although the initial electrical charge of both polysaccharides in solution was comparable (ζ-potential alginate: -36 mV; chitosan: 37 mV), chitosan layers presented larger values of surface ζ-potential (in terms of magnitude) than those observed in alginate layers. Likely, the differences in adsorption rates of both polysaccharides during the assembly of layers, or the ability of chitosan *free* chains to diffuse toward the surface could have increased the surface electrical charge of chitosan layers. Another important factor influencing the surface electrical charge of nanolaminates is the ionic strength; the greater material deposition on the forming layer induced by the

adsorption of coiled chains might also increase the magnitude of the electrical charge in the surface.

On the other hand, changes in the wetting properties of nanolaminates were investigated, depending on the outermost layer deposited. The contact angle (θ) found in aminolyzed PET sheets was 85º, as reported in previous studies (Carneiro-da-Cunha et al., 2010). After the first alginate layer deposition, there was a decrease in contact angle values ($\theta \approx 52º$). This was followed by a marked increase after the second chitosan layer was deposited ($\theta \approx 70º$), and this trend continued along the assembly process. This result was comparable to others reported for alginate/polyethyleneimine and κ-carrageenan/chitosan nanolaminates, where contact angles changed with the number of layers assembled (Gu et al., 2013; Pinheiro et al., 2012).

It has been described that chitosan behaves as a fully hydrophobic biopolymer, and the large θ values of chitosan-coated surfaces might be attributed to non-polar impurities contained in commercial chitosan samples, rather than the possible orientation of acetyl moieties at the solid/air interface (Farris et al., 2011). The hydrophilic properties of alginate molecules have been also stated for alginate-coated paperboards (Rhim, Lee, & Hong, 2006). The possibility of changing the wetting properties of a certain surface using the electrostatic deposition of two biopolymers with different water affinities may represent a useful feature for food applications.

The thermal properties of alginate/chitosan nanolaminates were assessed, using PET sheets as substrate. In general, the DSC profiles did not shown differences between the uncoated and coated substrate with 10-layer nanolaminates. The large mass ratio nanolaminate/substrate could explained this result since the film thickness of PET sheets was 36 μm, whereas nanolaminates were in the order of 100 nm thick. This suggests that the thermal properties of the composite material were dominated by PET.

A very slight increase in the enthalpy of melting (ΔH_m) was observed in coated PET compared to uncoated PET, probably because nanolaminates could have acted as barrier of the gases generated within the bulk during the thermal degradation, thus slowing down the process (Ayhan et al., 2015). Another possible factor responsible of this increase is the great concentration of carboxyl and amino groups on the surface or an increase in polymer

crystallinity, as suggested previously for alginate/chitosan nanolaminates assembled on PET sheets (Carneiro-da-Cunha et al., 2010).

The microscopic examination of alginate/chitosan nanolaminates also revealed the presence of densely packed polysaccharide structures, rather than stratified structures. Furthermore, it was possible to estimate an average thickness of ≈ 700 nm for 10-layer nanolaminates. A previous study demonstrated that nanolaminates that grows exponentially can reach thickness values of more than 10 μm, while same assemblies than grows linearly may have 100 nm thick containing equal number of layers (Richert et al., 2004). Other authors reported that exponential growing assemblies of chitosan/hyaluronan were about 6 μm thick, containing 24 layers (Etienne et al., 2005).

The topography of nanolaminates was also evaluated. The presence of big clusters connected through a polysaccharide net were observed, probably due to the formation of electrostatic complexes on the surface. This result matches well with others previously reported regarding the structure of chitosan/alginate assemblies (Martins, Mano, & Alves, 2011).

4. Effect of polysaccharide electrical charge: Nanolaminates buildup

The electrical charge (ζ-potential) of alginate and chitosan molecules in aqueous solutions can be simply modulated by changes in the pH media. As it was observed in the first study of this section, the degree of ionization of both polysaccharides also leads to conformational changes. Therefore, it was proposed that these changes might also have an effect on the assembly process of layer-by-layer nanolaminates. Consequently, the influence of different degrees of ionization of polysaccharides on the buildup of nanolaminates was studied. Firstly, alginate/chitosan nanolaminates were produced from *low*, *medium* and *high* charged polysaccharides. The pH of alginate solutions was adjusted to 7 (*high charge*), 5 (*medium charge*) and 3 (*low charge*) to obtain three levels of ionization. Chitosan solutions were adjusted to pH values of 3 (*high charge*), 4 (*medium charge*) and 7 (*low charge*).

The buildup of the different layer-by-layer assemblies was monitored by UV-visible spectroscopy, observing an absorbance increase as a function of the

number of layers deposited. However, there were significant differences in absorbance of nanolaminates depending on the initial electrical charge of polysaccharides. In fact, the absorbance (at 200 nm) per bilayer increased as the electrical charge of both polysaccharides decreased (*low*: 1.55; *medium*: 1.30; and; *high*: 0.23). The results obtained in this study are also comparable with those previously reported for alginate/chitosan assemblies (Yuan et al., 2007).

The differences found among the three nanolaminates were explained based on the conformation of polysaccharide chains. First, when both alginate and chitosan chains are fully charged, stiffness is increased due to the strong intra-molecular repulsion. This leads to less amount of material deposited per layer, and hence low values of absorbance. Contrarily, weakly charged polysaccharides adopt a coiled conformation, requiring higher amounts of material to compensate the oppositely charged surface, and thus absorbance increases. This behavior has been widely described for synthetic weak polyelectrolytes, wherein the pH changes of polyelectrolyte solutions results in different film thickness values (Shiratori & Rubner, 2000; Vidyasagar, Sung, Losensky, & Lutkenhaus, 2012).

Analyzing the growth regimes of nanolaminates, remarkable differences were also found. Nanolaminates obtained from *high* charge polysaccharides presented a linear growth type. In these assemblies, the amount of adsorbed mass per layer increases uniformly in each deposition. Moreover, nanolaminates prepared with *medium* and *low* charge chains grew exponentially, and hence the mass deposition per layer was significantly greater than in linearly growing nanolaminates.

A polysaccharides pair can form nanolaminates with different growth regime if the conditions of absorbing solutions are changed (Picart, 2008). A linear growth indicates that charged molecules in the solution interact exclusively with the outer layer of the multilayer system. However, when exponential growth occurs, one of the polyelectrolytes is able to diffuse within the film structure and these *free* chains can interact with the adsorbing solutions.

Results were in concordance with other studies (Xu et al., 2015); and confirmed that the degree of ionization in polysaccharide chains plays a key role in the formation of nanolaminates.

5. Effect of the polysaccharide electrical charge: Nanolaminates features

The potential impact of the electrical charge of polysaccharides on nanolaminates features was also investigated. Primarily, substantial differences in the surface ζ-potential of nanolaminates were observed, depending on the degree of ionization of polysaccharides. The surface of aminolyzed PET sheets was positively charged, and turned into negative after the first deposition with *high* and *medium* charge polysaccharides; this indicates the saturation of the surface by alginate chains. Nanolaminates prepared from *low* charge polysaccharides exhibited a completely different behavior. The sign of the surface electrical charge did not change, but a considerable decrease in the magnitude of the positive ζ-potential was observed. This was attributed to a sparse coverage of the substrate.

The weak positive charge of surface in this case, may be a result of the positive electrical charge of the substrate and the negative electrical charge of some alginate chains adsorbed. It has been stated that a minimum charge density of polyelectrolytes is necessary for creating a charge reversal on the surface during the layer-by-layer assembly. Below this threshold, there is not sufficient charge to achieve an overcompensation (de Villiers, Otto, Strydom, & Lvov, 2011; Klitzing & V Klitzing, 2006).

Nevertheless, these results evidence that the assembly of nanolaminates can be carried out even when polysaccharides are weakly charged. Hence, the presence of other non-electrostatic interactions might have contributed to the deposition of the initial alginate layer. In effect, hydrogen bonding between neutral molecules, van der Waals forces or steric interactions, play an important role on the process of adsorption. Other authors have pointed out the impact of non-electrostatic interactions on the deposition of cellulose/chitosan nanolaminate systems (Junka, Sundman, Salmi, Osterberg, & Laine, 2014). Furthermore, the synergetic interactions between electrostatic and non-electrostatic forces could be responsible of the formation of nanolaminates when polyelectrolytes are weakly charged (Salehi, Desai, Li, Steele, & Larson, 2015; Schoeler, Sharpe, Hatton, & Caruso, 2004).

In fact, after the deposition of next chitosan layer, all assemblies presented a positive surface charge and the charge reversal was observed as the number

of layers increased. Results were consistent with those reported for hyaluronan/chitosan nanolaminates (Richert et al., 2004), and (poly(allylamine hydrochloride)/poly(sodium 4-styrenesulfonate)) systems (Ladam et al., 2000), measured by streaming potential analysis. This supports the assumption that a new layer deposition leads to a surface charge reversal.

On the other hand, the degree of ionization of polysaccharide chains also affected the magnitude of the ζ-potential achieved in the surface of nanolaminates. In effect, nanolaminates assembled from *high* and *low* charge polysaccharides presented greater surface ζ-potentials (in terms of magnitude) than nanolaminates prepared with *medium* charge chains. The layers formed with *high* charge polysaccharides may present a greater number of ionizable groups on the surface that provide an electrical charge. In the case of the layers made of *low* charge polysaccharides, the high surface charge may be ascribed to the greater amount of polysaccharides chains needed to create the layer.

In addition, even layers (chitosan) were more charged than odd layers (alginate), suggesting a greater contribution of chitosan molecules to the surface electrical properties of nanolaminates. This result was further confirmed with a previous study that dealt with hyaluronic acid/collagen nanolaminates (Zhang et al., 2005). Remarkably, the magnitude of the surface ζ-potential remained relatively constant in all nanolaminates from the eighth layer. Then, the layer-by-layer systems became stable.

The wetting properties of nanolaminates prepared from *low*, *medium* and *high* charge polysaccharides were also explored. Marked differences in the water contact angle values (θ) of nanolaminates were observed, regarding to the degree of ionization of the polysaccharides chains. The contact angle values (θ) of the assemblies obtained with *low* and *medium* charge polysaccharides exhibited a zigzag trend when nanolaminates passed from alginate-ending layers to chitosan-ending layers. Nonetheless, this behavior was not observed in nanolaminates prepared from *low* charge polysaccharides. Nanolaminates obtained from *medium* and *low* charge polysaccharides showed an evident hydrophobic/hydrophilic behavior owing to the greater amount of material adsorbed per layer. This denotes that layers might be organized in stratified structures. In contrast, nanolaminates prepared from *high* charge

polysaccharides did not exhibit differences, probably because of the lower mass deposited, and hence layers might be fused.

From these observations, it was stated that wetting properties of the nanolaminates hinge on the experimental conditions used during the assembly of layers. Previous studies support this hypothesis indicating the strong relationship between layer thickness and wetting properties (Fu, Ji, Yuan, & Shen, 2005). In thin layer-by-layer assemblies, the surface properties are governed by the properties of the polysaccharide *blend* because of the high interpenetration among layers. The thick assemblies exhibit surface properties dictated by the outermost layer adsorbed (Ladam et al., 2000; Yoo, Shiratori, & Rubner, 1998).

Thus, the differences observed in the wetting properties of all nanolaminates might be explained by the differences in the amount of polyanion/polycation mass adsorbed. Other factors, such as the topography of nanolaminates, could have an impact on their wetting properties (Deng et al., 2014).

The contact angle of chitosan layers in nanolaminates increased as the degree of ionization of polysaccharides decreased. On the contrary, the contact angle values of alginate layers was lower in nanolaminates of *low* charged polysaccharides than in those formed from *high* charged chains. Hence, the hydrophobic/hydrophilic behavior in the surface also increases. The outermost layer and the thickness of individual layers seem to govern the wettability of nanolaminates. The possibility of modulate the wetting properties in nanolaminates basically by controlling the experimental parameters, may be interesting for some applications in foods, where the design of water-repelling surfaces (e.g. dried foods) or highly hydrophilic surfaces (e.g. high moisture foods) is desirable.

The microstructure and thermal properties of nanolaminates were also assessed in nanolaminates formed from *medium* charge polysaccharides. These assemblies presented the most uniform deposition, based on the results obtained from previous analyses. Microscopic examinations of the uncoated substrate (PET sheets) showed a rather smooth surface. The coated substrates containing 10-layer nanolaminates presented a thin film on the surface of irregular appearance. The estimated thickness was 297 nm.

The internal organization of layers in a cross section of the nanolaminates suggested their fusion, forming densely packed polysaccharide structures. Observations of the topography of nanolaminates showed the presence of small clusters with globule-like appearance connected through a network, which was ascribed to the polyelectrolyte complexation (Sæther, Holme, Maurstad, Smidsrød, & Stokke, 2008).

Regarding the thermal properties, no significant differences were observed between uncoated and coated PET sheets containing the nanolaminates. The glass transition temperature and melting temperature of uncoated PET sheets were in accordance with previous studies (de Oliveira Santos, Castro, Ruvolo-Filho, & Frollini, 2014; Grant, Alfouzan, Gough, Twigg, & Coates, 2013; Indest et al., 2008). The presence of nanolaminates on the PET surface did not cause any effect, probably due to differences in the mass ratio between the PET sheets and nanolaminates, predominating thermal properties of the substrate. The importance of thermal properties of a certain material relies on the influence in the mechanical behavior of the material.

However, the melting enthalpy of PET sheets coated by nanolaminates presented a slight increase, which might be associated to the ability of nanolaminates to act as gas barrier generated during the thermal degradation process, slowing down the polymer degradation (Ayhan et al., 2015). Finally, the surface modification caused by the presence of alginate and chitosan chains, as well as the increase in polymer crystallinity may also contribute to the enthalpy changes, as it was previously pointed out for PET sheets coated by alginate/chitosan nanolaminates (Carneiro-da-Cunha et al., 2010).

6. Alginate/chitosan nanolaminates as delivery systems of folic acid

The incorporation of active molecules into layer-by-layer assemblies have been studied for different applications in other science fields (Keeney et al., 2015), but it has been scarcely investigated in food technology. Food-grade nanolaminates, besides of their capacity of functionalizing foods surfaces, they might act as reservoirs of active food ingredients. Namely, nutraceutical compounds might be entrap into nanolaminates for their further application in food products.

The encapsulation of folic acid (hydrophilic nutraceutical) into polysaccharide-based nanolaminates was investigated in this study. Alginate/chitosan nanolaminates composed of 20 layers were obtained using the optimal conditions selected from the previous studies (Chapter IV and V). Straightaway, the loading and release mechanisms of folic acid in/from nanolaminates were also elucidated.

Formation of alginate/chitosan nanolaminates

The layer-by-layer buildup was assessed by UV-visible. Optical density of the substrate (measured by absorbance) increased with the number of layers deposited, confirming the formation of alginate/chitosan nanolaminates. UV-visible spectra recorded from the second to the eighth layer did not exhibit a defined absorption peak, even though the greatest absorbance was in the UV wavelength range. However, as the number of layers increased in nanolaminates (up to 20 layers), a large absorption peak appeared at 195 nm; this corresponded to N-acetyl-glucosamine and glucosamine residues of chitosan. The chitosan content in nanolaminates seems to be a possible cause in the differences among spectra. In the assemblies with less than 8 layers, the chitosan concentration could have been below the limit of detection, explaining the absence of an absorption peak in the spectrum.

Infrared spectra of uncoated and coated PET sheets also confirmed the formation of alginate/chitosan nanolaminates on the substrate. Firstly, infrared spectra of uncoated PET were in good agreement with literature. The three typical bands found in polyesters were observed at 1721 cm^{-1}, 1245 cm^{-1} and 1100 cm^{-1}, representing the C=O, C-C-O and O-C-C stretching vibrations of aromatic ester groups, respectively (Smith, 1999).

On the other hand, the presence of a nanolaminated coating on PET's surface led to important differences in the infrared spectra. Mainly, the bands located at 1410 cm^{-1} indicated the symmetric stretching vibrations of carboxyl (COO^-) groups of alginate molecules (Kumar, Chauhan, Gopal, Kumar, & Dilbaghi, 2015). Other bands at 1030 cm^{-1} and 1080 cm^{-1} were ascribed to C-O and C-O-C asymmetric stretching vibrations (respectively) of the skeletal vibrations of saccharine rings in both polysaccharides (Alves, Picart, & Mano, 2009; Lawrie et al., 2007). The presence of chitosan molecules was proved by the presence of three bands at 1650 cm^{-1}, 1515 cm^{-1} and 1150 cm^{-1} that

corresponded to the N-H-C=O stretching vibrations of amide I, the amide II stretching or N-H bending vibrations, and asymmetric C-O-C and C-N stretching vibrations, respectively (Aston, Wimalaratne, Brock, Lawrie, & Grøndahl, 2015).

Folic acid loading into nanolaminates

The folic acid encapsulation was performed by the post-diffusion method, in which the layer-by-layer assemblies previously formed are submerged into a solution containing the active substance. The effect of using different folic acid concentrations in the loading solution, as well as different immersion times was studied regarding the final loading achieved in nanolaminates.

The folic acid loading into alginate/chitosan assemblies was evaluated by UV-visible spectroscopy. Firstly, the typical peak at 195 nm found in nanolaminates without folic acid was completely absent in spectra of nanolaminates containing the active ingredient. Indeed, two new absorption peaks were observed at 295 nm and 373 nm. These peaks were ascribed to the heteroaromatic pterine chromophore of folic acid (Andrisano et al., 2003; Choy et al., 2004; Matias et al., 2014). Therefore, the presence of folic acid in nanolaminates could be proved. Another important fact is that nanolaminates became yellow after the incorporation of folic acid, and this color remained intense even after numerous washes with water.

The degree of swelling, hydrophilic/hydrophobic balance, surface charge density and pore size are intrinsic characteristics of nanolaminates that affect the loading process of small active molecules. In addition, the properties of the adsorbing molecules, such as size, charge and hydrophilicity play a key role in the process (Burke & Barrett, 2004). Based on the above-mentioned statement, it was proposed different scenarios that could explain the possible mechanisms whereby folic acid was entrapped into nanolaminates.

The loading of folic acid into nanolaminates was firstly based on the premise that the active ingredient is hydrophilic as the polysaccharide-based nanolaminates, and the small size of folic acid molecule would allow its diffusion into the layers. One of the mechanism proposed was the adsorption of folic acid with chitosan layers by electrostatic interactions, since this vitamin has negative charge (ζ-potential $\approx$ -34 mV) in alkaline conditions (loading solutions: pH 9). However, electrostatic interactions may not be the main

driven forces operating, since at the pH of the loading solutions chitosan molecules were probably uncharged.

The other mechanism proposed was the folic acid adsorption by hydrogen bonding with the polysaccharide layers. In addition, it has been reported that the swelling capacity of nanolaminates seems to contribute to the loading of small molecules by hydrogen bonding. A high swelling capacity of nanolaminates increases the loading rate of small molecules by creating more free volume for storage. This also allows small molecules to move within the structure, avoiding undesirable electrostatic forces and finding sites for more favorable non-electrostatic interactions (Burke & Barrett, 2004). A previous study have demonstrated that alginate/chitosan nanolaminates exhibit a great swelling capacity; assemblies in wet state may exhibit thickness values two times greater than assemblies in dried state (Caridade et al., 2013). In this regard, it was suggested that folic acid molecules were entrapped into nanolaminates by hydrogen bonding, also induced by the great swelling capacity of alginate/chitosan assemblies.

The concentration of loading solutions changed the final concentration of folic acid entrapped in nanolaminates. First, slight increases in the concentration of the loading solution (from 1-2.5 mg/mL) did not altered considerably the folic acid concentration in nanolaminates (from 9.8 to 11.6 μg/cm^2). A greater increase of the concentration in loading solutions up to 7.5 mg/mL originated nanolaminates that contained much higher folic acid content (53.3 μg/cm^2). Nonetheless, the final concentration of folic acid in the assemblies barely changed (54.4 μg/cm^2) when the concentration of the loading solution increased more (12.5 mg/mL). All this confirms the existence of a relationship between the initial active compound content in the loading solution and the final load in nanolaminates.

On the other hand, the folic acid concentration in nanolaminates was affected by the immersion time in the loading solution, at a fixed concentration (12.5 mg/mL). The vitamin content in nanolaminates increased logarithmically as a function of time. A fast rise was observed in the first 30 min, followed by a slower process up to 120 min. Longer immersion times (up to 240 min) did not increased the folic acid content in the assemblies. Analyzing the results, the immersion time where nanolaminates reach the maximum load was found

to be 120 min. Knowing the loading capacity of nanolaminates could be useful to optimize the quantities of active ingredients required for encapsulation.

Microstructural changes

The incorporation of folic acid within nanolaminates leads to marked changes in the microstructure. The initial topography of the assemblies changed drastically when the vitamin was included. It was characterized by the presence of polysaccharide globular structures. It was presumed that chitosan molecules were in great concentration on the surface, being the last polysaccharide deposited (layer 20). Some small zones along the surface having a different organization were also identified. In this case, it was ascribed to uncoated zones on the surface that led exposed the alginate layer located just above (layer 19). Examining these results together with those obtained for the loading capacity of assemblies, it was observed that the surface roughness may also have an important contribution in the entrapment of small molecules into nanolaminates. Uneven surfaces have larger surface area than smooth surfaces, and thus, a greater number of binding sites available to capture small molecules (Zhang, Li, Zhi, & Haynie, 2005).

Contrarily, the topography of nanolaminates was rather smooth in presence of folic acid. It is likely that strong molecular reorganizations have occurred when folic acid molecules were adsorbed within the polysaccharide assemblies and swelling took place. Examinations of the cross-section revealed the stratified structure in assemblies containing or not the vitamin, being more evident in the presence of the compound. Additionally, the estimated thickness was about 2.9 μm for nanolaminates without folic acid, and apparently decreased when the vitamin was encapsulated.

The distribution of folic acid along the structure was also investigated by Raman spectroscopy. Spectra of nanolaminates containing folic acid showed a small peak at 680 nm, which was also present in the spectra of powdered folic acid. The peak at 680 nm corresponds to the stretching of the C-N and C-C bounds of the pteridine ring and p-aminobenzoic acid fragment of folic acid, respectively (Castillo et al., 2015). The presence of the vitamin in the polysaccharide assemblies was also confirmed by this result.

In parallel, it was evaluated the possible changes in the peak intensity at 680 nm in a particular area of the polysaccharide coating. If the peak intensity

varies in a certain region of the nanolaminate this could indicate differences in the amount of folic acid entrapped in the structure. To avoid the incidence of the substrate (PET) on spectra, a cross section of the nanolaminated structure was hence examined. Raman spectra recorded along 1000 μm did not changed in any case, as well as the peak at 680 nm. This could indicate that the quantity of folic acid found in different sections of the structure is comparable, wherewith, the encapsulation process was carried out efficiently.

Photo-protection of folic acid

One of the shortcomings of using folic acid in food fortification is related with their instability to environmental conditions, namely to UV-light exposure. In this Doctoral Thesis, a goal proposed was to elucidate if nanostructured systems might offer a better protection to those active ingredients, which functionality depends on their chemical stability. Therefore, it was study the ability of polysaccharide-based nanolaminates to enhance the chemical stability of the folic acid molecules entrapped in the structure, being exposed to direct lighting with UV-light.

Changes in the folic acid molecules (encapsulated or not) at constant irradiation was assessed by UV-visible spectroscopy. In general, the vitamin was rapidly degraded in the first 20 min in the non-encapsulated form (solutions in buffer pH 9). Important changes in the UV-visible spectra could be observed, compared to the initially found. The two peaks (283 nm: pteridine moieties and 364 nm: *p*-aminobenzoic glutamate moieties) observed in the folic acid spectrum changed into a broader peak that ranged from 310 nm and to 374 nm. This effect was more evident increasing the exposure time to 120 min; in this case the vitamin was completely degraded.

Folic acid molecules are cleaved into biologically inactive photoproducts as a result of a reaction with the UV-light. It has been identified two main photoproducts: the FPT (6-formylpterin) and PCA (pterine-6-carboxylic acid), with adsorption peaks at 278 – 310 - 365 nm and 290 - 350 nm, respectively (Off et al., 2005). The increasing concentration of PCA and FPT results in wider peaks in the absorbance spectrum. Hence, changes observed in the folic acid spectra after being irradiated respond to the presence of photoproducts generated in the degradation reaction.

On the contrary, the encapsulation of folic acid molecules within polysaccharide-based nanolaminates seems to improve their stability. The absorbance spectra remained comparable, even with 120 min of UV-light exposure. Therefore, encapsulation of vitamins in layer-by-layer assemblies has a positive effect on their chemical stability. Based on this results, it can be state that nanolaminates certainly may be able to entrap and protect sensitive substances against external agents, which normally would be degraded, reducing their functional properties.

Folic acid release from nanolaminates

This last study evaluates the different release profiles of folic acid generated when nanolaminates are incubated either in acidic or alkaline pH conditions. The criteria used to select the pH conditions for the release experiments was based on the fact that absorption of vitamins mostly occurs in alkaline conditions of the small intestine. Nonetheless, the stability of folic acid may be altered by the acidic environment of the gastric digestion, compromising its bioactivity before reaching the targeted site of absorption. The pH values commonly reported in the literature for simulated gastrointestinal conditions are unconcise and vary from one study to another. An harmonized protocol published for *in vitro* static digestion point out that recommended pH values for mimic the gastric and intestinal phases are 3 and 7, respectively (Minekus et al., 2014). Therefore, the release studies were performed using these values.

As previously observed in the latter study, nanolaminates exhibited notable protection of folic acid against UV-light degradation. Hence, it would be expected some protective effect during digestion or at least, a pH-stimuli response that would lead to a controlled release of the vitamin from the structure. Nanolaminates incubated at pH 3 presented around 22% of folic acid released with regard to the initial load. The situation was rather different when nanolaminates stayed at pH 7; almost the total amount of folic acid encapsulated could be released. These results show the pH stimuli-responsive properties of nanolaminates.

The release profiles of folic acid from assemblies were comparable in both situations, although the release rate was clearly faster at pH 7. The profile was characterized by fast release of folic acid reaching 88% of the initial load

during the first hour, followed by a much slower behavior until the end of incubation time. To a lesser degree, the release of folic acid from nanolaminates incubated pH 3 was also rapid initially, but then reached a plateau. Literature refer that the kinetic release of active compounds from a vehicle is affected by the pH of the environment, normally following a biphasic behavior. This means that the initial burst release takes place during the first hour, being driven by an excess of the encapsulated substance on the vehicle's surface. In the second release stage, the concentration gradient decreases due to the presence of less content of encapsulated compound, which results in their slow release from the vehicle to the media (Anandhakumar, Gokul, & Raichur, 2016).

The differences found in the release profiles of folic acid in both pH conditions might be explained in terms of solubility of folic acid. In alkaline media the vitamin has great water solubility than in acidic media ($pK_a \approx 3.37$) (Gazzali et al., 2016). A previous study has showed that the solubility of the encapsulated compound may determine the release rate in certain conditions. In effect, it was observed how the drug release from microspheres coated by alginate/chitosan assemblies was increased by changing the pH of the media, where the drug was more soluble (X. Li, Du, Liu, et al., 2014).

In summary, it can be postulated that the folic acid release from alginate/chitosan nanolaminates was governed mainly by the solubility of the vitamin. This feature led to different release profiles when nanolaminates were incubated with either alkaline or acidic buffer. The most interesting aspect of this result is the fact that nanolaminates were able to suppress efficiently the release of the vitamin in acidic pH values that mimicked those found in the stomach. However, it was observed that nanolaminates behaves completely different at the alkaline conditions similar to the intestinal digestion, promoting a complete release of the vitamin. This suggests that nanolaminates may be used to improve delivery of nutraceuticals to the targeted site of absorption, having a remarkable value for the design of healthier food products.

References

Alves, N. M., Picart, C., & Mano, J. F. (2009). Self assembling and crosslinking of polyelectrolyte multilayer films of chitosan and alginate studied by QCM and IR spectroscopy. *Macromolecular Bioscience*, *9*(8), 776–85.

Aston, R., Wimalaratne, M., Brock, A., Lawrie, G., & Grøndahl, L. (2015). Interactions between Chitosan and Alginate Dialdehyde Biopolymers and Their Layer-by-Layer Assemblies. *Biomacromolecules*, *16*(6), 1807–17.

Ayhan, Z., Cimmino, S., Esturk, O., Duraccio, D., Pezzuto, M., & Silvestre, C. (2015). Development of Films of Novel Polypropylene based Nanomaterials for Food Packaging Application. *Packaging Technology and Science*, *28*(7), 589–602.

Bieker, P., & Schönhoff, M. (2010). Linear and Exponential Growth Regimes of Multilayers of Weak Polyelectrolytes in Dependence on pH. *Macromolecules*, *43*(11), 5052–5059.

Boddohi, S., Killingsworth, C. E., & Kipper, M. J. (2008). Polyelectrolyte multilayer assembly as a function of pH and ionic strength using the polysaccharides chitosan and heparin. *Biomacromolecules*, *9*(7), 2021–2028. JOUR.

Bonilla, J., Atarés, L., Vargas, M., & Chiralt, A. (2012). Effect of essential oils and homogenization conditions on properties of chitosan-based films. *Food Hydrocolloids*, *26*(1), 9–16.

Carneiro-da-Cunha, M. G., Cerqueira, M. A., Souza, B. W. S., Carvalho, S., Quintas, M. A. C. C., Teixeira, J. A., & Vicente, A. A. (2010). Physical and thermal properties of a chitosan/alginate nanolayered PET film. *Carbohydrate Polymers*, *82*(1), 153–159.

Davidov-Pardo, G., & McClements, D. J. (2015). Nutraceutical delivery systems: resveratrol encapsulation in grape seed oil nanoemulsions formed by spontaneous emulsification. *Food Chemistry*, *167*, 205–12.

de Oliveira Santos, R. P., Castro, D. O., Ruvolo-Filho, A. C., & Frollini, E. (2014). Processing and thermal properties of composites based on recycled PET, sisal fibers, and renewable plasticizers. *Journal of Applied Polymer Science*, *131*(12), 40386.

de Villiers, M. M., Otto, D. P., Strydom, S. J., & Lvov, Y. M. (2011). Introduction to nanocoatings produced by layer-by-layer (LbL) self-assembly. *Advanced Drug Delivery Reviews*, *63*(9), 701–715.

Deng, J., Liu, X., Ma, L., Cheng, C., Shi, W., Nie, C., & Zhao, C. (2014). Heparin-mimicking multilayer coating on polymeric membrane via LbL assembly of cyclodextrin-based supramolecules. *ACS Applied Materials & Interfaces*, *6*(23), 21603–14.

Dickinson, E. (2003). Hydrocolloids at interfaces and the influence on the properties of dispersed systems. *Food Hydrocolloids*, *17*(1), 25–39.

Dickinson, E. (2009). Hydrocolloids as emulsifiers and emulsion stabilizers. *Food Hydrocolloids*, *23*(6), 1473–1482.

Etienne, O., Schneider, A., Taddei, C., Richert, L., Schaaf, P., Voegel, J.-C., … Picart, C. (2005). Degradability of polysaccharides multilayer films in the oral environment: an in vitro and in vivo study. *Biomacromolecules*, *6*(2), 726–33.

Fabra, M. J., Pérez-Masiá, R., Talens, P., & Chiralt, A. (2011). Influence of the homogenization conditions and lipid self-association on properties of sodium caseinate based films containing oleic and stearic acids. *Food Hydrocolloids*, *25*(5), 1112–1121.

Farris, S., Introzzi, L., Biagioni, P., Holz, T., Schiraldi, A., & Piergiovanni, L. (2011). Wetting of Biopolymer Coatings: Contact Angle Kinetics and Image Analysis Investigation. *Langmuir*, *27*(12), 7563–7574.

Fu, J., Ji, J., Yuan, W., & Shen, J. (2005). Construction of anti-adhesive and antibacterial multilayer films via layer-by-layer assembly of heparin and chitosan. *Biomaterials*, *26*(33), 6684–6692.

Gazzali, A. M., Lobry, M., Colombeau, L., Acherar, S., Azaïs, H., Mordon, S., … Frochot, C. (2016). Stability of folic acid under several parameters. *European Journal of Pharmaceutical Sciences*, *93*, 419–430.

Grant, C. A., Alfouzan, A., Gough, T., Twigg, P. C., & Coates, P. D. (2013). Nano-scale temperature dependent visco-elastic properties of polyethylene terephthalate (PET) using atomic force microscope (AFM). *Micron (Oxford, England : 1993)*, *44*, 174–8.

Gu, C.-H., Wang, J.-J., Yu, Y., Sun, H., Shuai, N., & Wei, B. (2013). Biodegradable multilayer barrier films based on alginate/polyethyleneimine and biaxially oriented poly(lactic acid). *Carbohydrate Polymers*, *92*(2), 1579–85.

Gutierrez, J., Rodriguez, G., Barry-Ryan, C., & Bourke, P. (2008). Efficacy of plant essential oils against foodborne pathogens and spoilage bacteria associated with ready-to-eat vegetables: Antimicrobial and sensory screening. *Journal of Food Protection*, *71*(9), 1846–1854.

Han, J., & Gennadios, A. (2005). Edible films and coatings: a review. In *Innovations in Food Packaging* (pp. 239–262). Elsevier.

Harding, S. E. (1997). The intrinsic viscosity of biological macromolecules. Progress in measurement, interpretation and application to structure in dilute solution. *Progress in Biophysics and Molecular Biology*, *68*(2), 207–262.

Haynie, D. T., Zhang, L., Rudra, J. S., Zhao, W., Zhong, Y., & Palath, N. (2005). Polypeptide Multilayer Films. *Biomacromolecules*, *6*(6), 2895–2913.

Heurtault, B. (2003). Physico-chemical stability of colloidal lipid particles. *Biomaterials*, *24*(23), 4283–4300.

Indest, T., Laine, J., Ribitsch, V., Johansson, L.-S., Stana-Kleinschek, K., & Strnad, S. (2008). Adsorption of chitosan on PET films monitored by quartz crystal microbalance. *Biomacromolecules*, *9*(8), 2207–14.

Joye, I. J., Davidov-Pardo, G., & McClements, D. J. (2014). Nanotechnology for increased micronutrient bioavailability. *Trends in Food Science and Technology*, *40*(2), 168–182.

Junka, K., Sundman, O., Salmi, J., Osterberg, M., & Laine, J. (2014). Multilayers of cellulose derivatives and chitosan on nanofibrillated cellulose. *Carbohydrate Polymers*, *108*, 34–40.

Juven, B. J., Kanner, J., Schved, F., & Weisslowicz, H. (1994). Factors that interact with the antibacterial action of thyme essential oil and its active constituents. *Journal of Applied Bacteriology*, *76*(6), 626–631.

Keeney, M., Jiang, X. Y., Yamane, M., Lee, M., Goodman, S., & Yang, F. (2015). Nanocoating for biomolecule delivery using layer-by-layer self-assembly. *J. Mater. Chem. B*, *3*(45), 8757–8770.

Klitzing, R. V, & V Klitzing, R. (2006). Internal structure of polyelectrolyte multilayer assemblies. *Physical Chemistry Chemical Physics : PCCP*, *8*(43), 5012–33.

Kumar, S., Chauhan, N., Gopal, M., Kumar, R., & Dilbaghi, N. (2015). Development and evaluation of alginate–chitosan nanocapsules for controlled release of acetamiprid. *International Journal of Biological Macromolecules*, *81*, 631–637.

Ladam, G., Schaad, P., Voegel, J. C., Schaaf, P., Decher, G., & Cuisinier, F. (2000). In Situ Determination of the Structural Properties of Initially Deposited Polyelectrolyte Multilayers. *Langmuir*, *16*(3), 1249–1255.

Lawrie, G., Keen, I., Drew, B., Chandler-Temple, A., Rintoul, L., Fredericks, P., & Grøndahl, L. (2007). Interactions between alginate and chitosan biopolymers characterized using FTIR and XPS. *Biomacromolecules*, *8*(8), 2533–2541.

Lundin, M., Blomberg, E., & Tilton, R. D. (2010). Polymer dynamics in layer-by-layer assemblies of chitosan and heparin. *Langmuir*, *26*(5), 3242–3251.

Lundin, M., Solaqa, F., Thormann, E., MacAkova, L., & Blomberg, E. (2011). Layer-by-layer assemblies of chitosan and heparin: Effect of solution ionic strength and pH. *Langmuir*, *27*(12), 7537–7548. JOUR.

Maizura, M., Fazilah, A., Norziah, M. H., & Karim, A. A. (2007). Antibacterial activity and mechanical properties of partially hydrolyzed sago starch-alginate edible film containing lemongrass oil. *Journal of Food Science*, *72*(6), C324-30.

Martins, G. V, Mano, J. F., & Alves, N. M. (2011). Dual Responsive Nanostructured Surfaces for Biomedical Applications. *Langmuir*, *27*(13), 8415–8423.

McClements, D. J. (2005). *Food emulsions : principles, practices, and techniques*. (C. Press, Ed.). Boca Raton, Fla. : CRC Press. Retrieved from

McClements, D. J., & Rao, J. (2011). Food-grade nanoemulsions: formulation, fabrication, properties, performance, biological fate, and potential toxicity. *Critical Reviews in Food Science and Nutrition*, *51*(4), 285–330.

Milani, J., & Maleki, G. (2012). Hydrocolloids in food industry. In B. Valdez (Ed.), *Food Idustrial Processes–Methods and Equipment* (pp. 17–38). Intech.

Minekus, M., Alminger, M., Alvito, P., Ballance, S., Bohn, T., Bourlieu, C., … Brodkorb, A. (2014). A standardised static in vitro digestion method suitable for food - an international consensus. *Food & Function*, *5*(6), 1113–24.

Morariu, S., Brunchi, C. E., & Bercea, M. (2012). The Behavior of Chitosan in Solvents with Different Ionic Strengths. *Industrial & Engineering Chemistry Research*, *51*(39), 12959–12966.

Nuchuchua, O., Sakulku, U., Uawongyart, N., Puttipipatkhachorn, S., Soottitantawat, A., & Ruktanonchai, U. (2009). In vitro characterization and mosquito (Aedes aegypti) repellent activity of essential-oils-loaded nanoemulsions. *AAPS PharmSciTech*, *10*(4), 1234–42.

Picart, C. (2008). Polyelectrolyte multilayer film: From physico-chemical properties to the control of cellular processes. *Current Medicinal Chemistry*, *15*(7), 685–697.

Picart, C., Lavalle, P., Hubert, P., Cuisinier, F. J. G., Decher, G., Schaaf, P., & Voegel, J.-C. (2001). Buildup Mechanism for Poly(l -lysine)/Hyaluronic Acid Films onto a Solid Surface. *Langmuir*, *17*(23), 7414–7424.

Picart, C., Mutterer, J., Richert, L., Luo, Y., Prestwich, G. D., Schaaf, P., … Lavalle, P. (2002). Molecular basis for the explanation of the exponential growth of polyelectrolyte multilayers. *Proceedings of the National Academy of Sciences of the United States of America*, *99*(20), 12531–5.

Pinheiro, A. C., Bourbon, A. I., Medeiros, B. G. de S., da Silva, L. H. M., da Silva, M. C. H., Carneiro-da-Cunha, M. G., … Vicente, A. A. (2012). Interactions between κ-carrageenan and chitosan in nanolayered coatings—Structural and transport properties. *Carbohydrate Polymers*, *87*(2), 1081–1090. JOUR.

Pires, C., Ramos, C., Teixeira, B., Batista, I., Nunes, L., & Marques, A. (2013). Hake proteins edible films incorporated with essential oils: Physical, mechanical, antioxidant and antibacterial properties. *Food Hydrocolloids*, *30*(1), 224–231.

Radeva, T., Kamburova, K., & Petkanchin, I. (2006). Formation of polyelectrolyte multilayers from polysaccharides at low ionic strength. *Journal of Colloid and Interface Science*, *298*(1), 59–65.

Rao, J., & McClements, D. J. (2012). Impact of lemon oil composition on formation and stability of model food and beverage emulsions. *Food Chemistry*, *134*(2), 749–57.

Raybaudi-Massilia, R. M., Mosqueda-Melgar, J., & Martin-Belloso, O. (2008). Edible alginate-based coating as carrier of antimicrobials to improve shelf-life and safety of fresh-cut melon. *International Journal of Food Microbiology*, *121*(3), 313–327.

Rhim, J.-W., Lee, J.-H., & Hong, S.-I. (2006). Water resistance and mechanical properties of biopolymer (alginate and soy protein) coated paperboards. *LWT - Food Science and Technology*, *39*(7), 806–813.

Richert, L., Lavalle, P., Payan, E., Shu, X. Z., Prestwich, G. D., Stoltz, J.-F., … Picart, C. (2004). Layer by Layer Buildup of Polysaccharide Films: Physical Chemistry and Cellular Adhesion Aspects. *Langmuir*, *20*(2), 448–458.

Rojas-Graü, M. A., Avena-Bustillos, R. de J., Friedman, M., Henika, P. R., Martin-Belloso, O., & McHugh, T. H. (2006). Mechanical, barrier, and antimicrobial properties of apple puree edible films containing plant essential oils. *Journal of Agricultural and Food Chemistry*, *54*(24), 9262–7.

Rojas-Graü, M. A., Avena-Bustillos, R. de J., Olsen, C., Friedman, M., Henika, P. R., Martin-Belloso, O., … McHugh, T. H. (2007). Effects of plant essential oils and oil compounds on mechanical, barrier and antimicrobial properties of alginate-apple puree edible films. *Journal of Food Engineering*, *81*(3), 634–641. JOUR.

Sæther, H. V., Holme, H. K., Maurstad, G., Smidsrød, O., & Stokke, B. T. (2008). Polyelectrolyte complex formation using alginate and chitosan. *Carbohydrate Polymers*, *74*(4), 813–821.

Salehi, A., Desai, P. S., Li, J., Steele, C. A., & Larson, R. G. (2015). Relationship between Polyelectrolyte Bulk Complexation and Kinetics of Their Layer-by-Layer Assembly. *Macromolecules*, *48*(2), 400–409.

Salvia-Trujillo, L., Rojas-Graü, M. A., Soliva-Fortuny, R. C., & Martín-Belloso, O. (2013). Effect of processing parameters on physicochemical characteristics of microfluidized lemongrass essential oil-alginate nanoemulsions. *Food Hydrocolloids*, *30*(1), 401–407.

Sánchez-González, L., Chiralt, A., González-Martínez, C., & Cháfer, M. (2011). Effect of essential oils on properties of film forming emulsions and films based on hydroxypropylmethylcellulose and chitosan. *Journal of Food Engineering*, *105*(2), 246–253.

Schoeler, B., Sharpe, S., Hatton, T. A., & Caruso, F. (2004). Polyelectrolyte Multilayer Films of Different Charge Density Copolymers with Synergistic Nonelectrostatic Interactions Prepared by the Layer-by-Layer Technique. *Langmuir*, *20*(7), 2730–2738.

Sessa, M., Tsao, R., Liu, R., Ferrari, G., & Donsì, F. (2011). Evaluation of the Stability and Antioxidant Activity of Nanoencapsulated Resveratrol during in Vitro Digestion. *Journal of Agricultural and Food Chemistry*, *59*(23), 12352–12360.

Shimoni, G., Shani Levi, C., Levi Tal, S., & Lesmes, U. (2013). Emulsions stabilization by lactoferrin nano-particles under in vitro digestion conditions. *Food Hydrocolloids*, *33*(2), 264–272.

Shiratori, S. S., & Rubner, M. F. (2000). pH-Dependent Thickness Behavior of Sequentially Adsorbed Layers of Weak Polyelectrolytes. *Macromolecules*, *33*(11), 4213–4219.

Shirazi, M. H., Ranjbar, R., Eshraghi, S., Amin, G., Nouri, M. S., & Bazzaz, N. (2008). Inhibitory Effects of Sage Extract on the Growth of Enteric Bacteria. *Pakistan Journal of Biological Sciences*, *11*(3), 487–489.

Smith, B. C. (1999). *Infrared spectral interpretation : a systematic approach*. Boca Raton [etc.] : CRC Press.

Tokle, T., & McClements, D. J. (2011). Physicochemical properties of lactoferrin stabilized oil-in-water emulsions: Effects of pH, salt and heating. *Food Hydrocolloids*, *25*(5), 976–982.

Ultee, A., Bennik, M. H. J., & Moezelaar, R. (2002). The phenolic hydroxyl group of carvacrol is essential for action against the food-borne pathogen Bacillus cereus. *Applied and Environmental Microbiology*, *68*(4), 1561–1568.

Vidyasagar, A., Sung, C., Losensky, K., & Lutkenhaus, J. L. (2012). pH-Dependent Thermal Transitions in Hydrated Layer-by-Layer Assemblies Containing Weak Polyelectrolytes. *Macromolecules*, *45*(22), 9169–9176.

Xu, J., Yang, L., Hu, X., Xu, S., Wang, J., & Feng, S. (2015). The effect of polysaccharide types on adsorption properties of LbL assembled multilayer films. *Soft Matter*, *11*(9), 1794–9.

Yoo, D., Shiratori, S. S., & Rubner, M. F. (1998). Controlling Bilayer Composition and Surface Wettability of Sequentially Adsorbed Multilayers of Weak Polyelectrolytes. *Macromolecules*, *31*(13), 4309–4318.

Yuan, W., Dong, H., Li, C. M., Cui, X., Yu, L., Lu, Z., & Zhou, Q. (2007). pH-Controlled Construction of Chitosan/Alginate Multilayer Film: Characterization and Application for Antibody Immobilization. *Langmuir*, *23*(26), 13046–13052.

Zhang, J., Senger, B., Vautier, D., Picart, C., Schaaf, P., Voegel, J.-C., & Lavalle, P. (2005). Natural polyelectrolyte films based on layer-by layer deposition of collagen and hyaluronic acid. *Biomaterials*, *26*(16), 3353–61.

Zúñiga, R. N., Skurtys, O., Osorio, F., Aguilera, J. M., & Pedreschi, F. (2012). Physical properties of emulsion-based hydroxypropyl methylcellulose films: effect of their microstructure. *Carbohydrate Polymers*, *90*(2), 1147–58.

CONCLUSIONS

The key findings obtained from the different studies proposed in the present Doctoral Thesis are described as follows. Conclusions were organized according to the three nanostructured delivery systems investigated.

Section I: Essential oil nanoemulsions and edible films

- The essential oils of thyme, lemongrass and sage were successfully incorporated into nanoemulsions using the microfluidization technology. The reduction in the droplet size bellow 100 nm, as well as the presence of texturizing agents in the formulation (alginate) had a marked influence on the physicochemical properties of nanoemulsions.
- The characteristics of essential oil nanoemulsions determined the final physical properties of the resulting edible films. The most important features of nanoemulsions affecting the properties of edible films were the size and the electrical charge of oil droplets.
- Antimicrobial activity of nanoemulsion-based edible films was mostly governed by the affinity between each essential oil and the target microorganism, and not by the droplet size. In some cases, the nanometric size of oil droplets might have a self-defeating effect in the antimicrobial activity of edible films.

Section II: Multilayer emulsions

- The biopolymer concentration in the continuous phase was a crucial parameter to form interfacial layers on droplets and obtain stable emulsions. Either a scarce or excessive quantity of biopolymer in the continuous phase originated instability phenomena in the multilayer emulsions, such as bridging or depletion flocculation.
- The addition of polysaccharides and polypeptides at the interface of protein-coated droplets increased the stability of emulsions during storage. The resveratrol entrapped in the oil phase of single-layer and multilayer emulsions was better protected from chemical degradation than non-encapsulated resveratrol during storage. However, the number of interfacial layers on resveratrol-loaded oil droplets did not have any additional effect on the chemical stability of the nutraceutical.

- The physical stability of resveratrol-loaded oil droplets exposed to simulated gastrointestinal fluids depended on the composition of the interfacial layers of biopolymers. The outermost layer forming the interfacial coating certainly defined the interactions between coated droplets and other components of the gastrointestinal fluids; this consequently affected the emulsion stability and resveratrol bioaccessibility.

Section III: Nanolaminates

- Changes in the conditions of preparation, such as pH, ionic strength and concentration affected the physicochemical properties of the polysaccharide solutions used for the assembly of nanolaminates. Alginate/chitosan layer-by-layer assemblies were successfully obtained at slightly acidic pH conditions and high ionic strength.
- Alginate/chitosan nanolaminates grew exponentially in high ionic strength conditions, and their physicochemical properties, such as the surface charge and wettability, changed as a function of the outer layer deposited on the surface.
- The initial electrical charge of the polysaccharides used as building blocks had a substantial impact on the formation of nanolaminates. As the electrical charge of the oppositely charged polysaccharides increased, the amount of mass deposition decreased. The growth regime of nanolaminates changed from linear to exponential, affecting also their physicochemical properties.
- The viability of using alginate/chitosan nanolaminates to entrap folic acid molecules was confirmed. The final folic acid content in the assemblies depended on the initial vitamin concentration in the loading solution as well as the immersion time.
- Nanolaminates exhibited outstanding properties as delivery systems of hydrophilic nutraceuticals. On the one hand, encapsulated folic acid was more stable to UV-light than the non-encapsulated form, indicating the protective effect of nanolaminates. On the other hand, the different pH-stimuli responses observed in nanolaminates allowed controlling the vitamin release from the polysaccharide structure.

FUTURE RESEARCH

The results obtained in this Doctoral Thesis have shown that food grade nanostructures, either emulsion-based or layer-by-layer systems, can be used as delivery systems of active food ingredients. Although research conducted up to date has demonstrated the advantages of designing food materials at nanometric level, this technological approach requires more research in order to be utilized in the food industry.

Further investigations proposed for each one of the systems studied are described below:

Nanoemulsion-based edible films

- Evaluate the possibility of incorporated other active ingredients in the formulation of nanoemulsions that could enhanced the quality of food products, such as antioxidants, texture enhancers, flavors, etc.
- Investigate the functional performance of nanoemulsion-based edible films on wrapped food product and compare it with conventional edible films.

Mutillayer emulsions

- Explain the possible interactions happening when incorporating multilayer emulsions in real foods.
- Validate the efficacy of multilayer emulsions as delivery systems of nutraceuticals using *in vivo* models.

Nanolaminates

- Investigate the possibility of encapsulate active hydrophobic ingredients into nanolaminates as well as their functional properties.
- Apply the active nanolaminate coatings in real food models and evaluate their impact on shelf life and/or functional properties of coated foods.
- Assess the behavior of nanolaminates containing nutraceuticals during an *in vitro* digestion
- Evaluate consumers' acceptance of food products coated with nanolaminate systems.